Author/s:
Rathnapala, Gallallalage Upeksha Lakmini

Title:
Defining the roles of essential genes in the malaria parasite life cycle

Date:
2017

Persistent Link:
https://hdl.handle.net/11343/207955

Defining the roles of essential genes in the malaria parasite life cycle

Gallallalage Upeksha Lakmini Rathnapala

orcid.org/0000-0001-6259-616X

Submitted in total fulfilment of the requirements of the degree of Doctor of Philosophy

September 2017

School of BioSciences, Faculty of Science
The University of Melbourne

Abstract

The combination of drug resistance, lack of an effective vaccine and ongoing conflict and poverty mean that malaria remains a major global health crisis. Understanding metabolic pathways at all parasite life stages is important in prioritising and targeting novel anti-parasitic compounds. To overcome limitations of existing genetic tools to investigate all the parasite life stages, new approaches are vital. This project aimed to develop a novel genetic approach using post meiotic segregation to separate genes and bridge parasites through crucial life stages.

The unusual heme synthesis pathway of the rodent malaria parasite, *Plasmodium berghei*, requires eight enzymes distributed across the mitochondrion, apicoplast and cytoplasm. Deletion of the ferrochelatase (FC) gene, the final enzyme in the pathway, confirms that heme synthesis is not essential in the red blood cell stages of the life cycle but is required to complete oocyst development in mosquitoes. The lethality of FC deletions in the mosquito stage makes it difficult to study the impact of these mutations in the subsequent liver stage. To overcome this, I combined locus-specific fluorophore expression with a genetic complementation approach to generate viable, heterozygous oocysts able to produce a mix of FC expressing and FC deficient sporozoites. In the liver stage, FC deficient parasites can be distinguished by fluorescence and phenotyped. Parasites lacking FC exhibited a severe growth defect from early to mid-stages of liver development *in-vitro* and could not infect naïve mice, confirming liver stage arrest. These results validate the heme pathway as a potential target for prophylactic drugs targeting liver stage parasites.

Energy metabolism in malaria parasites varies remarkably over the parasite life cycle. Parasites depend solely on anaerobic glycolysis at blood stage but need Krebs cycle, the electron transport chain, and mitochondrial ATP synthase during mosquito stage development. Again, reverse genetic approaches to study the hepatic stage of *Plasmodium* have been thwarted because parasites with defects in energy pathways are unable to complete the mosquito stage. I used the genetic complementation approach established to study heme biosynthesis to bridge parasites lacking the β subunit of mitochondrial ATP synthase through mosquito stage and studied their development in the liver stage. ATPase knockouts were indistinguishable from wildtype in *in-vitro* liver stage assays of size, nuclear content, and merosome production. Robust progression to blood stage confirmed the dispensability of mitochondrial ATP synthesis

in liver stages. I extended this approach to explore the essentiality of upstream mitochondrial electron transport and Krebs cycle during the liver stage. I speculate that energy metabolism in the liver stage resembles that in the blood stage, relying predominantly on glycolysis for ATP production.

There are numerous genetic tools to manipulate the blood stage malaria parasite genome in general, but existing genetic tools to generate viable parasites with defects in blood stage essential genes are limited. To overcome this limitation, I have developed a novel strategy in which I first insert a complementary copy of the essential gene-of-interest, and then delete the endogenous gene, and then take advantage of meiosis and segregation during the mosquito stage to create haploid knockout sporozoites. I genotype the parasites along the way by fluorescence microscopy. As proof of principle, I created complemented knockouts of the blood stage essential 1-deoxy-D-xylulose-5-phosphate reductoisomerase (DXR) gene, crossed these with wildtype parasites, and then tracked the progeny through *in-vitro* and *in-vivo* liver development. Pre-complementation proved difficult, perhaps due to inappropriate expression of important metabolic genes. Additionally, problems with apparent silencing of the fluorophore tags compromised my ability to genotype cross progeny preventing any firm conclusion on the function of isoprenoid precursor pathway of liver stage parasites. Nevertheless, my success in generating a blood stage essential gene knockout via pre-complementation provides encouragement that this novel reverse genetic strategy can be implemented to investigate the role of blood stage-essential genes in sporozoite and liver stages of malaria parasites.

Declaration

This is to certify that:

1. The thesis comprises only my original work towards the PhD except where indicated in the Preface
2. Due acknowledgement has been made in the text to all other material used
3. The thesis is fewer than 100,000 words in length, exclusive of tables, maps, bibliographies and appendices.

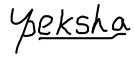

Gallallalage Upeksha Lakmini Rathnapala

Preface

This is a thesis submitted as a requirement for the degree of Doctor of Philosophy, University of Melbourne, resulting from a three and half year period of study funded by Melbourne International Research and Fee Remission Scholarships. The funding enabled Professor Geoff McFadden to fit me in to his Malaria research unit in School of BioSciences.

During these research studies I was able to develop a new technique (chapter 2) that could uncover potential treatment targets for malaria. This study was published in the journal PLOS Pathogens recently. The thesis also includes following other chapters which discuss, chapter 3: Mitochondrial energy metabolism of liver stage malaria parasites, chapter 4: Development of a new genetic technique which enables study of blood stage essential gene deficient parasites in liver stage.

These studies could not have been carried out without the collaboration and support stated below.

Dr Dean Goodman provided initial laboratory training. In addition, all the bacterial vectors used in this project were gifted by him. Vanessa Mollard provided training with mice handling. Anton Cozijnsen bred and maintained the mosquitoes and provided assistance with dissection for infections in salivary glands.

The *Plasmodium berghei* FC knockout vector was designed by Dr Goodman and the experiment included in the figure 2.6.5 (published in PLoS Pathogens) was performed by him. Dr Angelika Sturm generated and cloned the *P. berghei* ATPase knockout strain used in the chapter 3.

The *Pb ANKA* parasite lines expressing GFP and mCherry fluorescence markers were developed by Dr Goodman. The *Pb*nek-4ko strain was provided by Oliver Billker (Wellcome Trust Sanger Institute, Hinxton, Cambridge, UK) and The *Pbs*P48/45^{KO} strain was provided by Andy Waters (University of Glasgow, Glasgow, Scotland). The *Plasmo*GEM team at the Wellcome Trust Sanger Institute, UK provided the three *P. berghei* knockout vectors (SDH A and B, KDH) used in chapter 3 of this thesis.

Acknowledgements

I offer my grateful thanks to my two supervisors for their help and guidance. Professor Geoff McFadden kindly accepted me to work in his internationally famous research unit, introduced me to his field of research and guided me along with much patience. Dr Dean Goodman, observing my lack of experience, took over my initial all round training for the job in hand.

Besides my supervisors, I would like to thank the rest of my thesis committee: Dr Stuart Ralph and Dr Alex Johnson not only for their insightful comments and encouragement but also for their intricate and demanding questions which helped me to widen my research capability from various perspectives. A very special word of gratitude goes out to Vanessa Mollard who not only provided expert technical assistance and advice but also for being a great mentor. I am most grateful to Anton Cozijnsen for supporting me especially with his amazing mosquito dissecting skills. I also thank my fellow laboratory mates for the stimulating discussions and for all the fun we have had in the last three and half years. I also thank Dr Wilfred Samarawickrema, till recently Consultant to our Filariasis Research, Training and Service Unit back in the University of Ruhuna, Sri Lanka, now domiciled in Melbourne, for his constant encouragement and support.

The Melbourne International Research Scholarship and Melbourne International Fee Remission Scholarship funded me throughout my period of study. The University of Melbourne; Faculty of Science provided financial support through the RHD travel grant and Science Abroad Travel Scholarship to present research work at international conferences.

Finally, on a personal note, I am eternally grateful to my parents who brought up their only child in the way they had done and giving me the best education which has now equipped me for an academic career. Unfortunately my father passed away weeks before I arrived in Australia and since then my mother, who has been with me during much of my period of residence in Australia, who has been a tower of strength for me, has provided me with her companionship and guided me through with her moral and emotional support. I would like to dedicate this thesis to my father who, I am sure, would have considered this moment as one of the best in his life and to see that his little girl has now grown up.

Publication

Rathnapala UL, Goodman CD, McFadden GI (2017). A novel genetic technique in *Plasmodium berghei* allows liver stage analysis of genes required for mosquito stage development and demonstrates that *de novo* heme synthesis is essential for liver stage development in the malaria parasite. PLoS Pathog 13(6): e1006396. https://doi.org/10.1371/journal.ppat.1006396

Table of content

Chapter 4: Analysing liver-stage defects in parasites with knockouts in blood stage essential genes

Chapter 1: General introduction

1.1 Malaria mortality and morbidity

Malaria has yet again accounted for 429 000 deaths in 2015 with 212 million new cases worldwide. Among 91 countries reported as malaria endemic, Nigeria and Democratic Republic of the Congo shared more than a third of total deaths recoded worldwide. Similarly, amongst the five species that can infect humans, the majority of the deaths was caused by *Plasmodium falciparum*, with *P. vivax* being responsible for the second highest death rates (1).

Malaria parasites continue to threaten the world regardless of increased health care system, improved prevention measures along with adequate financial resources or even with intense focus on new diagnostic tools. The mortality rate has declined by 29% globally between 2010 and 2015, but the battle remains a large one. The health care systems in many counties with a high malaria burden remain under-resourced. Poor accessibility to hospitals and other health systems in these countries accounts for a larger proportion of reported malaria cases as well. Thus, there is an urgent need to increase in funding from domestic and international sources to take part in the mission against poverty combined with malaria.

Parasite resistance to artemisinin- the main component of the best available antimalarial drug- has been detected in five countries of the Greater Mekong sub region where the resistance first emerged (1). Mosquito resistance to insecticide treated mosquito nets (ITNs) and indoor residual spraying (IRS) has also been reported in 60 out of 73 malaria endemic countries in 2015 (1). On top of that, the continuous effort of scientists to come-up with a 100% effective vaccine or novel antimalarial compounds that work better against the parasite still seem far away. The majority of drugs tested in laboratories target the blood stage of malaria parasites as it is the symptomatic stage of life cycle. Still, there remains an on-going need to focus more on drugs that target different stages such as the liver and the transmission stage through the mosquito.

1.2 Life cycle of malaria parasites

1.2.1 Liver stage

A sporozoite first enters a new vertebrate host through the bite of an infected female *Anopheles* mosquito (2). Only a small proportion of these introduced sporozoites will pass into the blood stream (Fig 1.3.3) where they can gain the entry into hepatocytes to initiate the pre-erythrocytic cycle (2). After passing through several hepatic cells, the sporozoite invades a liver cell and starts multiplying asexually (2). At this stage, within two to three days in the case of *P. berghei*, the parasite forms a schizont containing thousands of daughter parasites called merozoites. Once the merozoites are fully mature, they egress from the hepatocyte and form a merozoite-filled vesicle called a merosome (3). This process of parasites detaching from the host hepatocyte as merosomes is not a synchronised process. The merosome is used by parasites to avoid the host immune system and reach the blood stream where they can continue growth in red blood cells (3).

1.2.2 Blood stage

The liver stage merozoites (Fig 1.3.3) begin a new stage of parasite life cycle by invading red blood cells that ultimately results in the formation of thousands of blood stage merozoites. While multiplying, blood stage parasites form a parasitophorous vacuole (PV), which ensures a complete physical separation from the host (4). Exchange of metabolites between the host and the parasite occurs exclusively through this parasitolphorous vacuole membrane (PVM). There are certain morphological changes that accompany parasite growth inside an erythrocyte. First, the parasite transforms into a ring stage and then a trophozoite stage. Next, schizogony, a process where nuclear division is followed by cellular division takes place to produce daughter merozoites. This stage, called a schizont, contains 16-24 merozoites (5). The time to reach schizogony depends on the species. For *P. berghei* it takes only 22-24 hours (6) whereas it takes 48 hours for *P. falciparum* (7). While the majority of merozoites released from a schizont continue to invade and grow asexually inside red blood cells (8), some develop into gametocytes. The commitment of parasites to become gametocytes occurs at the previous blood stage. (9, 10). Gametocytogenesis is the

process of formation of male and female gametocytes where, when they are taken up by a compatible mosquito species, transform into either male or female gametes.

1.2.3 Mosquito stage

Inside the mosquito midgut, gametocytes experience specific triggers which result in a rapid change of structure from gametocytes to gametes along with rupture of host erythrocyte (11). Typically, a temperature drop (approximately 5 ºC), pH increase (from 7.2 to 8) and exposure to exflagellation factor xanthurenic acid (XA; a metabolic intermediate in tryptophan catabolism) (12-16) are the triggers of gametocyte activation.

Within the mosquito midgut, the haploid male and female gametes fuse (Fig 1.3.4). This fusion is followed by endomitosis, producing a single tetraploid zygote nucleus with four haploid meiotic products (17). The zygote then transforms into a motile ookinete (18). This ookinete can traverse through the mosquito midgut epithelium where a protective cyst like structure develops on the outer surface of gut (18). The cyst, an oocyst, is a polyploid structure that eventually produces thousands of haploid sporozoites by sporogony (19). These sporozoites are next released into the mosquito hemocoel where they migrate into the salivary glands (Figs 1.3.3, 1.3.4). Upon the next blood feeding, salivary gland resident sporozoites are deposited into the skin of the new host as the feeding mosquito regurgitates saliva (20).

My entire thesis is centre on the sexual reproduction of *P. berghei*, which occurs inside the mosquito. As stated above, a malaria parasite undergoes drastic morphological changes and various chromosomal arrangements during this stage of the life cycle (Fig 1.3.4). Similarly, a large number of genes are specific for each of these stages as depicted in Table 1.3.3. The formation of gametes from gametocytes marks the beginning of this unique process.

1.2.4 Mosquito stage in depth

1.2.4. I Gametocyte to gamete development

Haploid male and female malaria gametocytes develop key differences in their molecular and cellular development. Female gametocytes represent a typical eukaryotic egg, which is ready for a speedy development into a zygote. Hence, it is equipped with well-developed organelles such as mitochondrion, apicoplast, and endoplasmic reticulum (ER). Conversely, mature male gametocytes contribute only their nucleus,

cytoplasm and an axoneme as cellular counterparts to zygote formation. Therefore male gametocytes carry a reduced amount of ribosome and ER (21).

1.2.4. II Activation and fertilization

Activation of gametocytes to form either male or female gametes commences when the gametocytes egress from their red blood cells. Within two minutes of the parasites being taken up into the mosquito, the parasitophorous vacuole membrane (PVM) ruptures so that erythrocyte membrane can be opened up for activated and rounded-up gametocytes to egress [(16), reviewed by (22)]. This egress from the host red blood cell is further facilitated by secretion of the osmophilic bodies [reviewed by (23)], and the overall increase in parasite cell volume (24). The releasing of extremely motile male gametes further make the cell weakens, enhancing discharge of the male gametocytes (16, 25, 26).

Once egressed from red blood cells, the female gametocytes produce a single extracellular and non-motile spherical female gamete while male gametes undergo the exflagellation to release eight male gametes. At this stage, three rapid rounds of mitotic replication of male gametocyte nucleus produce the eight haploid daughter nuclei. The resulting haploid male gametes are (27) extremely motile but tend to adhere to uninfected red blood cells probably for easy movement through the blood meal (28). Soon the male gametes detach from their exflagellation centre, their search for a female partner initiates (22).

Fertilisation:

Male and female gametes make contact with their plasma membranes and fuse with the help of specific parasite surface receptors (22). Fusion of these two plasma membranes, allow the male nucleus to enter the female cytoplasm. Nuclear fusion follows, taking place over the next three hours (29).

1.2.4. III Zygote

Fusion of gametes within the mosquito gut forms a diploid zygote (2n) which promptly undergoes meiosis to yield four haploid nuclei- no cytokinesis occurs yet (32). This newly formed zygote has a spherical shape at first but starts to polarize with time. Micro tubular structures extend from the diploid nucleus and give the zygote a new slender

shape (30). This follows a specific transcript regulation event where the parental alleles are differently regulated (22).

At this stage, parasites start genetic recombination. During meiosis, it has been found that each member of a particular pair of chromosomes segregates randomly. These genetic recombination events generate novel phenotypes of *Plasmodium sp* which sustains their genetic diversity. Consequently, it is not surprising we see mixtures of parasites with more than one genotype in natural conditions [reviewed by (31)].

1.2.4. IV Ookinetes

The zygote becomes tetraploid within 3 hours post fusion by meiosis and keeps this tetraploidy nature throughout the ookinete stage (22). It takes 19-36 hours post blood meal for parasites to completely mature into an ookinete (32-34). The ookinete has a characteristic banana shape and is motile so that they can escape the harsh mosquito gut lumen, which is rich in digestive proteases (35). The peritrophic membrane of the midgut is a protective cover of chitin, and it protects the midgut from food microbial infections [reviewed in (36)]. Breaching this membrane is one of the major tasks ookinetes face in their short life span, and it uses chitinase to hydrolyse the membrane polysaccharide, chitin (37-39). The apical and pellicular complexes of the ookinete facilitate the gliding motility allowing it to actively traverse multiple epithelial cells to reach the basal side of the haemocoel and settle down (17).

1.2.4. V Oocysts to sporozoites

The transition from ookinete to oocyst stage represents one of the major bottlenecks of malaria parasite development. The midgut stage of the parasite is exposed to components of the human immune system as well as midgut microbial flora and this cause a large reduction in parasite abundance. It has also been reported that the innate immune system of mosquito has a major impact on the later part of this transition (40).

Initiation of the oocyst stage commences when the motile ookinetes halt their movement upon reaching underneath the basal lamina and then round up and form a thick extracellular capsule. This capsule surrounds the oocyst while the apical complex and associated microtubules (which are no longer needed) are reabsorbed into the oocyst cytoplasm (41, 42).

Oocysts maturation

When the oocyst is formed, the developing sporoblast mother cell has a single nucleus containing four haploid products, placed centrally, which produces thousands of genomic centres by endomitosis. The endomitosis forms the characteristic polyploid cell where 10-11 rounds of DNA synthesis follows (41, 43). Due to this formation of thousands of genomes, the nucleus becomes extremely convoluted (17). Next, an apical complex is formed and the newly formed nucleus along with the necessary organelles which replicate simultaneously with DNA replication (41), are pulled into a protruberence. Eventually, the surface of the sporoblast mother cell elongates and detaches to form sporozoites (44). Meanwhile, the oocysts capsule prepares to release the forming sporozoites out into the surrounding haemolymph by becoming thinner and developing holes through which the sporozoites emerge (45). This sporozoite budding from the oocysts is believed to be an asynchronous process. Through accumulation of these small punctures however, a larger wound appears in the oocysts capsule leaving behind an empty, collapsed oocysts on the midgut surface (17).

Oocyst sporozoites release

Sporozoites budding off from the sporoblast is an active, protease dependent process (46). Motility of the sporozoites has been recognized as not directly responsible for the egress, rather protease activity (either intracellular or extracellular) triggers the sporozoites motility and the oocyst wall ruptures to release sporozoites (47). By using a series of time-lapse microscopy images, Klug and colleagues have put forward a model to show how the sporozoites egress from the oocyst. According to them, the release can occur in different ways (i) single sporozoite migrate through the holes of oocyst envelop (ii) formation of a structure called the sporosome; a sporozoite filled vesicle that buds off from the oocyst (iii) rapid rupture of the oocysts wall releasing emerging sporozoites suddenly (47).

Salivary gland sporozoites

The sporozoites emerging from their early space are now fully mature contain one haploid genome. They glide along with the haemolymph towards their next destination; the salivary glands (48). These invasive sporozoites use their characteristic gliding motility to invade and lodge in the lumen of salivary glands (17). When this mosquito

bites a new vertebrate host, sporozoites are released with saliva into the skin (49). Thus, a new journey into a new host begins.

1.2.4. VI Oocyst sporozoites and salivary gland sporozoites- A comparison

Sporozoites that reside in oocysts of midguts are morphologically similar to the sporozoites residing in salivary glands (20). While forming, midgut sporozoites are tight and rigid (50) but transform into a more flexible and motile structure once released (50, 51). In regards to the movement however, the sporozoites emerging from midguts show discontinuous gliding motility which is seen as a mere stretching and back-forth gliding. This is one of the major differences of oocyst sporozoites compared to the salivary gland sporozoites, which show characteristic circular gliding motility (20).

These two sporozoites have two different functions as well; the former is adapted to invade a vertebrate tissue while latter must leave the mosquito midgut (20, 52). Hence, the midgut sporozoites are non-infective and do not induce a protective immunity response in mammals (20). In addition to these differences between midgut and salivary gland sporozoites, there is a clear difference between their gene expression and protein expression profiles (20). Hence, sporozoites residing in midguts or salivary glands are recognized as two distinct invasive stages of malaria parasites.

Upon formation of numerous nuclei prior to cytokinesis, oocysts facilitate an excellent platform for experimental genetics. Fusion of two genetically different gametes at the beginning leads to heterokaryotic oocysts, consisting of genetically distinguishable nuclei within a shared cytoplasm. At this stage, lack of a gene product can be complemented by sharing a cytoplasm having a wildtype genome; therefore knockout parasites easily bypass the oocysts barrier due to being heterokaryons. Subsequently, sporozoites regain the haploid conditions once they bud off from the heterokaryotic oocyst and, are able to complete their transmission stage (53, 54). Taking advantage of this heterokaryotic nature of a multinucleate cell, several gene knockout cross experiments have been performed (Table 1.3.2).

1.2.5. Sexual reproduction and genetic recombination

Sexual reproduction arose just once, likely in the common ancestor of all eukaryotes; a single celled eukaryote. There are numerous theories as to how and why sex appeared in general, but for malaria parasites, sexual reproduction has served well. They can either self-fertilise or cross-fertilise in the presence of a second parasite strain at mosquito stage (55). To be more specific, genetically identical malaria parasites form male and female gametes, fuse the two genomes and recombine. Genetic recombination is "the occurrence of progeny with combinations of genes other than those that occurred in the parents, due to independent assortment or crossing over" (56). Within the definitive host, the mosquito, due to the cross-fertilization of the two gametes, a hybrid zygote forms and meiotic recombination follows (57). In addition to upholding genetic variation, sexual recombination make parasites to clear unwanted/ deleterious mutations from genome thus avoid accumulation of damaging mutations.

1.2.5. I History of experimental crosses

The very first experimental genetic cross in malaria history took place in 1954 with two strains of bird malaria parasites, *P. gallinaceum*: a non-lethal pyrimethamine sensitive strain, and a lethal pyrimethamine resistant strain. Greenberg and Trembley (58) used *Aedes aegypti* mosquitoes in this experiment as the definitive host, and they retrieved the crossed parasite progeny in chicks. Recombination had clearly taken place because pyrimethamine resistance was now present in the non-lethal strain.

The 1970's marks a significant era for the field of experimental malaria with the discovery of four rodent malaria parasite strains, establishment of a *P. falciparum in-vitro* culture system and the ability to feed culture grown gametocytes to mosquitoes. Thus, the possibility to study the complete *P. falciparum* life cycle within laboratory was established. Following the use of splenectomised chimpanzees to study liver stage of human malaria parasites, Walliker et al., 1987 (59) attempted the first experimental cross of *P. falciparum*. Gametocyte producing laboratory based human malaria strains, 3D7 and HB3 clonal lines were used to initiate this experiment where they witnessed recombination among P0 stage parasites.

The second experimental cross of *P. falciparum* was performed by Wellems and colleagues in 1990 (60) to investigate the gene/s responsible for chloroquine resistance in human malaria parasite. The parental strains: chloroquine sensitive HB3 (Honduras isolate Hondo-1) and chloroquine resistant Dd2 (W2-MEF line of the Indochina III isolate) strains were used for the cross, where 16 out of 76 of progeny clones were independent recombinants with even distribution of chloroquine sensitive and resistant forms. By the use of the cross experiment, it was revealed that the chloroquine resistance is not linked to the initially suspected *mdr*-like genes in *P. falciparum*. The third human malaria genetic cross using 7G8 (a clone of Brazilian isolate IMTM22-(61) and GB4 [a clone of isolate Ghana III/ CDC (62)] clones revealed the unique independent recombinants in the resultant population (63).

As with the genetic crossing of rodent and other malaria parasites, Yoeli and colleagues (64) performed an experiment with two *Plasmodium* strains, a pyrimethamine resistant *P. vinckei* and pyrimethamine sensitive *P. berghei*. They observed the drug resistance trait has been transferred from one strain to the other, but the reason behind the observation was not properly explained. Again in 1971 and 1973, Walliker and colleagues (65, 66) used two *P. berghei* strains which differed in isoenzyme type and drug sensitivity, to show recombination among the resultant progeny. In parallel to that in 1975, two *P. chabaudi* strains with three different characters (enzyme and drug selectable markers) were also crossed inside mosquitoes to observe recombination. Recombinant traits were observed among the three markers in the rodents infected with resulting sporozoites (67).

Even though mouse malaria models such as *P. berghei* provide ample opportunities to manipulate parasite genome in all stages, studies on *P. falciparum* has been limited mostly to blood and mosquito stages due to the restrictions of pre-erythrocytic stage development in human hepatocytes and chimpanzees (68). Thus, *P. falciparum* genetic crosses have become extremely technically difficult. With the recent discovery of human liver chimeric mice that support recovery of recombinant progeny to identify parasite traits and adaptations particularly linked to the emerging drug resistance (68), a powerful framework on human malaria studies have been initiated.

1.2.5. II Biased inheritance of the progeny of genetic crosses

One interesting observation to emerge from these earlier crosses was that there were more recombinants in resulting blood forms compared to either of the parental strains. It was assumed that if equal number of parasites/gametocytes from the two parents were mixed and fed to mosquitoes, half of the progeny should be identical to either of the parents while the other half must be recombinants which are the result of a cross-fertilisation. Hence, this finding inferred that cross fertilisation occurs randomly but frequently (69) in malaria parasites. The observed bias is probably due to the favoured growth of parasites with certain allelic combinations, ability of the male and female gametes to recognize self from non-self and favor cross-fertilization (70) or the variations in number of male and female gametocytes produced by the two parents (57).

1.2.5. III Genetic crosses today

In each step of parasite growth, specific gene/s are up or down regulated to fulfil a specific function. While there are likely to be hundreds even thousands of essential genes for such functions to be accomplished particularly at mosquito stage, only a handful has been characterised. In particular, the number of mosquito stage essential genes (~100 genes published so far) listed in Table 1.3.1 will provide only a glimpse of the actual numbers, which are yet to be discovered.

There is an ever growing list of mosquito stage essential genes (Table 1.3.1). When any of such genes is knocked-out in a parasite, the parasite cannot invade liver. Thus, there are large gaps of our understanding of the malaria parasites liver stage biology. However, this main obstacle has been overcome by crossing parasites with defects in mosquito stage essential genes to wildtype parasites. With the increasing success rate of cross-experiments, crossing of two strains (one with a gene deletion and the other one with a wildtype copy of that particular gene, coupled with easily distinguishable features inserted) in the lab and their follow up has been now a common procedure particularly with commonly used rodent malaria models. This method termed “genetic complementation” takes advantage of parasites’ sexual recombination and production of heterokaryotic, polyploid oocysts. A parasite with a deletion in a mosquito stage essential gene does not survive to complete the transmission stage. The effect of that

particular gene for liver stage development thus cannot be investigated. When we allow this knockout strain to cross fertilise with a wild-type strain for that particular gene, the parasites will recombine to produce novel genotypes. Due to the hetrokaryotic nature at the oocyst stage however, wild-type parasites and knockout parasite genes share a common cytoplasm. These knockouts even carryover the mRNA/transcript or protein they shared on to the sporozoite stage where that shared product may be sufficient enough for them to complete the mosquito stage of life cycle. So far, there are ~15 mosquito stage essential gene knockouts recovered by such genetic crossing experiments (Table 1.3.2).

We have further developed this commonly used method which complements the missing products of a knockout by crossing to a wildtype. By tagging the two strains with two fluorescent markers (Fig 1.3.5), their genetic content becomes readily detectable by live-imaging. PCR and immunofluorescence assays can be used as additional techniques to validate the fluorescent phenotyping strategy.

In addition, it is easy to extend this study to liver stage parasites, and even to P0 blood stage. Since parasites have their unique colours to assist with phenotyping, sporozoites from the cross can be used to infect liver cells as well as the following blood stage. Thus, the effect of this mosquito stage essential gene knockout on liver stage (if any) becomes a possibility. Earlier studies which used this crossing technique (Table 1.3.2) could never be expanded to liver stage with the complexity of genotypes of parasites post recombination. Due to this new colouring of parasites however, a novel technique which is simple and relatively easy could be introduced to study the liver stage of malaria parasites.

1.2.5. IV The genetic complementation approach

There are advantages of genetic crosses regardless of its occurrence in natural environment or under experimental conditions. It is beneficial for both sides, for parasites to maintain their genetic diversity through generating novel genotypes and for malariologists to better understand their main rival.

For scientists, performing a genetic cross experiment in a laboratory gives a good opportunity to link phenotype and genotype of the strains involved. This is particularly important for understanding a phonotype for which there’s no apparent responsible gene

in action. Geneticists can extract more data from linkage analysis of such an experimental cross as to what types of recombination occurs, in what frequency, how each loci contributes. This is particularly important in cases of finding the responsible gene loci for drug resistance. By comparing the genomes of the parent and progeny, and carefully cross-examining the loci, it is possible to identify which locus is responsible for a particular genetic variation post drug treatment. With the rapid spread of drug resistant parasites around the world, better understanding of population genetic of parasites with the combination of sexual reproduction has become crucial (71).

Apart from above, this genetic manipulation methodology performed in a laboratory has several advantages over any other conditional gene knockout system applicable in mosquito stage (1.2.6). There's no need of designing special gene constructs which require technical expertise and money. A conventional gene knockout structure for double cross-over recombination is the only requirement for this system. No special chemicals are needed for this process as this is entirely based on a natural system. This strategy can also be modified by adding florescent markers. If the knockout and wild-type carries two different fluorescent colours, the progeny is readily distinguishable therefore their phenotyping in next stages becomes remarkably easy. In addition, the sporozoites produced by this genetic complementation can be used to study liver stage in detail which is otherwise impossible with a mosquito stage essential gene. Particularly for genes that are assumed to be indispensable for liver stage but no clear phenotypic details available, this strategy can be easily expandable.

Thus, I used this technique to study malaria parasite heme biosynthesis pathway in liver stage (chapter 2) and is published in PLoS Pathogens (54). Since the essentiality of heme pathway genes during mosquito stage makes it hardly possible for heme deficient parasites to complete liver growth, there were no quantitative data as to when and how the heme is needed in liver. Through the genetic complementation of heme deficient parasites with a wildtype, we have demonstrated the indispensable nature of heme pathway in liver stage.

1.2.6 Other common methods of genetic manipulation at mosquito stage

As stated earlier, crossing of two strains (one with a gene deletion and the other strain containing a wildtype copy of that particular gene) to recover mosquito stage indispensable genes has long been a relatively popular strategy as a way of genetically manipulating malaria parasites. Among such methods which are very few in numbers compared to the number of techniques available to manipulate blood stage parasites, only few has been well established. One such method is FLP/ *frt* system.

FLP/*frt* system is used against *P. berghei* parasites to conditionally delete a gene of interest. The recombinase enzyme FLP activates and removes a gene of interest through recombination of two short *frt* sequences. And the gene deletion is non-reversible [reviewed by (72)]. One condition in this system is that the genetically modified parasites must transmit through mosquitoes so that the gene deletion occurs. Because the promoters developed to drive the FLP recombinase so far are specifically expressed in mosquito stage. For example, one promoter commonly used in this system is thrombospondin- related adhesive protein (TRAP) which is expressed in the mosquito midgut (72). UIS4 is expressed at salivary gland sporozoites hence the gene of interest must definitely pass through the sporozoite stage to FLP recombinase to express (73, 74). The system is rapid if the targeting construct is available. But generating it might be technically challenging and costly. Another major drawback of this system is being unable to excise the targeted gene 100% efficiently and difficulty in distinguishing parasites with and without the gene deletion [reviewed by (72)].

In addition to the above, tetracycline controlled transcription activation known as Tet system is a widely used method to control gene transcription. This system relies on a trans-activator which has a tetracycline repressor (TetRep) fused to an activating domain. This trans-activator binds with tet operator sequence (*TetO*) through the TetRep. A promoter is placed in front of this *TetO*. Binding of TetRep with *TetO* activates transcription of the gene of interest. Upon addition of either tetracycline or its analogue anhydro-tetracycline (ATc) however, transcription is turned off due to the reduced affinity of TetRep to *TetO* (75). Recently, this system has been improved with the establishment of additional trans-activating domains (TRAD) derived from transcription factor ApiAP2. This system has been well suited for blood stage *P. berghei* but has the potential to apply for both mosquito and liver stages. However, one

of the major downside of this system is limited accessibility of ATc to mosquito stage parasites (76).

In summary, blood stage malaria gametocytes undergo drastic morphological and metabolic changes once in the invertebrate host. Given the essentiality of majority of parasite genes/ metabolic pathways studied so far in the mosquito stage, genetic manipulation of such genes to study parasite liver stage becomes problematic. Among the available techniques which could be used to bypass the defects in mosquito stage essential genes, crossing of two strains to complement each other has become relatively common. The sexual recombination of parasites and the polyploid and heterokaryotic oocyst formation gives a good basis for this complementation strategy. When the two strains are equipped with two fluorescent markers, not only their genotyping becomes easy but also the study can be extended to the liver stage and further. Thus, this strategy can open up a new array of genetic manipulations of mosquito stage essential genes with the aim of in depth analysis of liver stage of malaria parasites.

1.3 Tables and figures

Table 1.3.1: A partial list of mosquito stage essential genes categorised according to the specific stage of parasites growth

Stage	Description of gene	Cellular function	Reference
Gametocyte to gamete and zygote	Calcineurin	Fertilization	(77)
	CDPK4	Cell cycle progression in male gametocytes	(78)
	DHHC2	Lipidation modification during zygote to ookinete conversion	(79)
	DOZI	Formation of the ribonucleoprotein complex	(80)
	GCS1	Gamete fusion	(81, 82)
	GEST	Gamete egress and sporozoite traversal	(83)
	HAP2	Gamete fusion	(82)
	MAPK-2	Male gamete formation	(84)
	PAT	A membrane component of osmiophilic bodies in gametocytes	(85)
	PPM1	Exflagellation	(86)
	Ps47	Microgamete-macrogamete attachment	(87, 88)
	Ps230	Microgamete-macrogamete attachment	(89)
	Ps48/45	Microgamete-macrogamete attachment	(90)
	ACO	Ookinete conversion	(91)
	Actin 2	Ookinete to oocyst formation	(92)
	Actin capping protein β subunit	Oocyst formation	(93)
	CDPK3	Ookinete motility, mosquito midgut invasion	(94, 95)
	CelTOS	Ookinete midgut traversal	(96)
	Chitinase/ CHT1	Hydrolysis of peritrophic memebrane during ookinete midgut traversal	(97, 98); *P. falciparum*
	enolase	Interaction with midgut epithelium	(99)
	Guanylate cyclase-β	Ookinete motility	(100, 101)
	M1 aminopeptidase	protein breakdown in ookinete	(27, 102-105)

		stages	
Ookinete	MAOP	Midgut invasion	(106)
	MDV-1/ PEG3	Egress of gametes from host cell and reduced ookinete transformation	(27, 107)
	Nek-2,4	Ookinete genome replication	(108)
	P25	Ookinete surface protein; ookinete survival in the mosquito midgut, traversal of the epithelium; ookinete-oocyst transformation	(109)
	P28	Ookinete surface protein; ookinete survival in the mosquito midgut, traversal of the epithelium; ookinete-oocyst transformation	(109)
	Palmityol transferase DHHC3	Gliding motility of ookinetes and sporozoites	(110)
	PANK1,2	Optimal ookinete formation and oocyst development	(111, 112)
	Phosphodiesterase δ	Gametogenesis and ookinete morphology	(101, 113)
	POS1-10	Ookinete surface protein	(114)
	PPLP3-5	Ookinete midgut traversal	(114, 115)
	Protein disulfide isomerase	Catalyses the oxidation, reduction and isomerisation of disulfide bonds	(27, 116, 117)
	Protein kinase G	Ookinete motility	(101) (118)
	PSOP 1,2,6,7,12	Ookinete-secreted proteins	(114)
	PSOP25	Ookinete maturation and formation of oocyst	(119)
	SHLP1	Ookinete formation	(120)
	SOAP	Ookinete midgut traversal	(121)
	SUB2	Possibly disrupting the actin cytoskeleton on midgut epithelium	(122)
	WARP	Ookinete midgut traversal	(123) (124)
	ALAS	Oocyst maturation	(125-127)
	ATP synthase β subunit	Oocyst formation	(128)

Oocysts	BCKDH	Oocyst maturation	(129)
	Cap380	Oocyst maturation	(130)
	CDPK3	Ookinete motility, mosquito midgut invasion	(94, 95)
	CPO	Oocyst maturation	(92); *P. falciparum*)
	CTRP	Oocyst formation	(131)
	CYC3	Oocyst development, maturation and sporozoite formation	(132)
	ECP1	Egress from midgut oocyst	(133)
	FabB/F	Oocyst to sporozoite development	(134); *P. falciparum*)
	FabI	Oocyst to sporozoite development	(134); *P. falciparum*)
	GGCS	Oocyst maturation	(135)
	GluS	Oocyst development	(111)
	GR	Oocyst maturation	(136, 137)
	HMGB2	Oocyst formation	(138); *P. yoelii*
	KGDH	Oocyst formation	(139); *P. falciparum*)
	LAP1/CCp3/SR	Oocyst maturation and sporozoite formation	(53, 140)
	LAP2/CCp1	Oocyst maturation and sporozoite formation	(53, 140)
	LAP3/CCp5	Oocyst maturation and sporozoite formation	(53, 140)
	LAP4/CCp2	Oocyst maturation and sporozoite formation	(53, 140)
	LAP5	Oocyst maturation and sporozoite formation	(53, 140)
	LAP6	Oocyst maturation and sporozoite formation	(53)
	MDH	Oocyst formation	(91)
	MISFIT (formin-like protein)	Oocyst development	(141)
	PBGD	Oocyst maturation	(127, 142, 143); *P. falciparum*
	PEPC	Oocyst formation	(91)
	PEPCK	Oocyst development	(111)
	PK7	Oocyst development and sporogony	(144)

	PPM5	Oocyst development	(86)
	SDH	Oocyst formation	(145)
	TRP1	Oocyst egress and salivary gland invasion	(146)
	Type II NADH: Ubiquinone dehydrogenase	Oocyst maturation	(147)
	UOS3	Oocysts sporozoites to infect salivary glands	(148)
	UROD	Oocyst maturation	(127, 143); *P. falciparum*
Sporozoites	Api ap2-sp	Sporogony	(149)
	Api ap2-sp2	Sporoblast formation	(149)
	Api ap2-sp3	Salivary gland invasion	(149)
	c-CAP	Sporozoite production	(150)
	CDLK	Sporozoite maturation	(144)
	CRMP1,2	Salivary gland invasion	(151)
	CSP	Sporozoite development within oocyst and sporozoite attachment to hepatocytes	(152)
	CYC3	Oocyst development, maturation and sporozoite formation	(132)
	FabB/F	Oocyst to sporozoite development	(134) *P. falciparum*
	FabI	Oocyst to sporozoite development	(134); *P. falciparum*
	GAK	Sporozoite development	(144)
	GEST	Gamete egress and sporozoite traversal	(83)
	Ik2	Latency of sporozoites in salivary glands	(153)
	IMC1a	Sporogony	(154)
	LIMP	Sporozoite gliding motility	(155)
	MAEBL	Salivary gland invasion	(156)
	PAT	A membrane component of osmiophilic bodies in micronemes of sporozoites	(85)
	PL/ UIS10	Sporozoite migration through cells	(157)
	PSOP13	Sporozoite development	(158)
	RON4	Sporozoite invasion of	(159)

		hepatocytes	
	S-acyl-transferase DHHC10	Sporozoite formation	(160)
	SPECT1/2	Sporozoite cell traversal	(161, 162)
	TLP	Sporozoites tissue traversal	(163)
	TRAP	Salivary gland invasion and infection of hepatocytes	(164)
	TRSP	Sporozoite host cell entry	(165)

ACO; Acotinase, ALAS; Aminolevulinic acid synthase, ApiAP2; AP2 DNA-binding domain, BCKDH; Branched-chain amino acid dehydrogenase, Cap380; Capsule protein 380, c-CAP; Cyclase-associated protein, CDLK; CDPK-like kinase, CDPK; Calcium-dependent protein kinase, CelTOS; Cell-traversal protein for ookinete and sporozoites, CPO; Coproporphyrinogen oxidase, CRMP; Cysteine repeat modular protein, CSP; Circumsporozoite protein, CTRP; Circumsporozoite protein and thrombospondin-related adhesive protein [TRAP]-related protein, CYC3; P-type cyclin 3, DHHC2; palmitoyl-S-acyl-transferase, DOZI; Development of zygote inhibited, ECP1; Egress cysteine protease I, FabB/F; β-ketoacyl-ACP synthase II, FabI; Enoyl-ACP reductase, GAK; Cyclin G-associated kinase, GCS1; generative cell specific 1, GEST; Gamete egress and sporozoite traversal, GGCS; Gamma-glutamylcystein synthetase, GluS; Glutamate synthase, GR; Glutathione reductase, HMGB; High mobility group protein, IK2; Initiation factor-2α kinase, IMC1a; Inner membrane complex protein, KGDH; α-keto-glutarate dehydrogenase, LAP; LCCL/ lectin adhesive-like protein 1, MAEBL; Apical membrane antigen/erythrocyte binding like protein, MAOP; Membrane-attack ookinete protein, MAPK; Mitogen-activated protein kinase, MDH; Malate dehydrogenase, Nek; NIMA-related kinase, PANK; Putative pantothenase Kinase, PBGD; Porphobilinogen deaminase, PEPC; Phosphoenolpyruvate carboxylase, PEPCK; Phosphoenolpyruvate carboxykinase, PK7; Protein kinase 7, PL; Phospholipase, POS; Putative ookinete surface-associated protein, PPLP; Plasmodial perforin-like protein, PPM1; metallo-dependent protein phosphatase 1, PSOP; Putative secreted ookinete proteins, RON; Rhoptry neck protein, SDH; Succinate dehydrogenase, SHLP; *Shewanellla*-like protein phosphatase, SOAP; Secreted ookinete adhesive protein, SPECT; Sporozoite microneme protein essential for cell traversal, TRAP; Thrombosponin-related adhesive proteinTRP1; Thrombosponidin-related protein, TRSP; Thrombospondin-related sporozoite protein, UOS; Upregulated in oocysts

sporozoites, UROD; Uroporphyrinogen decarboxylaseWARP; Von Willebrand factor A domain-related protein

Table 1.3.2: A partial list of mosquito stage essential genes genetically complemented/ cross-fertilised with either a wildtype or male/female sterile parasite strains

Description	Cellular function	Reference
ACO	Ookinete conversion	(111)
Actin 2	Ookinete to oocyst formation	(166)
Actin capping protein β subunit	Oocyst formation	(93)
ATP synthase β subunit	Oocyst formation	(128)
CTRP	Oocyst formation	(131)
CYC3	Oocyst development, maturation and sporozoite formation	(132)
FC	Oocyst formation and maturation	(54)
LAP1/CCp3/SR	Oocyst maturation and sporozoite formation	(53, 140)
LAP2/CCp1	Oocyst maturation and sporozoite formation	(53, 140)
LAP4/CCp2	Oocyst maturation and sporozoite formation	(53, 140)
LAP5	Oocyst maturation and sporozoite formation	(53, 140, 158)
LAP6	Oocyst maturation and sporozoite formation	(53)
MDH	Oocyst formation	(91)
MISFIT (formin-like protein)	Oocyst development	(141)
Palmityol transferase DHHC3	Gliding motility in ookinetes and sporozoites	(110)
PEPC	Oocyst formation	(91)
PPM5	Oocyst development	(86)
PSOP13	Sporozoite development	(158)
S-acyl-transferase DHHC10	Sporozoite formation	(160)
Type II NADH: Ubiquinone dehydrogenase	Oocyst maturation	(147)

All the crosses listed were performed with *P. berghei* unless indicated otherwise. ACO; Acotinase, CTRP; Circumsporozoite protein and thrombospondin-related adhesive protein [TRAP]-related protein, CYC3; P-type cyclin 3, LAP; LCCL/ lectin adhesive-

like protein 1, MDH; Malate dehydrogenase, PEPC; Phosphoenolpyruvate carboxylase, PPM; Metallo-dependent protein phosphatase, PSOP; Putative secreted ookinete proteins.

Figures

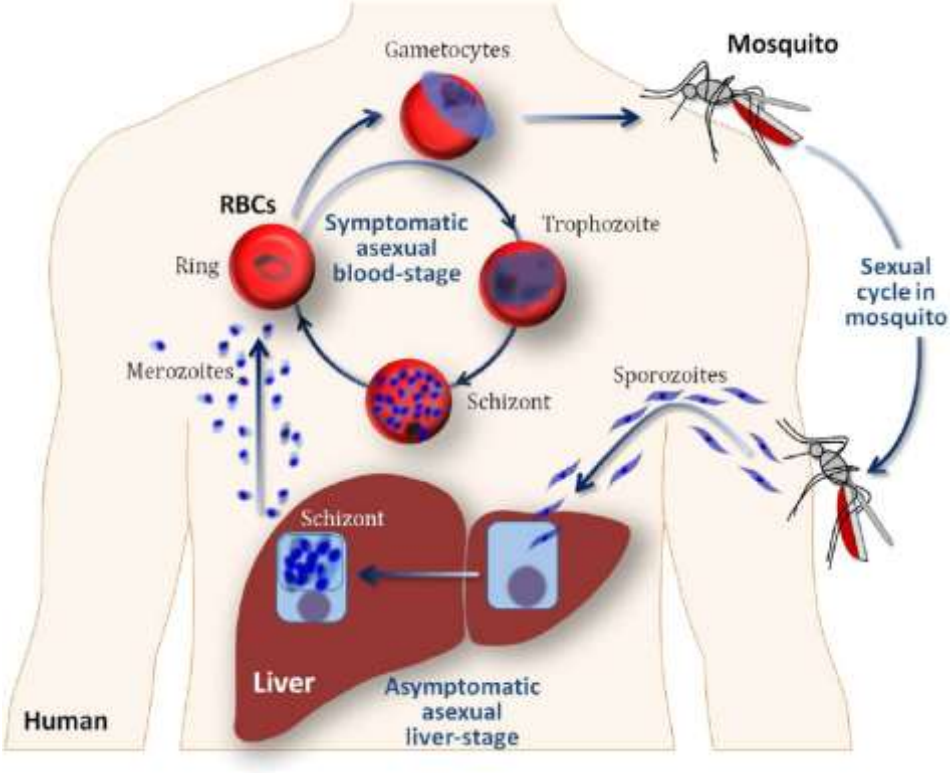

Figure 1.3.3 [adapted from (167)]: A simple illustration of life cycle of malaria parasites/ *Plasmodium falciparum*

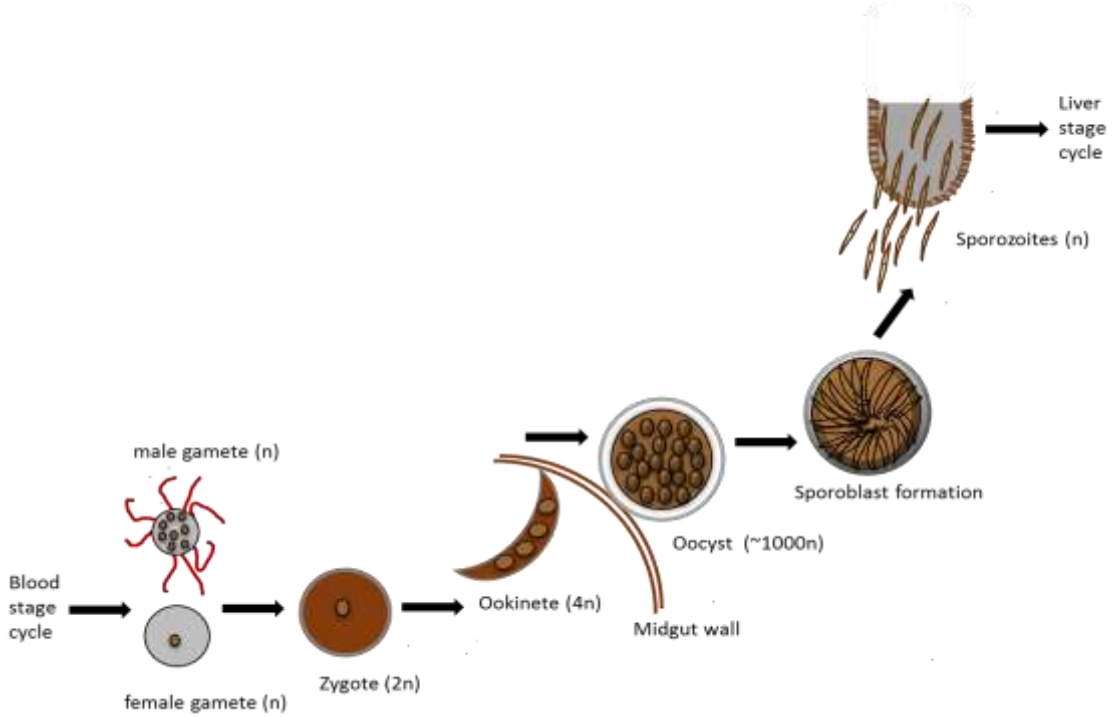

Figure 1.3.4: Different stages of the malaria parasite inside the mosquito

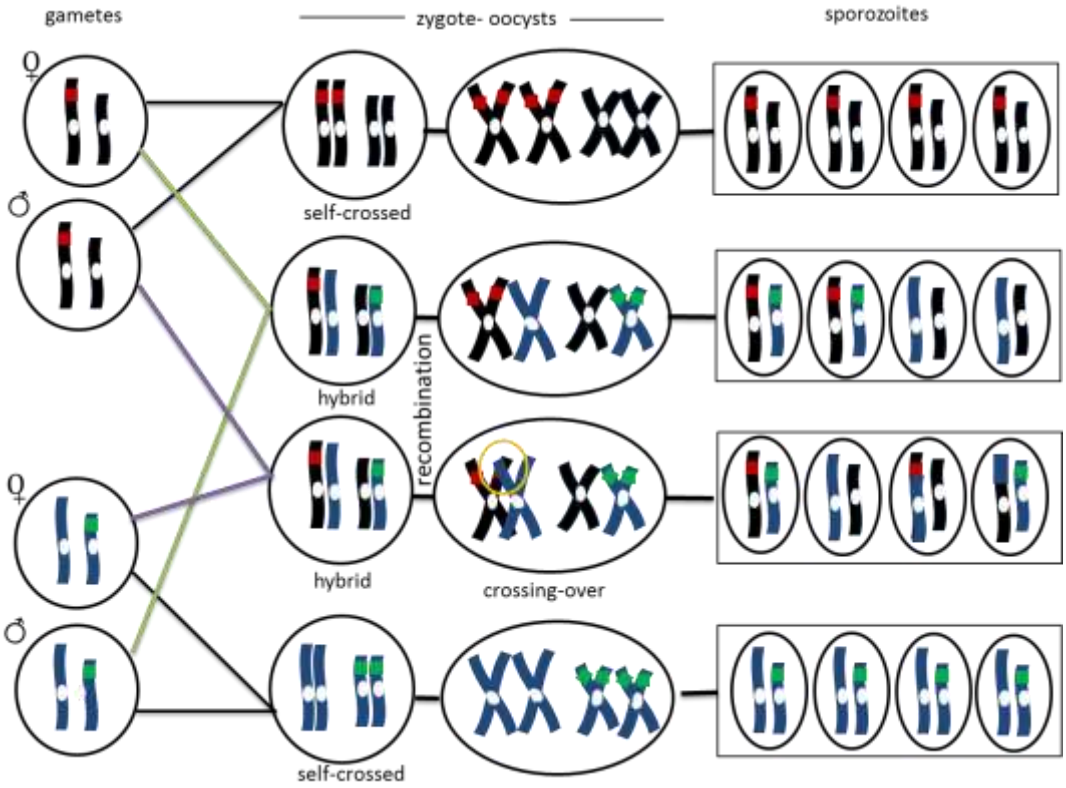

Figure 1.3.5 [adapted and modified from (168)]: Malaria parasite gene flow within the mosquito stage. In the first parasitic strain, which express red colour (denoted with

a red colour square), agene has been replaced with a red fluorescent protein (RFP). The other strain has a green fluorescent protein (GFP) inserted into a null locus of another chromosome (denoted as a green colour square). Upon mixing and introducing these two strains in the mosquito, both transform themselves into red or green gametes. These gametes can either self- fertilises or cross-fertilise which results in a diploid zygote. The zygote consists of chromosomes contributed from each parent arranged in pairs. Sexual reproduction and recombination between the parental chromosomes then follows while crossing-over of loci of homologous chromosomes can also take place. Finally, the arranged chromosomes segregate and assemble back into the haploid stage, which also contains recombinant chromosomes. As illustrated, by inserting the two fluorescent tags the gene flow can easily be followed. When a red colour parasite is seen, it shows the parasite has a knockout in the selected gene and survives. However, if the gene marked with RFP is essential for the completion of mosquito stage, no sporozoites should be produced by self-fertilization of two RFP expressing parasites. Green parasites means they are mainly coming from the self-fertilisation of green parent. A parasite having both red and green or no colour indicates recombination has taken place. Occasionally, due to the recombination with crossing over, either only red or only green colour parasites as well as red plus green or colourless parasites can be formed.

1.4 References

1. WHO. World malaria report 2016. Geneva: WHO. 2016;13.

2. Prudêncio M, Rodriguez A, Mota MM. The silent path to thousands of merozoites: The *Plasmodium* liver stage. Nature Reviews Microbiology. 2006;4:849-56.

3. Sturm A, Amino R, van de Sand C, Regen T, Retzlaff S, Rennenberg A, et al. Manipulation of host hepatocytes by the malaria parasite for delivery into liver sinusoids. Science. 2006;313:1287-90.

4. Bannister L, Mitchell G. The ins, outs and roundabouts of malaria. Trends in Parasitology. 2003;19:209-13.

5. Waters AP. Malaria parasites: Genomes and molecular biology: Horizon Scientific Press; 2004.

6. Janse CJ, Ramesar J, Waters AP. High-efficiency transfection and drug selection of genetically transformed blood stages of the rodent malaria parasite *Plasmodium berghei*. Nature Protocols. 2006;1:346-56.

7. Trager W, Jensen JB. Human malaria parasites in continuous culture. Science. 1976;193:673-75.

8. Salmon BL, Oksman A, Goldberg DE. Malaria parasite exit from the host erythrocyte: A two-step process requiring extraerythrocytic proteolysis. Proceedings of the National Academy of Sciences of the United States of America. 2001;98:271-76.

9. Baker DA. Malaria gametocytogenesis. Molecular and Biochemical Parasitology. 2010;172:57-65.

10. Bruce MC, Alano P, Duthie S, Carter R. Commitment of the malaria parasite *Plasmodium falciparum* to sexual and asexual development. Parasitology. 1990;100:191-200.

11. Martin SK, Miller LH, Nijhout MM, Carter R. *Plasmodium gallinaceum* - induction of male gametocyte exflagellation by phosphodiesterase inhibitors. Experimental Parasitology. 1978;44:239-42.

12. Kawamoto F, Alejoblanco R, Fleck SL, Sinden RE. *Plasmodium berghei* - ionic regulation and the induction of gametogenesis. Experimental Parasitology. 1991;72:33-42.

13. Billker O, Shaw MK, Margos G, Sinden RE. The roles of temperature, pH and mosquito factors as triggers of male and female gametogenesis of *Plasmodium berghei in-vitro*. Parasitology. 1997;115:1-7.

14. Billker O, Lindo V, Panico M, Etienne AE, Paxton T, Dell A, et al. Identification of xanthurenic acid as the putative inducer of malaria development in the mosquito. Nature. 1998;392:289-92.

15. Garcia GE, Wirtz RA, Barr JR, Woolfitt A, Rosenberg R. Xanthurenic acid induces gametogenesis in *Plasmodium*, the malaria parasite. Journal of Biological Chemistry. 1998;273:12003-05.

16. Sologub L, Kuehn A, Kern S, Przyborski J, Schillig R, Pradel G. Malaria proteases mediate inside-out egress of gametocytes from red blood cells following parasite transmission to the mosquito. Cellular Microbiology. 2011;13:897-912.

17. Baton LA, Ranford-Cartwright LC. Spreading the seeds of million-murdering death : Metamorphoses of malaria in the mosquito. Trends in Parasitology. 2005;21:573-80.

18. Shahabuddin M, Kaslow DC. *Plasmodium* - parasite chitinase and its role in malaria transmission. Experimental Parasitology. 1994;79:85-88.

19. Sinden RE. Excystment by sporozoites of malaria parasites. Nature. 1974;252:314-14.

20. Kappe SH, Kaiser K, Matuschewski K. The *Plasmodium* sporozoite journey: A rite of passage. Trends in Parasitology. 2003;19:135-43.

21. Sinden RE, Carter R, Drakeley C, Leroy D. The biology of sexual development of *Plasmodium*: The design and implementation of transmission-blocking strategies. Malaria Journal. 2012;11.

22. Bennink S, Kiesow MJ, Pradel G. The development of malaria parasites in the mosquito midgut. Cellular Microbiology. 2016;18:905-18.

23. Sinden RE. The cell biology of malaria infection of mosquito: Advances and opportunities. Cellular Microbiology. 2015;17:451-66.

24. Sinden RE, Croll NA. Cytology and kinetics of microgametogenesis and fertilization in *Plasmodium yoelii nigeriensis*. Parasitology. 1975;70:53-65.

25. Deligianni E, Morgan RN, Bertuccini L, Wirth CC, de Monerri NCS, Spanos L, et al. A perforin-like protein mediates disruption of the erythrocyte membrane during egress of *Plasmodium berghei* male gametocytes. Cellular Microbiology. 2013;15:1438-55.

26. Wirth CC, Glushakova S, Scheuermayer M, Repnik U, Garg S, Schaack D, et al. Perforin-like protein PPLP2 permeabilizes the red blood cell membrane during egress of *Plasmodium falciparum* gametocytes. Cellular Microbiology. 2014;16:709-33.

27. Lal K, Prieto JH, Bromley E, Sanderson SJ, Yates JR, Wastling JM, et al. Characterisation of *Plasmodium* invasive organelles; an ookinete microneme proteome. Proteomics. 2009;9:1142-51.

28. Innes EA, Wright SE, Maley S, Rae A, Schock A, Kirvar E, et al. Protection against vertical transmission in bovine neosporosis. International Journal for Parasitology. 2001;31:1523-34.

29. Janse CJ, Vanderklooster PFJ, Vanderkaay HJ, Vanderploeg M, Overdulve JP. DNA-synthesis in *Plasmodium berghei* during asexual and sexual development. Molecular and Biochemical Parasitology. 1986;20:173-82.

30. Shahabuddin M, Costero A. Spatial distribution of factors that determine sporogonic development of malaria parasites in mosquitoes. Insect Biochemistry and Molecular Biology. 2001;31:231-40.

31. Lobo CA, Kumar N. Sexual differentiation and development in the malaria parasite. Parasitology Today. 1998;14:146-50.

32. Aikawa M, Carter R, Ito Y, Nijhout MM. New observations on gametogenesis, fertilization, and zygote transformation in *Plasmodium gallinaceum*. The Journal of Protozology. 1984;31:403-13.

33. Sinden RE. A cell biologist's view of host cell recognition and invasion by malarial parasites. Transactions of the Royal Society of Tropical Medicine and Hygiene. 1985;79:598-605.

34. Vlachou D, Zimmermann T, Cantera R, Janse CJ, Waters AP, Kafatos FC. Real-time, *in-vivo* analysis of malaria ookinete locomotion and mosquito midgut invasion. Cellular Microbiology. 2004;6:671-85.

35. Billingsley PF, Hecker H. Blood digestion in the mosquito, *Anopheles stephensi* liston (diptera, culicidae), activity and distribution of trypsin, aminopeptidase, and alpha-glucosidase in the midgut. Journal of Medical Entomology. 1991;28:865-71.

36. Lehane MJ. Peritrophic matrix structure and function. Annual Review of Entomology. 1997;42:525-50.

37. Vinetz JM, Dave SK, Specht CA, Brameld KA, Xu B, Hayward R, et al. The chitinase PfCHT1 from the human malaria parasite *Plasmodium falciparum* lacks proenzyme and chitin-binding domains and displays unique substrate preferences. Proceedings of the National Academy of Sciences of the United States of America. 1999;96:14061-66.

38. Vinetz JM, Valenzuela JG, Specht CA, Aravind L, Langer RC, Ribeiro JMC, et al. Chitinases of the avian malaria parasite *Plasmodium gallinaceum*, a class of enzymes necessary for parasite invasion of the mosquito midgut. Journal of Biological Chemistry. 2000;275:10331-41.

39. Langer RC, Hayward RE, Tsuboi T, Tachibana M, Torii M, Vinetz JM. Micronemal transport of *Plasmodium* ookinete chitinases to the electron-dense area of the apical complex for extracellular secretion. Infection and Immunity. 2000;68:6461-65.

40. Vaughan JA, Noden BH, Beier JC. Sporogonic development of cultured *Plasmodium falciparum* in six species of laboratory-reared *Anopheles* mosquitoes. American Journal of Tropical Medicine and Hygiene. 1994;51:233-43.

41. Sinden RE, Strong K. An ultrastructural study of the sporogonic development of *Plasmodium falciparum* in *Anopheles gambiae*. Transactions of the Royal Society of Tropical Medicine and Hygiene. 1978;72:477-91.

42. Mehlhorn H, Peters W, Haberkorn A. The formation of kinetes and oocyst in *Plasmodium gallinaceum* (haemosporidia) and considerations on phylogenetic-relationships between haemosporidia, piroplasmida and other coccidia. Protistologica. 1980;16:135-54.

43. Howells RE, Davies EE. Nuclear division in the oocyst of *Plasmodium berghei*. Annals of Tropical Medicine and Parasitology. 1971;65:451-9.

44. Schrevel J, Asfaux-Foucher G, Hopkins J, Robert V, Bourgouin C, Prensier G, et al. Vesicle trafficking during sporozoite development in *Plasmodium berghei*: Ultrastructural evidence for a novel trafficking mechanism. Parasitology. 2008;135:1-12.

45. Meis J, Wismans P, Jap P, Lensen A, Ponnudurai T. A scanning electron microscopic study of the sporogonic development of *Plasmodium falciparum* in *Anopheles stephensi*. Acta tropica. 1992;50:227-36.

46. Aly AS, Vaughan AM, Kappe SH. Malaria parasite development in the mosquito and infection of the mammalian host. Annual Review of Microbiology. 2009;63:195-221.

47. Klug D, Frischknecht F. Motility precedes egress of malaria parasites from oocysts. Elife. 2017;6:e19157.

48. Smith RC, Vega-Rodriguez J, Jacobs-Lorena M. The *Plasmodium* bottleneck: Malaria parasite losses in the mosquito vector. Memorias Do Instituto Oswaldo Cruz. 2014;109:644-61.

49. Frischknecht F, Baldacci P, Martin B, Zimmer C, Thiberge S, Olivo-Marin JC, et al. Imaging movement of malaria parasites during transmission by *Anopheles* mosquitoes. Cellular Microbiology. 2004;6:687-94.

50. Sinden R, Matuschewski K. The sporozoite. Molecular approaches to malaria: American Society of Microbiology; 2005. p. 169-90.

51. Sinden RE, Garnham PCC. A comparative study on the ultrastructure of *Plasmodium* sporozoites within the oocyst and salivary glands, with particular reference

to the incidence of the micropore. Transactions of the Royal Society of Tropical Medicine and Hygiene . 1973;67:631-37.

52. Rodriguez MH, Hernandez-Hernandez FD. Insect-malaria parasites interactions: The salivary gland. Insect Biochemistry and Molecular Biology. 2004;34:615-24.

53. Raine JD, Ecker A, Mendoza J, Tewari R, Stanway RR, Sinden RE. Female inheritance of malarial lap genes is essential for mosquito transmission. PLoS Pathogens. 2007;3.

54. Rathnapala UL, Goodman CD, McFadden GI. A novel genetic technique in *Plasmodium berghei* allows liver stage analysis of genes required for mosquito stage development and demonstrates that *de novo* heme synthesis is essential for liver stage development in the malaria parasite. PLoS Pathogens. 2017;13:e1006396.

55. Beverley JK, Watson WA. Prevention of experimental and of naturally occurring ovine abortion due to Toxoplasmosis. Veterinary Record. 1971;88:39-and.

56. King RC, Mulligan P, Stansfield W. A dictionary of genetics: Oxford University Press; 2013.

57. Walliker D. Genetic recombination in malaria parasites. Experimental Parasitology. 1989;69:303-09.

58. Greenberg J, Trembley HL. Infections produced by mixed strains of *Plasmodium gallinaceum* in chicks. The Journal of Parasitology. 1954;40:336-40.

59. Walliker D, Quakyi IA, Wellems TE, Mccutchan TF, Szarfman A, London WT, et al. Genetic-analysis of the human malaria parasite *Plasmodium falciparum*. Science. 1987;236:1661-66.

60. Wellems TE, Panton LJ, Gluzman IY, Do Rosario VE, Gwadz RW, Walker-Jonah A, et al. Chloroquine resistance not linked to mdr-like genes in a *Plasmodium falciparum* cross. Nature. 1990;345:253-55.

61. Burkot TR, Williams JL, Schneider I. Infectivity to mosquitoes of *Plasmodium falciparum* clones grown *in-vitro* from the same isolate. Transactions of the Royal Society of Tropical Medicine and Hygiene. 1984;78:339-41.

62. Sullivan JS, Sullivan JJ, Williams A, Grady KK, Bounngaseng A, Huber CS, et al. Adaptation of a strain of *Plasmodium falciparum* from Ghana to *Aotus lemurinus griseimembra*, a-nancymai, and a-vociferans monkeys. American Journal of Tropical Medicine and Hygiene. 2003;69:593-600.

63. Hayton K, Gaur D, Liu A, Takahashi J, Henschen B, Singh S, et al. Erythrocyte binding protein PfRH5 polymorphisms determine species-specific pathways of *Plasmodium falciparum* invasion. Cell Host and Microbe. 2008;4:40-51.

64. Yoeli M, Upmanis RS, Most H. Drug-resistance transfer among rodent *Plasmodia*. Parasitology. 1969;59:429-47.

65. Walliker D, Carter R, Morgan S. Genetic recombination in malaria parasites. 1971.

66. Walliker D, Carter R, Morgan S. Genetic recombination in *Plasmodium berghei*. Parasitology. 1973;66:309-20.

67. Walliker D, Carter R, Sanderson A. Genetic studies on *Plasmodium chabaudi*: Recombination between enzyme markers. Parasitology. 1975;70:19-24.

68. Vaughan AM, Pinapati RS, Cheeseman IH, Camargo N, Fishbaugher M, Checkley LA, et al. *Plasmodium falciparum* genetic crosses in a humanized mouse model. Nature Methods. 2015;12:631-33.

69. Ranford-Cartwright LC, Balfe P, Carter R, Walliker D. Genetic hybrids of *Plasmodium falciparum* identified by amplification of genomic DNA from single oocysts. Molecular and Biochemical Parasitology. 1991;49:239-43.

70. Ranford-Cartwright LC, Balfe P, Carter R, Walliker D. Frequency of cross-fertilization in the human malaria parasite *Plasmodium falciparum*. Parasitology. 1993;107 (Pt 1):11-8.

71. Kooij TW, Matuschewski K. Triggers and tricks of *Plasmodium* sexual development. Current Opinion in Microbiology. 2007;10:547-53.

72. de Koning-Ward TF, Gilson PR, Crabb BS. Advances in molecular genetic systems in malaria. Nature Review Microbiology. 2015;13:373-87.

73. Combe A, Giovannini D, Carvalho TG, Spath S, Boisson B, Loussert C, et al. Clonal conditional mutagenesis in malaria parasites. Cell Host and Microbe. 2009;5:386-96.

74. Lacroix C, Giovannini D, Combe A, Bargieri DY, Spath S, Panchal D, et al. Flp/frt-mediated conditional mutagenesis in pre-erythrocytic stages of *Plasmodium berghei*. Nature Protocols. 2011;6:1412-28.

75. Pino P. From technology to biology: A malaria genetic toolbox for the functional dissection of essential genes. Molecular Microbiology. 2013;88:650-54.

76. Pino P, Sebastian S, Kim EA, Bush E, Brochet M, Volkmann K, et al. A tetracycline-repressible transactivator system to study essential genes in malaria parasites. Cell Host and Microbe. 2012;12:824-34.

77. Philip N, Waters AP. Conditional degradation of *Plasmodium* calcineurin reveals functions in parasite colonization of both host and vector. Cell Host and Microbe. 2015;18:122-31.

78. Billker O, Dechamps S, Tewari R, Wenig G, Franke-Fayard B, Brinkmann V. Calcium and a calcium-dependent protein kinase regulate gamete formation and mosquito transmission in a malaria parasite. Cell. 2004;117:503-14.

79. Santos JM, Kehrer J, Franke-Fayard B, Frischknecht F, Janse CJ, Mair GR. The *Plasmodium* palmitoyl-s-acyl-transferase DHHC2 is essential for ookinete morphogenesis and malaria transmission. Scientific Reports. 2015;5.

80. Mair GR, Braks JA, Garver LS, Wiegant JC, Hall N, Dirks RW, et al. Regulation of sexual development of *Plasmodium* by translational repression. Science. 2006;313:667-69.

81. Hirai M, Arai M, Mori T, Miyagishima S, Kawai S, Kita K, et al. Male fertility of malaria parasites is determined by GCS1, a plant-type reproduction factor. Current Biology. 2008;18:607-13.

82. Liu YJ, Tewari R, Ning J, Blagborough AM, Garbom S, Pei JM, et al. The conserved plant sterility gene HAP2 functions after attachment of fusogenic membranes

in *Chlamydomonas* and *Plasmodium* gametes. Genes and Development. 2008;22:1051-68.

83. Talman AM, Lacroix C, Marques SR, Blagborough AM, Carzaniga R, Ménard R, et al. PbGEST mediates malaria transmission to both mosquito and vertebrate host. Molecular Microbiology. 2011;82:462-74.

84. Rangarajan R, Bei AK, Jethwaney D, Maldonado P, Dorin D, Sultan AA, et al. A mitogen-activated protein kinase regulates male gametogenesis and transmission of the malaria parasite *Plasmodium berghei*. Eurpean Molecular Biology Organization Reports. 2005;6:464-69.

85. Kehrer J, Singer M, Lemgruber L, Silva PA, Frischknecht F, Mair GR. A putative small solute transporter is responsible for the secretion of G377 and TRAP-containing secretory vesicles during *Plasmodium* gamete egress and sporozoite motility. PLoS Pathogens. 2016;12:e1005734.

86. Guttery DS, Poulin B, Ramaprasad A, Wall RJ, Ferguson DJ, Brady D, et al. Genome-wide functional analysis of *Plasmodium* protein phosphatases reveals key regulators of parasite development and differentiation. Cell Host and Microbe. 2014;16:128-40.

87. van Schaijk BC, van Dijk MR, van de Vegte-Bolmer M, van Gemert GJ, van Dooren MW, Eksi S, et al. Pfs47, paralog of the male fertility factor Pfs48/45, is a female specific surface protein in *Plasmodium falciparum*. Molecular and Biochemical Parasitology. 2006;149:216-22.

88. Molina-Cruz A, Garver LS, Alabaster A, Bangiolo L, Haile A, Winikor J, et al. The human malaria parasite Pfs47 gene mediates evasion of the mosquito immune system. Science. 2013;340:984-87.

89. Eksi S, Czesny B, van Gemert GJ, Sauerwein RW, Eling W, Williamson KC. Malaria transmission-blocking antigen, Pfs230, mediates human red blood cell binding to exflagellating male parasites and oocyst production. Molecular Microbiology. 2006;61:991-98.

90. van Dijk MR, Janse CJ, Thompson J, Waters AP, Braks JAM, Dodemont HJ, et al. A central role for P48/45 in malaria parasite male gamete fertility. Cell. 2001;104:153-64.

91. Srivastava A, Creek DJ, Evans KJ, De Souza D, Schofield L, Muller S, et al. Host reticulocytes provide metabolic reservoirs that can be exploited by malaria parasites. PLoS Pathogens. 2015;11.

92. Andreadaki M, Morgan RN, Deligianni E, Kooij TW, Santos JM, Spanos L, et al. Genetic crosses and complementation reveal essential functions for the *Plasmodium* stage-specific actin2 in sporogonic development. Cellular Microbiology. 2014;16:751-67.

93. Ganter M, Schuler H, Matuschewski K. Vital role for the *Plasmodium* actin capping protein (CP) beta-subunit in motility of malaria sporozoites. Molecular Microbiology. 2009;74:1356-67.

94. Ishino T, Orito Y, Chinzei Y, Yuda M. A calcium-dependent protein kinase regulates *Plasmodium* ookinete access to the midgut epithelial cell. Molecular Microbiology. 2006;59:1175-84.

95. Siden-Kiamos I, Ecker A, Nyback S, Louis C, Sinden RE, Billker O. *Plasmodium berghei* calcium-dependent protein kinase 3 is required for ookinete gliding motility and mosquito midgut invasion. Molecular Microbiology. 2006;60:1355-63.

96. Kariu T, Ishino T, Yano K, Chinzei Y, Yuda M. CelTOS, a novel malarial protein that mediates transmission to mosquito and vertebrate hosts. Molecular Microbiology. 2006;59:1369-79.

97. Dessens JT, Mendoza J, Claudianos C, Vinetz JM, Khater E, Hassard S, et al. Knockout of the rodent malaria parasite chitinase PbCHT1 reduces infectivity to mosquitoes. Infection and Immunity. 2001;69:4041-7.

98. Tsai YL, Hayward RE, Langer RC, Fidock DA, Vinetz JM. Disruption of *Plasmodium falciparum* chitinase markedly impairs parasite invasion of mosquito midgut. Infection and Immunity. 2001;69:4048-54.

99. Ghosh AK, Coppens I, Gardsvoll H, Ploug M, Jacobs-Lorena M. *Plasmodium* ookinetes coopt mammalian plasminogen to invade the mosquito midgut. Proceedings of the National Academy of Sciences of the United States of America. 2011;108:17153-58.

100. Hirai M, Arai M, Kawai S, Matsuoka H. PbGCbeta is essential for *Plasmodium* ookinete motility to invade midgut cell and for successful completion of parasite life cycle in mosquitoes. Journal of Biochemistry. 2006;140:747-57.

101. Moon RW, Taylor CJ, Bex C, Schepers R, Goulding D, Janse CJ, et al. A cyclic GMP signalling module that regulates gliding motility in a malaria parasite. PLoS Pathogens. 2009;5.

102. Florent I, Derhy Z, Allary M, Monsigny M, Mayer R, Schrevel J. A *Plasmodium falciparum* aminopeptidase gene belonging to the M1 family of zinc-metallopeptidases is expressed in erythrocytic stages. Molecular and Biochemical Parasitology. 1998;97:149-60.

103. Allary M, Schrevel J, Florent I. Properties, stage-dependent expression and localization of *Plasmodium falciparum* M1 family zinc-aminopeptidase. Parasitology. 2002;125:1-10.

104. Sahi S, Rai S, Chaudhary M, Nain V. Modeling of human M1 aminopeptidases for *in silico* screening of potential *Plasmodium falciparum* alanine aminopeptidase (PfA-M1) specific inhibitors. Bioinformation. 2014;10:518-25.

105. Drinkwater N, Bamert RS, Sivaraman KK, Paiardini A, McGowan S. X-ray crystal structures of an orally available aminopeptidase inhibitor, tosedostat, bound to anti-malarial drug targets PfA-M1 and PfA-M17. Proteins-Structure Function and Bioinformatics. 2015;83:789-95.

106. Kadota K, Ishino T, Matsuyama T, Chinzei Y, Yuda M. Essential role of membrane-attack protein in malarial transmission to mosquito host. Proceedings of the National Academy of Sciences of the United States of America. 2004;101:16310-15.

107. Ponzi M, Siden-Kiamos I, Bertuccini L, Curra C, Kroeze H, Camarda G, et al. Egress of *Plasmodium berghei* gametes from their host erythrocyte is mediated by the MDV-1/PEG3 protein. Cellular Microbiology. 2009;11:1272-88.

108. Reininger L, Billker O, Tewari R, Mukhopadhyay A, Fennell C, Dorin-Semblat D, et al. A NIMA-related protein kinase is essential for completion of the sexual cycle of malaria parasites. Journal of Biological Chemistry. 2005;280:31957-64.

109. Tomas AM, Margos G, Dimopoulos G, van Lin LHM, de Koning-Ward TF, Sinha R, et al. P25 and P28 proteins of the malaria ookinete surface have multiple and partially redundant functions. European Molecular Biology Organization Journal. 2001;20:3975-83.

110. Hopp CS, Balaban AE, Bushell ES, Billker O, Rayner JC, Sinnis P. Palmitoyl transferases have critical roles in the development of mosquito and liver stages of *Plasmodium*. Cellular Microbiology. 2016;18:1625-41.

111. Srivastava A, Philip N, Hughes KR, Georgiou K, MacRae JI, Barrett MP, et al. Stage-specific changes in *Plasmodium* metabolism required for differentiation and adaptation to different host and vector environments. PLoS Pathogens. 2016;12.

112. Hart RJ, Cornillot E, Abraham A, Molina E, Nation CS, Ben Mamoun C, et al. Genetic characterization of *Plasmodium* putative pantothenate kinase genes reveals their essential role in malaria parasite transmission to the mosquito. Scientific Reports. 2016;6.

113. Taylor CJ, McRobert L, Baker DA. Disruption of a *Plasmodium falciparum* cyclic nucleotide phosphodiesterase gene causes aberrant gametogenesis. Molecular Microbiology. 2008;69:110-18.

114. Kaneko I, Iwanaga S, Kato T, Kobayashi I, Yuda M. Genome-wide identification of the target genes of AP2-O, a *Plasmodium* AP2-family transcription factor. PLoS Pathogens. 2015;11.

115. Wirth CC, Bennink S, Scheuermayer M, Fischer R, Pradel G. Perforin-like protein PPLP4 is crucial for mosquito midgut infection by *Plasmodium falciparum*. Molecular and Biochemical Parasitology. 2015;201:90-99.

116. Florenta I, Mouray E, Ali FD, Drobecq H, Girault S, Schrevel J, et al. Cloning of *Plasmodium falciparum* protein disulfide isomerase homologue by affinity purification using the antiplasmodial inhibitor 1,4-bis{3-[n-(cyclohexyl

methyl)amino]propyl}piperazine. Federation of European Biochemical Societies Letters. 2000;484:246-52.

117. Mahajan B, Noiva R, Yadava A, Zheng H, Majam V, Mohan KVK, et al. Protein disulfide isomerase assisted protein folding in malaria parasites. International Journal for Parasitology. 2006;36:1037-48.

118. Brochet M, Collins MO, Smith TK, Thompson E, Sebastian S, Volkmann K, et al. Phosphoinositide metabolism links cGMP-dependent protein kinase G to essential Ca(2)(+) signals at key decision points in the life cycle of malaria parasites. PLoS Biology. 2014;12:e1001806.

119. Zheng WQ, Liu F, He YW, Liu QY, Humphreys GB, Tsuboi T, et al. Functional characterization of *Plasmodium berghei* PSOP25 during ookinete development and as a malaria transmission-blocking vaccine candidate. Parasites and Vectors. 2017;10.

120. Patzewitz EM, Guttery DS, Poulin B, Ramakrishnan C, Ferguson DJP, Wall RJ, et al. An ancient protein phosphatase, SHLP1, is critical to microneme development in *Plasmodium* ookinetes and parasite transmission. Cell Reports. 2013;3:622-29.

121. Dessens JT, Siden-Kiamos I, Mendoza J, Mahairaki V, Khater E, Vlachou D, et al. SOAP, a novel malaria ookinete protein involved in mosquito midgut invasion and oocyst development. Molecular Microbiology. 2003;49:319-29.

122. Han YS, Thompson J, Kafatos FC, Barillas-Mury C. Molecular interactions between *Anopheles stephensi* midgut cells and *Plasmodium berghe*i: The time bomb theory of ookinete invasion of mosquitoes. European Molecualr Biology Organization Journal. 2000;19:6030-40.

123. Li FW, Templeton TJ, Popov V, Comer JE, Tsuboi T, Torii M, et al. *Plasmodium* ookinete-secreted proteins secreted through a common micronemal pathway are targets of blocking malaria transmission. Journal of Biological Chemistry. 2004;279:26635-44.

124. Yuda M, Yano K, Tsuboi T, Torii M, Chinzei Y. Von willebrand factor a domain-related protein, a novel microneme protein of the malaria ookinete highly conserved throughout *Plasmodium* parasites. Molecualr and Biochemical Parasitology. 2001;116:65-72.

125. Nagaraj VA, Sundaram B, Varadarajan NM, Subramani PA, Kalappa DM, Ghosh SK, et al. Malaria parasite-synthesized heme is essential in the mosquito and liver stages and complements host heme in the blood stages of infection. PLoS Pathogens. 2013;9.

126. Ke HJ, Sigala PA, Miura K, Morrisey JM, Mather MW, Crowley JR, et al. The heme biosynthesis pathway is essential for *Plasmodium falciparum* development in mosquito stage but not in blood stages. Journal of Biological Chemistry. 2014;289:34827-37.

127. Rizopoulos Z, Matuschewski K, Haussig J. Distinct prominent roles for enzymes of *Plasmodium berghei* heme biosynthesis in sporozoite and liver stage maturation. Infection and Immunity. 2016.

128. Sturm A, Mollard V, Cozijnsen A, Goodman CD, McFadden GI. Mitochondrial ATP synthase is dispensable in blood-stage *Plasmodium berghei* rodent malaria but essential in the mosquito phase. Proceedings of the National Academy of Sciences of the United States of America. 2015;112:10216-23.

129. Oppenheim RD, Creek DJ, Macrae JI, Modrzynska KK, Pino P, Limenitakis J, et al. BCKDH: The missing link in apicomplexan mitochondrial metabolism is required for full virulence of *Toxoplasma gondii* and *Plasmodium berghei*. PLoS Pathogens. 2014;10:e1004263.

130. Srinivasan P, Fujioka H, Jacobs-Lorena M. PbCap380, a novel oocyst capsule protein, is essential for malaria parasite survival in the mosquito. Cellular Microbiology. 2008;10:1304-12.

131. Yuda M, Sakaida H, Chinzei Y. Targeted disruption of the *Plasmodium berghei* CTRP gene reveals its essential role in malaria infection of the vector mosquito. Journal of Experimental Medicine. 1999;190:1711-6.

132. Roques M, Wall RJ, Douglass AP, Ramaprasad A, Ferguson DJP, Kaindama ML, et al. *Plasmodium* P-type cyclin CYC3 modulates endomitotic growth during oocyst development in mosquitoes. PLoS Pathogens. 2015;11.

133. Aly ASI, Matuschewski K. A malarial cysteine protease is necessary for *Plasmodium* sporozoite egress from oocysts. Journal of Experimental Medicine. 2005;202:225-30.

134. van Schaijk BCL, Kumar TRS, Vos MW, Richman A, van Gemert GJ, Li T, et al. Type II fatty acid biosynthesis is essential for *Plasmodium falciparum* sporozoite development in the midgut of *Anopheles* mosquitoes. Eukaryotic Cell. 2014;13:550-59.

135. Vega-Rodriguez J, Franke-Fayard B, Dinglasan RR, Janse CJ, Pastrana-Mena R, Waters AP, et al. The glutathione biosynthetic pathway of *Plasmodium* is essential for mosquito transmission. PLoS Pathogens. 2009;5:e1000302.

136. Pastrana-Mena R, Dinglasan RR, Franke-Fayard B, Vega-Rodriguez J, Fuentes-Caraballo M, Baerga-Ortiz A, et al. Glutathione reductase-null malaria parasites have normal blood stage growth but arrest during development in the mosquito. Journal of Biological Chemistry. 2010;285:27045-56.

137. Buchholz K, Putrianti ED, Rahlfs S, Schirmer RH, Becker K, Matuschewski K. Molecular genetics evidence for the *in-vivo* roles of the two major NADPH-dependent disulfide reductases in the malaria parasite. Journal of Biological Chemistry. 2010;285:37388-95.

138. Gissot M, Ting L-M, Daly TM, Bergman LW, Sinnis P, Kim K. High mobility group protein HMGB2 is a critical regulator of *Plasmodium* oocyst development. Journal of Biological Chemistry. 2008;283:17030-38.

139. Ke H, Lewis IA, Morrisey JM, McLean KJ, Ganesan SM, Painter HJ, et al. Genetic investigation of tricarboxylic acid metabolism during the *Plasmodium falciparum* life cycle. Cell Reports. 2015;11:164-74.

140. Trueman HE, Raine JD, Florens L, Dessens JT, Mendoza J, Johnson J, et al. Functional characterization of an LCCL-lectin domain containing protein family in *Plasmodium berghei*. Journal of Parasitology. 2004;90:1062-71.

141. Bushell ESC, Ecker A, Schlegelmilch T, Goulding D, Dougan G, Sinden RE, et al. Paternal effect of the nuclear formin-like protein MISFIT on *Plasmodium* development in the mosquito vector. PLoS Pathogens. 2009;5.

142. Sigala PA, Crowley JR, Henderson JP, Goldberg DE. Deconvoluting heme biosynthesis to target blood-stage malaria parasites. Elife. 2015;4.

143. Posayapisit N, Songsungthong W, Koonyosying P, Falade MO, Uthaipibull C, Yuthavong Y, et al. Cytochrome c and c1 heme lyases are essential in *Plasmodium berghei*. Molecular and Biochemical Parasitology. 2016;210:32-36.

144. Tewari R, Straschil U, Bateman A, Bohme U, Cherevach I, Gong P, et al. The systematic functional analysis of *Plasmodium* protein kinases identifies essential regulators of mosquito transmission. Cell Host and Microbe. 2010;8:377-87.

145. Hino A, Hirai M, Tanaka TQ, Watanabe Y, Matsuoka H, Kita K. Critical roles of the mitochondrial complex II in oocyst formation of rodent malaria parasite *Plasmodium berghei*. Journal of Biochemistry. 2012;152:259-68.

146. Klug D, Frischknecht F. Motility precedes egress of malaria parasites from oocysts. Elife. 2017;6.

147. Boysen KE, Matuschewski K. Arrested oocyst maturation in *Plasmodium* parasites lacking type II NADH:Ubiquinone dehydrogenase. Journal of Biological Chemistry. 2011;286:32661-71.

148. Mikolajczak SA, Silva-Rivera H, Peng X, Tarun AS, Camargo N, Jacobs-Lorena V, et al. Distinct malaria parasite sporozoites reveal transcriptional changes that cause differential tissue infection competence in the mosquito vector and mammalian host. Molecular and Cellular Biology. 2008;28:6196-207.

149. Modrzynska K, Pfander C, Chappell L, Yu L, Suarez C, Dundas K, et al. A knockout screen of ApiAP2 genes reveals networks of interacting transcriptional regulators controlling the *Plasmodium* life cycle. Cell Host and Microbe. 2017;21:11-22.

150. Hliscs M, Sattler JM, Tempel W, Artz JD, Dong A, Hui R, et al. Structure and function of a G-actin sequestering protein with a vital role in malaria oocyst development inside the mosquito vector. Journal of Biological Chemistry. 2010;285:11572-83.

151. Thompson J, Fernandez-Reyes D, Sharling L, Moore SG, Eling WM, Kyes SA, et al. *Plasmodium* cysteine repeat modular proteins 1-4: Complex proteins with roles throughout the malaria parasite life cycle. Cellular Microbiology. 2007;9:1466-80.

152. Menard R, Sultan AA, Cortes C, Altszuler R, vanDijk MR, Janse CJ, et al. Circumsporozoite protein is required for development of malaria sporozoites in mosquitoes. Nature. 1997;385:336-40.

153. Zhang M, Fennell C, Ranford-Cartwright L, Sakthivel R, Gueirard P, Meister S, et al. The *Plasmodium* eukaryotic initiation factor-2alpha kinase IK2 controls the latency of sporozoites in the mosquito salivary glands. Journal of Experimental Medicine. 2010;207:1465-74.

154. Khater EI, Sinden RE, Dessens JT. A malaria membrane skeletal protein is essential for normal morphogenesis, motility and infectivity of sporozoites. Journal of Cell Biology. 2004;167:425-32.

155. Santos JM, Egarter S, Zuzarte-Luís V, Kumar H, Moreau CA, Kehrer J, et al. Malaria parasite LIMP protein regulates sporozoite gliding motility and infectivity in mosquito and mammalian hosts. Elife. 2017;6:e24109.

156. Kariu T, Yuda M, Yano K, Chinzei Y. MAEBL is essential for malarial sporozoite infection of the mosquito salivary gland. Journal of Experimental Medicine. 2002;195:1317-23.

157. Bhanot P, Schauer K, Coppens I, Nussenzweig V. A surface phospholipase is involved in the migration of *Plasmodium* sporozoites through cells. Journal of Biological Chemistry. 2005;280:6752-60.

158. Ecker A, Bushell ES, Tewari R, Sinden RE. Reverse genetics screen identifies six proteins important for malaria development in the mosquito. Molecular Microbiology. 2008;70:209-20.

159. Giovannini D, Späth S, Lacroix C, Perazzi A, Bargieri D, Lagal V, et al. Independent roles of apical membrane antigen 1 and rhoptry neck proteins during host cell invasion by apicomplexa. Cell Host and Microbe. 2011;10:591-602.

160. Santos JM, Duarte N, Kehrer J, Ramesar J, Avramut MC, Koster AJ, et al. Maternally supplied S-acyl-transferase is required for crystalloid organelle formation and transmission of the malaria parasite. Proceedings of the National Academy of Sciences of the United States of America. 2016;113:7183-88.

161. Ishino T, Chinzei Y, Yuda M. A *Plasmodium* sporozoite protein with a membrane attack complex domain is required for breaching the liver sinusoidal cell layer prior to hepatocyte infection. Cellular Microbiology. 2005;7:199-208.

162. Ishino T, Yano K, Chinzei Y, Yuda M. Cell-passage activity is required for the malarial parasite to cross the liver sinusoidal cell layer. PLoS Biology. 2004;2:e4.

163. Moreira CK, Templeton TJ, Lavazec C, Hayward RE, Hobbs CV, Kroeze H, et al. The *Plasmodium* TRAP/MIC2 family member, TRAP-like protein (TLP), is involved in tissue traversal by sporozoites. Cellular Microbiology. 2008;10:1505-16.

164. Mueller AK, Kohlhepp F, Hammerschmidt C, Michel K. Invasion of mosquito salivary glands by malaria parasites: Prerequisites and defense strategies. International Journal for Parasitology. 2010;40:1229-35.

165. Labaied M, Camargo N, Kappe SH. Depletion of the *Plasmodium berghei* thrombospondin-related sporozoite protein reveals a role in host cell entry by sporozoites. Molecualr and Biochemical Parasitology. 2007;153:158-66.

166. Andreadaki M, Morgan RN, Deligianni E, Kooij TWA, Santos JM, Spanos L, et al. Genetic crosses and complementation reveal essential functions for the *Plasmodium* stage-specific actin2 in sporogonic development. Cellular Microbiology. 2014;16:751-67.

167. Bautista JM, Marín-García P, Diez A, Azcárate IG, Puyet A. Malaria proteomics: Insights into the parasite–host interactions in the pathogenic space. Journal of Proteomics. 2014;97:107-25.

168. Culleton RL, Abkallo HM. Malaria parasite genetics: Doing something useful. Parasitology International. 2015;64:244-53.

Chapter 2

Investigating the function of heme biosynthesis pathway in the liver stage of *Plasmodium berghei*

2.1 Introduction

Malaria is a life-threatening disease caused by five species of *Plasmodium* parasites, with *P. falciparum* being the most deadly. The on-going emergence of drug resistance threatens malaria control efforts (1) and highlights the need for new drugs and novel approaches for controlling the spread of this disease. *Plasmodium berghei* is a widely-used mouse malaria model and a dominant tool for reverse genetic studies in malaria (2). The *P. berghei* genome is largely homologous to the genome of the human parasites, which permits experiments that are difficult to perform with human subjects (3). Experimental access to the entire life cycle is arguably the most important advantage of rodent malaria parasites as it facilitates study of transmission dynamics, exoerythrocytic stage vaccines, and prophylactic drugs.

Genome manipulation is an essential tool for understanding key events in the *Plasmodium* life cycle. Stable transfection of the parasite and modification of its genome by homologous recombination are now common procedures (4). A significant limitation of the method is that the parasite genes essential at one life stage cannot be characterized in subsequent stages. In the growing list of loss of function mutations that can survive the blood stages, many are found to fail during development in the mosquito; possibly due to the increased metabolic requirements in this stage of the life cycle (5). Failure to produce infective sporozoites limits the possibilities for studying the role of these genes in the liver stage. Given the unique features of the hepatic stage of the life cycle, particularly the low parasite burden and the role in generation of sterile immunity (6), understanding parasite biology at this stage is of great importance. Thus, temporal gene inactivation is needed in functional studies to test protein function during liver stage development. A small number of genes essential in other life stages have been successfully ablated using conditional knockout strategies in *P. berghei* to analyse liver stage function (7, 8), and other conditional strategies are available. But these strategies can present significant limitations in terms of which species can be tested, the complexity of plasmid construction, the need for specific parasite lines, requirements

for specific chemical or physical treatments during the life cycle, and unpredictable variations in the effectiveness of the gene ablation. Such drawbacks have limited the use of these techniques and severely hampered analysis of parasite liver stage responses to gene deletion (9, 10) largely precluding reverse genetic approaches to this important life cycle stage.

Heme is essential in malaria parasites, playing an important role as a precursor for cytochrome production in the mitochondrial electron transport chain. *Plasmodium* parasites encode and express all the enzymes for a complete heme biosynthesis pathway (Fig 2.6.3), and heme biosynthesis was initially considered a potential drug target against malaria parasites (11). However, the *de novo* heme synthesis pathway enzymes are dispensable during the blood stage of the parasite life cycle (12-15). It appears that parasites still require heme, but in the blood stage they can scavenge pathway intermediates, heme and/or heme synthesizing enzymes, from the host red blood cell (12, 14, 16). However, these alternate sources are apparently not sufficient or accessible enough during the mosquito stages of the parasite life cycle, where parasites lacking heme-synthesizing enzymes fail to complete sporozoite development in the oocyst (12, 13, 15).

Given the essentiality of the endogenous heme biosynthesis pathway in the mosquito stages of the parasite life cycle, it is hardly surprising that there is minimal data available about the liver stage growth of heme deficient parasites. Parasites lacking the first enzyme in the heme biosynthesis pathway, aminolevulinic acid synthase (ALAS) can only complete the life cycle if mosquitoes are fed aminolevulinic acid (d-ALA), the product of ALAS (12, 15). This chemical complementation approach has been effectively employed to generate infective ALAS-minus sporozoites and demonstrate that parasites can scavenge d-ALA from the host liver and, thereby, partially restore parasite viability (15). While it is clear that parasites can survive the loss of ALAS, this finding does not directly address whether parasite synthesized heme is essential for liver stage development. Aminolevulinic acid is a stable compound that appears to be available for uptake from the host cell cytoplasm, possibly by the same mechanism that imports parasite synthesized d-ALA into the apicoplast where the next steps in the pathway are localized. It remains unclear if the other compensatory mechanisms available to parasites in the red blood cell, particularly the ability to scavenge FC and/or heme, are available to the parasite during liver stage infection.

A chemical complementation approach is not available for the final stage of the heme biosynthesis pathway (Fig 2.6.3), namely conversion of protoporphyrin IX and iron to heme by ferrochelatase (FC) in the mitochondrion, so I set out here to address this limitation by applying a genetic complementation method to rescue parasites with a deletion of the FC gene. By combining locus-specific fluorescence tagging with the ability of sexual outcrossing to bridge parasites through the mosquito life stages (17), I generated viable sporozoites that lacked the FC gene but were capable of infecting liver cells *in-vitro* and *in-vivo*. The specific fluorescent labelling of parasites lacking FC allowed detailed exploration of the reliance on heme for parasite development in the liver stage. This fluorescence-tagging complementation strategy gives a straightforward method for reverse genetic analysis of various blood-stage dispensable/mosquito-stage essential genes that is useable in all genetically tractable, fertile *Plasmodium* species and requires no special conditions.

2.2 Materials and Methods

2.2.1 Experimental animals

Male asmu:Swiss mice aged between 4-6 weeks obtained from Monash Animal Research platform were used in all the experiments.

2.2.2 Ethics statement

All animal experiments were carried out as per the National Health and Medical Research Council - Australian Code for the Care and Use of Animals for Scientific Purposes 2013 (8^{th} edition) guidelines and were permitted by the University of Melbourne Animal Ethics committee under Ethics ID 1413078.1.

2.2.3 Parasites

The *Pb*nek-4ko strain (18) was provided by Oliver Billker (Wellcome Trust Sanger Institute, Hinxton, Cambridge, UK). *Pb ANKA* parasites lines expressing GFP, tdTomato and mCherry fluorescence markers were developed by Dr Dean Goodman based on (19). See Supplementary methods 2.7.1 for a full description of the generation of these lines.

2.2.4 Generation of *Plasmodium berghei* ^{FC} knockout parasites

To generate the *P. berghei* FC (Pb ANKA_114070) knockout parasites (FC^{KOmCh}), the selection cassette from pLChSKD, a modified version of pL0006 (MRA-775) with the *h*DHFR replaced by mCherry fused to *h*DHFR via a viral 2A skip peptide (20), was ligated into the *Xho*I/*Bgl*II sites of pL0006 containing regions flanking the FC gene (16) to create pFCChSKD. See Supplementary methods (2.7.1.I) for a full description of pLChSKD plasmid construction. *Pb*ANKA parasites were transfected with *Hind*III/*Eco*RI linearized pFCChSKD, genotyped by PCR (see Table 2.7.3.I for primer sequences) and cloned as previously described (5, 21). PCR conditions used are as follows.

Initial denaturation	95 ºC	2 min
35 cycles	95 ºC	15 sec
	58 ºC	15 sec
	65 ºC	2 min
Final extension	68 ºC	5 min

2.2.5 Infection of *Anopheles stephensi*

All parasite strains used for coinfection crossing experiments were inoculated by intraperitoneal injection into naïve mice and assessed for fluorescence and genotype at day 3. 2.5 x 10^5 parasites from each strain were mixed and used to infect a naïve mouse by intravenous (IV) injection. The mice were infected with the following combinations of *P. berghei* parasitic strains.

1. FC^{KOmCh} x FC^{WT}-GFP – Parasites having FC replaced with ChSKDHFR mixed with parasites having a wildtype FC locus and expressing GFP from a different genetic locus
2. FC^{KOmCh} nek-4wt x FC^{WT}-nek-4ko - Parasites with a wildtype nek4 locus and having FC replaced with ChSKDHFR mixed with parasites carrying a wildtype FC gene but lacking nek-4.
3. FC^{WT}-mCh x FC^{WT}-GFP – parasites with a wildtype FC locus and expressing mCherry from another genetic locus mixed with FC wildtype parasites expressing GFP from another genetic locus.
4. FC^{WT-}mCh x FC^{WT}-nek-4ko - parasites with wildtype FC and nek4 loci and expressing mCherry from another genetic locus mixed with non-fluorescent parasites with a wildtype FC locus but lacking nek-4.

To complement the effect of FC deletion, I crossed the knockout parasites with two strains carrying wildtype FC genes. First, the cross with FC^{WT} parasites expressing GFP (FC^{WT}-GFP) (number 1) allows easy follow up of self-fertilized knockout (red), wildtype (green) and recombinants (orange). As the control experiment, a wildtype parasite carrying intact FC gene but mCherry inserted in to chromosome 6 (FC^{WT}-mCh) was crossed with the same FC^{WT} parasites expressing GFP (number 3). Second, I crossed a female sterile FC^{WT}-nek-4ko strain with the FC^{KOmCh} to increase the number of recombinant parasites of the cross as self-fertilized nek-4ko parasites do not form oocysts (number 2). To control any effect of fluorophore expression, above FC wildtype parasites expressing mCherry (FC^{WT}-mCh) was crossed to the same nek-4ko (number 4).

Adult females of *A. stephensi* (MR4) reared under standard insectary conditions (adult mosquitoes were grown at 27 ºC with humidity of 80% and light: dark photoperiod of 14:10 hours with a 1 hour ramp in) were allowed to feed on 4-6 weeks old Swiss mice

anesthetized with ketamine/xylazine 3 days following coinfection. A minimum of three independent infections were done for all crosses.

2.2.6 Assessment of mosquito stage development

Twelve days after infection, mosquito midguts were removed, imaged using a Leica DM 2500 epifluorescence microscope (20X) and counted. Oocyst size was measured using Fiji (ImageJ 1.46a, Wayne Rasband, National Institutes of Health).

Salivary gland sporozoite numbers were counted using a standard haemocytometer and averaged per mosquito. The sporozoite motility 21 days post-infection was analysed by immunofluorescence assay (IFA) (22). First, sporozoites were let to settle down on a 3% Bovine Serum Albumine (BSA; Sigma Aldrich) coated coverslip at 37 ºC for 15 minutes. After that, 4% paraformaldehyde (PFA) was used for 10 minutes at room temperature for sporozoites to fix. Next, 0.2% TritonX-100 (Fisher Scientific) was added and let 15 minutes at room temperature to permeabilize sporozoites. Blocking of sporozoites in 3% BSA/0.2% Triton X-100/ phosphate buffered saline (PBS) at room temperature for 20 minutes was followed by staining with mouse anti-circumsporozoite protein (mouse anti-CSP) in 1: 500 dilution (a gift from Louis Schofield, Walter and Eliza Hall Institute) and rabbit anti-mCherry antibody (1: 250; Abcam ab167453). FC^{KOmCh} nek-4wt x FC^{WT}-nek-4ko parasites were probed with Alexa Fluor 488 goat anti-mouse IgG and Alexa Fluor 546 goat anti-rabbit IgG (1:1000; Molecular Probes/ Thermo Fisher) secondary antibodies. FC^{KOmCh} x FC^{WT}-GFP parasites were probed with Alexa Fluor 633 goat anti-mouse IgG and Alexa Fluor 546 goat anti-rabbit IgG (1:1000; Molecular Probes/Thermo Fisher) secondary antibodies. In between and after antibody incubation, washing with 1% PBS was done. From the images developed after the IFA, presence of trails and the number of circles sporozoites have moved was reported. Salivary gland sporozoite gDNA was extracted and used as template for nested PCR to confirm the presence of FC^{KOmCh} parasites.

2.2.7 In-*vitro* liver stage development analysis

Growth and IFAs of pre-erythrocytic forms were performed as described (23). HepG2 cells were seeded in 24-well plates one day prior to the addition of 20,000 sporozoites from each combination of parasites. After the addition of sporozoites, HepG2 cells were incubated for 2 hours at 37 ºC. Two hours post incubation: culture media [Alpha

Modification of Eagle's Medium/AMEM (Gibco), 10% heat inactivated Fetal Bovine Serum/FBS (Gibco), 1% penStrep (Gibco), 2mM Glutamax (Gibco) and 0.1% amphotericin] was replaced with fresh media containing 2% of amphotericin. The process continued for 68 hours with media changing twice a day. Once the duration of infection reached 24, 48 and 68 hours respectively, cells were fixed with 4% paraformaldehyde (PFA) for 20 minutes and permeabilized with ice-cold methanol overnight at -20 ºC. After removing methanol and washing the cells with 1X PBS two times, the cells were blocked with 3% BSA (Sigma Aldrich) in 1X mouse PBS ([Dulbecco's Phosphate Buffered Saline (Thermo Fisher Scientific)] for 30 minutes. In between and after antibody incubation, the cells were washed with 1X PBS for two times each. The DNA stain Hoechst 33342 (5µg/ ml/ Thermo Fisher Scientific) was included in to the first washing of the last washing step after the secondary antibody incubation. Then the coverslips were carefully washed with distilled water and removed remaining water drops. Finally a drop of Dako (Agilent) at 4 ºC was added to a cleaned glass slide and the coverslip with cells was mounted on to the glass slide.

To determine the size and nuclear content, parasites were stained with rabbit anti-mCherry (1: 250; Abcam ab167453)/Alexa Fluor 546 goat anti-rabbit IgG (1:1000; Molecular Probes/Thermo Fisher) and Hoechst 33342 (5µg/ ml). Images collected at 40X magnification with the Leica DM 2500 microscope were analysed in Fiji to measure parasite size in μm^2. Student t-test (unpaired) was used to compare the average growth size differences 24, 48 and 68 hours post infection for parasites pooled from 6 independent experiments. For nuclear content, Chi-squared analysis was used to assess pooled data from two independent experiments.

To further assess parasites development in liver cells, parasites grown for 68 hours in three independent experiments were stained with both rabbit anti-mCherry, (1: 250; Abcam ab167453) and mouse anti-Pf merozoite surface protein-1 (MSP-1) (1: 100; a gift from Paul Gilson, Burnet Inst) followed by Alexa Fluor 546 goat anti-rabbit IgG Probes and Alexa Fluor 488 goat anti-mouse IgG (1:1000; Molecular Probes/Thermo Fisher) for the FC^{KOmCh}-nek4-wt x FC^{WT}-nek4-ko. For the FC^{KOmCh} x FC^{WT}-GFP cross, Alexa Fluor 633 goat anti-mouse IgG and Alexa Fluor 546 goat anti-rabbit IgG (1:1000; Molecular Probes/Thermo Fisher) were used as secondary antibodies. MSP-1 expression was compared using Fisher's exact test of data pooled from three independent experiments (801 parasites assessed).

To determine the ability of parasites to complete liver stage development *in-vitro*, merosomes were counted at 70 hpi using an Olympus CKX41 compound fluorescence microscope at 40X magnification.

To confirm the presence of FC knockout parasites in liver by PCR, naïve mice were (IV) infected with 20,000 sporozoites. Forty to 42 hours post infection, mice were sacrificed, their livers harvested and genomic DNA was extracted for use as template in a nested PCR reaction. See Table 2.7.3.I, Fig 2.7.2.I for primer sequences and PCR strategy.

2.2.8 Analysis of sporozoite infectivity and ability to infect naïve mice

For bite-back infection, mosquitoes were given access to anesthetized Swiss mice (4-6 weeks old) until at least 20 mosquitoes had fed. For IV infection, salivary gland sporozoites were isolated from salivary glands 21-24 days after infection, counted and IV injected at 1000 or 10000 sporozoites/mouse. Time to patency and the subsequent development of asexual stage parasites, were monitored by fluorescence microscopy and Giemsa stained blood smears from 3 days post infection onwards. Genotyping by PCR was done as described above.

For each pyrimethamine selection of FC^{KOmCh} parasites, two mice were simultaneously infected from a single cage of mosquitoes. One mouse was given pyrimethamine in its drinking water (70µg/ ml: Sigma) while the other was not treated. Once parasites were detected in the untreated mice, they were analysed for fluorescence and genotype and then given pyrimethamine in drinking water (70µg/ ml) to clear all the parasites. After parasites were cleared (day 4) pyrimethamine was removed and mice were observed for 7 days to test for recrudescence.

2.2.9 Statistical analysis

All statistical analysis was done using GraphPad Prism (GraphPad Software, La Jolla California USA).

2.3 Results

2.3.1 Deletion of the ferrochelatase gene arrests parasite development in the oocysts stage

Pb ANKA_114070 encodes FC, the last enzyme of the heme biosynthesis pathway (24). The *Pb* ANKA_114070 locus was interrupted by double cross over homologous recombination introducing the selectable marker, human dihydrofolate reductase (*h*DHFR) fused to a fluorescent mCherry tag and driven by the constitutive *Pb* EF-1α promoter, into the FC coding sequence (Fig 2.7.2.I). Parasites carrying this FC deletion are denoted as FC^{KOmCh}. When *Anopheles stephensi* mosquitoes fed on mice infected with FC^{KOmCh}, oocysts developed in these mosquitoes but no salivary gland sporozoites were observed (Table 2.6.1). This is consistent with previous reports that FC is dispensable at the blood stage and early sexual stages but crucial for completion of sporozoite development (12,13,16).

2.3.2 Crossing ferrochelatase deficient parasites with those carrying a wildtype ferrochelatase gene complements the defect in oocyst development and sporozoite production

To determine if the effects of the FC deletion during the mosquito stage could be complemented by a wildtype copy of the allele (denoted FC^{WT}), I crossed the FC^{KOmCh} with two different strains carrying intact FC genes: either FC^{WT} parasites expressing GFP inserted into the intergenic locus of chromosome 6 (19), or a female sterile line FC^{WT}-nek-4ko (18). To control for any effects of fluorophore expression on oocyst generation and development, I also generated control crosses of the fluorescent lines with parasites with a wildtype FC locus. Mice were dual infected and *A. stephensi* mosquitoes fed on these dual infected mice to generate the various crosses. Expected genotypes of the oocysts and sporozoites from the two crosses are depicted in Figs 2.6.4. A, B.

The replacement of the FC coding region with *h*DHFR fused to mCherry in FC^{KOmCh} parasites allows tracking of FC^{KO} genotype throughout sexual reproduction. In mosquitoes fed on mice infected with both FC^{KOmCh} and FC^{WT}-GFP, after sexual recombination and oocyst formation in mosquitoes, three oocyst genotypes could be

identified 12 days post infection: FC^{KOmCh} (red), FC^{WT}-GFP (green), and FC^{KOmCh} x FC^{WT}-GFP recombinants (orange) (Fig 2.6.4.C).

Mosquito infectivity, as measured by infection rate and oocyst load, was not significantly different (P>.05, one-way ANOVA) between FC^{KOmCh} and FC^{WT}-mCh parasites when crossed to either FC^{WT}-GFP or FC^{WT}-nek-4ko parasites (Table 2.6.1). This confirms previous findings (12, 15) that the parasite heme synthesis enzymes do not play an essential role in the early mosquito life stages in *P. berghei*.

FC deletion restricts the growth of oocysts (Figs 2.6.4. C, D). Fluorescence tags allowed determining the genotype (presence/absence of active FC gene) of each oocyst. In the FC^{KOmCh} x FC^{WT}-GFP cross, oocysts with only mCherry fluorescence (red) are the product of FC^{KOmCh} self-fertilization, and they exhibit the reduced oocyst growth phenotype (Figs 2.6.4. C, D) characteristic of parasites lacking ferrochelatase, or other heme synthesizing enzymes (15). FC^{KOmCh} self-fertilized parasites (red in the cross) are not significantly different in size to oocysts produced when mosquitoes are infected with FC^{KOmCh} alone (Fig 2.6.4.D). In contrast, orange oocysts, which carry both FC^{KOmCh} and FC^{WT}-GFP genes, are significantly larger than exclusively FC^{KO} oocysts (red) and equivalent in size to FC^{WT}-GFP oocysts (green), which are self-fertilized progeny of the GFP containing parent from FC^{KOmCh} x FC^{WT}-GFP.

A comparable increase in size was also seen in the oocysts from the FC^{KOmCh}-nek-4wt x FC^{WT}-mCh-nek-4ko cross. Because the FC^{WT}-mCh-nek-4ko line is female sterile (18), no colourless oocysts were produced, and in the absence of a second fluorophore it is not possible to distinguish FC^{KOmCh} nek-4wt self-fertilization oocysts (red) from FC^{KOmCh} nek-4wt x FC^{WT}-mCh-nek-4ko recombinants (red). Nevertheless, the mCherry expressing oocysts from the FC^{KOmCh} nek-4wt x FC^{WT}-mCh-nek-4ko cross are, on average, significantly larger than oocysts arising from infections with FC^{KOmCh} alone (Fig 2.6.4.D).

Complementation of the FC knockout by crossing to FC^{WT} strains not only restored normal oocyst growth but also enabled development of sporozoites, with robust numbers of salivary gland sporozoites produced in all our crosses (Table 2.6.1). Red sporozoites could be observed in the mosquito midgut at day 17 and in the salivary glands at day 21 post-infection (Fig 2.6.4.E). Sporozoites contain only a single haploid nucleus, so red sporozoites predict the presence of FC^{KOmCh} genotype in the sporozoites

generated by the cross and this was confirmed by PCR (Fig 2.6.4.F). Therefore, it is concluded that introduction of a wildtype FC gene by sexual crossing can restore oocyst growth and sporozoite production to FC^{KO} parasites. It was noted that all the sporozoites from the FC^{KOmCh} nek-4wt x FC^{WT}-nek-4ko cross were red, despite the expectation that half of the sporozoite population should carry the colourless FC^{WT} genotype and, therefore, not fluoresce. The presence of both FC^{KOmCh} and FC^{WT} parasites was confirmed by PCR (Fig 2.6.4.F). This suggests that fluorescent protein was being carried over from the oocyst and interfering with visual genotyping of sporozoites in the midgut and salivary glands.

To further examine the apparent carryover of fluorescent protein from the oocyst to the sporozoites, the parasites with either GFP or tdTomato inserted in the same genetic locus (Fig 2.6.5.A), namely the intergenic region of chromosome 6 (19) were crossed (the experiment was performed by Dr Dean Goodman). Oocysts from this cross exhibited three different colours (green, red and orange) indicating that the lines had successfully crossed and also self-fertilised (Fig 2.6.5.B). Unlike the polyploid oocysts, haploid sporozoite progeny from this cross can inherit only one fluorophore gene, either GFP or tdTomato (Fig 2.6.5.A). Nevertheless, in addition to exclusively green or red sporozoites, many sporozoites that contained both fluorophores were observed (orange parasites highlighted with arrows in Fig 2.6.5.C). I conclude that sporozoite formation involves carryover of significant oocyst cytoplasm, resulting in dual-coloured sporozoites emerging from the heterozygous oocysts. All parasites had reverted to exclusively GFP or tdTomato once the sporozoites invaded liver cells and developed into early exoerythrocytic forms (Fig 2.6.5.B). Similarly, only red or green parasites were observed when these parasites progressed in to blood stage following bite-back (Fig 2.6.5.B).

2.3.3 FC^{KO} sporozoites are liver infective both *in-vitro* and *in-vivo* but have severe growth defects and fail to complete liver stage development

To examine the viability of FC^{KOmCh} sporozoites, their motility *in-vitro*, and infectivity both *in-vitro* and *in-vivo* were tested. No significant difference between the number of motile sporozoites, or in their levels of motility, was observed between FC^{KOmCh} and FC^{WT} sporozoites (Table 2.7.3.II, Fig 2.7.2.II). FC^{WT} parasites had slightly more

sporozoites with maximal motility (> 10 trails), but this difference was not statistically significant (P>0.05).

Sporozoites recovered from complemented FC^{KOmCh} lines were used to infect *in-vitro* cultures of HepG2 liver cells, and parasite development was assessed by IFA at 24, 48 and 68 hours. By 24 hours, any residual fluorescent protein seen in the sporozoites is lost and the liver parasites can be unequivocally genotyped by fluorescence expression, with mCherry expression denoting the FC^{KOmCh} genotype. FC^{KOmCh} liver parasites (red) could be detected at 24, 48 and even 68 hours post infection from either of the complementation crosses (Fig 2.6.6.A). The FC^{KOmCh} (red) parasites were smaller than FC^{WT} parasites at all three time points, although the difference only becomes statistically significant at 48 and 68 hours (Figs 2.6.6. A,B). This size defect correlated with a significant reduction (P<0.0001) in the number of nuclei produced in FC^{KOmCh} parasites at 68 hpi (Fig 2.6.6.C). To further assess progress through liver stage development, the production of merozoite surface protein-1 (MSP-1) was measured in FC^{KOmCh} parasites. Significantly fewer FC^{KOmCh} parasites (45%) were MSP-1 positive than FC^{WT} type parasites (79%) (Fig 2.6.6.D, P<0.001) suggesting a mid-stage liver stage defect (25-28).

To determine if the smaller size, reduced nuclear content, and impaired MSP-1 expression in FC^{KOmCh} liver stage parasites foreshadowed an inability to complete the liver stage of the life cycle merosomes were counted, which are groups of membrane-bound merozoites that bud off the infected liver cell and represent the end-product of the parasite's liver stage development (29). Merosomes were readily recovered, but none contained red fluorescent parasites, indicating that FC^{KOmCh} parasites could not complete the liver stage *in-vitro* (Table 2.6.2). Thus, it was concluded that FC^{KOmCh} parasites can infect liver cells *in-vitro* but cannot complete liver stage development.

To assay FC^{KOmCh} liver development *in-vivo*, both bite-back and IV injection of purified salivary gland sporozoites were used to infect naïve mice. Positive PCR of FC^{KOmCh} parasites in mice livers 40-42 hours after IV injection of complemented sporozoites demonstrate that these parasites can successfully infect mouse hepatocytes *in-vivo* (Fig. 2.6.4.F). To test if FC^{KOmCh} parasites could complete the liver stage in naïve mice, blood stage parasites were tested by microscopy and PCR. Blood stage patency was achieved in standard times frames from either mosquito bites or intravenous injection of

sporozoites from each of crosses, including those with FC^{KOmCh} parasites as one parent (Table 2.6.1). However, fluorescence microscopy revealed no mCherry expressing parasites in any of the infected mice (Fig 2.6.7.A) indicating that parasites carrying FC^{KOmCh} could not complete the liver stage *in-vivo*. All other expected gene combinations following recombination were detected by PCR, including the nek-4ko allele transmitted via the male FC^{WT}-nek-4ko gamete, confirming that recombination had occurred (Figs 2.6.7.B, 2.7.2.III).

To exclude the possibility that FC^{KOmCh} parasites were present at levels below the threshold of detection by microscopy or PCR, pyrimethamine selection was applied to the P0 mice infected with sporozoites generated by the FC^{KOmCh} x FC^{WT}-GFP cross. The FC^{WT}-GFP parasites lack pyrimethamine resistance, so drug pressure should selectively recover any FC^{KOmCh} parasites (in which *h*DHFR disrupts their FC gene) that had completed the liver stage. Following infection with sporozoites from the FC^{KOmCh} x FC^{WT}-GFP cross, one group of mice was immediately treated with pyrimethamine. These mice remained free of parasites for 14 days after infection. A second group of mice were left untreated following sporozoite infection and then treated with pyrimethamine after the infection was established (7 days after infection). All parasites were cleared after four days of pyrimethamine treatment, and no recrudescence was detected. These experiments eliminate the possibility that a small number of FC^{KOmCh} parasites complete the liver stage but are being masked by a larger population of FC^{WT} parasites. This confirms that the deletion of FC is lethal during the exoerythrocytic stage of *P. berghei*. FC^{KOmCh} parasites can establish, but not complete, a liver stage infection and this prevents them from generating a blood stage infection.

2.4 Discussion

I confirmed that *P. berghei* rodent malaria parasites with a disrupted FC gene are viable during blood stage, can infect mosquitos and produce oocysts, but that these oocysts fail to produce sporozoites. As with many other mutants with their first observable effect in the mosquito stage, the absolute block in sporozoite production by heme pathway deletion mutants essentially prevents any subsequent assessment of the viability of these mutants in the sporozoite and liver stages. Aim of this study was to create a simple genetic system to complement the deletion of any mosquito stage essential gene using a heme enzyme as a test case. It has been a common strategy in *Plasmodium* parasites that can be transmitted in the lab, to complement mosquito stage defects by crossing mutant parasites to wildtype parasites (Table 2.7.3.III). This simple technique takes advantage of the heterokaryotic, polyploid nature of the mosquito stages to determine if the deleted gene is essential for transmission. However, this approach does not allow phenotypic analysis in the early stages of the mammalian infection because it yields a mixed population of wildtype and mutants parasites that are indistinguishable from each other. By inserting a fluorescent marker into the deleted locus, I can definitively identify mutant parasites following recombination, thus enabling phenotypic characterization of these parasites during liver stages. Using this technique, I analysed the late mosquito, and early mammalian stage phenotype of the final enzyme in heme synthesis, FC.

It was possible to generate haploid FC^{KO} sporozoites (Fig 2.6.4.F), and (in agreement with findings for parasites lacking ALAS but chemically complemented with d-ALA) these FC^{KOmCh} sporozoites showed no significant defects in motility (Fig 2.7.2.II, Table 2.7.3.II) and could infect liver cells both *in-vivo* and *in-vitro* (Figs 2.6.4.F, 2.6.6). ALAS is the first enzyme in the heme synthesis pathway and FC is the last, so it is reasonable to assume that the entire synthesis pathway is not essential for sporozoites. It is noted, however, that all sporozoites from the forced outcross to a colourless, female sterile parasite line (FC^{WT}-nek-4ko) contained mCherry, even though the genotyping confirmed the presence of sporozoites carrying the non-fluorescent FC^{WT} locus (Fig 2.6.4.F). This suggested significant carryover of mRNA, protein and/or heme from the cytoplasm of the multinucleate oocyst that could transiently complement FC^{KOmCh} sporozoites. By crossing parasites expressing different fluorophores from the same genetic locus it was confirmed that sporozoites can contain proteins expressed in the oocyst even when they lack the gene encoding these proteins (Fig 2.6.5). Therefore, the

FC^{KOmCh} sporozoite phenotypic data must be interpreted with caution until further studies clarify the nature and persistence of the products carried over from the shared oocyst cytoplasm to the haploid sporozoite.

Parasites in mosquito and hepatic cells are postulated to have fewer host cell resources available to them in comparison to parasites in the erythrocytic environment (14). Indeed, mitochondrial chemiosmotic respiration is significantly increased as parasites transition to the non-red blood cell stages, reflecting the activation of oxidative phosporyhylation to generate ATP (30). Thus, it is not surprising that this stage has high demands for heme cores for cytochromes and that *de novo* heme biosynthesis is essential during the protracted oocyst stage of the *Plasmodium* life cycle, (5, 12, 13, 15). Supplementing ALAS deficient parasites by exogenously applying the product of this enzyme during the mosquito stages has proven an elegant method to look at the role of the initial heme synthesis enzyme in the liver stage of parasite development (12, 15). However, the complexity of the *Plasmodium* heme biosynthetic pathway, particularly being spread over three cellular compartments, suggests that the parasite may have differential abilities to compensate for loss of heme pathway components.

In this system, the specific phenotype of FC deficient parasites could be assessed throughout the entirety of liver stage development. Reassuringly, at the first phenotypic assessment at 24 hours, parasites could be definitively classified based on the expression of mCherry, suggesting there is no detectable carry-over of fluorphores, and presumably other proteins, from the sporozoite at this early liver stage. It remains possible that very early liver stage development could be affected by residual protein from the oocyst, although the absence of any oocyst derived fluorphores at 24 hours post infection suggest a very limited contribution of oocyst derived products to overall development in the liver stage. mCherry expressing FC knockout parasites were present throughout the life cycle up to 68 hpi, but these had significant growth defects that arrest their progress in the middle of liver stage development. The reduced expression of MSP-1 (Fig 2.6.6.D) further suggests that FC^{KOmCh} parasites are significantly impaired in the ability to develop normally beyond ~50 hours after liver cell invasion, the point at which MSP-1 is detectable (25). This developmental block was confirmed by the slower growth rate (Figs 2.6.6. A,B), reduced number of nuclear division (Fig 2.6.6.C) and inability to complete development, as demonstrated by the inability to produce merosomes (Table 2.6.2).

In-vivo transmission confirmed the *in-vitro* liver stage phenotype of FC^{KOmCh} parasites. Mutant parasites could be detected in the mouse liver 40-42 hours after infection with sporozoites (Fig 2.6.4.F) but could not be detected in the subsequent blood stage infection by fluorescence or PCR, even when mice were infected by 10-fold more sporozoites than are required to generate 100% infection rates in the naïve mouse strain tested (Figs 2.6.7.B, 2.7.2.III, Table 2.6.1). Recovery of all other combinations possible from sexual recombination confirmed successful crossing and infection of the naïve mice (Figs 2.6.7.B, 2.7.2.III). The ability to specifically select for FC^{KOmCh} parasites using pyrimethamine treatment provided a further tool to assay for parasites carrying the FC^{KOmCh} locus, ensuring that no population of mutant parasites was present at levels below the sensitivity of our PCR screen and masked or overgrown by FC^{WT} parasites during subsequent blood stage infection. These screens also support the specific link between the observed phenotype and the FC locus. Rigorous, discipline-standard experimental technique in the development of the FC^{KOmCh} parasite line strongly supports a single, specific integration in this parasite line. However, the strict correlation observed between fluorescence, drug resistance and the FC gene deletion following sexual recombination and drug selection confirms that the observed phenotype is specifically caused by deletion of the FC locus.

Deletion of FC causes a different defect in parasite liver stage growth both *in-vitro* and *in-vivo* than that observed for parasites lacking the upstream heme pathway enzyme ALAS (15). Although it was initially reported that ALAS activity is essential to generate infectious sporozoites (12), a subsequent study found that *P. berghei* parasites can partially compensate for the loss of ALAS activity (15) allowing them to maintain limited infectivity *in-vivo* (15). An *in-vitro* analysis showed that these parasites can complete the liver stage and produce a limited number of merosomes in the absence of ALAS activity (15) presumably by scavenging sufficient d-ALA from the host cell to compensate for the loss of this enzyme. In contrast, our data suggest such scavenging cannot compensate for the lack of FC activity. The *in-vitro* liver stage phenotype observed for FC^{KOmCh} parasites is far more severe than that for parasites lacking ALAS and no merosome production was observed. This agrees with the *in-vivo* findings that FC^{KOmCh} parasites can infect the liver but not complete this life stage.

The marked difference between knockouts of the first enzyme in the synthesis pathway and the last, likely relates to differences in the stability of the two products and their localization within the host cell. Heme is a highly reactive molecule that can be a significant generator of oxygen radicals (31), whereas d-ALA is stable enough to survive prolonged periods in culture or in sucrose solution fed to mosquitoes. After d-ALA formation by ALAS in the host mitochondrion, this substrate is transported to the host cell cytoplasm where ALAD, the next enzyme in the pathway is located. This makes it much more likely that salvageable levels of d-ALA are available in the host liver cell cytoplasm. In contrast, in a hepatic cell FC, and the heme it produces, are located in the mitochondrion. This organellar localization is likely to restrict the free diffusion of reactive heme into the liver cell cytoplasm, where the parasite is located, thus preventing the parasite from salvaging enough heme to compensate for a loss of the FC enzyme. By contrast, red blood cells lack any internal cellular structure, so parasites are surrounded by all the enzymes of the heme pathway and by copious amounts of cytosolic haemoglobin. Parasites are also actively degrading haemoglobin in their food vacuole, making more heme available and apparently rendering FC dispensable at this stage (12, 13, 16).

The essential nature of FC during the *P. berghei* liver stages described here completes the picture of heme requirements, either endogenous or scavenged, for survival across all stages of the parasite life cycle. It also contrasts the differing ability of the parasite to scavenge host resources to compensate for a loss of enzymes in the *de novo* synthesis pathway. In the red blood cell, the abundance of freely accessible heme, heme pathway intermediates and host cell enzymes allows the parasite to rely on scavenging to meet its heme needs. Host resources appear less available or less accessible during the mosquito stages, making a loss of any heme-synthesizing enzyme during the insect stage lethal. Sporozoites apparently do not require heme synthesis, perhaps having sufficient heme on board after sporogony to underpin their needs. Alternatively, sporozoites would have to scavenge for their heme requirements in the mosquito hemocoel, vertebrate skin, blood capillaries and liver. The liver stage appears more complicated, with the parasites able to partially compensate for the loss of ALAS by scavenging d-ALA from the host cytoplasm. However, in the absence of FC parasites are unable to access sufficient quantities of host heme (or FC) to survive this stage. This suggests that targeting heme synthesis with prophylactic drugs in the parasite and host cells is still

possible, but must be carefully considered, given the ability of the parasite to compensate for the loss of certain steps in the pathway. In contrast, the phenotype of parasites lacking FC suggests that heme synthesis may not be an ideal pathway to target for genetic attenuation vaccine strategies, which are more effective the longer the parasite grows in the liver (32).

Despite its importance in vaccine development and prophylaxis, hepatic growth of malaria parasites remains one of the least explored areas of parasite biology. Reverse genetic approaches to liver stage analysis have been hampered by two aspects of *Plasmodium* molecular genetics: only blood stages can be genetically modified, and getting from the blood stage to the liver stages means that these genetically modified parasites must traverse the entire life cycle. Thus, analysis of liver stage phenotypes was compromised by the difficulty in generating infectious sporozoites in mutant parasites with lethal phenotypes at earlier life stages. The complementation strategy outlined here presents a straightforward, simple to implement, and widely applicable approach to extending the analysis window for the burgeoning list of gene mutations (Table 2.7.3.III) that show their first effects during the mosquito stages. Thus, complementation provides a powerful tool to dissect the biology of the parasite during its earliest, most vulnerable stage in the mammalian host.

2.5 References

1. WHO. World malaria report 2013: World Health Organization; 2014.
2. Jambou R, El-Assaad F, Combes V, Grau GE. *In-vitro* culture of *Plasmodium berghei*-ANKA maintains infectivity of mouse erythrocytes inducing cerebral malaria. Malaria Journal. 2011;10:346.
3. Kooij TW, Carlton JM, Bidwell SL, Hall N, Ramesar J, Janse CJ, et al. A *Plasmodium* whole-genome synteny map: Indels and synteny breakpoints as foci for species-specific genes. PLoS Pathogens. 2005;1:e44.
4. Carvalho TG, Thiberge S, Sakamoto H, Menard R. Conditional mutagenesis using site-specific recombination in *Plasmodium berghei*. Proceedings of the National Academy of Sciences of the United States of America. 2004;101:14931-6.
5. Sturm A, Mollard V, Cozijnsen A, Goodman CD, McFadden GI. Mitochondrial ATP synthase is dispensable in blood-stage *Plasmodium berghei* rodent malaria but essential in the mosquito phase. Proceedings of the National Academy of Sciences of the United States of America. 2015;112:10216-23.
6. Prudencio M, Mota MM, Mendes AM. A toolbox to study liver stage malaria. Trends in Parasitology. 2011;27:565-74.
7. Lacroix C, Giovannini D, Combe A, Bargieri DY, Spath S, Panchal D, et al. Flp/frt-mediated conditional mutagenesis in pre-erythrocytic stages of *Plasmodium berghei*. Nature Protocols. 2011;6:1412-28.
8. Kalanon M, Bargieri D, Sturm A, Matthews K, Ghosh S, Goodman CD, et al. The *Plasmodium* translocon of exported proteins component EXP2 is critical for establishing a patent malaria infection in mice. Cellular Microbiology. 2016;18:399-412.
9. Suarez C, Volkmann K, Gomes AR, Billker O, Blackman MJ. The malarial serine protease SUB1 plays an essential role in parasite liver stage development. PLoS Pathogens. 2013;9:e1003811.
10. de Koning-Ward TF, Gilson PR, Crabb BS. Advances in molecular genetic systems in malaria. Nature Reviews Microbiology. 2015;13:373-87.
11. Surolia N, Padmanaban G. *De novo* biosynthesis of heme offers a new chemotherapeutic target in the human malarial parasite. Biochemical and Biophysical Research Communications. 1992;187:744-50.

12. Nagaraj VA, Sundaram B, Varadarajan NM, Subramani PA, Kalappa DM, Ghosh SK, et al. Malaria parasite-synthesized heme is essential in the mosquito and liver stages and complements host heme in the blood stages of infection. PLoS Pathogens. 2013;9:e1003522.

13. Ke HJ, Sigala PA, Miura K, Morrisey JM, Mather MW, Crowley JR, et al. The heme biosynthesis pathway is essential for *Plasmodium falciparum* development in mosquito stage but not in blood stages. Journal of Biological Chemistry. 2014;289:34827-37.

14. Sigala PA, Crowley JR, Henderson JP, Goldberg DE. Deconvoluting heme biosynthesis to target blood-stage malaria parasites. Elife. 2015;4.

15. Rizopoulos Z, Matuschewski K, Haussig J. Distinct prominent roles for enzymes of *Plasmodium berghei* heme biosynthesis in sporozoite and liver stage maturation. Infection and Immunity. 2016.

16. Smith CM, Jerkovic A, Puy H, Winship I, Deybach JC, Gouya L, et al. Red cells from ferrochelatase-deficient erythropoietic protoporphyria patients are resistant to growth of malarial parasites. Blood. 2015;125:534-41.

17. Trueman HE, Raine JD, Florens L, Dessens JT, Mendoza J, Johnson J, et al. Functional characterization of an LCCL–lectin domain containing protein family in *Plasmodium berghei*. Journal of Parasitology. 2004;90:1062-71.

18. Reininger L, Billker O, Tewari R, Mukhopadhyay A, Fennell C, Dorin-Semblat D, et al. A NIMA-related protein kinase is essential for completion of the sexual cycle of malaria parasites. Journal of Biological Chemistry. 2005;280:31957-64.

19. Kooij TW, Rauch MM, Matuschewski K. Expansion of experimental genetics approaches for *Plasmodium berghei* with versatile transfection vectors. Molecular and Biochemical Parasitology. 2012;185:19-26.

20. Straimer J, Lee MCS, Lee AH, Zeitler B, Williams AE, Pearl JR, et al. Site-specific genome editing in *Plasmodium falciparum* using engineered zinc-finger nucleases. Nature Methods. 2012;9:993-+.

21. Janse CJ, Ramesar J, Waters AP. High-efficiency transfection and drug selection of genetically transformed blood stages of the rodent malaria parasite *Plasmodium berghei*. Nature Protocols. 2006;1:346-56.

22. Combe A, Moreira C, Ackerman S, Thiberge S, Templeton TJ, Menard R. TREP, a novel protein necessary for gliding motility of the malaria sporozoite. International Journal for Parasitology. 2009;39:489-96.

23. Sturm A, Graewe S, Franke-Fayard B, Retzlaff S, Bolte S, Roppenser B, et al. Alteration of the parasite plasma membrane and the parasitophorous vacuole membrane during exo-erythrocytic development of malaria parasites. Protist. 2009;160:51-63.

24. Ralph SA, van Dooren GG, Waller RF, Crawford MJ, Fraunholz MJ, Foth BJ, et al. Tropical infectious diseases: Metabolic maps and functions of the *Plasmodium falciparum* apicoplast. Nature Review Microbiology. 2004;2:203-16.

25. Combe A, Giovannini D, Carvalho TG, Spath S, Boisson B, Loussert C, et al. Clonal conditional mutagenesis in malaria parasites. Cell Host Microbe. 2009;5:386-96.

26. Yu M, Kumar TR, Nkrumah LJ, Coppi A, Retzlaff S, Li CD, et al. The fatty acid biosynthesis enzyme FabI plays a key role in the development of liver-stage malarial parasites. Cell Host Microbe. 2008;4:567-78.

27. Annoura T, Ploemen IH, van Schaijk BC, Sajid M, Vos MW, van Gemert GJ, et al. Assessing the adequacy of attenuation of genetically modified malaria parasite vaccine candidates. Vaccine. 2012;30:2662-70.

28. Falkard B, Kumar TR, Hecht LS, Matthews KA, Henrich PP, Gulati S, et al. A key role for lipoic acid synthesis during *Plasmodium* liver stage development. Cellular Microbiology. 2013;15:1585-604.

29. Sturm A, Amino R, van de Sand C, Regen T, Retzlaff S, Rennenberg A, et al. Manipulation of host hepatocytes by the malaria parasite for delivery into liver sinusoids. Science. 2006;313:1287-90.

30. Jacot D, Waller RF, Soldati-Favre D, MacPherson DA, MacRae JI. Apicomplexan energy metabolism: Carbon source promiscuity and the quiescence hyperbole. Trends in Parasitology. 2016;32:56-70.

31. Sigala PA, Goldberg DE. The peculiarities and paradoxes of *Plasmodium* heme metabolism. Annual Review of Microbiology, Vol 68. 2014;68:259-78.

32. Butler NS, Schmidt NW, Vaughan AM, Aly AS, Kappe SH, Harty JT. Superior antimalarial immunity after vaccination with late liver stage-arresting genetically attenuated parasites. Cell Host Microbe. 2011;9:451-62.

2.6 Tables and figures

Table 2.6.1 Life cycle progression and infectivity of FC^{KOmCh} parasites following outcrossing

Parasite lines	Number of infections	Infection rate (%)/ Oocysts per mosquito* (n=number of infected mosquitoes)	Sporozoites per mosquito (n= number of mosquitoes dissected)	Transmission to naïve mice**		Time to patency (days) **
				IV injection (n = number of sporozoites injected)	bite-back	
FC^{KOmCh} parent	2	47 ± 29/ 203 ± 34 (n=13)	0 n=22	(NA)***	0/1	N/A
FC^{KOmCh} x FC^{WT}-GFP	4	79 ± 5/ 172 ± 30 (n=33)	6367± 1206 n=72	n=1000 - 1/1 n=10000 - 1/1	4/4	4.5
FC^{WT}-mCh x FC^{WT}-GFP	3	80 ± 2/ 161 ± 33 (n=24)	6101± 233 n=78	(ND)	3/3	5
FC^{KOmCh}nek-4wt x FC^{WT}-nek-4ko	8	86 ± 4/ 181 ± 21 (n=75)	5330± 906 n=142	n=1000 - 1/1 n=10000 - 1/1	4/4	4.75
FC^{WT}-mCh-nek-4wt x FC^{WT}-nek-4ko	5	79 ± 6/ 241± 28 (n=43)	10913± 3482 n=94	n=10000 - 1/1	3/3	4.5

*The number of oocysts per midgut reflect only mCherry expressing oocysts from infected mosquitoes **Transmission and days to patency data do not include results of experiments involving pyrimethamine treatment. ****Pb* FC^{KOmCh} parasites do not produce salivary gland sporozoites when self-fertilized, so IV injection was not possible. NA= not applicable. ND = Not done. Table 2.6.2 Production of FC^{KOmCh} merosomes following outcrossing (no. of trials=3)

Table 2.6.2 Production of FC^{KOmCh} merosomes following outcrossing (no. of trials=3)

	FC^{KOmCh}	FC^{WT}-mCh
70 hours post infection	0	21.6 ± 6

Figures

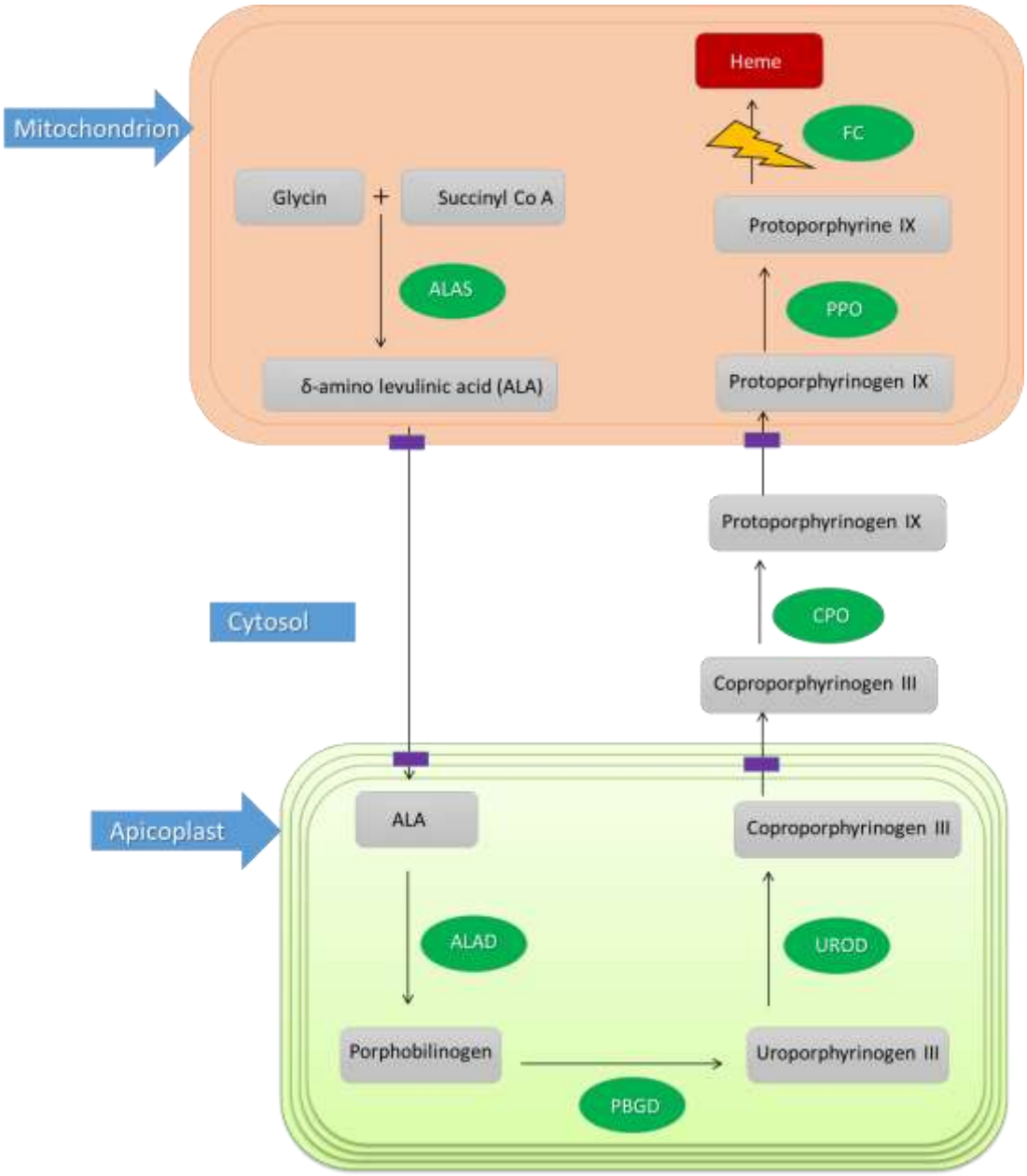

Figure 2.6.3 Heme biosynthestic pathway of malaria parasites. The seven enzymes are localized in mitochondrion, apicoplast and cytosol (12). The transporters involved in the shuttling of intermediate products are depicted as purple colour bars and are yet to be identified. The yellow colour sign in the mitochondrion shows the disruption of the pathway be deleting the FC gene.

ALAS, aminolevulinic acid synthase; ALAD**,** aminolevulinic acid dehydratase; PBGD, porphobilinogen deaminase; UROD, uroporphyrinogen decarboxylase; CPO, coproporphyrinogen oxidase; PPO, protoporphyrinogen oxidase; FC, ferrochelatase

Figure 2.6.4

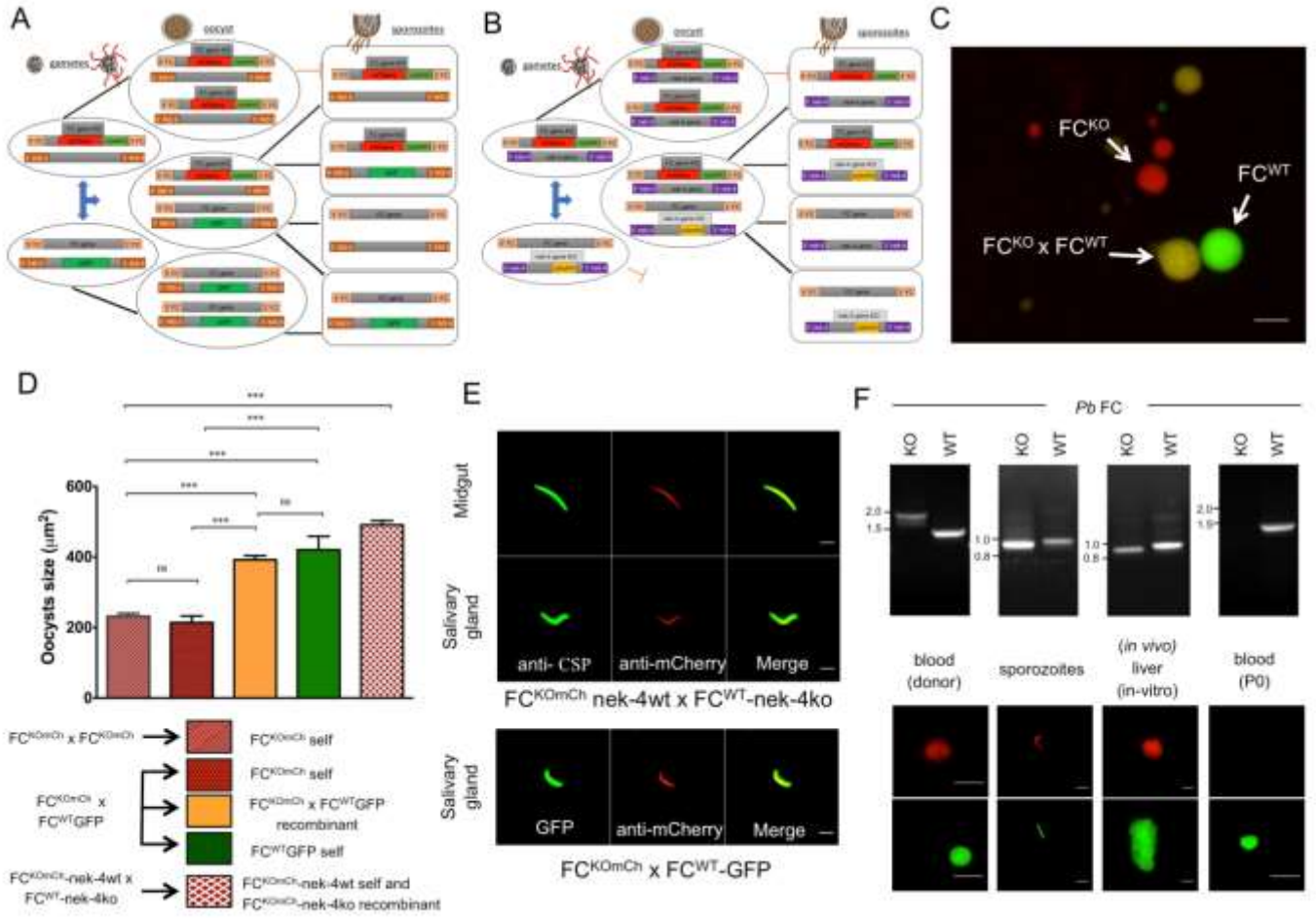
A
B
C
FC^KO
FC^WT
FC^KO x FC^WT
D
Oocysts size (µm²)
600
400
200
0
***
ns
FC^KOmCh x FC^KOmCh
FC^KOmCh self
FC^KOmCh x FC^WTGFP
recombinant
FC^WTGFP self
FC^KOmCh-nek-4wt x FC^WT-nek-4ko
FC^KOmCh-nek-4wt self and FC^KOmCh-nek-4ko recombinant
E
Midgut
Salivary gland
anti- CSP
anti-mCherry
Merge
FC^KOmCh nek-4wt x FC^WT-nek-4ko
GFP
FC^KOmCh x FC^WT-GFP
F
Pb FC
KO
WT
blood (donor)
sporozoites
(in vivo) liver (in-vitro)
blood (P0)

Figure 2.6.4 Crossing FC^{KOmCh} to FC^{WT} parasites allows normal development of FC^{KOmCh} sporozoites. (A) Schematic representation of the predicted parasite genotypes at the polyploid oocyst stage and haploid sporozoite stage after allowing mosquitoes to feed on mice dually infected with FC^{KOmCh} and FC^{WT}-GFP parasites. Three genetic combinations are possible in the polyploid oocyst: self- fertilization yielding oocysts with only the FC^{KOmCh} or the FC^{WT}-GFP allele or outcrossing creating an oocyst with both FC^{KOmCh} and the FC^{WT}-GFP alleles. Following sporogony, the parasite returns to the haploid state yielding four possible genetic combinations of the FC^{KOmCh} and the FC^{WT}-GFP genes: The original FC^{KOmCh} or FC^{WT}-GFP alleles alone, a combination of both the FC^{KOmCh} and FC^{WT}-GFP alleles or parasites carrying neither allele. (B) Schematic representation of the predicted parasite genotypes at the polyploid oocyst stage and haploid sporozoite stage after allowing mosquitoes to feed on mice dually infected with FC^{KOmCh}–nek4-wt and FC^{WT}-nek4-ko parasites. The nek4ko mutation prevents self-fertilization of this parasite line, so two genetic combinations are possible in the polyploid oocyst: self- fertilization yielding oocysts with only the FC^{KOmCh} allele or outcrossing creating an oocyst with both FC^{KOmCh} and the FC^{WT}-nek4ko alleles. Following sporogony, the parasite returns to the haploid state yielding four possible genetic combinations of the FC^{KOmCh} and the FC^{WT}-nek4ko genes: The original FC^{KOmCh} or FC^{WT}-nek4ko alleles alone, a combination of both the FC^{KOmCh} and FC^{WT}-nek4ko alleles or parasites carrying neither allele. (C) A midgut infected by feeding on an FC^{KOmCh} x FC^{WT}-GFP infected mouse showing the presence of the three oocyst phenotypes. Red oocysts are self-fertilized FC^{KOmCh} parasites, green are self-fertilized FC^{WT}-GFP, and orange oocysts are FC^{KOmCh} x FC^{WT}-GFP recombinants. Scale bar: 20µm. (D) Complementation of the FC^{KO} phenotype demonstrated by comparing the mean surface area of oocysts from FC^{KOmCh} self-fertilization with oocysts produced by the FC^{KOmCh} x FC^{WT}-GFP and FC^{KOmCh} nek-4wt x FC^{WT}-nek-4ko crosses. The female specific defect resulting from the nek4-ko genotype prevents development of colourless FC^{WT}-nek-4ko oocysts, so all oocysts produced from FC^{KOmCh} nek-4wt x FC^{WT}-nek-4ko crosses carry the FC^{KOmCh} and are red in colour. ns; not significant, *** - *P* value <0.0001 (Student t test) (E) Immunofluorescence assay showing the presence of mCherry fluorescence, and hence the presence of the FC^{KOmCh} allele in midgut (day 17 post infection) and salivary gland (day 21 post infection) sporozoites from the FC^{KOmCh} nek-4wt x FC^{WT}-nek-4ko cross and the salivary gland sporozoites from the FC^{KOmCh} x FC^{WT}-GFP cross. Scale bar: 10µm F) FC genotype (by PCR) and matching fluorescent

phenotype of parasites through the complete life cycle showing the presence of parasites carrying both the FC^{KOmCh} and FC^{WT} genes from donor blood stage, sporozoites to the liver stage of the life cycle. Liver stage; PCR shows the *in-vivo* parasite growth and the corresponding fluorescence image shows the *in-vitro* liver parasites. Parasites carrying the FC^{KOmCh} fail to complete liver stage development so neither red fluorescence nor the FC^{KOmCh} gene are detectable in the subsequent blood stage infection. Sporozoite and liver stage genotypes were assessed with a nested PCR reaction, yielding a band of different size to that seen in blood stages. Scale bar: 10μm

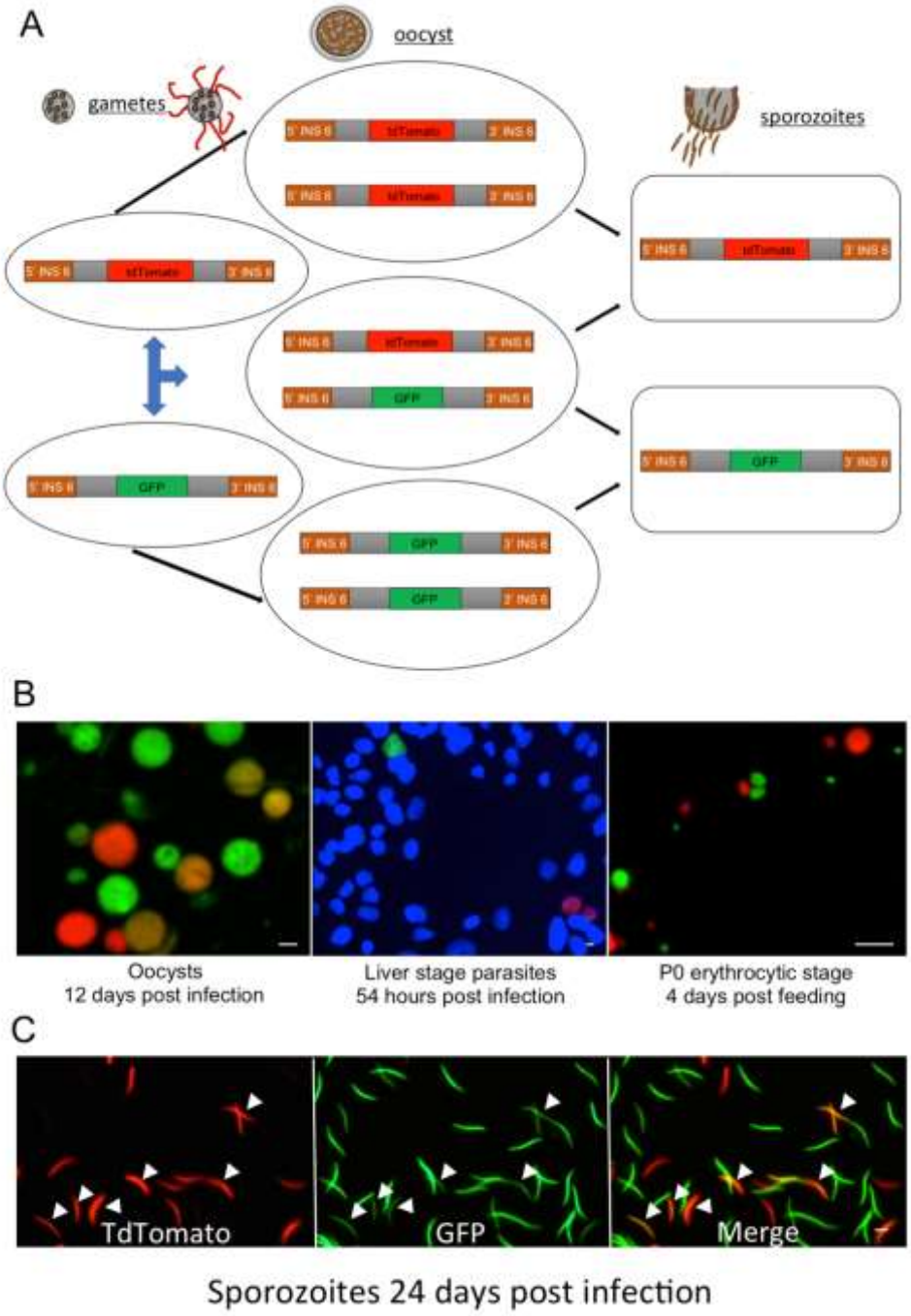

Figure 2.6.5 Sporozoite development involves significant carryover of oocyst cytoplasm. (A) Schematic representation of the predicted parasite genotypes at the polyploid oocyst stage and haploid sporozoite stage after allowing mosquitoes to feed on mice dually infected with parasites expressing either GFP or tdTomato. The fluorophore is inserted into the same genetic locus in each parasite line, so three genetic combinations are possible in the polyploid oocyst: self- fertilization yielding oocysts with either the GFP or tdTomato allele, whereas outcrossing generates a heterzygous

oocyst with both the GFP and tdTomato alleles. Following sporogony, the parasite returns to the haploid state and can carry either the GFP or tdTomato allele, but not both. (B) Progeny of the GFP x tdTomato cross through the life cycle. Three oocyst phenotypes are present, GFP only (green) and tdTomato only (red) from self-fertilizations and heterozygous, polyploid parasites expressing both fluorophores (orange). Only two phenotypes, GFP (green) or tdTomato (red) are present in haploid liver and red blood cell stages. (C) Sporozoites generated from crossing GFP and tdTomato parasites showed many haploid sporozoites still carrying both fluorphores (arrow heads). Single colour (green or red) sporozoites are presumably offspring from self-fetilizations, while two-colour (orange) sporozoites are from recombinant oocysts.

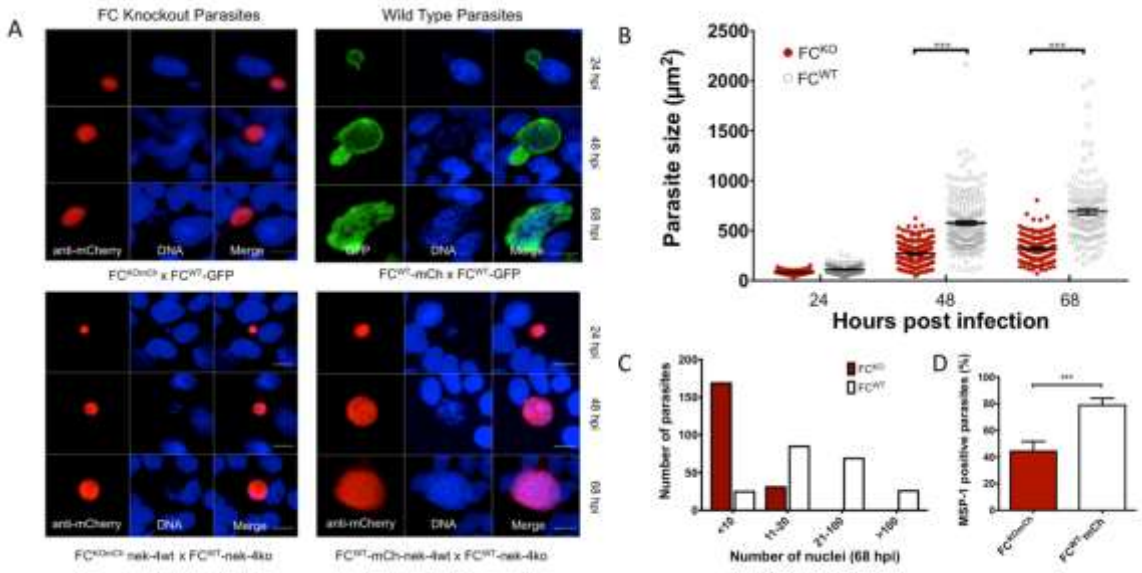

Figure 2.6.6 Parasites lacking FC have a severe liver stage growth phenotype.

(A) Immunofluorescence assay of FC^{KOmCh} and FC^{WT} parasites grown in HepG2 liver cells for 24, 48 and 68 hours post infection (hpi) showing the reduced growth of FC^{KOmCh} parasites. Scale bar 20µm. (B) Quantification of liver stage parasite size showing that FC^{KOmCh} parasites are significantly smaller than FC^{WT} parasites after 48 and 68 hours of incubation in HepG2 cells. *** - P value < 0.0001 (Student t-test), data pooled from six independent experiments. (C) Quantification of parasite nuclei 68 hours after infection showing that FC^{KOmCh} parasites produced significantly fewer nuclei than FC^{WT} parasites by 68 hpi. P value <0.0001 (χ^2). (D) Immunofluorescence assay of MSP-1 expression: a marker for mid to late stage parasite development in the liver stage. FC^{KOmCh} parasites have a defect in MSP-1 expression, with only 45% of FC^{KOmCh} parasites producing MSP-1 compared to 79% of FC^{WT}. *** - P value <0.001(Fisher's exact test) 801 parasites assessed, pooled from three independent experiments with no fewer than 58 parasites measured in any one sample. Error bars show 99% confidence interval.

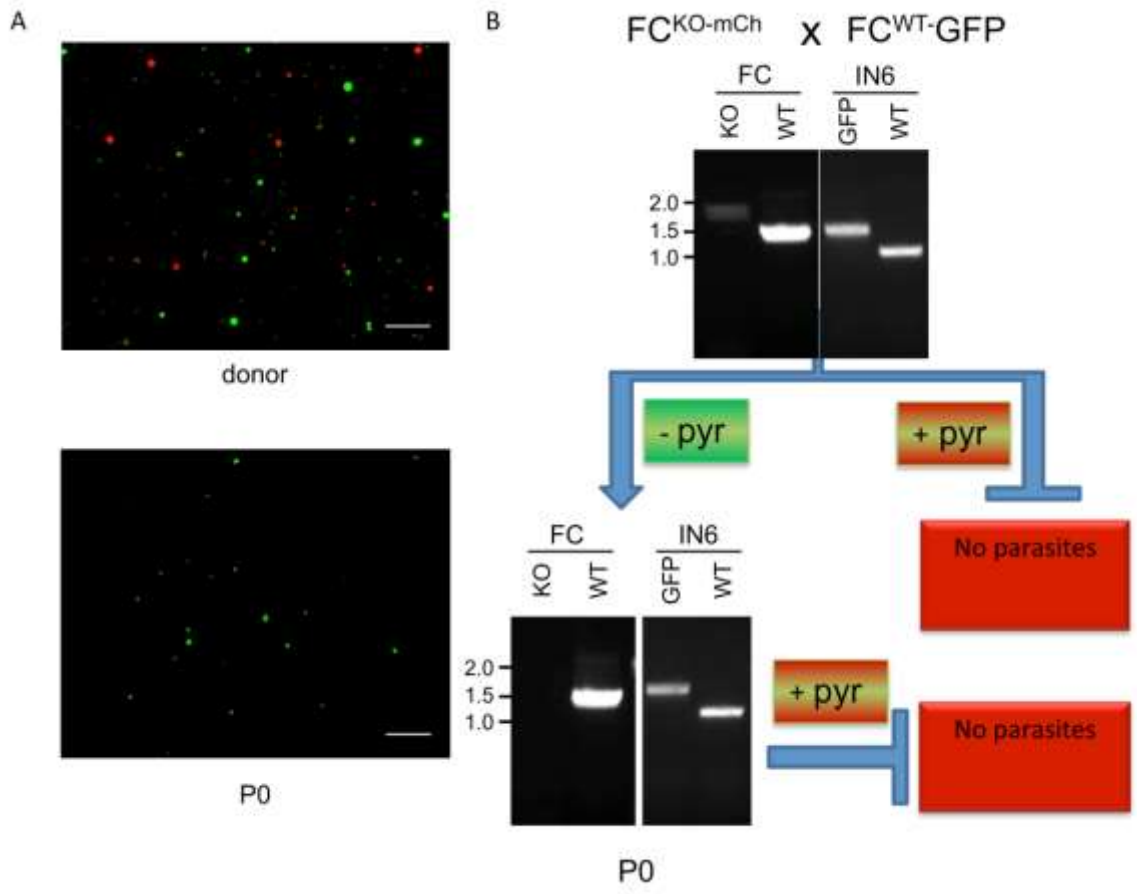

Figure 2.6.7 FC deficient parasites cannot complete the liver stage *in-vivo*

(A) Epi-fluorescent images comparing the expression of mCherry and GFP before and after transmission. Both GFP and mCherry are visible in parasites recovered from the blood of a donor mouse dual infected with FC^{KOmCh} and FC^{WT}-GFP parasites (upper panel). In contrast only GFP expression is observed in a naive mouse infected with the progeny of this cross, confirming the essential nature of FC during liver stage development. Scale bar: 100µm. (B) Summary of the genotypes and pyrimethamine resistance phenotype following infection of naïve mice with sporozoites from the FC^{KOmCh} x FC^{WT}-GFP cross. PCR screening detects parasites with both of the FC and GFP alleles in the donor mouse used to infect mosquitoes. The FC^{KOmCh} genotype cannot be detected in the blood of mice infected by parasites found in those mosquitoes, demonstrating its lethality in the liver stage. Pyrimethamine selection for parasites carrying the *h*DHFR inserted in the FC locus kills all parasites, confirming that FC^{KOmCh} sporozoites cannot infect naïve mice. FC^{WT}-GFP parasites are susceptible to pyrimethamine treatment and are, therefore, not present after drug treatment.

2.7 Supplementary data

2.7.1 Supplementary Methods

2.7.1.I Generation of pChSKLD plasmid

Human DHFR from pL0006 (MRA-775) and mCherry from pBAT (1) were amplified using primers D355-D296 and D356-D354 (Table 2.7.3.I), respectively. These primers added overlapping portions of the Viral 2A skip peptide (2) to each PCR product. The resultant fragments were used as the overlapping template in PCR with primers D356 and D296 to generate the mCherry-Skip-hDHFR insert that was cut with *BspHI*/*Xba*I and cloned into the *Xba*I/*Nco*I sites of PL0006 to create pLChSKD.

2.7.1.II Generation of FCWT-GFP, FCWT-tdTomato, and FCWT-mCherry parasite lines.

Lines expressing GFP or mCherry in the absence of a selectable marker were created in a two-step process. 5' and 3' flanks of the intergenic region of chromosome 6 corresponding to those detailed in (1) were generated by PCR using primers D331-D332 and D326-D327 (Table 2.7.3.I), respectively and cloned into the *EcoR*I/*Not*I (5') and *Apa*I/*Afl*II (3') sites of pDONR-P2/P3 (Invitrogen) to create the plasmid pINT65'3'P2-P3. The *h*DHR/*y*fcu positive-negative selectable marker cassette from pL0034 (MRA-849) was cloned into pINT65'3'P2-P3 using *Xma*I/*Pst*I. The construct was linearized with *Not*I/*Asc*I and transfected into *Pb* ANKA parasites as described in material and methods 2.2.4. Transfectants were cloned and correct integration confirmed by PCR.

GFP flanked by the HSP70 (1) 5' and 3' UTRs in pbc-GFP@hsp70 (a kind gift of Robert Menard, Institute Pasteur) was inserted into the *Sac*I/*Xma*I sites of pBluescript (Agilent) to create pBSKHG. The mCherry sequence was cut out of pLChSKD with *Avr*II/*BamH*I and cloned into the *Nhe*I/*Bgl*II site of pBSKHG, replacing the GFP to create pBSKHCh. The tdTomato sequence was amplified and cloned into pL0006 as mCherry for pLChSKD, cut with *Avr*II/*BamH*I and cloned into the *Nhe*I/*Bgl*II site of pBSKHG to create pBSKHTm. pBSKHG, pBSKHTm and pBSKHCh were cut with *Sac*I/*Xma*I to liberate the HSP705'-FP-HSP703' cassette, which was inserted into pINT65'3'P2-P3 to create pINT65'3'HG, pINT65'3'HTm, and pINT65'3'HCh. These

plasmids were linearized and transfected as above, with selection on 5-FC, and cloned. Correct gene insertion was confirmed by PCR. All parasite lines were tested in the complete life-cycle to confirm previous findings that HSP70 5' driven expression of GFP, tdTomato and mCherry in this locus does not impair parasite development (1). The fidelity of all PCR amplified products was confirmed by sequencing.

2.7.2 Supplementary figures

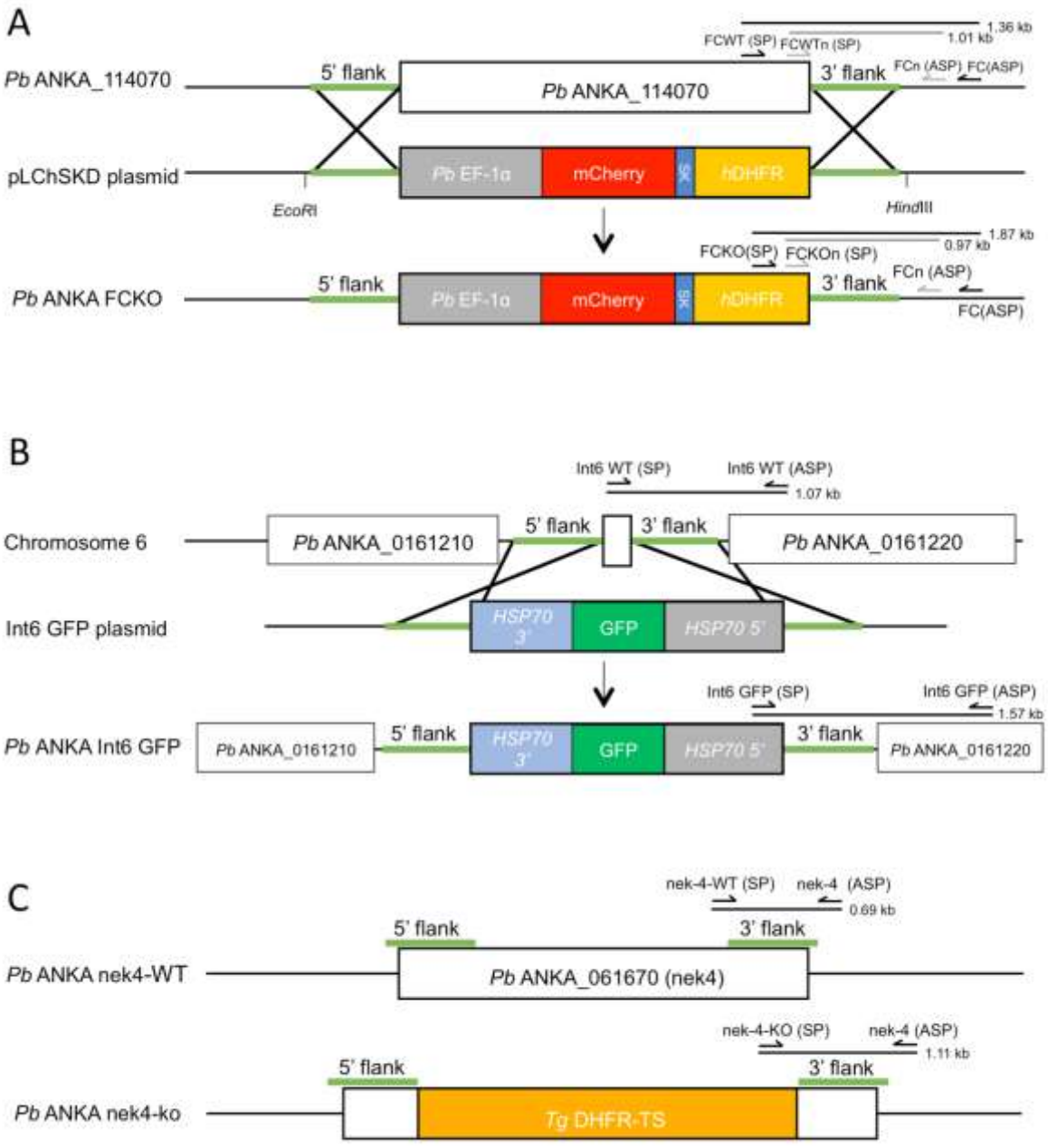

Figure 2.7.2.I: Generation of FC^{KOmCh} and FC^{WT}-GFP and PCR genotyping strategy. (A) FC^{KOmCh} (B) GFP in intergenic region of chromosome 6 (C) nek4-ko (3)

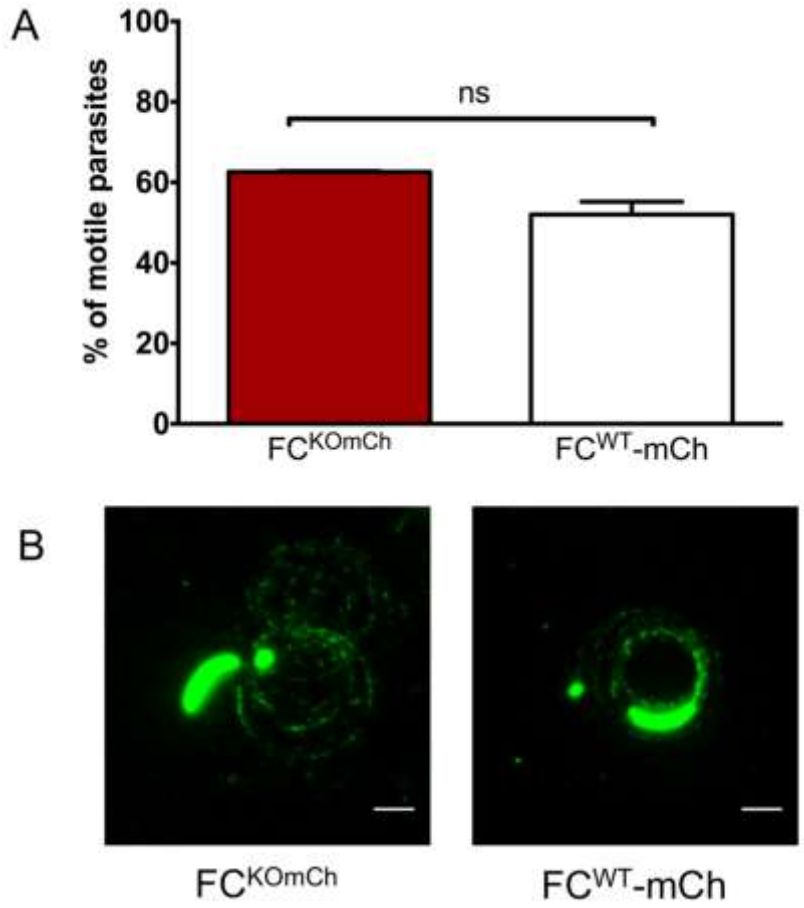

Figure 2.7.2.II: Motility of FC^{KOmCh} salivary gland sporozoites. (ns; not significant; P>.05, χ^2 test); A) percentage of motile sporozoites observed B) representative image of a motile sporozoites and trails labelled with anti-CSP/AlexaFluor 488 antibodies (green). Scale bar: 10µm

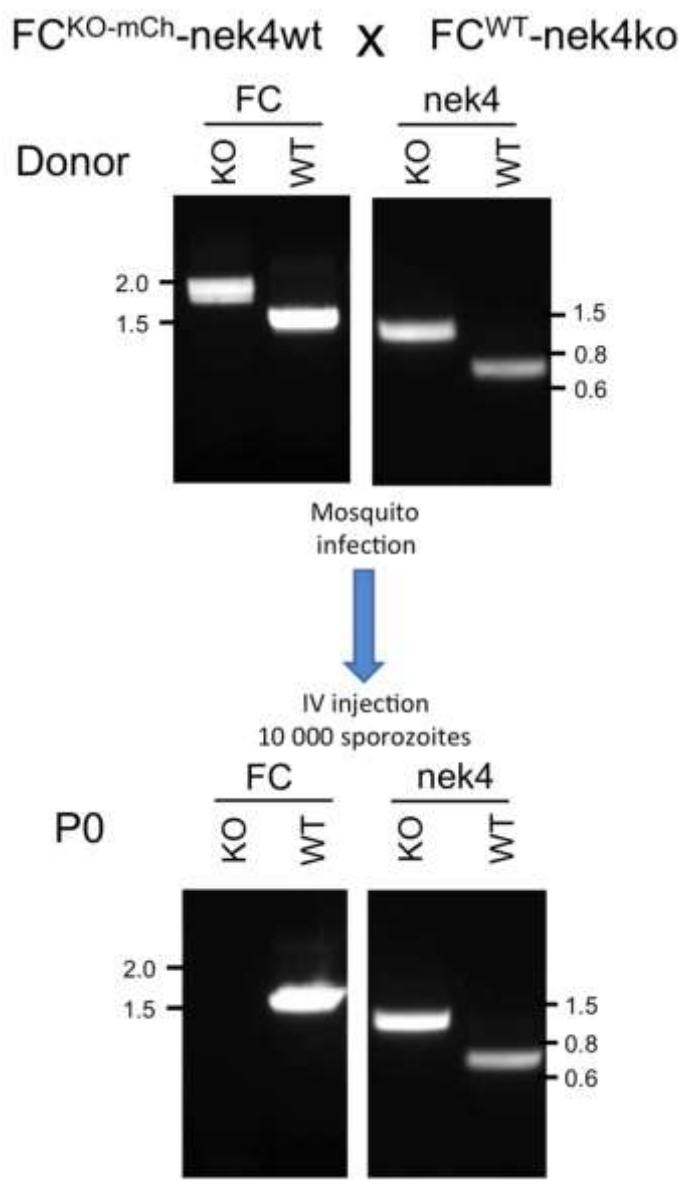

Figure 2.7.2.III: PCR genotyping of donor parasites and P0 parasites generated by crossing FC^{KOmCh} nek-4wt x FC^{WT}-mCh-nek-4ko.

2.7.3 Supplementary tables

Table 2.7.3.I: List of PCR primers and predicted product sizes

Primers	Primer sequence (restriction sites in italics)	
Vector construction		
pLChSKD		
D296 (ASP)	5'*CCTAGG*CCATCATTCTTCTCATATACTTC3'	
D354 (ASP)	5'TCCACGTCACCGATGTTAGAAGACTTCCTCTGCCCTCC CTAGGCTTGTACAGCTCGTCCATG3'	
D355 (SP)	5'AACATGCGGTGACGTGGAGGAGAATCCCGGCCCTGTC GACGTTGGTTCGCTAAACTGCA3'	
D356 (SP)	5'*TCATGA*TCATGGTGAGCAAGGGCGAGGAG3'	
FC^{WT}-GFP / FC^{WT}-mCherry		
D326 (SP)	5'*GGGCCC*GGGTTCAGGAAACTTTTGTGTG3'	
D327 (ASP)	5'*CTTAAG*GCGCGCGCCATTCAGTTTGCCTATTTGC3'	
D332 (SP)	5'*GCGGCCGC*GTTTGTATTATGCACGCAAC3'	
D333 (ASP)	5'*GAATTCGGCGCGCC*TCATTTCCCCTGAATATAG3'	
Genotype screening		
FCKO		Product size (bp)
Pb FCKO (SP)	5'GAATCACCCAGGCCATCTTA3'	1868
Pb FC (ASP)	5'TGCATCATTTTTGTGGCTTG3'	
Pb FCWT (SP)	5'TAATTTGCCCATCCTTTTCG3'	1362
Pb FC (ASP)	5'TGCATCATTTTTGTGGCTTG3'	
Pb FCKOn (SP)	5'TTTTTCCTTCAATTTCGATGGGTAC3'	965
Pb FCn (ASP)	5'ACCGAGTAACTGGATCTTCCA3'	
Pb FCWTn (SP)	5'TTCAATCATATGGAAATGGACAGTT3'	1014
Pb FCn (ASP)	5'ACCGAGTAACTGGATCTTCCA3'	
nek-4KO		
Pb nek-4 (SP)	5'TCCAGATGGAGATGGCTGTC3'	1112
Pb nek-4 (ASP)	5'CGAAGTTACATATTCAAATAGCCAAT3'	
Pb nek-4 (SP)	5'TTAGATCCCCGATTTACCAAA3'	691
Pb nek-4 (ASP)	5'CGAAGTTACATATTCAAATAGCCAAT3'	

GFP		
Pb Int6 GFP (SP)	5'AACTGAAAAAGAGCGCAAATG3'	1568
Pb Int6 GFP(ASP)	5'CCCAGAATTCCCATGAACTG3'	
Pb Int6 WT (SP)	5'GCGGCCGCGTTTGTATTATGCACGCAAC3'	1074
Pb Int6 WT (ASP)	5'TCTTGAGGAACGGATAGACAC3'	

Table 2.7.3.II: Motility of FC^{KOmCh} salivary gland sporozoites

	Trails					
	0	linear or 1/2	1	2-5	6-10	>10
$FC^{KO\text{-}mCh}$	35± 4	25± 2	12± 6	20± 3	2	0
FC^{WT}-mCh	53± 10	13± 9	9	23± 2	7± 2	4± 2

Table 2.7.3.III: Partial list of *Plasmodium* spp. pathways/genes shown to be essential for mosquito stage development that could be candidates for analysis with the described genetic complementation strategy

Description	Cellular function	Reference
ACO*	Ookinete conversion	(4)
Actin 2*	Ookinete to oocyst formation	(5)
Actin capping protein β subunit*	Oocyst formation	(6)
ALAS	Oocyst maturation	(7-9) (*P. falciparum)*
Api ap2-sp	Sporogony	(10)
Api ap2-sp2	Sporoblast formation	(10)
Api ap2-sp3	Salivary gland invasion	(10)
ATP synthase β subunit*	Oocyst formation	(11)
BCKDH	Oocyst maturation	(12)
Cap380	Oocyst maturation	(13)
c-CAP	Sporozoite production	(14)
CDLK	Sporozoite maturation	(15)
CDPK3	Ookinete motility, mosquito midgut invasion	(16, 17)
CelTOS	Ookinete midgut traversal	(18)
Chitinase	Hydrolysis of peritrophic memebrane during ookinete midgut traversal	(19, 20) (*P. falciparum*)
CPO	Oocyst maturation	(21) (*P. falciparum*)
CRMP1,2	Salivary gland invasion	(22)
CSP	Sporozoite development within oocyst and sporozoite attachment to hepatocytes	(23)
CTRP*	Oocyst formation	(24)
CYC3*	Oocyst development, maturation and sporozoite formation	(25)
ECP1	Egress from midgut oocyst	(26)
FabB/F	Oocyst to sporozoite development	(27) (*P. falciparum*)
FabI	Oocyst to sporozoite development	(27) (*P. falciparum*)

GAK	Sporozoite development	(15)
GGCS	Oocyst maturation	(28)
GluS	Oocyst development	(29)
GR	Oocyst maturation	(30, 31)
Ik2	Latency of sporozoites in salivary glands	(32)
IMC1a	Sporogony	(33)
KGDH	Oocyst formation	(34) (*P. falciparum*)
LAP1/CCp3/SR*	Oocyst maturation and sporozoite formation	(35, 36)
LAP2/CCp1*	Oocyst maturation and sporozoite formation	(35, 36)
LAP3/CCp5	Oocyst maturation and sporozoite formation	(35, 36)
LAP4/CCp2*	Oocyst maturation and sporozoite formation	(35, 36)
LAP5*	Oocyst maturation and sporozoite formation	(35-37)
LAP6*	Oocyst maturation and sporozoite formation	(36)
MAEBL	Salivary gland invasion	(38)
MAOP	Midgut invasion	(39)
MDH*	Oocyst formation	(4)
MISFIT (formin-like protein)*	Oocyst development	(40)
Nek-2,4	Ookinete genome replication	(3)
P25	Ookinete surface protein; ookinete survival in the mosquito midgut, traversal of the epithelium; ookinete-oocyst transformation	(41)
P28	Ookinete surface protein; ookinete survival in the mosquito midgut, traversal of the epithelium; ookinete-oocyst transformation	(41)
Palmityol transferase DHHC3*	Gliding motility in ookinetes and sporozoites	(42)

PANK1,2	Optimal ookinete formation and oocyst development	(30, 43)
PBGD	Oocyst maturation	(9, 21, 44) (*P. falciparum*)
PEPC*	Oocyst formation	(4)
PEPCK	Oocyst development	(29)
PK7	Oocyst development and sporogony	(15)
POS1-10	Ookinete surface protein	(45)
PPLP3-5	Ookinete midgut traversal	(45, 46)
PPM5*	Oocyst development	(47)
PSOP 1,2,6,7,12	Ookinete-secreted proteins	(45)
PSOP13*	Sporozoite development	(37)
PSOP25	Ookinete maturation and formation of oocyst	(48)
S-acyl-transferase DHHC10*	Sporozoite formation	(49)
SDH	Oocyst formation	(50)
SHLP1	Ookinete formation	(51)
SOAP	Ookinete midgut traversal	(52)
TRAP	Salivary gland invasion and infection of hepatocytes	(53)
TRP1	Oocyst egress and salivary gland invasion	(54)
Type II NADH: Ubiquinone dehydrogenase*	Oocyst maturation	(55)
UROD	Oocyst maturation	(9, 44)
WARP	Ookinete midgut traversal	(56, 57)

* Genes where knockouts have been complemented through the mosquito stage by genetic crossing but not analysed for phentoypes in the liver stage. All the genes listed here are performed with *P. berghei* unless indicated otherwise. ACO; Acotinase, ALAS; Aminolevulinic acid synthase, ApiAP2; AP2 DNA-binding domain, BCKDH; Branched-chain amino acid dehydrogenase Cap380; Capsule protein 380, c-CAP; Cyclase-associated protein, CDLK; CDPK-like kinase, CDPK; Calcium-dependent protein kinase, CelTOS; Cell-traversal protein for ookinete and sporozoites, CPO; Coproporphyrinogen oxidase, CRMP; Cysteine repeat modular protein, CSP; Circumsporozoite protein, CTRP; Circumsporozoite protein and thrombospondin-

related adhesive protein [TRAP]-related protein, CYC3; P-type cyclin 3, ECP1; Egress cysteine protease I, FabB/F; β-ketoacyl-ACP synthase II, FabI; Enoyl-ACP reductase, GAK; Cyclin G-associated kinase, GGCS; Gamma-glutamylcystein synthetase, GluS; Glutamate synthase, GR; Glutathione reductase, IK2; Initiation factor-2α kinase, IMC1a; Inner membrane complex protein, KGDH; α-keto-glutarate dehydrogenase, LAP; LCCL/ lectin adhesive-like protein 1, MAEBL; Apical membrane antigen/erythrocyte binding like protein, MAOP; Membrane-attack ookinete protein, MDH; Malate dehydrogenase, Nek; NIMA-related kinase, PANK; Putative pantothenase Kinase, PBGD; Porphobilinogen deaminase, PEPC; Phosphoenolpyruvate carboxylase, PEPCK; Phosphoenolpyruvate carboxykinase, PK7; Protein kinase 7, POS; Putative ookinete surface-associated protein, PPLP; Plasmodial perforin-like protein, PPM; Metallo-dependent protein phosphatase, PSOP; Putative secreted ookinete proteins, SDH; Succinate dehydrogenase, SHLP; *Shewanellla*-like protein phosphatase, SOAP; Secreted ookinete adhesive protein, TRAP; Thrombosponin-related adhesive protein, TRP1; Thrombosponidin-related protein, UROD; Uroporphyrinogen decarboxylase, WARP; Von Willebrand factor A domain-related protein

2.7.4 Supplementary References

1. Kooij TW, Rauch MM, Matuschewski K. Expansion of experimental genetics approaches for *Plasmodium berghei* with versatile transfection vectors. Molecular and Biochemical Parasitology. 2012;185:19-26.

2. Straimer J, Lee MCS, Lee AH, Zeitler B, Williams AE, Pearl JR, et al. Site-specific genome editing in *Plasmodium falciparum* using engineered zinc-finger nucleases. Nature Methods. 2012;9:993-98.

3. Reininger L, Billker O, Tewari R, Mukhopadhyay A, Fennell C, Dorin-Semblat D, et al. A NIMA-related protein kinase is essential for completion of the sexual cycle of malaria parasites. Journal of Biological Chemistry. 2005;280:31957-64.

4. Srivastava A, Creek DJ, Evans KJ, De Souza D, Schofield L, Muller S, et al. Host reticulocytes provide metabolic reservoirs that can be exploited by malaria parasites. PLoS Pathogens. 2015;11.

5. Andreadaki M, Morgan RN, Deligianni E, Kooij TW, Santos JM, Spanos L, et al. Genetic crosses and complementation reveal essential functions for the *Plasmodium* stage-specific actin2 in sporogonic development. Cellular Microbiology. 2014;16:751-67.

6. Ganter M, Schuler H, Matuschewski K. Vital role for the *Plasmodium* actin capping protein (CP) beta-subunit in motility of malaria sporozoites. Molecular Microbiology. 2009;74:1356-67.

7. Nagaraj VA, Sundaram B, Varadarajan NM, Subramani PA, Kalappa DM, Ghosh SK, et al. Malaria parasite-synthesized heme is essential in the mosquito and liver stages and complements host heme in the blood stages of infection. PLoS Pathogens. 2013;9.

8. Ke HJ, Sigala PA, Miura K, Morrisey JM, Mather MW, Crowley JR, et al. The heme biosynthesis pathway is essential for *Plasmodium falciparum* development in mosquito stage but not in blood stages. Journal of Biological Chemistry. 2014;289:34827-37.

9. Rizopoulos Z, Matuschewski K, Haussig J. Distinct prominent roles for enzymes of *Plasmodium berghei* heme biosynthesis in sporozoite and liver stage maturation. Infection and Immunity. 2016.

10. Modrzynska K, Pfander C, Chappell L, Yu L, Suarez C, Dundas K, et al. A knockout screen of Apiap2 genes reveals networks of interacting transcriptional regulators controlling the *Plasmodium* life cycle. Cell Host Microbe. 2017;21:11-22.

11. Sturm A, Mollard V, Cozijnsen A, Goodman CD, McFadden GI. Mitochondrial ATP synthase is dispensable in blood-stage *Plasmodium berghei* rodent malaria but essential in the mosquito phase. Proceedings of the National Academy of Sciences of the United States of America. 2015;112:10216-23.

12. Oppenheim RD, Creek DJ, Macrae JI, Modrzynska KK, Pino P, Limenitakis J, et al. BCKDH: The missing link in apicomplexan mitochondrial metabolism is required for full virulence of *Toxoplasma gondii* and *Plasmodium berghei*. PLoS Pathogens. 2014;10:e1004263.

13. Srinivasan P, Fujioka H, Jacobs-Lorena M. PbCap380, a novel oocyst capsule protein, is essential for malaria parasite survival in the mosquito. Cellular Microbiology. 2008;10:1304-12.

14. Hliscs M, Sattler JM, Tempel W, Artz JD, Dong A, Hui R, et al. Structure and function of a G-actin sequestering protein with a vital role in malaria oocyst development inside the mosquito vector. Journal of Biological Chemistry. 2010;285:11572-83.

15. Tewari R, Straschil U, Bateman A, Bohme U, Cherevach I, Gong P, et al. The systematic functional analysis of *Plasmodium* protein kinases identifies essential regulators of mosquito transmission. Cell Host Microbe. 2010;8:377-87.

16. Ishino T, Orito Y, Chinzei Y, Yuda M. A calcium-dependent protein kinase regulates *Plasmodium* ookinete access to the midgut epithelial cell. Molecular Microbiology. 2006;59:1175-84.

17. Siden-Kiamos I, Ecker A, Nybäck S, Louis C, Sinden RE, Billker O. *Plasmodium berghei* Calcium-dependent protein kinase 3 is required for ookinete gliding motility and mosquito midgut invasion. Molecular Microbiology. 2006;60:1355-63.

18. Kariu T, Ishino T, Yano K, Chinzei Y, Yuda M. CelTOS, a novel malarial protein that mediates transmission to mosquito and vertebrate hosts. Molecular Microbiology. 2006;59:1369-79.

19. Dessens JT, Mendoza J, Claudianos C, Vinetz JM, Khater E, Hassard S, et al. Knockout of the rodent malaria parasite chitinase PbCHT1 reduces infectivity to mosquitoes. Infection and Immunity. 2001;69:4041-7.

20. Tsai YL, Hayward RE, Langer RC, Fidock DA, Vinetz JM. Disruption of *Plasmodium falciparum* chitinase markedly impairs parasite invasion of mosquito midgut. Infection and Immunity. 2001;69:4048-54.

21. Sigala PA, Crowley JR, Henderson JP, Goldberg DE. Deconvoluting heme biosynthesis to target blood-stage malaria parasites. Elife. 2015;4.

22. Thompson J, Fernandez-Reyes D, Sharling L, Moore SG, Eling WM, Kyes SA, et al. *Plasmodium* cysteine repeat modular proteins 1-4: Complex proteins with roles throughout the malaria parasite life cycle. Cellular Microbiology. 2007;9:1466-80.

23. Menard R, Sultan AA, Cortes C, Altszuler R, vanDijk MR, Janse CJ, et al. Circumsporozoite protein is required for development of malaria sporozoites in mosquitoes. Nature. 1997;385:336-40.

24. Yuda M, Sakaida H, Chinzei Y. Targeted disruption of the *Plasmodium berghei* CTRP gene reveals its essential role in malaria infection of the vector mosquito. Journal of Experimental Medicine. 1999;190:1711-6.

25. Roques M, Wall RJ, Douglass AP, Ramaprasad A, Ferguson DJ, Kaindama ML, et al. *Plasmodium* P-type cyclin CYC3 modulates endomitotic growth during oocyst development in mosquitoes. PLoS Pathogens. 2015;11:e1005273.

26. Aly ASI, Matuschewski K. A malarial cysteine protease is necessary for *Plasmodium* sporozoite egress from oocysts. Journal of Experimental Medicine. 2005;202:225-30.

27. van Schaijk BCL, Kumar TRS, Vos MW, Richman A, van Gemert GJ, Li T, et al. Type II fatty acid biosynthesis is essential for *Plasmodium falciparum* sporozoite development in the midgut of *Anopheles* mosquitoes. Eukaryotic Cell. 2014;13:550-59.

28. Vega-Rodriguez J, Franke-Fayard B, Dinglasan RR, Janse CJ, Pastrana-Mena R, Waters AP, et al. The glutathione biosynthetic pathway of *Plasmodium* is essential for mosquito transmission. PLoS Pathogens. 2009;5:e1000302.

29. Srivastava A, Philip N, Hughes KR, Georgiou K, MacRae JI, Barrett MP, et al. Stage-specific changes in *Plasmodium* metabolism required for differentiation and adaptation to different host and vector environments. PLoS Pathogens. 2016;12:e1006094.

30. Pastrana-Mena R, Dinglasan RR, Franke-Fayard B, Vega-Rodriguez J, Fuentes-Caraballo M, Baerga-Ortiz A, et al. Glutathione reductase-null malaria parasites have normal blood stage growth but arrest during development in the mosquito. Journal of Biological Chemistry. 2010;285:27045-56.

31. Buchholz K, Putrianti ED, Rahlfs S, Schirmer RH, Becker K, Matuschewski K. Molecular genetics evidence for the *in-vivo* roles of the two major NADPH-dependent disulfide reductases in the malaria parasite. Journal of Biological Chemistry. 2010;285:37388-95.

32. Zhang M, Fennell C, Ranford-Cartwright L, Sakthivel R, Gueirard P, Meister S, et al. The *Plasmodium* eukaryotic initiation factor-2α kinase IK2 controls the latency of sporozoites in the mosquito salivary glands. Journal of Experimental Medicine. 2010;207:1465-74.

33. Khater EI, Sinden RE, Dessens JT. A malaria membrane skeletal protein is essential for normal morphogenesis, motility and infectivity of sporozoites. Journal of Cell Biology. 2004;167:425-32.

34. Ke H, Lewis IA, Morrisey JM, McLean KJ, Ganesan SM, Painter HJ, et al. Genetic investigation of tricarboxylic acid metabolism during the *Plasmodium falciparum* life cycle. Cell Reports. 2015;11:164-74.

35. Trueman HE, Raine JD, Florens L, Dessens JT, Mendoza J, Johnson J, et al. Functional characterization of an LCCL-lectin domain containing protein family in *Plasmodium berghei*. Journal of Parasitology. 2004;90:1062-71.

36. Raine JD, Ecker A, Mendoza J, Tewari R, Stanway RR, Sinden RE. Female inheritance of malarial lap genes is essential for mosquito transmission. PLoS Pathogens. 2007;3.

37. Ecker A, Bushell ES, Tewari R, Sinden RE. Reverse genetics screen identifies six proteins important for malaria development in the mosquito. Molecular Microbiology. 2008;70:209-20.

38. Kariu T, Yuda M, Yano K, Chinzei Y. MAEBL is essential for malarial sporozoite infection of the mosquito salivary gland. Journal of Experimental Medicine. 2002;195:1317-23.

39. Kadota K, Ishino T, Matsuyama T, Chinzei Y, Yuda M. Essential role of membrane-attack protein in malarial transmission to mosquito host. Proceedings of the National Academy of Sciences of the United States of America. 2004;101:16310-15.

40. Bushell ESC, Ecker A, Schlegelmilch T, Goulding D, Dougan G, Sinden RE, et al. Paternal effect of the nuclear formin-like protein MISFIT on *Plasmodium* development in the mosquito vector. PLoS Pathogens. 2009;5.

41. Tomas AM, Margos G, Dimopoulos G, van Lin LHM, de Koning-Ward TF, Sinha R, et al. P25 and P28 proteins of the malaria ookinete surface have multiple and partially redundant functions. European Molecular Biology Organization Journal. 2001;20:3975-83.

42. Hopp CS, Balaban AE, Bushell ES, Billker O, Rayner JC, Sinnis P. Palmitoyl transferases have critical roles in the development of mosquito and liver stages of *Plasmodium*. Cellular Microbiology. 2016;18:1625-41.

43. Hart RJ, Cornillot E, Abraham A, Molina E, Nation CS, Ben Mamoun C, et al. Genetic characterization of *Plasmodium* putative pantothenate kinase genes reveals their essential role in malaria parasite transmission to the mosquito. Scientific Reports. 2016;6.

44. Posayapisit N, Songsungthong W, Koonyosying P, Falade MO, Uthaipibull C, Yuthavong Y, et al. Cytochrome c and c1 heme lyases are essential in *Plasmodium berghei*. Molecular and Biochemical Parasitology. 2016;210:32-36.

45. Kaneko I, Iwanaga S, Kato T, Kobayashi I, Yuda M. Genome-wide identification of the target genes of AP2-O, a *Plasmodium* AP2-family transcription factor. PLoS Pathogens. 2015;11:e1004905.

46. Wirth CC, Bennink S, Scheuermayer M, Fischer R, Pradel G. Perforin-like protein PPLP4 is crucial for mosquito midgut infection by *Plasmodium falciparum*. Molecular and Biochemical Parasitology. 2015;201:90-99.

47. Guttery DS, Poulin B, Ramaprasad A, Wall RJ, Ferguson DJ, Brady D, et al. Genome-wide functional analysis of *Plasmodium* protein phosphatases reveals key regulators of parasite development and differentiation. Cell Host Microbe. 2014;16:128-40.

48. Zheng W, Liu F, He Y, Liu Q, Humphreys GB, Tsuboi T, et al. Functional characterization of *Plasmodium berghei* PSOP25 during ookinete development and as a malaria transmission-blocking vaccine candidate. Parasites and vectors. 2017;10:8.

49. Santos JM, Duarte N, Kehrer J, Ramesar J, Avramut MC, Koster AJ, et al. Maternally supplied s-acyl-transferase is required for crystalloid organelle formation and transmission of the malaria parasite. Proceedings of the National Academy of Sciences of the United States of America. 2016;113:7183-88.

50. Hino A, Hirai M, Tanaka TQ, Watanabe Y, Matsuoka H, Kita K. Critical roles of the mitochondrial complex II in oocyst formation of rodent malaria parasite *Plasmodium berghei*. Journal of Biochemistry. 2012;152:259-68.

51. Patzewitz EM, Guttery DS, Poulin B, Ramakrishnan C, Ferguson DJP, Wall RJ, et al. An ancient protein phosphatase, SHLP1, is critical to microneme development in *Plasmodium* ookinetes and parasite transmission. Cell Reports. 2013;3:622-29.

52. Dessens JT, Siden-Kiamos I, Mendoza J, Mahairaki V, Khater E, Vlachou D, et al. SOAP, a novel malaria ookinete protein involved in mosquito midgut invasion and oocyst development. Molecular Microbiology. 2003;49:319-29.

53. Mueller A-K, Kohlhepp F, Hammerschmidt C, Michel K. Invasion of mosquito salivary glands by malaria parasites: Prerequisites and defense strategies. International Journal for Parasitology. 2010;40:1229-35.

54. Klug D, Frischknecht F. Motility precedes egress of malaria parasites from oocysts. Elife. 2017;6:e19157.

55. Boysen KE, Matuschewski K. Arrested oocyst maturation in *Plasmodium* parasites lacking type II NADH:Ubiquinone dehydrogenase. Journal of Biological Chemistry. 2011;286:32661-71.

56. Li FW, Templeton TJ, Popov V, Comer JE, Tsuboi T, Torii M, et al. *Plasmodium* ookinete-secreted proteins secreted through a common micronemal pathway are targets of blocking malaria transmission. Journal of Biological Chemistry. 2004;279:26635-44.

57. Yuda M, Yano K, Tsuboi T, Torii M, Chinzei Y. Von willebrand factor a domain-related protein, a novel microneme protein of the malaria ookinete highly conserved throughout *Plasmodium* parasites. Molecular and Biochemical Parasitology. 2001;116:65-72.

Chapter 3

Investigation of mitochondrial energy metabolism in the liver stage of *P. berghei*

3.1 Introduction

Recently it has emerged that malaria parasites adopt starkly different modes of energy metabolism in different parts of their life cycle. Most eukaryotes produce their ATP using either of two routes: glycolysis, or glycolysis followed by oxidative phosphorylation. Glycolysis takes place in the cytosol. If access to oxygen is limited within the cell, glucose (the main energy precursor) will be converted to either lactate or ethanol after glycolysis. During aerobic conditions however, the end product of glycolysis will be pyruvate, which is then transformed into acetyl CoA inside the mitochondrion. In the next step, acetyl-CoA is modified through a series of chemical reactions to produce ATP through the tricarboxylic acid (TCA) cycle. The cycle also consumes oxygen, reduces NAD^+ to NADH, and produces carbon dioxide and water as waste by-products. The NADH generated by the TCA cycle is fed into the oxidative phosphorylation/electron transport chain (ETC), which builds up a proton gradient to drive mitochondrial ATP synthesis. The net result of these two closely linked pathways is the oxidation of nutrients to produce usable chemical energy in the form of ATP.

Whereas animals switch between glycolysis and oxidative phosphorylation depending on oxygen availability, malaria parasites make this switch when changing hosts, seemingly independent of oxygen availability. For example, blood stage malaria parasites mainly depend on anaerobic glycolysis. Despite having access to oxygen, parasites convert glucose scavenged from the host to lactate (1). Even though glycolysis provides the main source of ATP for blood stage malaria parasites, mitochondrial electron transport is not completely inactive in the blood stage. Rather, parasites utilize a conventional ETC cycle to regenerate ubiquinone for pyrimidine synthesis (2). In contrast, genetic knockout studies and chemical inhibition assays have demonstrated the essentiality of TCA cycle enzymes during sexual differentiation (1-4). Similarly, the majority of the genes associate with TCA cycle and electron transport chain are known to be essential for the mosquito stage but dispensable in blood stage, which is consistent with glycolysis being the main source of ATP (5). The energy metabolism of the hepatic stage of *Plasmodium*, on the other hand, is largely unstudied

by reverse genetics due to inability of these knockout parasites to survive through the mosquito stage.

ATP synthase, also known as complex V of the ETC (Fig 3.6.6), is the enzyme complex that catalyses ATP synthesis from ADP using the proton gradient generated across the inner mitochondrial membrane (6). ATP synthase consist of two major functional domains: a membrane-extrinsic F1 domain; and a membrane-intrinsic F0 domain, which are joined together by central and peripheral stalks. F1 is the catalytic part of the enzyme where ATP is formed from ADP and Pi, whereas F0 contains a motor to generate rotation (6). The F1 domain of the ATP synthase is an assembly of five globular proteins, α, β, γ, δ and ε, with the stoichiometry α3β3γ 1δ1ε1 (7).

Sturm et al. in 2015 (2) generated a gene knockout of the β subunit of ATP synthase in *P. berghei* that grew well at blood stage implying that mitochondrial ATP synthesis was dispensable in blood stage parasites, which is again consistent with a primary role for glycolysis in generating ATP (1). However, the ATP synthase β subunit was shown to be essential during mosquito stage, particularly for ookinete to oocyst development (2). Given the observed defects in the mosquito stage it was not possible to study the effect of the ATP synthase knockout in liver stage development. Therefore, this gene was a good candidate to apply the complementation system that I established (chapter 2) and to explore energy metabolism in the malaria parasite liver stage.

In this Chapter I complemented the ATP synthase β subunit knockout with wildtype ATP synthase β subunit by crossing the red fluorophore tagged gene deletion parasites with green fluorophore tagged wildtype parasites. By carefully analyzing the genetically complemented ATP synthase β subunit knock out sporozoites *in-vitro* using cultured liver cells, I could observe their growth and development in the absence of mitochondrial ATP synthesis. I was also able to study their development *in-vivo* by allowing mosquitoes with complemented ATP synthase mutants to bit naïve mice and assay for the recovery of a P0 blood stage, which I could genotype and drug select (the knockouts are pyrimethamine resistant). Complementation allowed me to bridge the ATP synthase β subunit knockout through the mosquito stage and produce sporozoites with no ATP synthase β subunit, which were then used to infect liver cells *in-vitro* and mice by mosquito bites. In this way I explored the viability of ATP synthase β subunit deficient parasites in liver stage and provide the first evidence that liver stage rodent

malaria parasites are not dependent on mitochondrial ATP synthesis, which is the first insight into their energy metabolism.

To extend the investigations of energy metabolism in liver stage malaria parasites, I applied my complementation strategy to knockouts in energy metabolism genes upstream of ATP synthase β subunit, namely two subunits of complex II of mitochondrial ETC (flavoprotein subunit of succinate dehydrogenase [SDH A] and iron-sulfur subunit of succinate dehydrogenase [SDH B]), and the 2-oxoglutarate dehydrogenase E2 component (KDH) of the mitochondrial TCA cycle (Table 3.6.3, Fig 3.6.6). Deletion of the SDH A subunit gene is inconsequential in blood stage but causes defects in ookinete growth in *P. berghei* (8) and blocks mosquito stage transmission of *P. falciparum* (4). Similarly, the E1 subunit of KDH gene is dispensable at blood stage but essential for ookinete to oocyst development in *P. falciparum* (4). Thus, the three selected genes associated with mitochondrial ATP generation were assumed to play important roles in mosquito stage transmission. However, their liver stage functions remained unknown as knockout parasites do not survive during mosquito stage to infect liver. In this Chapter I complemented the three knockouts with wildtype alleles of the genes in an attempt to bridge these gene deletions through the mosquito stage, which would allow me to explore their essentiality in liver stage parasites. Because of time restrictions, I did not generate fluorophore-tagged versions of these three knockouts. Rather, I made use of the off-the-shelf *Plasmo*GEM constructs to generate these knockouts quickly. Nevertheless, I tracked the knockout alleles by PCR across the mosquito, liver, and P0 mouse stages to dissect where and when these genes are necessary during malaria parasite development across its digenetic life cycle.

3.2 Materials and methods

3.2.1 Parasites

A clonal population of *P. berghei* ATP synthase β knockouts carrying the mCherry fluorescent marker and *h*DHFR (drug selectable marker) was generated by Dr Angelika Sturm (2).

The *Pbs*P48/45^{KO} strain (9) was provided by Andy Waters (University of Glasgow, Glasgow, Scotland). *Pb ANKA* parasite lines expressing GFP and mCherry fluorescence markers were developed by Dr Dean Goodman based on (10).

3.2.2 Infection of *Anopheles stephensi*

Adult females of *A. stephensi* reared under standard insectary conditions (adult mosquitoes were grown at 27 ºC with humidity of 80% and light: dark photoperiod of 14:10 hours with a 1 hour ramp in) were allowed to feed on anesthetised mice that had been infected with the following combinations ($2x10^5$ parasites from each strain were mixed and two independent experiments from each coinfection (total four coinfections) was performed).

- ATPβ^{KOmCh} [parasites having ATPβ replaced with, *h*DHFR gene fused to mCherry fluorescent marker (2)]
- ATPβ^{KOmCh} x ATPβ^{WT}-GFP [parasites having ATPβ replaced with *h*DHFR fused to mCherry, mixed with a wildtype ATPβ locus expressing GFP from a different genetic locus (11)]
- ATPβ^{WT}mCh x ATPβ^{WT}-GFP (parasites with a wildtype ATPβ locus and expressing mCherry from another genetic locus mixed with ATPβ wildtype parasite expressing GFP from another genetic locus)
- Pbs48/45^{KO} [parasites lacking Pbs48 and 45; non-fluorescent strain (9)]
- ATPβ^{KOmCh} Pbs48/45^{WT} x ATPβ^{WT} P48/45^{KO} (parasites having ATPβ replaced with *h*DHFR fused to mCherry fluorescents maker, with a wildtype Pbs48/45 loci and mixed with parasites carrying a wildtype ATPβ gene but lacking Pbs 48/45)
- ATPβ^{WT}mCh Pbs48/45^{WT} x ATPβ^{WT} Pbs48/45^{KO} (parasites with wildtype ATPβ and Pbs48/45 loci and expressing mCherry from another

genetic locus mixed with non-fluorescent parasites with a wildtype ATPβ locus but lacking Pbs48/45)

To complement the effect of ATPase β subunit deletion, I crossed the knockout parasites ($ATP\beta^{KOmCh}$) with two strains carrying wildtype ATPβ genes. First, the cross with $ATP\beta^{WT}$ parasites expressing GFP inserted ($ATP\beta^{WT}$-GFP) allows easy follow up of self-fertilized and recombinant parasites by colour. As the control experiment, a wildtype parasite carrying intact ATPase β subunit but mCherry inserted in to chromosome 6 ($ATP\beta^{WT}$mCh) was crossed with the same $ATP\beta^{WT}$ parasites expressing GFP ($ATP\beta^{WT}$-GFP). Next, I crossed a male sterile $ATP\beta^{WT}$ $P48/45^{KO}$ strain with the $ATP\beta^{KOmCh}$ $Pbs48/45^{WT}$ to increase the number of recombinant parasites as self-fertilized $Pbs48/45^{KO}$ parasites do not form oocysts. To control any effect of fluorophore expression, above $ATP\beta^{WT}$mCh $Pbs48/45^{WT}$parasites expressing mCherry was crossed to the same $ATP\beta^{WT}$ $Pbs48/45^{KO}$.

First, the donor parasitic strain $ATP\beta^{KOmCh}$ was used to infect mosquitoes as a preliminary experiment. Screening of ATPβ knockout and wildtype parasites was performed with the primers listed in Table 3.6.1 using the following PCR conditions.

Initial denaturation	95 ºC	3 min
34 cycles	95 ºC	15 sec
	55 ºC	20 sec
	72 ºC	3 min
Final extension	72 ºC	5 min

The aim of this trial was to confirm the absence of oocysts in midguts of the mosquitoes and hence the essentiality of ATP synthase β subunit for mosquito stage transmission of parasites (Fig 3.6.8).

Next, the oocysts from the mosquito midguts day 12 post infection, and salivary gland sporozoites day 21 post infection for the two cross experiments and equivalent controls were analysed. An IFA was used to detect fluorescent expression of $ATP\beta^{KOmCh}$ $Pbs48/45^{WT}$ x $ATP\beta^{WT}$ $P48/45^{KO}$ salivary gland sporozoites as described (in materials and methods of chapter 2) using rabbit anti-mCherry (1: 250; Abcam ab167453)/Alexa Fluor 546 goat anti-rabbit IgG (1:1000; Molecular Probes/ThermoFisher) for $ATP\beta^{KOmCh}$ x $ATP\beta^{WT}$-GFP. The number of oocysts and sporozoites per mosquito was recorded and the ratio of sporozoites/oocysts was compared between parasites of

$ATP\beta^{KOmCh}$ x $ATP\beta^{WT}$-GFP and $ATP\beta^{WT}$mCh x $ATP\beta^{WT}$-GFP from two independent experiments using student t test.

3.2.3 Sporozoite infections of HepG2 cells

All the sporozoites from each cross experiment were incubated with HepG2 cells (20,000 sporozoites per well) for 68 hours with cells fixed at 68 hours post incubation (hpi). An IFA was carried out (refer to materials and methods of chapter 2) for wells fixed at 68 hours by staining parasites with rabbit anti-mCherry (1: 250; Abcam ab167453)/Alexa Fluor 546 goat anti-rabbit IgG (1:1000; Molecular Probes/ThermoFisher) and Hoechst 33342 (5µg/ ml). Next, the number of nuclei per parasite and the area of each parasite were compared to their corresponding control parasites using images taken at 40X magnification of the Leica DM 2500 epifluorescence microscopy. Images were analysed by ImageJ (1.46a, Wayne Rasband, National Institutes of Health) software. Student t-test (unpaired) was used to compare the average growth size differences 68 hours post infection and χ^2 analysis for nuclear content for parasites pooled from 4 independent experiments. At 70 hpi, detached cells and merosome production were observed and counted using an Olympus CKX41 compound fluorescence microscope at 40X magnification (Table 3.6.2).

3.2.4 Sporozoite infections in mice

Infected mosquitoes day 21 post infection were allowed to feed on naïve mice (P0 population by biting) and dissected salivary gland sporozoites were IV injected into naïve mice as 1000 and 10000 sporozoites per mouse (P0 by sporozoite IV). Mice infected with $ATP\beta^{KOmCh}$ x $ATP\beta^{WT}$-GFP were treated with pyrimethamine (70µg/ml: Sigma) once the parasitemia reached approximately 5% and followed up for a further 14 days. In addition to the pyrimethamine treatment, fluorescence microscopy and PCR analysis (primers; Table 3.6.1) were used to genotype the resultant parasites from each experiment.

3.2.5 Screening of three, TCA and ETC associated genes to analyse the gene function in liver

Three genes with functions in either the TCA cycle or the ETC (Table 3.6.3) were selected and the knockout constructs were obtained from the *Plasmodium* Genetic Modification facility (*Plasmo*GEM) (http://plasmogem.sanger.ac.uk).

3.2.5.I Blood stage knockout parasites of SDH A, SDH B and KDH genes

The vectors with knockout constructs obtained from the *Plasmo*GEM were confirmed by screening restriction digestions and DNA amplified by Maxi prep (Promega) and cut with *Not*I-HF to linearize the constructs prior to transfection. The constructs were transfected into wildtype *PbANKA* parasites (10) and selected by pyrimethamine (70µg/ml). Screening primers used to confirm the knockout parasites are listed in Table 3.6.1 and the PCR conditions used were as follow.

Initial denaturation	95 ºC	3 min
34 cycles	95 ºC	15 sec
	58 ºC	30 sec
	70 ºC	3 min
Final extension	70 ºC	5 min

3.2.5.II Infection of *A. stephensi*

As described above, the mosquitoes were infected with following strains/ combinations;

- SDH A^{KO} (parasites having SDH A replaced with 3xHA-*h*dhfr-*y*FCU selection cassette)
- SDH B^{KO} (parasites having SDH B replaced with 3xHA-*h*dhfr-*y*FCU selection cassette)
- KDH^{KO} (parasites having KDH replaced with 3xHA-*h*dhfr-*y*FCU selection cassette)
- SDH A^{KO} x SDH A^{WT}-GFP (parasites having SDH A replaced with 3xHA-*h*dhfr-*y*FCU mixed with, a wildtype SDH A locus expressing GFP from a different genetic locus
- SDH B^{KO} x SDH B^{WT}-GFP (parasites having SDH B replaced with 3xHA-*h*dhfr-*y*FCU mixed with, a wildtype SDH B locus expressing GFP from a different genetic locus

- KDH^{KO} x KDH^{WT}-GFP (parasites having KDH replaced with 3xHA-*h*dhfr-*y*FCU mixed with, a wildtype KDH locus expressing GFP from a different genetic locus

Next, the oocysts from the above mosquito midguts day 12 post infections were analysed with mercurochrome staining as the knockout constructs lack fluorescent markers. First, the dissected mosquito midguts were added to 20 µl of 0.2% mercurochrome in 1X phosphate buffered saline (PBS) on a glass side and stained for 10 minutes. Then, the midguts were transferred to 20 µl of distilled water on a second glass slide and de-stained for 10 minutes.

3.2.5.III P0 parasite generation to study liver stage

The infected mosquitoes from above six combinations (day 21 post infection) were allowed to feed on naïve mice (P0 population by biting). The number of mice infected (by biting) with three mixed parasite populations was duplicated, and one set of mice was given pyrimethamine (70µg/ml) in their drinking water. The salivary gland sporozoites of mosquitoes infected with the three mixed populations were IV injected into naïve mice as 1,000 and 10,000 sporozoites per mouse (P0 by sporozoite IV), which were immediately treated with pyrimethamine (70µg/ ml). Confirmation of parasite genotypes was performed by PCR using primers (Table 3.6.1) and conditions listed above.

3.2.6 Statistical analysis

All statistical analysis was done using GraphPad Prism (GraphPad Software, La Jolla California USA).

3.3 Results

3.3.1 Parasites with ATP synthase β subunit gene deletion (PbATPβ^{KOmCh}) show slightly impaired growth during blood stage but fail to infect mosquitoes

All the experiments from generating the PbATPβ^{KOmCh} strain, transfection, sub-cloning to generate a single parasitic strain and their blood stage growth experiments were done by Dr Angelika Sturm. This work confirmed that the ATPβ^{KO} parasites complete blood stage growth, suffering only a slight growth defect (2). Further, when the knockout strain was introduced to *A. stephensi* mosquitoes, parasites failed to produce any oocysts (2). Hence, it was confirmed the β subunit of the ATPase gene is not essential for erythrocytic development but required for parasite transmission through mosquitoes (2).

To further verity the above finding, the cloned ATPβ^{KOmCh} was PCR genotyped (Fig 3.6.8.A) using primers listed in Table 3.6.1 and fed to mosquitoes. The absence of oocysts in the midgut infected with the knockout compared to the wildtype control (Fig 3.6.8.B) corroborated the published result (2).

3.3.2 Crossing to wildtype parasites complements the ATP synthase β subunit gene knockout defect in mosquito stage development

To determine if the effects of β subunit of ATPase gene deletion (ATPβ^{KOmCh}) on parasite growth during mosquito stage could be complemented by crossing to parasites carrying a wildtype copy of the allele (ATPβ^{WT}), *A. stephensi* mosquitoes were fed on mice co-infected with (I) ATPβ^{KOmCh} x ATPβ^{WT}-GFP and (II) ATPβ^{KOmCh} Pbs48/45^{WT} x ATPβ^{WT} P48/45^{KO} with their equivalent control strains.

The replacement of the ATPβ coding region with mCherry fused to *h*DHFR in ATPβ^{KOmCh} parasites allows tracking of ATPβ^{KO} genotype after sexual reproduction. Following sexual recombination in mosquitoes and encystment, oocysts were seen 12 days post infection. As expected (Fig 3.6.7), there were only two phenotypes of oocysts present; orange colour recombinants carrying both ATPβ^{KOmCh} and ATPβ^{WT}-GFP genes and green colour self-fertilized oocysts with ATPβ^{WT}-GFP (Fig 3.6.9.A). Due to the growth defect of ATPβ gene deletion, self-fertilized ATPβ^{KOmCh} parasites expressing only the red colour will not complete their oocysts development, which explains why I

saw no red only oocysts (2). Nevertheless, salivary gland sporozoites with mCherry expression could be seen (Fig 3.6.9.A) confirming the survival of parasites having knockout ATP synthase β gene in mosquito stage. Hence, complementation of the ATPβ^{KO} in the oocyst restored sporozoite production in both co-infections. In addition, there was no significant difference (P=0.6448; student t-test) between the ratio of sporozoites/oocysts developed by the ATPβ^{KOmCh} x ATPβ^{WT}-GFP compared to the control (Fig 3.6.9.B). Due to the low level of mCherry expression seen in ATPβ^{KOmCh}-Pbs48/45^{WT} x ATPβ^{WT}mCh-Pbs48/45^{KO} cross; the number of red colour oocysts could not be counted. However, all the sporozoites from the ATPβ^{KOmCh}-Pbs48/45^{WT} x ATPβ^{WT}mCh-Pbs48/45^{KO} cross showed mCherry fluorescence (by using the anti-mCherry antibody to enhance the red colour expression) despite having a mix of ATPβ^{KOmCh} and ATPβ^{WT} genotypes. This suggests significant carry-over of transcripts and/or protein from the shared cytoplasm of the oocyst that could mask any phenotype resulting from the loss of ATP synthase β subunit activity in sporozoites (10).

3.3.3 The role of parasite-synthesized ATP synthase β subunit gene in liver stage development

Sporozoites recovered from the test and control crosses were used to infect *in-vitro* cultures of HepG2 liver cells, and parasite development was assessed by IFA at 68 hours post infection. By 24 hours, any residual fluorescent mCherry protein seen in the sporozoites is lost and the parasites can be genotyped by fluorescence expression (10). As seen in images (Figs 3.6.10 A,B), there were red colour ATPβ^{KOmCh} parasites present 68 hours post infection as fluorescence expression allowed us to correlate liver stage parasite size with the presence of an active ATPase β subunit gene. In the ATPβ^{KOmCh} x ATPβ^{WT}-GFP cross, parasites with only the red colour as well as orange colour parasites are products of recombination of orange colour oocysts which came from cross fertilization of ATPβ^{KOmCh} and ATPβ^{WT}-GFP (Fig 3.6.7). Similarly, parasites which express only green colour can be a result of either self-fertilization of ATPβ^{WT}-GFP or from the recombination of orange colour oocysts (Fig 3.6.10 A). A similar pattern was seen in the parasites from the ATPβ^{KOmCh} Pbs48/45^{WT} x ATPβ^{WT}mCh Pbs48/45^{KO} co-infection 68 hpi (Fig 3.6.10 B). In the absence of a second fluorophore however it is not possible to distinguish ATPβ^{KOmCh} Pbs48/45^{WT} self-fertilization from ATPβ^{KOmCh} Pbs48/45^{WT} x ATPβ^{WT}mCh Pbs48/45^{KO} recombinants. Depending on the size of each

parasite according to the red colour they expressed, there was no significant difference (P value=0.2292; student t-test) in between the cross and control parasite development at 68 hours of infection (Fig 3.6.10 C). The similarity in parasite size correlated with similar numbers of nuclei present (Fig 3.6.10 D) in ATPβ^{KOmCh} parasites at 68 hpi compared to their wildtype equivalent (P value=0.0389; χ^2). Both ATPβ^{KOmCh} and wildtype lines produced parasites containing more than 100 nuclei.

Production of detached cells and merosomes was assayed at 70 hours post infection (Table 3.6.2) and the presence of mCherry expressing detached cells and merosomes in both cross infections confirmed ATPβ^{KOmCh} ability to complete the hepatic stage replication in *in-vitro*.

The ability of ATPβ^{KOmCh} parasites to complete liver stage in naïve mice *in-vivo* was tested using both bite-back and injection of purified salivary gland sporozoites. Mice infected by either strategy became infected within the expected period for a wildtype parasite (day 4-5), and fluorescence microscopy revealed the presence of mCherry expressing parasites in the infected mice, demonstrating that parasites carrying ATPβ^{KOmCh} could complete the liver stage (Figs 3.6.11.A I and II). However, the proportion of red colour parasites was very low in comparison to the green colour parasites as both self-fertilized 'green' and recombinant 'green' colour parasites will also survive through the liver stage to infect erythrocytesNevertheless, all gene combinations expected as P0 following recombination, were detected by PCR screen, including the Pbs48/45^{KO} allele, presumably transmitted via the male ATPβ^{WT} Pbs48/45^{KO} gamete (Fig 3.6.11.A III).

To further verify the presence of ATPβ^{KOmCh} parasites, and to enhance the number of parasites present in the population, I selected for mutant parasites using pyrimethamine resistance linked to the ATPβ^{KOmCh} locus (Fig 3.6.11.B I). Following infection with sporozoites from the ATPβ^{KOmCh} x ATPβ^{WT}-GFP cross, the mice were treated with pyrimethamine after the infection was established (7 days post infection). All parasites except mCherry expressing parasites were cleared after 4 days of pyrimethamine treatment and did not reappear over further days of observation as confirmed by the PCR (Fig 3.6.11.B II).

3.3.4 Screening of three, TCA and ETC associated genes to analyse the gene function in liver

3.3.4.I Parasites with SDH A, SDH B or KDH gene deletions have no marked growth defect during blood stage but fail to complete mosquito stage

The knockout constructs obtained from the *Plasmodium* Genetic Modification (*Plasmo*GEM) were transfected into mice and the parasites were recovered day 7 post infections. PCR using primers in Table 3.6.1 confirmed the expected gene knockouts (Fig 3.6.12). These results are consistent with published work demonstrating that these genes are dispensable during the rodent malaria parasite blood stage (4, 8, 12).

3.3.4.II Crossing to wildtype parasites complements the gene knockout defects in oocyst development

First, the PCR confirmed knockout parasites (uncloned) were used to feed *A. stephensi* mosquitoes and oocyst development observed on day 12 of infection. The three strains were not sub-cloned to remove the wildtype parasites remaining in the transfectant population as the presence of these parasites would not affect the outcrossing to wildtype parasites or the PCR-based genotyping of the progeny. Therefore, while majority of the midguts dissected were devoid of oocysts for all three gene deletions (Fig 3.6.13.A I), occasional oocysts were present in some midguts (Fig 3S). These oocysts might have originated from the residue of wildtype parasites in the uncloned population because these genes have previously been shown to essential for oocyst development (4, 8). Because the *Plasmo*GEM knockout vectors lack a fluorophore, I was not able to genotype individual oocysts by microscopy.

To determine if the effects of these gene deletions on parasite growth during mosquito stage could be complemented by crossing to parasites carrying a wildtype copy of the allele, *A. stephensi* mosquitoes were fed on mice co-infected with (I) SDH A^{KO} x SDH A^{WT}-GFP (II) SDH B^{KO} x SDH B^{WT}-GFP (III) KDH^{KO} x KDH^{WT}-GFP. Mosquito midguts were dissected at day 12 of infection, which indeed confirmed the formation of oocysts (Fig 3.6.13.A II), and salivary gland sporozoites were recovered day 21 post infection (Table 3.6.4).

3.3.4.III The role of gene knockouts in liver stage development

To further investigate if any knockout oocysts observed without cross to a wildtype allele produce sporozoites in mosquitoes, three naïve mice were infected by mosquito bite-back with following strains; (I) SDH A^{KO} (II) SDH B^{KO} (III) KDH^{KO}. The mice were free of parasites for 14 days post infection (Table 3.6.5) confirming the indispensable nature of TCA and ETC related genes for mosquito stage transmission (2, 4, 8).

The ability of, the knockout parasites mixed with parasites having the wildtype allele of the gene, to complete liver stage in naïve mice *in-vivo* was tested using both bite-back and injection of purified salivary gland sporozoites. Mice infected by biting but not treated with pyrimethamine became infected (Table 3.6.5) within the expected period for a wildtype parasite (day 4), and fluorescence microscopy revealed the presence of GFP expressing parasites in the infected mice. Genotypes of parasites were studied by PCR screen, and the wildtype parasites were present for all three genes. However, knockout parasites were absent in blood for all the three genes (Fig 3.6.13.B) except a very faint PCR band for SDH B^{KO}.

To further verify the absence of knockout parasites, or to enhance (if present) the number of knockout parasites in the P0 population, the mutant parasites were selected using pyrimethamine resistance linked to the knockout locus and the pyrimethamine sensitivity of WT^{GFP} parasites (Fig 3.6.13.B). Following infection with sporozoites from the mixed infections (by biting, by IV 1000 and 10000 sporozoites/mouse), the mice were immediately treated with pyrimethamine. All the mice were free of infection up to 14 days post infection for both SDH A and B, regardless of the strategy used to infect mice (Table 3.6.5). The mouse infected with KDH^{KO} x KDH^{WT}-GFP by biting (with pyrimethamine) was positive for parasites from day seven post infection, which is a significant delay compared to that of a wildtype parasite (day 4). PCR confirmed presence of KDH knockout and absence of wildtype parasites in the mouse blood (Fig 3.6.13.B). However, the mice infected with KDH^{KO} x KDH^{WT}-GFP sporozoites injection (both 1,000 and 10,000 per mouse under pyrimethamine treatment) was negative for parasites (Table 3.6.5).

3.4 Discussion

In this chapter I have used a reverse genetic strategy to make one of the first explorations of energy metabolism in the liver stage of malaria parasites. Previously, energy metabolism has been difficult to assay in liver stage malaria parasites. The liver is difficult to access, and the number of parasite is relatively miniscule. An additional problem is that the liver cells are metabolically active, so teasing out the parasite metabolic activity from that of the host is problematic. To address this, I applied my genetic complementation strategy to bridge knockout alleles of mitochondrial ATP synthase, mitochondrial electron transport and TCA cycle through mosquitoes and then on to liver stages to assess essentiality of these genes in liver stage parasites.

The ATP synthase β subunit has been the subject for genetic manipulation in both *P. falciparum* and *P. berghei* strains. An early report concluded that the β subunit of ATP synthase was essential in *P. falciparum* blood stage on the grounds that no knockout could be obtained after concerted effort (13). In contrast, a knockout of the β subunit of ATP synthase was obtainable in *P. berghei* parasites and caused only a minor growth defect (2), which is consistent with a global knockout program for several ATP synthase subunits in which most were found to be dispensable (12). What can we make of this apparent difference between reliance on mitochondrial ATP synthase in rodent and human malaria parasites? One possible explanation is that *P. falciparum* preferentially invades mature erythrocytes whereas *P. berghei* utilises reticulocytes, which can perhaps provide more metabolic resources than mature erythrocytes. Reticulocytes have a complex, enriched metabolic profile than mature erythrocytes and thus a greater metabolic overlap between parasites occupying reticulocytes and mature erythrocytes has been observed from multiple knockout studies (14). A potential confounding factor is the reliance on absolute gene knockouts in *P. falciparum* rather than conditional knockouts. Indispensability is often inferred by the lack of ability to procure a knockout. However, if a gene knockout incurs a growth rate cost, it can be difficult to recover knockout parasites. It will be interesting to learn if mitochondrial ATP synthase is dispensable or not in human malaria parasites at blood stage.

When the β subunit of ATP synthase knockout *P. berghei* parasites were introduced into the mosquito stage, progression from ookinete to oocysts was found to fail (2). Similar to many of the genes related to either TCA cycle or electron transport chain,

these mitochondrial ATP synthase knock-out parasites appear unable to scavenge sufficient resources from the mosquito to sustain their development. Trehalose rather than glucose becomes the key sugar molecule in the mosquito hemolymph (15) and the accessible quantity may be limiting in comparison to the erythrocyte stage (8). Indeed, a picture is gradually emerging that parasite maturation and proliferation in the mosquito is constrained by the accessibility of limited metabolites, which is manifested by parasite death at various stages in the mosquito midgut for different metabolic knockouts (16). In addition to any limitation of resources in the mosquito hemolymph, it is also possible that the protective cyst wall is a substantial barrier for the exchange of metabolites. Whatever the case, it is clear that the parasites require a robust, functioning mitochondrial energy generating system to sustain themselves within mosquitoes (1, 2, 5, 12).

Reliance on a complete system of mitochondrial ATP synthesis machinery in malaria parasite mosquito stages creates an obvious blockade for reverse genetic studies of liver stages. In Chapter 2, I presented a genetic complementation strategy that allowed me to produce gene of interest deficient sporozoites despite the fact that the gene was essential for mosquito stage development of sporozoites (10). In this chapter I applied the same approach to observe liver stage growth of the ATP synthase β subunit deficient *P. berghei* strain. By crossing to two different strains having ATPβ^{WT} , first a wildtype *P. berghei* having GFP inserted into a dispensable locus of a chromosome [chromosome 6; (11)] and second a male sterile line Pbs 48/45 (9), the lack of the active ATPβ subunit in the knockout strain was compensated. By using two fluorophores in the ATPβ^{WT}mCh x ATPβ^{WT}-GFP cross, I could easily follow up the self-crossed parasites and recombinants. The ATPβ knockout parasites become female sterile once introduced into the mosquito (2) therefore I used the male sterile strain to cross with, with the aim of increasing the number of recombinant parasites in the resulting progeny.

With the cross of ATPβ knockout parasites into the parasites with wildtype locus of ATPβ, I could restore the growth of oocysts and the observed progeny had no detectable difference in terms of production of oocysts or salivary gland sporozoites (Fig 3.6.9). Similarly, mCherry expressing sporozoites were readily recovered from both crosses. Since the reported phenomena of “carry-over” of oocysts proteins into the sporozoites (10), all the sporozoites I recovered were red in color. Therefore, I did not attempt to

further analyze the motility of the sporozoites as it can be misleading with the carry-over of foreign products.

I observed normal growth of ATPβ knockout parasites (genotyped by their red fluorescence) in *in-vitro* liver cells (Fig 3.6.10), with no significant difference in average size, nuclear content nor merosomes produced between ATPβ deficient and wildtype parasites (Table 3.6.2) strongly suggesting that a functional ATP synthase gene is not required for liver stage development.

To further confirm normal growth of these knockout parasites in *in-vivo* liver stage, I next studied the capacity of mutants to progress to the next blood stage/P0 by infecting naïve mice with the complemented sporozoites from the cross. Parasites were recovered from mice infected with both by bite-back and IV sporozoite injection (1,000 and/or 10,000 sporozoites per mouse) within time frames (d 4-5) equivalent to wildtype parasites, strongly suggesting that the ATPβ deficient parasites successfully completed liver stage development *in-vivo* as well as *in-vitro*. Fluorescent microscopy observations revealed the presence of only a small proportion of red fluorescent parasites with a higher proportion of parents and recombinants recovered (Figs 3.6.11.A I,II). The fact that the knockout parasites have a slight growth delay in blood stage (2) perhaps explains the low numbers of red fluorescent parasites present in the P0 progeny. To increase the knockout parasite population in the ATPβ^{KOmCh} x ATPβ^{WT}-GFP cross, I treated infected mice with pyrimethamine once they reached approximately 5% parasitemia. Since the GFP expressing parasites are pyrimethamine sensitive, the treatment enriched red color parasites (Fig 3.6.11.B. I). It was not possible to treat ATPβ^{KOmCh} Pbs48/45^{WT} x ATPβ^{WT} P48/45^{KO} infected mice with pyrimethamine as both ATPβ^{KO} and Pbs48/45^{KO} have *h*DHFR inserted and are thus pyrimethamine resistant. Phenotyping of parasites by PCR further confirmed the presence of ATPβ^{KOmCh} parasites (Figs 3.6.11.A III and B II) as well as the recovery of other genetic combinations of parasites post recombination (Fig 3.6.11.A III).

With careful analysis of ATPβ^{KOmCh} parasite growth in liver stage and further into the P0 blood stage, I here confirm the dispensability of the presence of a functional ATP synthase complex in the inner mitochondrial membrane during liver stage development. It has been previously reported by (17) that the complex I of electron transport chain, the NADH:ubiquinone dehydrogenase complex is also not essential for liver stage

growth of *P. berghei.* Boysen and Matuschewski (17) used a similar approach to generate sporozoites with the gene knockout and to recover the P0 knockout parasites without my refinement of fluorescently tagging knockout parasites. Nevertheless, my findings are in line with this early work suggesting mitochondrial energy metabolism is dispensable in rodent malaria parasite liver stage.

In the absence of the complex V of electron transport chain, the parasites must either use a different approach to yield ATP driven by the proton gradient across the inner mitochondrial membrane or a different mechanism rather than depending on the ATP synthase complex. The most likely hypothesis is that rodent malaria parasites rely primarily on glycolysis for their ATP production in liver stages just as they do in blood stages.

To explore this further I sought to repeat my complementation strategy to generate liver stage rodent malaria parasites with knockouts in genes for components of the mitochondrial ATP generation system upstream of ATP synthase, namely the TCA cycle and electron transport chain. If malaria parasite ATP can be produced solely by glycolysis at liver stage, genes for TCA cycle and/or ETC might also be dispensable at liver stage. I selected three more genes for this approach: one belongs to TCA cycle (KDH) and two, associated with both TCA and ETC (subunit A and B of SDH). Deleting the three genes in blood stage had no effect on parasite growth (Fig 3.6.12), confirming previous screens indicating they are dispensable at blood stage (4, 8, 12). Similarly, I also confirmed that these genes are critical for the production of oocysts by introducing the knockouts into mosquitoes (Fig 3.6.13.A I). In the interests of time, I did not clone any of these knockouts, which apparently resulted in wildtype parasites (presumably with spurious insertions of the selectable marker) self-fertilising and producing oocysts (Fig 3S). When the knockout parasites were crossed to a wildtype and fed to mosquitoes, I observed robust oocysts development (Fig 3.6.13.A II) and copious salivary gland sporozoites were generated (Table 3.6.4). Since the knockout parasites were not tagged with a fluorescent marker, PCR was used to genotype parasites in each stage (Fig 3.6.13.B).

I next used P0 blood stage to assess *in-vivo* liver stage growth of the crossed parasites. Parasites with knockouts in subunit A of complex II of the ETC (SDH A) did not survive in P0 blood stage. Regardless of the strategy used to infect naïve mice, no

parasites were recovered even upon pyrimethamine treatment while the untreated mice were positive only with the wildtype counterpart (Fig 3.6.13.B). Presence of knockout SDH A along with the wildtype parasites was consistent from blood stage to sporozoites but knockout parasites disappeared at P0 (Fig 3.6.13.B). This is potentially an indication of a severe liver stage growth defect of knockout parasites, perhaps preventing them from completing development and then infecting erythrocytes. The absence of knockout parasites was further confirmed by drug selection. By allowing the mixed infected mosquitoes to bite on naïve mice (without drug selection), I could clearly recover wildtype SDH B parasites but a very faint band to indicate SDH B^{KO} was also seen in PCR. Nevertheless, the mice immediately treated with pyrimethamine post biting/sporozoites IV were free from parasites for 14 days (Fig 3.6.13.B). The fact that SDH B^{KO} parasites were seen only by biting without drug selection (Table 3.6.5), makes it impossible to conclude whether or not the SDH B gene is essential at liver stage at this point.

SDH functions as a linker between the TCA cycle and ETC by oxidising succinate to fumarate in TCA cycle and then reducing the fumarate at ETC. SDH is also one of the TCA cycle members that generate NADH, the substrate for NDH2 in ETC (8). Pyrimidine biosynthesis is the main function of the ETC during the blood stage. The ETC is required to maintain the ubiquinone turnover essential for dihydoorotate oxidation by dihydroorotate dehydrogenase (DHOD) (18). Blood stage parasites can survive without functional SDH complex because the ubiquinone turnover is maintained at sufficient levels by complex III of the ETC (5). When the parasites reach liver stage, their metabolic requirements vary considerably from blood stage. For instance, the heme biosynthesis pathway which has no function in blood stage becomes essential for hepatic stage (10, 19, 20). Heme biosynthesis needs succinyl Co-A, which is generated via TCA cycle (19, 21). Thus, parasites in the liver need both pyrimidine and heme synthesis and so require at least minimal function of both the ETC and the TCA cycle. Therefore, parasites must have a functional SDH to sustain pyrimidine and heme biosynthesis. Hence, it is not surprising that mosquito-stage phenotype of SDH knockouts could be rescued by complementing to wildtype parasites, but the knockout sporozoites have a growth arrest in the hepatic stage. However, the fact that detection in P0 blood stages of small numbers SDH B knockout parasites compared to the complete

absence of SDH A knockout parasites, highlights the need of further experiments on these strains including a detailed study of the liver stage.

The recovery of KDH^{KO} parasites in P0 performed by bite-back indicates the KDH gene deletion has no major impact on liver stage parasites. Surprisingly, neither injecting 1,000 nor 10,000 sporozoites IV resulted in a P0 blood stage infection (Table 3.6.5). Since P0 KDH knockouts were recovered only by bite-back strategy (with pyrimethamine), it is necessary to repeat these experiments to investigate reasons behind the absence of parasites via IV injection. It can be hypothesized that only a small proportion of knockout parasites have been survived and managed to continue through the liver stage to infect red blood cells. Only by eliminating the wildtype parasites via drug treatment, can the knockout parasites be permitted to expand and be detectable. One reason why only a small number of knockout parasites survived compared to the wildtype could be that there might be a mild growth defect either as oocysts, sporozoites or during liver stage and that the defect was not strong enough to prevent the parasites from completing the liver stage. Genotyping of KDH^{KO} x KDH^{WT} further supports this suggestion since there were no knockout parasites at oocysts and sporozoites according to the PCR analysis. Another explanation is that the PCR analysis was not sensitive enough to detect such a minor population. Whatever the case, the knockouts reappeared once the wildtype parasites were removed via drug treatment (Fig 3.6.13.B). These somewhat anomalous findings serve to emphasise the importance of further experiments on the KDH gene with a detailed study during liver stage, preferably using fluorophore tagging of the knocked out locus and cloning of knockouts prior to mosquito infection.

The KDH gene has been subjected to genetic manipulations both in blood and mosquito stages of *P. falciparum* where the gene deletion has shown no effect on parasite erythrocyte growth. As observed by (4), the knockout parasites adapted to use glutamine-derived α-ketoglutarate to generate malate in blood stage while the gene deletion prevented parasites from using glutamine as a carbon source for TCA cycle thus parasite transmission was blocked. This is indicative of a flexible carbon metabolism in malaria parasites, which may be ultimately essential for them to make transitions between different environments during life cycle. My preliminary finding that KDH knockout parasite survive the liver stage further supports this hypothesis and the parasites may have altered their carbon flux to bypass the KDH in liver.

In summary, in accordance with (17), complex I (NADH-ubiquinone dehydrogenase) of malaria ETC is not essential for liver stage. Similarly, I have found parasites with defects in complex V (ATP synthase) could also complete the liver stage. On the other hand, complex III (cytochrome *bc* complex) of ETC is the target of the drug atovaquone, which robustly inhibits the liver stage, implying the crucial nature of the complex III (22). Similarly, my finding that SDH A subunit gene deletion prevented parasites from completing the liver stage tentatively suggests that complex II of ETC might be essential for exo-erythrocytic parasite development. Yet, KDH of the TCA cycle seems to be less vulnerable to genetic manipulation as the knockouts could complete liver stage.

This first foray into the reverse genetics of malaria parasite liver stage energy metabolism provides a preliminary finding that hepatic stages of the rodent malaria parasite probably don't require mitochondrial ATP synthesis. My tentative conclusion is that liver stage parasites resemble blood stage parasites in relying on glycolysis to generate most of their ATP, but the initial experiments with TCA and ETC knockout parasites are somewhat inconsistent and bear repetition and refinement. Clearly, it would be advantageous to fluorophore tag null alleles to better genotype individual parasites. Additionally, it would be optimal to clone knockout lines rather than relying on the asserted lack of spurious integration of *Plasmo*GEM vectors, which perhaps confounded some of my assays. Nevertheless, I demonstrate the excellent utility of my complementation strategy to undertake reverse genetic studies of liver stage malaria parasite energy metabolism for which there has previously been an impasse.

3.5 References

1. MacRae JI, Dixon MW, Dearnley MK, Chua HH, Chambers JM, Kenny S, et al. Mitochondrial metabolism of sexual and asexual blood stages of the malaria parasite *Plasmodium falciparum*. BioMed Central Biology. 2013;11:67.
2. Sturm A, Mollard V, Cozijnsen A, Goodman CD, McFadden GI. Mitochondrial ATP synthase is dispensable in blood-stage *Plasmodium berghei* rodent malaria but essential in the mosquito phase. Proceedings of the National Academy of Sciences. 2015;112:10216-23.
3. Oppenheim RD, Creek DJ, Macrae JI, Modrzynska KK, Pino P, Limenitakis J, et al. BCKDH: The missing link in apicomplexan mitochondrial metabolism is required for full virulence of *Toxoplasma gondii* and *Plasmodium berghei*. PLoS Pathogens. 2014;10:e1004263.
4. Ke H, Lewis IA, Morrisey JM, McLean KJ, Ganesan SM, Painter HJ, et al. Genetic investigation of tricarboxylic acid metabolism during the *Plasmodium falciparum* life cycle. Cell Reports. 2015;11:164-74.
5. Jacot D, Waller RF, Soldati-Favre D, MacPherson DA, MacRae JI. Apicomplexan energy metabolism: Carbon source promiscuity and the quiescence hyperbole. Trends in Parasitology. 2016;32:56-70.
6. Walker JE. The atp synthase: The understood, the uncertain and the unknown. Portland Press Limited; 2013.
7. Walker J, Fearnley I, Gay N, Gibson B, Northrop F, Powell S, et al. Primary structure and subunit stoichiometry of F1-ATPase from bovine mitochondria. Journal of Molecular Biology. 1985;184:677-701.
8. Hino A, Hirai M, Tanaka TQ, Watanabe Y-i, Matsuoka H, Kita K. Critical roles of the mitochondrial complex II in oocyst formation of rodent malaria parasite *Plasmodium berghei*. The Journal of Biochemistry. 2012;152:259-68.
9. van Dijk MR, Janse CJ, Thompson J, Waters AP, Braks JA, Dodemont HJ, et al. A central role for P48/45 in malaria parasite male gamete fertility. Cell. 2001;104:153-64.
10. Rathnapala UL, Goodman CD, McFadden GI. A novel genetic technique in *Plasmodium berghei* allows liver stage analysis of genes required for mosquito stage development and demonstrates that *de novo* heme synthesis is essential for liver stage development in the malaria parasite. PLoS Pathogens. 2017;13:e1006396.

11. Kooij TW, Rauch MM, Matuschewski K. Expansion of experimental genetics approaches for *Plasmodium berghei* with versatile transfection vectors. Molecular and Biochemical Parasitology. 2012;185:19-26.

12. Bushell E, Gomes AR, Sanderson T, Anar B, Girling G, Herd C, et al. Functional profiling of a *Plasmodium* genome reveals an abundance of essential genes. Cell. 2017;170:260-72. e8.

13. Nina PB, Morrisey JM, Ganesan SM, Ke H, Pershing AM, Mather MW, et al. ATP synthase complex of *Plasmodium falciparum* dimeric assembly in mitochondrial membranes and resistance to genetic disruption. Journal of Biological Chemistry. 2011;286:41312-22.

14. Srivastava A, Creek DJ, Evans KJ, De Souza D, Schofield L, Müller S, et al. Host reticulocytes provide metabolic reservoirs that can be exploited by malaria parasites. PLoS Pathogens. 2015;11:e1004882.

15. Liu K, Dong Y, Huang Y, Rasgon JL, Agre P. Impact of trehalose transporter knockdown on *Anopheles gambiae* stress adaptation and susceptibility to *Plasmodium falciparum* infection. Proceedings of the National Academy of Sciences. 2013;110:17504-09.

16. Goodman CD, Buchanan HD, McFadden GI. Is the mitochondrion a good malaria drug target? Trends in Parasitology. 2017;33:185-93.

17. Boysen KE, Matuschewski K. Arrested oocyst maturation in *Plasmodium* parasites lacking type II NADH: Ubiquinone dehydrogenase. Journal of Biological Chemistry. 2011;286:32661-71.

18. Painter HJ, Morrisey JM, Mather MW, Vaidya AB. Specific role of mitochondrial electron transport in blood-stage *Plasmodium falciparum*. Nature. 2007;446:88.

19. Nagaraj VA, Sundaram B, Varadarajan NM, Subramani PA, Kalappa DM, Ghosh SK, et al. Malaria parasite-synthesized heme is essential in the mosquito and liver stages and complements host heme in the blood stages of infection. PLoS Pathogens. 2013;9:e1003522.

20. Rizopoulos Z, Matuschewski K, Haussig J. Distinct prominent roles for enzymes of *Plasmodium berghei* heme biosynthesis in sporozoite and liver stage maturation. Infection and Immunity. 2016.

21. Ke HJ, Sigala PA, Miura K, Morrisey JM, Mather MW, Crowley JR, et al. The heme biosynthesis pathway is essential for *Plasmodium falciparum* development in

mosquito stage but not in blood stages. Journal of Biological Chemistry. 2014;289:34827-37.

22. Davies C, Pudney M, Nicholas J, Sinden R. The novel hydroxynaphthoquinone 566C80 inhibits the development of liver stages of *Plasmodium berghei* cultured *in-vitro*. Parasitology. 1993;106:1-6.

3.6 Tables and figures

Table 3.6.1: List of primers used for screening of genes

Gene		5'-3'	Expected size (bp)
ATPβ			
KO	SP	CCGCTCAGGAACGAATTTAG	2670
	ASP	TGTGAATTCCGTCCCAACAAACAATTAACA	
WT	SP	TGATTTTAGTGGTTCAAAAGCTG	807
	ASP	TGTGGATCCCATTTGTTTAGCCATTTC	
P48/45			
KO	SP	CATTCATACATACATGTGTATGG	1300
	ASP	ACGCATTATATGAGTTCATTTTAC	
WT	SP	TTTTGGGAACAGCCGTTTT	689
	ASP	TTTGTTTGCACGCTAGCACT	
GIMO GFP			
GFP	SP	AACTGAAAAAGAGCGCAAATG	1570
	ASP	CCCAGAATTCCCATGAACTG	
No GFP	SP	GCGGCCGCGTTTGTATTATGCACGCAAC	1070
	ASP	TCTTGAGGAACGGATAGACAC	
SDH A			
KO	SP	GGTGAGGCTTCGGAACCATT	1426
	ASP	AGGGGCCATACTATGCTTGG	
WT	SP	TGATGGGCAAGGACCTGAGCA	350
	ASP	AGCAGCATAAACATCTCGGCCTGA	
KDH			
KO	SP	TTGTTACTGGTGCCCTCGAC	1468
	ASP	GACGCACCTCAAGAAGAAGGA	
WT	SP	TGCCACAATCAGCCATATTAGGT	1012
	ASP	GACGCACCTCAAGAAGAAGGA	
SDH B			
KO	SP	TTGTTACTGGTGCCCTCGAC	1110
	ASP	TGCTTAATGTTTGCAAGCTCAA	
WT	SP	TGGATGGAAGAGAAGCCGTACA	360
	ASP	TTGCAATTTATGGGATGCCA	

Table 3.6.2: Number of mCherry expressing merosomes generated by each strain at 70 hpi in the ATPβ^{KOmCh} study

Strain	Number of mCherry expressing merosomes (number of trails=4)
ATPβ^{KOmCh} x ATPβ^{WT}-GFP	45±11
ATPβ^{WT}mCh x ATPβ^{WT}-GFP	25±34
ATPβ^{KOmCh} Pbs48/45^{WT} x ATPβ^{WT} P48/45^{KO}	31±34
ATPβ^{WT}mCh Pbs48/45^{WT} x ATPβ^{WT} Pbs48/45^{KO}	55±9

Table 3.6.3: List of selected genes associated with TCA and ETC

*Plasmo*DB ID	*Plasmo*GEM ID	Gene name and the abbreviation used	Associated pathway
PBANKA_0518200	275858	Flavoprotein subunit of succinate dehydrogenase (SDH A)	TCA and ETC
PBANKA_1428800	111006	Iron-sulfur subunit of succinate dehydrogenase (SDH B)	TCA and ETC
PBANKA_1419100	110413	Dihydrolipoamide succinyl transferase (E2) of 2-oxoglutarate dehydrogenase complex (KDH)	TCA

Table 3.6.4: Number of salivary gland sporozoites/ mosquito produced

Strain	Salivary gland sporozoites/ mosquito (number of trials=1)
SDH A^{KO} x SDH A^{WT}-GFP	28,609
SDH B^{KO} x SDH B^{WT}-GFP	14,819
KDH^{KO} x KDH^{WT}-GFP	10,667

Table 3.6.5: Results of P0 infection in mice

Gene	KO	Cross			
	bite-back	bite-back		sporozoite IV	
		pyr -	pyr +	1000 (pyr +)	10000 (pyr +)
SDH A	NP	WT	NP	NP	NP
SDH B	NP	WT+ KO	NP	NP	NP
KDH	NP	WT	KO	NP	NP

NP; no parasites recovered WT; wildtype parasites KO; knockout parasites pyr +/-; with and without pyrimethamine treatment. Number of trials=1

Figures

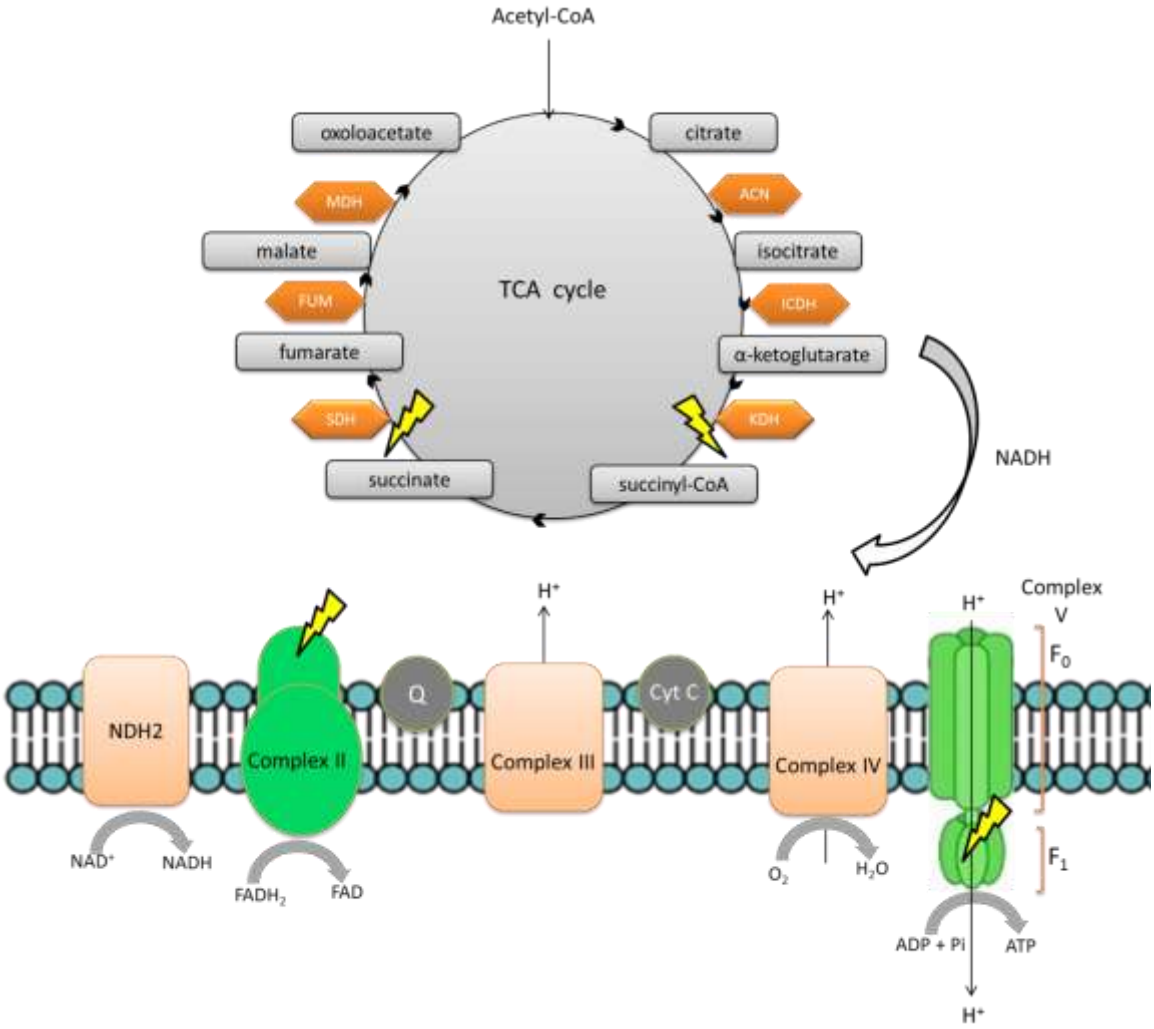

Figure 3.6.6: A diagram showing mitochondrial tricarboxylic acid cycle (TCA) and electron transport chain (ETC) to represent the gene candidtats of the study. The α-ketoglutarate dehydragenase (KDH) gene which converts α-ketoglutarate to succinyl-CoA belongs to the TCA cycle and succinate dehydrogenase (SDH) oxidizes succinate to produce fumarate as a TCA cycle member and it reduces fumarate at the complex II of ETC. ATP synthase is the complex V of ETC which harvest ATP, generated through the mitochondrial membrane proton gradient. Yellow arrows depict the disruption of pathway by deleting particular genes.

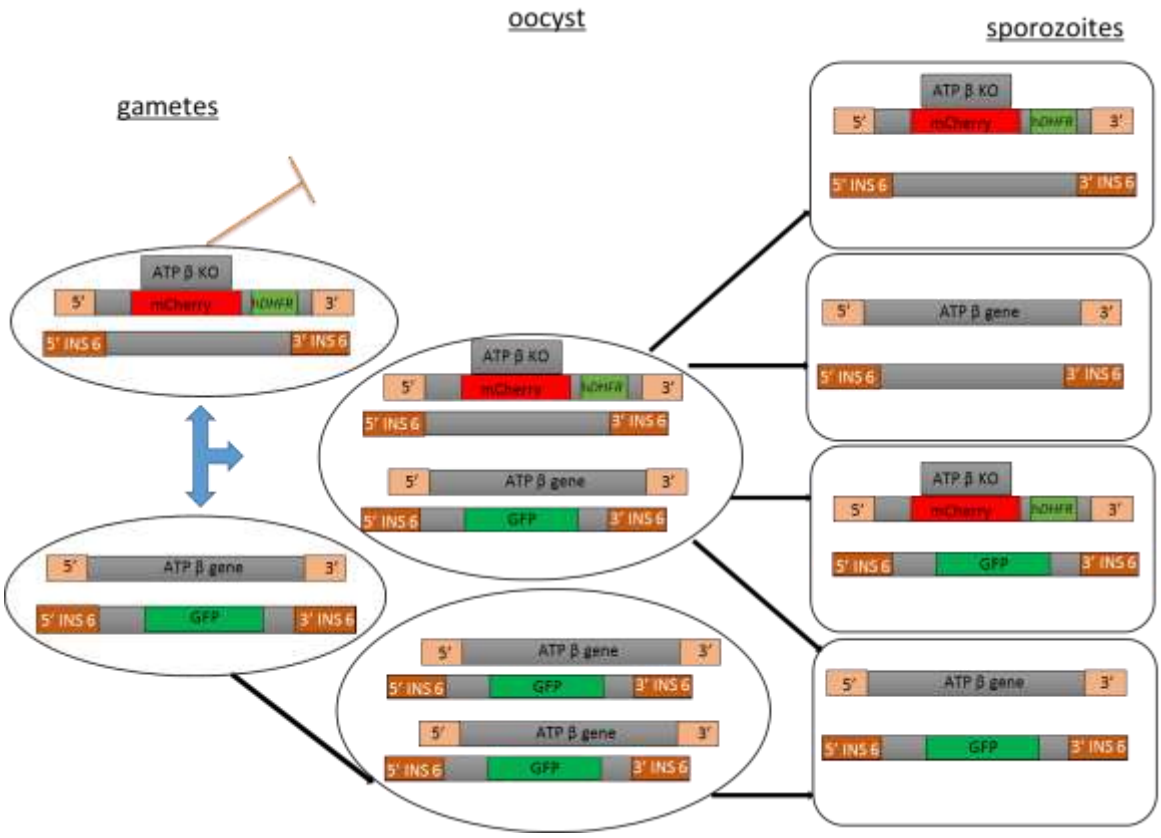

Figure 3.6.7: Schematic representation of the predicted parasite genotypes at the polyploid oocyst stage and haploid sporozoite stage after allowing mosquitoes to feed on mice dually infected with ATPβ^{KOmCh} and ATPβ^{WT}-GFP parasites. The ATPβ^{KO} mutation prevents self-fertilization of this parasite line, so two genetic combinations are possible in the polyploidy oocyst: outcrossing creating an oocyst with both ATPβ^{KOmCh} and the ATPβ^{WT}-GFP alleles (orange phenotype) and self- fertilization yielding oocysts with only the ATPβ^{WT}-GFP allele (green phenotype). Following sporogony, the parasite returns to the haploid state yielding four possible genetic combinations of the ATPβ^{KOmCh} and the ATPβ^{WT}-GFP genes: The original ATPβ^{KOmCh} (red) or ATPβ^{WT}-GFP (green) alleles alone, a combination of both the ATPβ^{KOmCh} and ATPβ^{WT}-GFP alleles (orange) or parasites carrying neither allele (colourless).

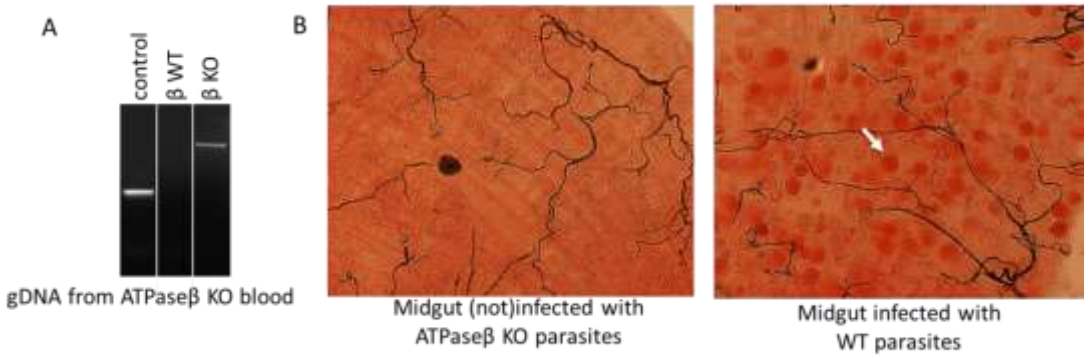

Figure 3.6.8: Confirmation of ATPaseβ knockout clone (A) PCR reaction showing the ATPaseβ gene knockout/ deletion of the ATPase β gene. Primers used are, control; to amplify a known region in the parasite genome, β WT; to amplify the wildtype gene, β KO; to amplify the knockout gene (Table 3.6.1) (B) Mosquito midguts infected with (I) ATPaseβ KO (II) control wildtype *P. berghei* to compare the absence of knockout oocysts in the mercurochrome stained midguts (arrow head shows an oocyst)

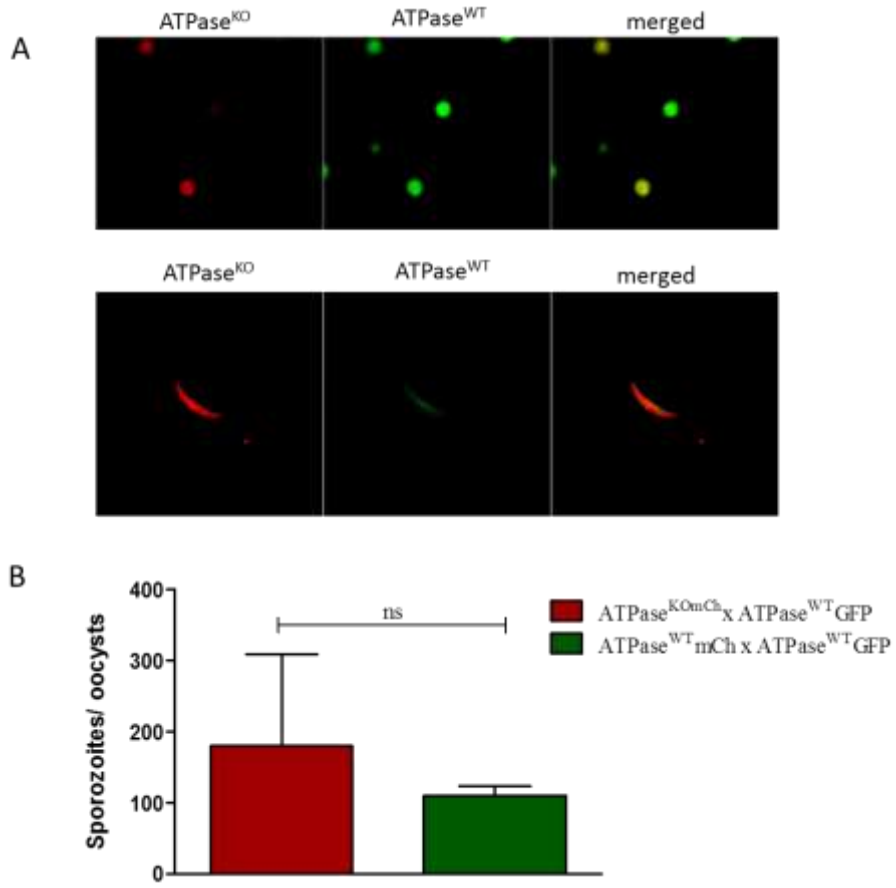

Figure 3.6.9: Mosquito stage development of ATPβ^{KOmCh} x ATPβ^{WT}-GFP dual infected parasites (A) Orange colour oocysts at day 12 post infection expressing mCherry (ATPase^{KOmCh}) with GFP (ATPβ^{WT}-GFP) and oocysts with GFP alone (ATPβ^{WT}-GFP). The salivary gland sporozoites day 21 post infection are stained with anti-mCherry antibody to show the presence of ATPβ^{KOmCh} (B) Graph showing a comparison of the ratios of salivary gland sporozoites/ oocysts between cross and control strains (P=0.6448; student t-test) ns; not significant

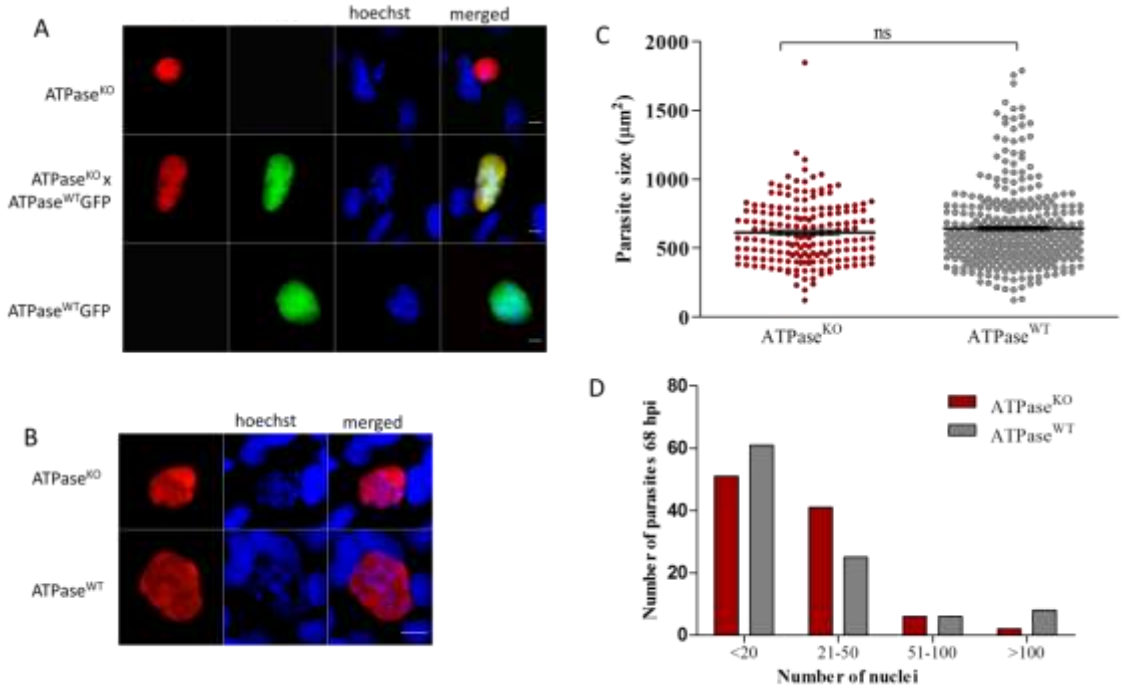

Figure 3.6.10: In-*vitro* liver stage growth of ATPβ^{KOmCh} parasites (A) ATPβ^{KOmCh} x ATPβ^{WT}-GFP; the parasites are stained with anti-mCherry antibody and DNA stain Hoechst (68 hours post infection (hpi) to show the presence of, parasites having only red colour, both red and green colours and only green colour. The red colour parasites contain the ATPβ^{KOmCh} allele and are originated from the recombination (Fig 3.6.7). Similarly, the orange colour parasite is a recombinant. The green colour parasites come from either self-fertilized green colour oocyst or from the heterozygous orange colour oocyst (Fig 3.6.7) (B) ATPβ^{KOmCh} Pbs48/45^{WT} x ATPβ^{WT} P48/45^{KO}; represented as ATPase^{KO} and their equivalent control parasites (represented as ATPase^{WT}, a wildtype *P. berghei* strain expressing mCherry mixed with P48/45^{KO}) stained with anti-mCherry antibody and Hoechst, 68 hpi. Scale bar 20 µm (C) Graph showing a comparison of average size (in µm^2) of β knockout parasites and the equivalent control strain 68 hpi where the differences is not statistically significant (P=0.2292; student t-test) ns; not significant (D) A comparison of number of nuclei produced by each strain of parasites 68 hpi. Both ATPβ^{KOmCh} and wildtype lines producing parasites with more than 100 nuclei (P value=0.0389; χ^2).

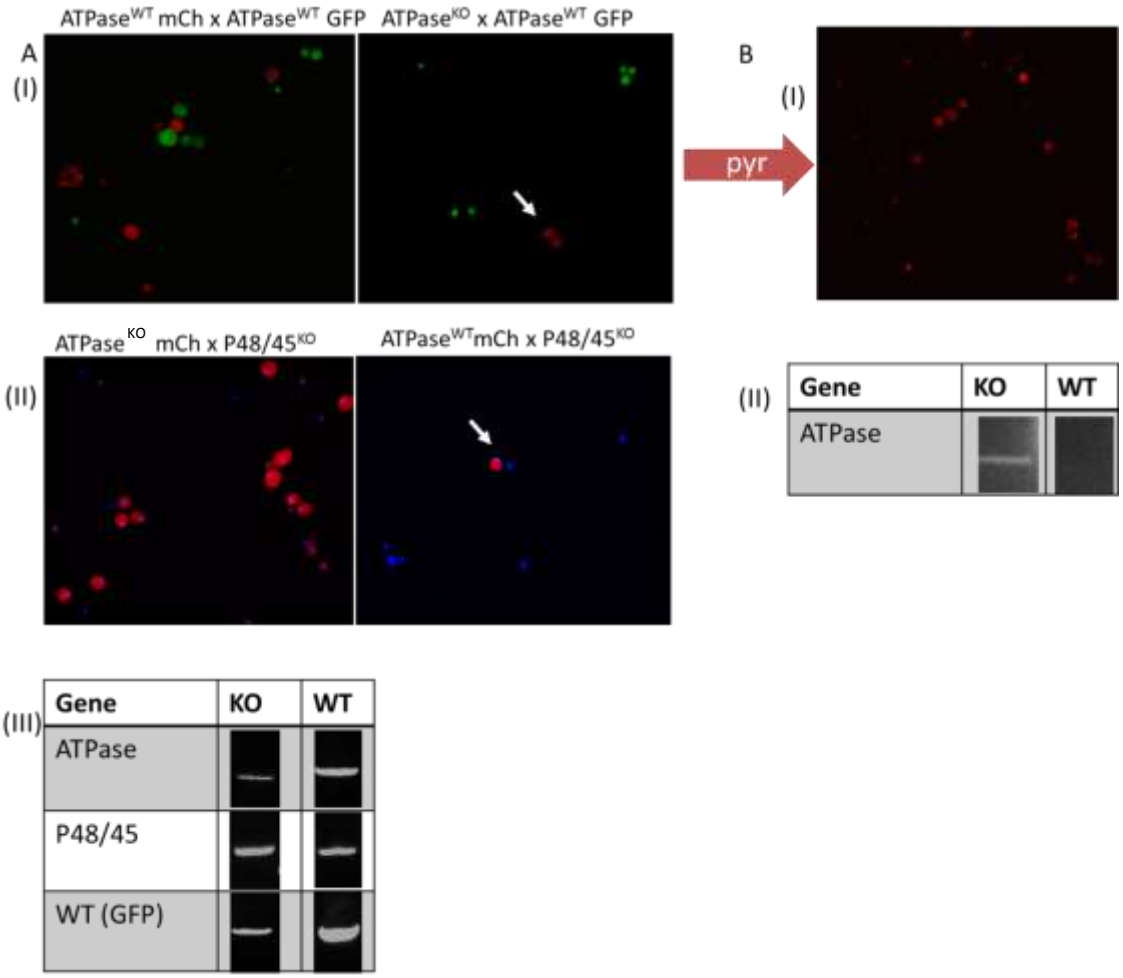

Figure 3.6.11: P0 blood stage growth of ATPβ^{KOmCh} parasites (A) Fluorescence microscopy images showing (I) recovery of ATPβ^{WT}mCh x ATPβ^{WT}-GFP parasites with both GFP and mCherry expression and knockout parasites expressing mCherry (arrow head) and GFP, from ATPβ^{KOmCh} x ATPβ^{WT}-GFP cross. The propotion of mCherry expressing knockout parasites is very low compared to the green colour (either self-fertilized or recombinants) parasites (II) images of red colour ATPβ^{KOmCh} parasites (arrow head) mixed with P48/45^{KO} and the equivalent control. In both the original cross (with ATPβ^{KOmCh}) and the control (with ATPβ^{WT}mCh); the P48/45^{KO} strain has no intact fluorescent marker hence only the red colour expression can be seen. (Parasite DNA has been strained and seen in blue colour) (III) genotypes of parasites recovered as P0 by PCR which include all the expected genotypes post recombination at mosquito stage; (1) knockout ATPase and wildtype copy of ATPase (2) knockout P48/45 and wildtype P48/45 and (3) parasites with GFP (KO) and without (WT) GFP expression. Primers in Table 3.6.1 (B) (I) pyrimethamine selection of P0 ATPβ^{KOmCh} x ATPβ^{WT}-GFP parasites showing the elimination of drug sensitive GFP expressing wildtype

parasites while the number of mCherry expressing ATPβ^{KOmCh} parasites show a drastic increase over 2-3 days post treatment (II) genotype (PCR) of parasites recovered through the drug treatment where all the parasites have knocked-out ATPaseβ gene (note the absence of a PCR amplification for the wildtype ATPase gene).

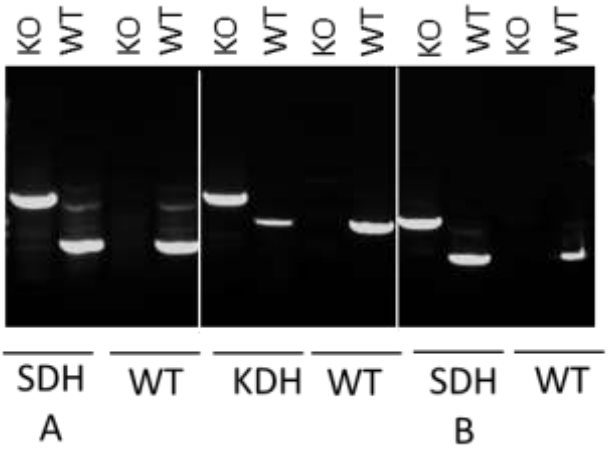

Figure 3.6.12: Confirmation of blood stage SDH A^{KO}, KDH^{KO} and SDH B^{KO} post transfection by PCR. The primers (Table 3.6.1) were used to amplify a knockout (KO) in the gene and a wildtype (WT) region of the selected genes respectively. For each gene, not only the gDNA from the transfected population (SDH A, KDH and SDH B respectively) but also wildtype (WT) gDNA was used for additional confirmation of the gene knockout of parasites.

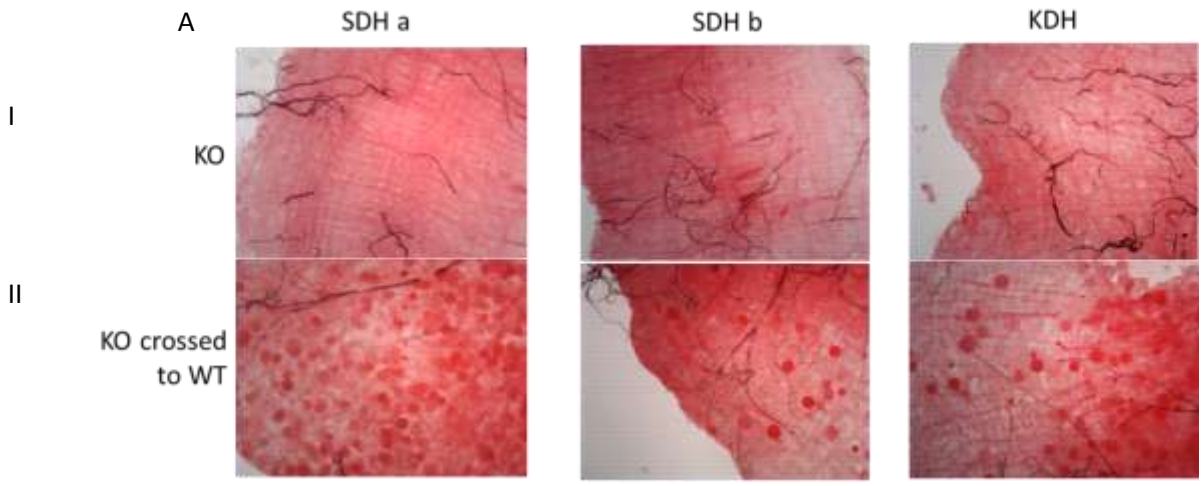

B

	Mixed blood		oocysts		Sporozoites		P0 (- pyr)		P0 (+ pyr)	
	KO	WT	KO	WT	KO	WT	KO	WT	KO	WT
SDH a									NP	NP
SDH b									NP	NP
KDH (b)										

Figure 3.6.13: Analysis of growth of SDH A, SDH B and KDH knockout parasites throughout the life cycle (A) Mercurochrome stained midguts infected with (I) uncloned strains of SDH A^{KO}, SDH B^{KO} and KDH^{KO} respectively showing the absence of oocysts. Occasionally some oocysts appeared probably originated from the wildtype parasites in the uncloned population (Fig 3S). Similarly, no parasites were recovered as P0 by bite-back confirming the essentiality of the genes for parasite transmission (II) oocysts generated from dual-infected SDH A^{KO} x SDH A^{WT}-GFP, SDH B^{KO} x SDH B^{WT}-GFP and KDH^{KO} x KDH^{WT}-GFP parasites respectively. (B) Recovered genotypes of mixed infected strains in blood, oocysts, salivary gland sporozoites and P0 blood stages respectively. The number of mice infected to generate P0 (Table 3.6.5) by biting were doubled and one set of mice were treated with pyrimethamine (pyr +) and the other set of mice left untreated (pyr -). NP; no parasites recovered. For SDH A^{KO} x SDH A^{WT}-GFP and SDH B^{KO} x SDH B^{WT}-GFP, both knockout and wildtype genes are present from the initial mixed blood stage to until the formation of sporozoites. As for the P0 infection of the SDH A^{KO} cross-infection, knockout parasites are clearly absent

as per the PCR, confirming a growth defect during liver stage. As for the SDH B^{KO}, a similar pattern of knockout and wildtype parasites are present from the first blood stage to sporozoites, but a faint PCR band along with a strong wildtype PCR band indicate the recovery of knockout parasites as P0. Upon pyrimethamine treatment however, the knockout parasites were not recovered. The KDH^{KO} parasites along with a wildtype copy of the gene are seen in the blood stage but the knockout is next seen with the recovery as P0 with the drug treatment (day 7 post-infection). Presence of only a small number of knockout parasites must have caused the knockout (KO) PCR band to disappear throughout the mosquito stage as well as in the P0 without drug selection. Only by removing the drug sensitive wildtype parasites, the knockout population reached to a detectable level. The recovery of KDH^{KO} with a substantial delay of days of patency (day 7) confirmed the gene has no apparent function in liver stage but might have a mild growth defect, most probably during their mosquito stage, which was not strong enough to prevent parasites from completing the liver stage. All the mice infected by sporozoite IV injection and immediately treated with pyrimethamine to generate P0, were negative for all three types of strains (Table 3.6.5).

Supplementary figure

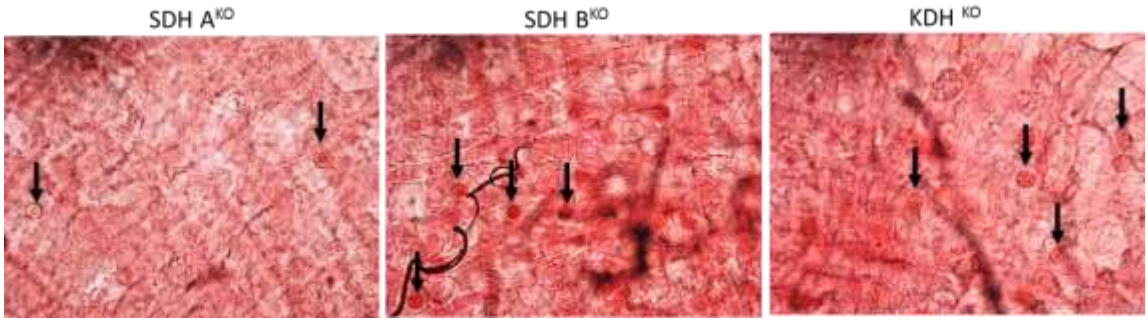

Figure 3S: Presence of mercurochrome stained oocysts in SDH A, SDH B and KDH knockout strains. Since the knockout parasites were uncloned, the few numbers of oocysts present (arrow heads) must be wildtype origin.

Chapter 4

Analyzing liver-stage defects in parasites with knockouts in blood stage essential genes

4.1 Introduction

The isoprenoids are a large class of natural products and metabolites that serve various functions including protein prenylation and protein anchoring, quinone production, cell membrane maintenance, and synthesis of hormones (1). There are two routes of biosynthesis of isoprenoids: one starting with mevalonate and one starting with non-mevalonate substrate. Malaria parasites use the pathway starting with a non-mevalonate substrate, known as 2-C-methyl-D-erythritol-4-phosphate (MEP), which is also known as the 1-deoxy-D-xylulose-5-phosphate (DOXP) (Fig 4.6.5). In addition to malaria parasites, higher plant plastids, most algae and bacteria all use the MEP/ DOXP pathway. In contrast, mammals, Archaea, a few bacteria, fungi, and the cytosol and mitochondria of plants utilize the other mevalonate (MVA) based pathway (2, 3). Humans/ mammals thus lack the non-mevalonate (MEP or DOXP) pathway, which suggests that inhibitors specific for MEP/DOXP should represent useful antimalarial drugs (3).

The discovery that fosmidomycin (Fos) and its derivative FR-900098 inhibit the malaria parasite apicoplast MEP pathway (4) confirmed that MEP is a valid antimalarial drug candidate, and Fos went into clinical trials. Fos inhibits deoxyxylulose phosphate reductoisomerase (DXR), which is the second of seven MEP isoprenoid synthesis pathway enzymes (Fig 4.6.5) (5). MMV008138 is an antimalarial candidate from the Malaria Box collection of antimalarials that targets IspD (MEP cytidyltransferase) of isoprenoid biosynthesis pathway (Fig 4.6.5) (6, 7). DXS and IspF (2C-Methyl-D-erythritol-2,4-cyclodiphosphate synthase) are also promising drug targets, with DXS being involved in the biosynthesis of both vitamin B1 and vitamin B6 (8) and IspF playing a crucial role in the regulation of the MEP pathway (3)

Howe et al in 2013 (9) demonstrated that Fos treatment reduced protein prenylation of *P. falciparum*, proving that the MEP pathway is responsible for generation of the isoprenoid precursors used in protein prenylation. Further, along with inhibition of the isoprenoid biosynthesis, parasites show late developmental arrest with morphological

defects in the food vacuole, which is consistent with a loss of protein prenylation (9). Isoprenoid biosynthesis also plays a major role in the production of ubiquinone, an electron carrier and a cofactor for the dihydroorotate dehydrogenase (DHODH) enzyme of the pyrimidine biosynthesis pathway (10).

The substrates for apicoplast MEP come from the parasite cytosol. *Plasmodium* parasites have two triose phosphate/phosphate transporters, oTPT and iTPT, known to reside in the outermost and innermost membranes of the four-membraned apicoplast respectively (11). oTPT has 10 transmembrane domains and lacks a canonical bipartite leader sequence but still targets to the outer membrane of the apicoplast (11, 12). iTPT also has 10 transmembrane domains plus a classic bipartite leader thought to target it to the inner apicoplast membrane (11). These transporters are responsible (among other duties) for import of initial substrates of isoprenoid precursor synthetic pathway, dihydroxyacetone phosphate (DHAP) and phosphoenol pyruvate (PEP), into the apicoplast (Fig 4.6.5). To provide the necessary isoprenoid pathway substrates (13), imported DHAP is converted to glyceraldehyde-3-phosphate (Gly3P) by apicoplast triose phosphate isomerase (TPI), and PEP is converted to pyruvate by apicoplast localized pyruvate kinase (PK). Banerjee et al, in 2012 (14) have tested knockouts of these two transporters in *P. berghei* and found that oTPT knockout is indispensable for erythrocytic *P. berghei* while iTPT knockouts grew similar to wildtype parasites. To be more specific, they have claimed that oTPT knockout parasites do survive in erythrocytic stage but not beyond a few growth cycles, which they thus termed essential for growth (14). On the other hand, the absence of iTPT in mosquito and liver stages negatively affected parasite growth blocking development (14).

Yeh and DeRisi (15) demonstrated that inhibition of the *P. falciparum* isoprenoid biosynthesis pathway at blood stage by Fos could be rescued by adding high concentrations of the MEP pathway product isopentenyl pyrophosphate (IPP) to the growth media. Further, this IPP supplementation can reverse parasite death following antibiotic treatment that targets apicoplast housekeeping and results in apicoplast loss. These “apicoplast-minus” parasites can survive when provided with exogenous IPP, which neatly demonstrated that isoprenoid precursor biosynthesis is the only essential function of the apicoplast during parasite erythrocytic development (15).

There are only limited data available on the role of isoprenoid biosynthesis during mosquito and liver life stages. Proteomic studies showed that the enzymes of the isoprenoid synthesis pathway are expressed in these stages (16). By generating apicoplast-minus *P. falciparum* gametocytes (which had been supplemented with IPP during blood stage), Wiley and colleagues (1) demonstrated that gametocytes that lack apicoplasts exhibit growth defects and produce fewer and smaller oocysts and no sporozoites when used to infect mosquitoes. Even though this provides evidence of essentiality of the apicoplast for establishing an infection in the mosquito, it does not necessarily mean that the isoprenoid biosynthesis pathway is essential in mosquito stage parasites. Indeed, we already know (see Chapter 2) that apicoplast heme synthesis is essential in mosquitoes, so apicoplast minus parasites would be expected to fail in mosquitoes. Furthermore, apicoplast fatty acid biosynthesis is also essential for *P. falciparum* parasites in the oocysts stage, so apicoplasts are required for multiple reasons in mosquito stages. We thus have no direct evidence for the requirement (or not) of apicoplast MEP in mosquitoes.

Similarly, our understanding of the role of apicoplast MEP in liver stages is also incomplete. So far, studies manipulating the isoprenoid pathway in liver stage have relied on Fos treatment, and have provided conflicting results. Nair et al., in 2011 (17) showed *P. berghei* liver stage parasite growth was inhibited by Fos as parasites produced a reduced number of merosomes. They suggested the pathway must be required for *P. berghei* liver growth (17). In contrast, other groups (18-20) saw no effect of Fos on liver stage *P. berghei*, and concluded that the parasites are unaffected by Fos due to its inability to enter hepatocytes. Accordingly, Sparr and colleagues (20) developed a mechanism to increase the cell penetration of Fos by tagging it with cell penetrating peptides consisting of octa-arginine. Using this method, they concluded that Fos has a mild effect on liver stage *P. berghei* maturation by reducing the number of merosomes parasites produced, thereby providing evidence of the importance of the MEP pathway in hepatic stage development. While these inhibitor studies hint at a crucial role for apicoplast MEP in liver stages, there is no direct reverse genetic confirmation of whether or not apicoplast isoprenoid biosynthesis is necessary in either mosquito or liver stages, but herein lays a problem. Because the MEP pathway genes are essential at blood stage (21), one can't generate MEP knockout parasites and

passage them through the life cycle. In this Chapter I explore strategies to address this impasse.

The MEP pathway has well-established regulatory machinery. This is probably because synthesis is metabolically expensive; two ATPs and three $NADH_2$ are required for the conversion of a single glucose molecule into a single molecule of IPP (22). In order to optimize the energy requirements, it is important for a cell to regulate this energy demanding process, and this regulation can operate at three basic levels. It can be either at gene level, at protein regulation or by controlling the metabolic activity within the cell (23). At the transcript level, it has been demonstrated in *Arabidopsis thaliana*, that an RNA-processing protein called Rif10 can control the MEP pathway enzymes at their transcript level (24). In *P. falciparum* however, chemical inhibition did not result in significant changes in the transcript levels of MEP pathway enzymes (25). Evidence of isoprenoid biosynthesis pathway regulation by metabolic intermediates has drawn much interest recently. Products of the MEP pathway, IPP and DMAPP cause feed-back inhibition of DXS in *Populus trichocarpa* (14). A feed-forward mechanism of regulation has also been detected in *E. coli*, where IspF is activated by the upstream intermediates of MEP pathway (3). Haloacid dehalogenase-like hydrolase (HAD) 1 is a cytosolic sugar phosphate member. HAD catalyses the dephosphorylation of cytosolic phosphometabolites particularly of glycolysis. HAD1 activity thus decreases the availability of sugar phosphates, and by extension, the substrates of the MEP pathway. Hence HAD negatively regulates the MEP pathway (Fig 4.6.5). In Fos resistant parasites, HAD1 activity is lost and the level of MEP metabolites (particularly DXR) increases, hence the competitive inhibition of Fos with DXR diminishes. Therefore HAD is a major regulator of the MEP pathway (26).

The objective of this Chapter is to develop a new stage-specific knockout strategy using selected genes of the blood stage essential isoprenoid biosynthesis pathway. My general strategy was to first introduce a complementary copy of the gene slated for knockout and then perform a knockout of the blood stage-essential endogenous gene. The two constructs (complementary and knockout) are tagged with different fluorescent markers to facilitate parasite genotyping. Importantly, the complementary copy of the gene is inserted in a null locus on a different chromosome to the knockout locus. With this complemented knockout line in hand, I would then exploit sex and segregation in the

mosquito to separate the complementary copy of the gene from the knockout copy during sporogony to produce null mutant sporozoites hopefully able to invade liver cells. This strategy is similar to the use of independent assortment of genes during sexual recombination exploited in Chapter 2, but in this case the gene has to be introduced in blood stage before making the knockout and sex, recombination, and segregation back to haploidy does the rest (Figs 4.6.6 I, 4.6.7). Effectively, this strategy was planned to give me stage specific (sporogony) knockouts of genes known to be essential in an earlier life cycle stage, namely blood stage. In this way, it was envisaged that the effects of isoprenoid production gene knockouts on transmission and subsequently liver stage growth could be studied. Most importantly this strategy is the first to allow such separation and direct study of, blood stage essential genes in liver stage by means of natural segregation.

I selected three genes to explore whether I could make knockouts of blood stage essential genes by first introducing a complementary gene copy at a remote locus:

(1) oTPT (outer-triose phosphate transporter); a gene essential for phosphoenolpyruvate transport, a primary source of both energy and carbon backbones for isoprenoid biosynthesis (11).
(2) DXR (1-deoxy-D-xylulose-5-phosphate reductoisomerase (also known as IspC); a gene in the MEP pathway and the target of antimalarial drug fosmidomycin (6).
(3) IspF (2C-methyl-D-erythritol-2,4-cyclodiphosphate synthase); a gene in the MEP pathway which is assumed to play an important role in pathway regulation (3).

Here I describe successes (and failures) in prior complementation and subsequent knockout of these three blood stage essential genes. I also describe the crossing of one complemented knockout (DXR) with wildtype parasites in mosquitoes that allowed me to generate the first knockout sporozoites of a MEP pathway gene and infect liver cells to test the role of MEP in the malaria parasite hepatic stage.

4.2 Materials and methods

4.2.1 Generation of gene constructs

4.2.1.I Generation of gene knockouts (oTPT/IspF/DXR KO^{Tm})

To generate the gene knockout constructs, first the 5' and 3' flanks of the genes were PCR amplified using Phusion High-Fidelity DNA Polymerase (primers; Table 4.6.1). PCR conditions used for the above reaction are as follows;

Initial denaturation	98 ºC	30 sec
35 cycles	98 ºC	10 sec
	57 ºC	30 sec
	68 ºC	1 min
Final extension	68 ºC	10 min

Then, the sequences were ligated into the intermediate vector pGEM-T Easy (Promega), and verified by Sanger sequencing with primers SP6 and T7 (Promega). Next, the 3' flank was ligated into the pLSKDTm (27) vector using *Sac*II and *Hind*III-HF (BioLabs) enzymes (Table 4.6.3). The correct insertion was confirmed by PCR, and DNA was amplified by bacterial transformation. Following a restriction digestion of DNA screen to further confirm the insertion, the 5' flank was ligated into the resulting vector using *Nhe*I and *Kpn*I enzymes. Finally, the knockout constructs were confirmed with a series of screen restriction digestions pre transfection. The confirmed vector with the gene knockout construct was bacterial transformed and DNA amplified (Promega). Then the final vector was linearized using restriction enzymes *Hind*III-HF and *Nhe*I, gel purified (Bioline) and DNA ethanol precipitated. Finally, the transfection of the knockout constructs was performed as per (28) using blood stage *P. berghei* wildtype parasites (*Pb*ANKA) as the recipient strain.

4.2.1.II Generation of gene complementary (oTPT/IspF/DXR Comp^{GFP}) line

Generation of oTPT complementary (oTPT Comp^{GFP}) line

To generate the gene oTPT complementation vector, first the corresponding region of the gene coding sequence was amplified from *P. berghei* genomic DNA using Phusion High-Fidelity DNA Polymerase (primers in Table 4.6.1). The primers omitted the oTPT stop codon so that the translation could continue into the hemagglutinin (HA) tag. This sequence was cloned into the intermediate vector pGEM-T Easy (Promega), verified by

Sanger sequencing with primers SP6 and T7 (Promega), then ligated into the multiple cloning site of the "Int6HSP70GFPcam3'rc" (Table 4.6.2). The resulting complementation vector contained the gene sequence fused to N-terminal HA tag. Due to the failure of getting bacterial colonies post transformation despite several attempts, a new vector was designed by ligating HSP70GFPcam3'rc and "pBART sil6" (vector I, Table 4.6.2). Next, the oTPT gene complementation construct in pGEM-T was ligated into the newly made vector. After that, the promoter peptide deformylase (PDF); PBANKA_0809300 (kindly given by Dr Goodman) was ligated into the resulting vector which has the gene complementation construct (vector II). The confirmed vector with the gene complementary construct was bacterial transformed and DNA amplified (Promega). Restriction digestion and PCR screening was used to confirm the correct integration. Next, the final vector was linearized using restriction enzymes *Bgl*II and *Nae*I, gel purified (Bioline), and DNA ethanol precipitated prior to transfection. After that, the newly made construct was transfected into *P. berghei* infected with *Pb*ANKA Gene Insertion Marker Out (GIMO) P0 parasites with the positive and negative selectable markers fused (*h*DHFR:*y*FCU) (29). As the last step, the parasites were selected by 5 FC (5-fluorocytosine) drug (1mg/ml) treatments given in the mice's drinking water to select parasites without the *h*DHFR:*y*FCU marker.

To insert a multiple cloning site in-order to ensure the final restriction digestion performs an efficient double cross-over recombination, a new fragment (PCR amplified, primers; Table 4.6.1) was ligated into the 3' prime region of the previous vector pBART sil 6 (forming pBART sil6+ DG3). Next, the resulting vector was ligated to vector I. In this way, the 3' flank of the previous vector was replaced with the new fragment with multiple cloning sites (vector III: Table 4.6.2). With the resulting vector, the same procedure was followed to insert the oTPT complementary sequence (vector IV) and next, the promoter PDF (vector V). Finally the transfection was performed as described above.

Next, the EF-1α region (primers in Table 4.6.1) was PCR amplified with Phusion High-Fidelity DNA Polymerase using the vector pLSKDTm as template. This sequence was cloned into the intermediate vector pGEM-T Easy (Promega), verified by Sanger sequencing with primers SP6 and T7 (Promega). This intermediate vector was then ligated to the *Kas*I site of the vector from last step (vector V), to replace the PDF with

the new promoter EF-1α. Following the new promoter insertion, another transfection was performed as described above.

As the next step, Int6 HSP70 GFPHA in pBKS was used as the new vector to ligate the complementary gene construct. After ligating the oTPT Comp into this new vector (vector VI: Table 4.6.2) followed by promoter EF-1α ligation, a transfection was completed with *Pb*ANKA GIMO as the parental strain.

Generation of IspF and DXR complementary (IspF/DXR Comp^{GFP}) line

First, the corresponding region of the gene coding sequence was (the primers were selected similar to that for the oTPT construct) amplified from *P. berghei* genomic DNA using Phusion High-Fidelity DNA Polymerase (primers: Table 4.6.1). This sequence was cloned into the intermediate vector pGEM-T Easy (Promega), verified by Sanger sequencing with primers SP6 and T7 (Promega). Then the intermediate vector was ligated into the multiple cloning site of the vector Int6 HSP70 GFPHA in pBKS (Table 4.6.2). Next, the PCR amplified, sequence confirmed EF-1α in pGEM intermediate vector was ligated into the vector VII. Finally the resulting vector was linearized using *Asc*I and *Not*I-HF restriction enzymes, gel purified (Bioline), DNA precipitated. As the last step, the final vector VII with EF-1α promoter was transfected into blood stage *Pb*ANKA GIMO P0 parasites. Parasites were selected using 5-FC treatment (1mg/ml).

4.2.2 Analysing of blood stage parasites

Screening of blood stage parasites post transfection was done using fluorescence microscopy (Leica DM 2500 epifluorescence microscope) and PCR. Screening PCR primers are listed in Table 4.6.1. The PCR conditions used to screen are as follows.

Initial denaturation	95 ºC	2 min
35 cycles	95 ºC	15 sec
	58 ºC	15 sec
	65 ºC	2 min
Final extension	68 ºC	5 min

To detect the HA tag expression of parasites, a western blot was performed as follows.

Saponin lysis and sample preparation

Blood stage parasites were isolated by saponin lyses. First, the blood was mixed with 10X volumes of saponin (0.15 % w/v; Sigma-Aldrich) in 1X phosphate buffered saline (PBS) and incubated for 5 minutes on ice. Then parasites were centrifuged at 4000 rpm for 5 minutes at 4 ºC followed by multiple washings of the pellet with ice-cold 1X PBS. As the last step, the parasites were mixed with reducing buffer [4X NuPAGE LDS sample buffer (Thermo Fisher Scientific) mixed with β-mercaptoethanol] to a final concentration of 1X and samples were boiled for 5 minutes before storing at -20 ºC.

Membrane transfer and western blotting

The above prepared samples were loaded on to a NuPAGE Bis-Tris gel (Thermo Fisher Scientific) and run at 200 V for 35 minutes with the running buffer (1X NuPAGE MES SDS Running Buffer; Thermo Fisher Scientific). Next, the separated proteins were transferred from the gel to a methanol soaked 0.45 µm polyvinyl difluoride (PVDF) membrane (Thermo Fisher Scientific) in 1X transfer buffer with 10% methanol using 30 V for 75 minutes. After that, the membrane was blocked for overnight with 5% skim milk in 1X TTBS [1X tris buffered saline (TBS) with Tween 20 (Merck Millipore)] buffer. Both primary antibodies and horseradish peroxidase (HRP)-conjugated antibodies were diluted with 5% skim milk in 1X TTBS for incubation for 1-2 hours. To detect the HA tag expression, rat anti-HA (Roche) in 1:250 dilution/ goat anti-rat horseradish peroxidase (HRP) conjugated antibody (Thermo Fisher Scientific) in 1:1000 dilution were used. In between and after antibody incubations, the membrane was washed 4 times with 1X TTBS for 5 minutes each at room temperature. After that, the protein bands were detected on a ChemiDoc (BIO-RAD) using the SuperSignal West Pico Chemiluminescent Substrate (Thermo Fisher Scientific).

4.2.3 Optimising selection of post-transfected parasites

To optimize the number of GFP/tdTomato expressing parasites post transfection, the FACs sorting facility at Peter Doherty Institute for Infection and Immunity, University of Melbourne (PC2 MoFlo Astrios cell sorter) was used.

4.2.4 Drug treatment to select transfected parasites

The parasites with the gene complementary construct transfected into GIMO parasites were selected using 5- FC (5-fluorocytosine) drug (Sigma). For the selection of parasites with the knockout construct inserted, pyrimethamine (Sigma) as 70µg/ml was used.

4.2.5 Sub-cloning of transfected parasites

A single parasite having the desired genetic construct was selected by serial dilution and IV infecting into 10 naïve mice, as one parasite/ 1.5 parasite and 2 parasites per mouse (28).

4.2.6 Preliminary investigation of DXR Comp^{GFP} KO^{Tm} growth in blood, mosquitoes and in *in-vitro* liver

Blood stage

To confirm the tdTomato expression and HA of blood stage knockout parasites, a western blot was performed as described in 4.2.2 using following antibodies; polyclonal rabbit anti-mCherry (1: 250; Abcam ab167453)/ rabbit-anti HRP (1:1000; Thermo Fisher Scientific). In addition, a PCR screen was followed using primers, tdTomato of DXR KO (Table 4.6.1) to detect the tdTomato expression. Same primers were used to amplify the region (including tdTomato) using Phusion High-Fidelity DNA Polymerase and was cloned into the intermediate vector pGEM-T Easy (Promega). The plasmids were confirmed by screen restriction digestion and sent for Sanger sequencing with primers SP6 and T7 (Promega). In addition, an immunofluorescence assay (IFA) was performed on DXR Comp^{GFP} parasites as follows.

First, the coverslips with hydrophobic rings drawn were pre-coated with 0.5 mg/ml Concanavalin (conA, type V, sigma Aldrich) for 30 minutes at 37 ºC. Meanwhile, the blood was centrifuged at 4000 rpm for 2 minutes and supernatant removed. After

multiple washing steps [wash buffer; RPMI HEPES (Walter and Eliza Hall Institute) with sodium bicarbonate], the blood was re-suspended to 1% in wash buffer and added to the above pre-coated coverslips. After incubating the cells at 37 ºC for 15 minutes, the coverslips were washed with 1X mouse PBS [Dulbecco's Phosphate Buffered Saline (Thermo Fisher Scientific)] to remove unbound cells. Next, the cells were fixed with 4% paraformaldehyde and 0.005% glutaraldehyde in 1X mouse PBS by incubating for 20 minutes. Then the cells were washed with 1X mouse PBS and were permeabilised for 10 minutes with 0.1% Tx100 (Fisher Scientific). After washing the cells with 1X mouse PBS three times, the cells were blocked with 3% bovine serum albumin (BSA; Sigma Aldrich) in 1X mouse PBS for 30 minutes. The antibodies used on DXR $Comp^{GFP}$ parasites were; rat anti-HA (1:250; Thermo)/ Alexa Fluor 546 goat anti-rabbit IgG (1:1000; Molecular Probes/ThermoFisher). Similarly, another IFA was carried out for DXR $Comp^{GFP}$ KO^{Tm} parasites with rabbit anti-mCherry (1: 250; Abcam ab167453)/Alexa Fluor 546 goat anti-rabbit IgG (1:1000; Molecular Probes/ThermoFisher). In between and after antibody incubations, the cells were washed with 1X mouse PBS for 5 minutes each for up to 5 times. The DNA stain Hoechst 33342 (5µg/ ml/ Thermo Fisher Scientific) was included into the first two washings of the last washing step. Finally, a drop of Dako (Agilent) at 4 ºC was added to the coverslip and mounted on to a cleaned glass slide.

Mosquito and liver stages

The growth of DXR $Comp^{GFP}$ KO^{Tm} inside mosquitoes was examined. The experiment was done prior to the sub-cloning of the parasitic line. Adult females of *Anopheles stephensi* reared under standard insectary conditions (adult mosquitoes were grown at 27 ºC with humidity of 80% and light: dark photoperiod of 14:10 hours with a 1 hour ramp in) were used to feed on an anesthesized mouse that had been infected with DXR $Comp^{GFP}$ KO^{Tm}. Next, the growth of oocysts from the mosquito midguts were observed day 12 post infections and salivary gland sporozoites day 21 post infection. Further, the recovered salivary gland sporozoites were incubated in HepG2 cells (20,000 sporozoites per well) and fixed the cells at 48 hours post incubation (hpi). An IFA was carried out (refer to materials and methods of chapter 2) for one set of fixed sporozoites and one set of HepG2 cells fixed (refer to materials and methods of chapter 2) at 48 hours by staining with rabbit anti-mCherry (1: 250; Abcam ab167453)/Alexa Fluor 546 goat anti-

rabbit IgG (1:1000; Molecular Probes/ThermoFisher) and Hoechst 33342 (5µg/ ml). As the final step, the infected mosquitoes were allowed to bite on naïve mice to generate P0 parasites.

4.2.7 Crossing of DXR Comp^{GFP} KO^{Tm} into wildtype *P. berghei*

4.2.7.I Generation of clonal population

Once the DXR Comp^{GFP} KO^{Tm} parasites were confirmed by fluorescence microscopy, western blot and PCR as previously described, the population was sub-cloned by serial dilution (2 parasites/ mouse) to obtain a single parasite with the desired genetic combination.

4.2.7.II Infection of *A. stephensi*

Adult females of *A. stephensi* (reared under standard insectary conditions) were used to feed on anesthesized mice that had been infected with following combinations of parasites in equal numbers (2.5 x 10^5 parasites from each strain).

- DXR Comp^{GFP} KO^{Tm} x DXR^{WT} (parasites having extra DXR gene in chromosome 6 and endogenous DXR replaced with SKDTm mixed with a wildtype *P. berghei* without a fluorescent marker)
- DXR WT^{GFP} x DXR WT^{RFP} (parasites with a wildtype DXR locus and expressing GFP from another genetic locus (27) mixed with DXR wildtype parasite expressing RFP from another genetic locus (30)

To segregate the extra DXR gene copy (DXR Comp^{GFP}) from the knockout DXR (DXR KO^{Tm}) post recombination during mosquito stage development (Fig 4.6.7), I crossed the DXR Comp^{GFP} KO^{Tm} strain with a wildtype strain (without any fluorescent marker) denoted as DXR^{WT}. To control any effect of fluorophore expression, two wildtype strains expressing GFP and RFP (DXR WT^{GFP} x DXR WT^{RFP}) were crossed as follows.

Next, the oocysts from the mosquito midguts were analysed day 12 post infections and salivary gland sporozoites day 21 post infection. Genomic DNA extracted from oocysts and salivary gland sporozoites were used to perform a PCR reaction (primers; Table 4.6.1).

In addition, the mice infected with two parental strains; DXR Comp^{GFP} and DXR Comp^{GFP} KO^{Tm} were also put on *A. stephensi* individually to observe oocysts growth day 12 post infection. A PCR reaction to screen the DXR knockout region was performed using the genomic DNA extracted from mosquito midguts (primers; Table 4.6.1).

4.2.7.III Sporozoite infection in HepG2 cells

The purified salivary gland sporozoites from the cross experiment and control were incubated in HepG2 cells (20,000 sporozoites per well) with cells fixed at 68 hpi. An IFA was carried out (refer to material and methods of chapter 2) for wells fixed at 68 hours by staining parasites with rabbit anti-mCherry (1: 250; Abcam ab167453)/Alexa Fluor 546 goat anti-rabbit IgG (1:1000; Molecular Probes/ThermoFisher) and Hoechst 33342 (5µg/ ml). Next, the area of each resulting parasites was compared to their corresponding control parasites using images taken at 40X magnification of the Leica DM 2500 epifluorescence microscopy. Images were analysed by ImageJ software (ImageJ 1.46a, Wayne Rasband, National Institutes of Health). At 70 hpi, detached cells and merosome production was observed and were counted using Olympus CKX41 compound fluorescence microscope at 40X magnification.

4.2.7.IV Sporozoite infection in mice

The infected mosquitoes day 21 post infection were used to feed on naïve mice (P0 population by bite-back) and dissected sporozoites were IV injected into naïve mice as 1,000 and 10,000 sporozoites (P0 by sporozoite IV). Half of the mice infected with DXR Comp^{GFP} KO^{Tm} x DXR^{WT} were treated with pyrimethamine (70µg/ ml: Sigma) through mice drinking water while the other set of mice were not treated. All of the mice were followed up to 14 days and recorded their parasitemia. In addition to the pyrimethamine treatment, fluorescence microscopy (Leica DM 2500 epifluorescence microscopy) and PCR analysis (primers: Table 4.6.1) were used to genotype the resultant parasites from each experiment.

4.3 Results

4.3.1 Knocking out of selected blood stage essential genes

First, the three knockout constructs generated for oTPT, IspF and DXR genes (one construct for each gene; oTPT/DXR/IspF KO in pLDSKTm; Table 4.6.3) were transfected into wildtype parasites individually (three biological replicates for each gene) to confirm their essentiality for blood stage growth. In agreement with Banerjee et al., 2012 (14) for *P. berghei* oTPT, DXR of *P. falciparum* (31) and *P. berghei* (*Plasmodium* Genetic Modification database; http://plasmogem.sanger.ac.uk), no parasites were recovered despite three attempts. Similarly, IspF knocked-out parasites did not survive post transfection, further confirming the indispensable nature of isoprenoid pathway for blood stage parasites.

4.3.2 Generation of oTPT complementary (oTPT Comp^{GFP}) line

The construct carrying a complementary copy of oTPT (coTPT) driven by the PDF promoter and GFP fluorescent marker (vector II; Table 4.6.2) was transfected into GIMO parasites (which contain the positive-negative selectable marker; *h*DHFR: *y*FCU; Fig 4.6.6.I) allowing negative selection of the parasites. Thus, only the marker free parasites were expected post transfection but only ~10% of parasites contained the GFP expressing construct (Fig 4.6.8 A). To generate a population with higher proportion of GFP expressing parasites, a fluorescence assisted cell sort (FACs) was attempted following two more transfections (with a new vector construct (Vector V, Table 4.6.2) to separate the GFP parasites. All these attempts increased the number of parasites with GFP up to ~60% (Fig 4.6.8 A) and with this population I set about to knock out the endogenous oTPT gene as per the study plan. It was expected to obtain oTPT knockout parasites from this transfection assuming the donor strain already has the complementary oTPT (~60%) and the fact that oTPT knocked-out parasites did not survive on their own. However, there were no tdTomato expressing parasites (from the oTPT knockout) post transfection.

The simplest explanation of the inability of the complementary construct to support knockout of the endogeneous gene is lack of expression of the complementary copy of oTPT. To test this, a western blot was performed with antibodies against the hemagglutinin (HA) tag at the 3' end of coTPT, and there was no HA signal detected

(Fig 4.6.8). One explanation for this observation is that the chosen PDF promoter was not strong enough to drive sufficient expression of the coTPT. Thus, the PDF promoter was replaced with strong and constitutive *P. berghei* EF-1α promoter.

Multiple independent transfections with this new construct (Vector VI; Table 4.6.2) resulted in a maximum of ~60% parasites carrying the construct as confirmed by GFP expression and PCR genotyping (Fig 4.6.8 B). FACs sorting increased the level of GFP expressing parasites in the population to 90%. However, even with the majority of parasites carrying the coTPT construct, western blotting failed to detect expression of the HA tagged (Fig 4.6.8 B) protein. At this point, attempts to generate a complemented knockout of oTPT were abandoned.

4.3.3 Generation of IspF and DXR complementary (IspFComp^{GFP}/ DXRComp^{GFP}) line

The same procedure used for the oTPT gene was followed to make the complementary gene constructs of the IspF and DXR genes but this time with the Vector VII (Table 4.6.2), EF-1α promoter, C terminal HA tag and GFP. The EF-1α promoter was used instead of PDF to drive the complementary copies of IspF and DXR since more GFP expressing parasites were obtained by using EF-1α compared to the PDF promoter in previous oTPT gene study.

4.3.4 Transfection of IspF complementary (IspF Comp^{GFP}) line

The construct carrying a complementary copy of IspF (coIspF) driven by the EF-1α promoter and GFP fluorescent marker (vector VII; Table 4.6.2) was transfected into GIMO parasites and ~55% of parasites were observed to express GFP. Despite the fact that more than half the population carried the coIspF construct, no HA expression of coIspF was observed by western blot (Fig 4.6.9).

4.3.5 Transfection of DXR complementary (DXR Comp^{GFP}) line

After multiple attempts to transfect (Fig 4.6.10.I) the DXR complementary gene (EF-1α as the promoter to drive the extra DXR in Vector VI; Table 4.6.2), an enhanced population of parasites (~85%) with complementary DXR (coDXR) was obtained. Expression of complementary DXR gene was confirmed by a western blot against the HA tag in which a band of about the expected mass was detected (Fig 4.6.10.IIA). The western blot performed with antibodies raised against HA showed a clear protein band

with a mass of ~49 kDa, which is slightly less than the predicted mass of 57 kDa for the entire open reading frame. The most likely reconciliation is that the bipartite leader of the DXR was removed during apicoplast import- a common phenomenon in apicoplast targeted proteins (11). An IFA performed with antibodies against apicoplast resident acyl carrier protein (ACP) and HA further confirmed that the complementary DXR is localized to the apicoplast. Therefore, parasites with the confirmed DXR comp^{GFP} gene were sub-cloned into 10 mice to get a single parasitic line and were confirmed by PCR and continued expression of the coDXR was confirmed by western blot (Fig 4.6.10.II A).

4.3.6 Transfection of the DXR knockout into the DXR complementary (DXR Comp^{GFP} KO^{Tm}) line

The clonal line of DXR Comp^{GFP} was used as the recipient for the DXR knockout (DXR KO^{Tm}) construct. As a positive control, ferrochelatase knockout (FCKO) with mCherry expression, which is known to be non-essential for blood stage growth of parasites (32), was also transfected into the DXR Comp^{GFP} line. Parasites appeared within standard time frames (7 days to patency), and parasites expressing both red (mCherry from FCKO) and green colours were obtained. For the DXR gene, parasites bearing both GFP and tdTomato from the transfected mouse were observed on day 8 post infection. However, only ~60% of the population expressed both fluorescent colours with the remainder expressing only GFP. PCR analysis of the transfected population confirmed the presence of DXR KO as well as parasites still possessing the complementary DXR (DXR Comp^{GFP}) (Fig 4.6.10.II B).

4.3.7 Sub-cloning of DXR Comp^{GFP} KO^{Tm} line

My first attempt to knockout the endogenous DXR gene by inserting tdTomato and drug selectable marker into DXR Comp^{GFP} parasites was only partially successful as the population contained a sizeable proportion of what appeared to be the recipient strain (green) along with the dual red/green parasites (complemented knockouts). Even among the assumed knockouts, one set of parasites was bright red with green yet another set had very weak red fluorescence (with green) in comparison to the first population (Fig 4.6.10.I). Thus, the recovery of a pure population of knockout parasites was unsuccessful even after another transfection attempt and five sub-cloning attempts

where FACs sorted parasites were used as donors for the last two sub-cloning (Fig 4.6.10.I).

Meanwhile, a new vector construct was designed for the knockout DXR replacing the tdTomato tag with positive-negative selectable marker; *h*DHFR:*y*FCU (Fig 4.6.10.I). Integration of the original knockout construct into the endogenous locus followed by transcription, translation, maturation of tdTomato as well as the stabilizing of protein chimera are among the stages where the earlier observed less-bright red phenotype must have originated (33). Thus, it was decided to first make the knockout without a fluorescent marker. Once the knockout was confirmed, my plan was to subsequently replace the drug selectable marker with tdTomato in parasites. Unfortunately, this transfection with positive-negative selectable marker in the place of tdTomato was not successful (Fig 4.6.10.I). However, as a positive control for the transfection, the original DXR knockout with tdTomato was transfected into DXR Comp^{GFP} parasites and this gave rise to a population of almost 100% knockout parasites. But the red color was still dimmer. Nevertheless, these parasites were sub-cloned and I obtained a single parasitic line having both coDXR and a knockout in the endogenous DXR (Fig 4.6.10.II B).

4.3.8 Confirmation of the pale red color expression as a "modified tdTomato"

My next goal was to confirm that the pale red fluorescence is indeed the visual genotyping cue of tdTomato in the knockout construct. Therefore, an IFA was performed using a polyclonal anti-mCherry antibody, which cross reacts with tdTomato. The HA tag was observed to be localized to the apicoplast in a separate IFA but the IFA results for the tdTomato expression were not-promising (Fig 4.6.10.II B-e).

Therefore, a western blot to confirm the tdTomato expression was carried out with the same anti-mCherry antibody. A protein band was seen but it was not in the expected range of mass, being 35 kDa instead of the expected 52 kDa (Fig 4.6.11A). As the anti-mCherry antibody could detect the limited fluorophore expression of the protein, it was suspected that an open reading frame that could at lease code for a functional monomeric protein must be present even after the protein rearrangement. In addition, a set of primers (Table 4.6.1) designed to amplify the tdTomato region of these parasites to confirm the integrity of the "tdTomato tag" gave a much smaller PCR band than expected (~1.5 Kb instead of the expected ~2.1 Kb; Fig 4.6.11A). Therefore, I sequenced the PCR product, which revealed a "modified tdTomato" region where

approximately 100 base pairs at the beginning and at the end of the amplified tdTomato region were still intact.

4.3.9 Preliminary investigation of DXR Comp^{GFP} KO^{Tm} growth in mosquitoes and in *in-vitro* liver

To confirm whether this weak red fluorescence is visible in other stages of the life cycle, an uncloned parasite population (from the donor mouse used for sub-cloning this parasite line) was used to feed mosquitoes (Figs 4.6.11B, C). Oocysts in mosquito midguts showed a dimmer red colour along with the GFP, and sporozoites were GFP positive but the red colour was hard to detect (Fig 4.6.11B). Following 48 hours of *in-vitro* liver cell infection, HepG2 cells were observed by fluorescence microscopy and confirmed a bright green with dimmer red colour in parasites (Fig 4.6.11C). An IFA using anti-mCherry antibody enhanced the tdTomato signal for both salivary gland sporozoites and HepG2 infected parasites, making them clearly visible by microscopy (Figs 4.6.11 B,C). P0 infections were also performed using the mosquitoes infected (by bite-back). Even though the red colour was barely visible, GFP expressing P0 parasites were detected. The genotyping of P0 parasites showed parasites marked with GFP as well as parasites with the knockout in DXR (Fig 4.6.11D). Even though the primary population was uncloned, no parasites with wildtype DXR were detected in P0 stage which is similar to the initial PCR of the transfectant (Fig 4.6.10.II B-d). Hence, the tdTomato expression observed throughout the mosquito and liver stages was confirmed as sufficient to continue with the original plan.

4.3.10 Crossing of DXR Comp^{GFP} KO^{Tm} into wildtype *P. berghei*

Blood stage

After the confirmation of DXR Comp^{GFP} KO^{Tm} by fluorescence microscopy, PCR, and western blot, the planned cross experiment was completed as follows.

(1) The cloned population of DXR KO and DXR Comp^{GFP} was mixed with a *P. berghei* wildtype strain (DXR Comp^{GFP} KO^{Tm} x DXR^{WT})

(2) *P. berghei* GIMO GFP (27) mixed with Pbs 733 RFP strain (30) as the control (DXR WT^{GFP} x DXR WT^{RFP})

To segregate the extra DXR gene copy (DXR Comp^{GFP}) from the knockout DXR (DXR KO^{Tm}) post recombination during mosquito stage development (Fig

4.6.7), I crossed the DXR Comp^{GFP} KO^{Tm} strain with a wildtype strain (without any fluorescent marker) denoted as DXR^{WT}. To control any effect of fluorophore expression, two wildtype strains expressing GFP and RFP (DXR WT^{GFP} x DXR WT^{RFP}) were crossed.

After mixing of the parasites in above combination and infecting into naïve mice, the number of exflagellation events of DXR cross and the control was counted and recorded (9.5 vs 3.6 exflagellations per 1x10^4 red blood cells respectively) prior to infecting mosquitoes.

Mosquito stage

Mosquitoes infected with the two strains (above) were dissected at day 12 post infection to observe oocyst formation in midguts. The majority of the oocysts expressed both red and green, but small populations of oocysts with either only red or only green fluorescence were also present (Fig 4.6.12A). This result was unexpected as per the predicted genotype of oocysts (Fig 4.6.7). All the oocysts originating from the DXR Comp^{GFP} KO^{Tm} must bear both red and green colours (Fig 4.6.7) thus; the observation of only red/ only green colour oocysts needs an explanation. Since it is important to confirm that all the parental genotypes are present in oocysts stage , a PCR reaction was performed using oocyst DNA. The PCR was used to confirm the presence of parasites with knockout (DXR KO^{Tm}) and parasites with the GFP marker intact (DXR Comp^{GFP}) as well as wildtype DXR (Fig 4.6.12B). In one midgut a mixture of red only (few), green only (few) and orange colour oocysts (majority) were present. Since the PCR was performed using the whole midgut regardless of the colour of the oocysts present, all the genetic combinations of parasites were expected.

The salivary glands of the infected mosquitoes were removed 21 days post infection and used to perform an IFA and a PCR reaction to genotype the parasites. From the sporozoite IFA, two parasitic populations were observed. There were sporozoites exhibiting only red fluorescence while another population showed both red and green fluorescence (Fig 4.6.13). According to the expected outcome of the cross (Fig 4.6.7), there should be red-only, green-only, red/green dual fluorescent, and colourless sporozoites post segregation. Due to the reported GFP proteins carry over from the shared cytoplasm of oocysts (34), it is expected that all the sporozoites will fluoresce

green initially. Yet, green fluorescence was clearly lost at oocyst stage (red only oocysts), so perhaps these red only oocysts produced red only sporozoites. Nevertheless, a PCR reaction of the salivary gland sporozoites confirmed existence of the parasites with knockout and wildtype DXR as well as the GFP marker intact (Fig 4.6.13B).

Due to the unexpected outcome of oocysts and sporozoites development from the crossed parasitic strain (observation of red only/ green only parasites), the two parental strains (DXR $Comp^{GFP}$ and DXR $Comp^{GFP}$ KO^{Tm}) were also passed through the mosquitoes individually and the fluorescence colour at oocyst stage was observed. A small percentage of oocysts from the DXR $Comp^{GFP}$ and DXR $Comp^{GFP}$ KO^{Tm} were seen without any colour (Fig 4.6.14A), which was unexpected. As all the parasites from DXR $Comp^{GFP}$ clonal line must be green in colour, the colourless parasites must have arisen through loss of GFP expression. This explains the observation of red only oocysts and sporozoites from the DXR $Comp^{GFP}$ KO^{Tm} x DXR^{WT} cross. The fact that a few parasites with only green fluorescence were also seen suggest that the tdTomato experienced occasional loss of expression.

To further validate the above results, a set of PCR reactions was performed from mosquito midgut DNA of the two donors. As shown in Fig 4.6.14B, there were no GIMO parents (these should have been removed by the sub-cloning of DXR $Comp^{GFP}$ strain removing the colourless GIMO) in any of the populations. This genotyping reconfirmed the presence of only the anticipated genotypes (only knockout DXR with GFP parasites in DXR^{Tm} $Comp^{GFP}$ infected midguts and only wildtype DXR with GFP parasites in DXR $Comp^{GFP}$ midguts), which lends further support to the hypothesis that the fluorescent markers were somehow being occasionally silenced to generate unexpected oocyst fluorescent patterns.

Liver stage

Next, the purified sporozoites from the mixed infections were used to infect *in-vitro* liver cells (HepG2 cells; as 20,000 sporozoites per well). The parasites were fixed and IFA performed at various intervals post infection (hpi) (Fig 4.6.15A). Starting from 24 hpi, a clear separation of parasite colours was seen (as red-only, green-only, red and green as well as colourless parasites; not shown). At 68hpi, an in-depth analysis on proportions of parasites having various fluorescent colour combinations was completed.

The number of parasites bearing only red colour was less in comparison to the other parasites. Thus, it was not possible to conclude whether a significant size difference among the three types of parasites; red-only, green-only, and red/green is present (Fig 4.6.15B). Finally, the number of detached cells and merosomes at 70 hpi were recorded according to parasite fluorescence (Table 4.6.4). Clearly red colour detached cells and merosomes were observed, which potentially indicates that the "knockout" parasites have the ability to complete their liver stage replication (35), however the apparent loss of fluorescence expression limits my ability to make a firm conclusion.

P0 blood stage

The sporozoites recovered from the mixed infections were used to inject naïve mice intravenously, and mice were also infected by the bite-back method to assay the completion of liver stage *in-vivo* and subsequent progression to blood stage. All the mice infected (regardless of the method of infection) but not treated with pyrimethamine were positive for parasites day 4 post infection onwards (Fig 4.6.16A). Among the pyrimethamine treated mice, only the mouse infected by IV injecting 1,000 sporozoites was positive but the days to reach patency was delayed (day 8). Genotyping of these parasites (Fig 4.6.16B i) revealed presence of GFP inserted parasites as well as parasites with knockout DXR. Since the DXR wildtype parasites are pyrimethamine sensitive, their observed absence from the population was expected. The PCR performed using the untreated parasites recovered as P0 showed no knockout DXR as well as GFP fluorescent marker insertion (Fig 4.6.16B ii). Nevertheless, green colour parasites were visible from the mouse infected with 10,000 sporozoites (Fig 4.6.16A). Regrettably, it was difficult to clarify whether the green fluorescent parasites were DXR $Comp^{GFP}$ or DXR $Comp^{GFP}$ KO^{Tm} due to the weakness of the red fluorescence. The absence of a PCR band for the GFP insertion (regardless of the observation of GFP under microscopy) could be due to the presence of a very low proportion of green colour parasites among a larger population of colourless parasites.

4.4 Discussion

I chose three MEP pathway related genes as candidates for studying the MEP pathway in malaria parasite liver stage via reverse genetics, namely oTPT, an apicoplast IPP substrate importer (11); and DXR and IspF, two enzymes in the MEP pathway (36). Attempts at straight knockouts of these three genes failed to grow in blood stage, providing further confirmation that isoprenoid biosynthesis pathway related genes are indispensable for erythrocyte growth and potentially good drug targets.

Generation of complementary gene carrying lines proved difficult with only one out of the three genes (DXR) being expressed according to western blotting of the HA tags attached to the trans genes. Switching to a stronger promoter (EF-1α) did not enhance oTPT or IspF protein production, in spite of the fact that the majority of parasites were GFP positive and presumably carried the transgene. One explanation for the lack of HA-tagged oTPT and IspF can be that the HA tag interferes with the expression of complementary gene resulting in the protein degradation. Nevertheless, the EF-1α promoter could generate parasites with an expressed complementary DXR (as judged by HA tag) also expressing GFP. This perhaps indicates that expression of a complementary gene might not be so much dependent on the chosen promoter but on some other factor(s).

My inability to generate parasites expressing complementary copies of oTPT and IspF might be explained by the regulatory mechanism of parasites that suppress the transcription/translation. For instance, the isoprenoid precursor biosynthesis pathway has a clear mechanism to regulate certain products of the pathway (3, 23, 37). IspF is responsible for the pathway regulatory mechanism as it is involved with feedback inhibition of isoprenoid biosynthesis. Bitok and Meyers, 2012 (3) have observed that the IspF activity is sustained through MEP (2-C-methyl-D-erythritol 4-phosphate). So it might be that parasite does not favour having extra IspF, which has the potential to interrupt this regulatory process. Mullin et al., 2006 (11) attempted to find the substrate of oTPT by expressing TPT of *P. falciparum* on *Xenopus laevis* oocytes but failed. Similarly, Lim et al., 2016 (12) could not target their constructs containing different combinations of transmembrane domains (TMD) of *P. falciparum* oTPT protein to the apicoplast. As in the case of gene expression in isoprenoid biosynthesis pathway, the IPP transporters might also be subjected to an unknown regulatory mechanism. In

addition, DXR is also directly involved in with MEP pathway regulation at IspD level (38). Nevertheless, I was successfully able to introduce a complementary copy of DXR that was expressed as protein and apparently imported into the apicoplast.

Coupled with the regulatory mechanisms, extra gene products of oTPT and IspF might have caused direct inhibitory effects on parasites. As shown with experiments performed using other organisms, presence of certain extra gene products/over expression in a cell can alter growth. In potato tubers non-mevalonate isoprenoid production is disturbed by over-expressing a bacterial DXS gene (39). Similarly, Brown et al., 2010 (40) used *Mycobacterium tuberculosis* to show over-expression of DXS (deoxyxylulose 5-phosphate synthase) is inhibitory to bacterial growth. They have also found that, while over-expression of DXR is inhibitory to the organism, over expression of DXR has no effect on *M. tuberculosis* (40). Conversely, *Escherichia coli* studies showed that expression of an exogenous isopentenyl diphosphate isomerase gene could enhance isoprenoid biosynthesis (41). In parallel, increased DXS activity up-regulates plastid isoprenoid biosynthesis in *Arabidopsis thaliana*, and over-expressing DXR shows increased accumulation of plastid isoprenoids (42). Based on these findings, it is apparent that DXR over-expression is not inhibitory to any of the organisms studied. Similar to studies in other organisms (40, 42), I was able to express extra DXR in malaria parasites (Fig 4.6.10.II), but over-expressing oTPT or IspF was not feasible. Installation of a complementary copy of DXR gene, followed by deletion of the endogenous gene is proof of principle that my stage (sporozoite) specific knockout concept can successfully be put into practice. However, the lack of success with oTPT and IspF means that the target gene may need to be carefully considered.

My strategy relies on the exogenous (complementary) copy of DXR being sufficient to complement the loss of the native DXR gene by insertional mutagenesis (knock-out). PCR confirmed that the transfected parasites have a disruption in this essential gene; DXR (Fig 4.6.10.II) so my strategy effectively allows me to generate parasites with a knockout of a blood stage essential gene so long as a complementary copy is successfully installed beforehand.

A crucial part of my strategy was to link a fluorophore to the knockout locus and a second fluorophore to the complementing locus to allow facile genotyping at any stage by simple fluorescence microscopy. However, the tdTomato expression of knockout

parasites was barely visible despite PCR being positive for knockout DXR. The weak fluorescence is probably due to some modification of the marker. Sequencing and PCR revealed a rearrangement of tdTomato marker akin to a "loop-over" or oligomerization perhaps exacerbated by the tandem nature of the fluorophore gene (Fig 4.6.11A). Diminished expression of fluorophore markers in *Plasmodium* is occasionally encountered and consideration of markers and constructs is prudent in future strategies. Nevertheless, I decided that I could proceed with the subsequent stages of my strategy by resorting to the less convenient, but still effective, strategy of immunofluorescent genotyping of individual parasites (Figs 4.6.11B, C).

As shown in Fig 4.6.7, parasites in mosquito stage are expected to have certain phenotypes which correlate with their genotype. Hence, it is essential to confirm the presence of such colour combinations in mosquito stage prior to the studies in subsequent liver stage. However, there were red-only and green-only oocysts, implying that GFP and/or tdTomato expression had been silenced in selected parasites (Fig 4.6.12). Similarly, red-only sporozoites were detected in salivary glands (Fig 4.6.13). According to the expected genotypes of the cross post recombination (Fig 4.6.7), the red only sporozoites must be present unless the isoprenoid biosynthesis is essential for salivary gland sporozoite development. However, considering the reported stability/long half-life of GFP proteins in cells (34), and the carry-over of proteins such as GFP from the shared cytoplasm of oocysts into sporozoites (which I have observed in experiments of both chapter 2 and 3), it is unlikely to observe red-only sporozoites. . One explanation for this observation is that in some parasites, the GFP expression must have been shut-off. To test this explanation, I passed the donors individually (DXR $Comp^{GFP}$ and DXR $Comp^{GFP}$ KO^{Tm} parasites) into mosquitoes and revealed an unexpected outcome. Some parasites were colourless despite our expectation that all parasites arise from these clonal lines must be green/ orange in colour respectively (Fig 4.6.14). It is thus evident that GFP from the complementary construct in the crossed population has undergone some form of silencing, which explains the presence of red-only parasites. Likewise, observation of green-only oocysts can be explained by silencing of the tdTomato fluorophore.

One possibility is that the presence of excess DXR caused an inhibitory effect on parasites via mis-regulation of isoprenoid biosynthesis pathway, which interferes with the expression of fluorescent markers. More likely however, is that excess GFP or

tdTomato protein expressed in these parasites has a negative consequence. There are reports where aggregation of GFP protein caused cellular toxicity effects, sometimes even inducing apoptosis (43). Anecdotal reports from various malaria labs tell of fluorophore 'loss', and these are believed to boost growth rate leading to eventual out-competition of tagged lines by 'silenced' variants. What is not clear is why I observed seemingly random loss of colour expression in a minority of parasites. It will be important to understand the basis of this colour-loss as it confounds interpretations of parasite genetic content by colour, which was a major benefit of my strategy.

Despite these difficulties, I was able to infect liver cells with parasites believed to be knockout for DXR on the basis of their staining with anti-mCherry antibody and apparent lack of GFP expression (Fig 4.6.15A). Nevertheless, there were very few parasites with only red colour in the DXR cross, making it statistically challenging to make a conclusion by comparing their growth size to that of control parasites. As red fluorescing detached cells/merosomes were also observed at 70 hpi (Table 4.6.4), it is apparent that red fluorescent parasites, which should be DXR null, were able to successfully complete liver stage replication. However, it is an open possibility that the observed red colour liver stage parasites are knockout recombinants with silenced GFP (i.e. carry the complementary DXR gene copy). One way to exclude this possibility would be to extend the IFA protocol to detect the HA tag on the complementary DXR gene product in future experiments.

At P0 blood stage, I anticipated three out of four possible genetic combinations (Fig 4.6.7) to be recovered: parasites with the endogenous DXR gene abrogated and no copy of the complementary DXR, should not survive in blood stage even if they were able to complete the liver stage. Indeed, PCR confirmed that all the parasites that did not receive pyrimethamine via mice drinking water have wild-type DXR gene regardless of the method used to introduce parasites into naïve mice (Fig 4.6.16). Consistent with the DXR knockout without a complementary gene copy being lethal to blood stage parasites, there were no parasites with knockout DXR gene as P0. Upon treating with pyrimethamine however, parasites with *h*DHFR inserted (i.e. DXR $Comp^{GFP}$ KO^{Tm} parasites) should survive. Nevertheless, by bite-back or by IV injecting 1000 sporozoites, no GFP expressing parasites were recovered, and this was confirmed by PCR. Meanwhile a small proportion of GFP expressing parasites from 10000 IV injected mouse were detected (Fig 4.6.16). The only mouse which was positive with the

drug selection became positive day 8 post injection, which is a substantial delay compared to the standard days to patency for P0 wildtype parasites (d4). Probably, the DXR Comp^{GFP} KO^{Tm} parasites have a mild growth defect and therefore represented a minority in the population which caused them to appear late in the P0 parasite blood.

The fluorescent expression in all parasites is absolutely essential for this experiment to succeed. Therefore, based on the results I cannot with any degree of certainty draw the conclusion that the DXR gene is essential/not essential for liver stage growth of *P. berghei*. The limiting factor was the unreliability of fluorescent or even IFA genotyping in the face of spontaneous silencing of these reporters, which was apparent in mosquito stage. Due to lack of time to redesign new gene constructs and to execute a complete life cycle, this study was put on hold and remains inconclusive with regard to the MEP pathway in liver stage rodent malaria parasites.

Nevertheless, a very important achievement of this study was that I could confirm the validity of my original concept. With improvement I believe this strategy can be employed to experiment on DXR deficient liver stage parasites. Future progress will just be a matter of redesigning genetic constructs to include different epitope tags for each construct in addition to florescent markers. It is speculated that tagging can sometimes affect the protein of interest leading to a non-functional protein. Hence, it will be safe to either choose the endogenous locus for tagging or not to use epitope tag at all for complex genetic constructs. Apart from engineering reliable expression cassettes however, choosing a suitable promoter for driving the gene is extremly essential. At the same time, choosing a gene to study must be given a special consideration. In my experience, only one gene out of three in the isoprenoid pathway was capable of withstanding expression of exogenous gene products. Thus, it is uncertain which gene/s will be amenable for this approach; we need to learn how to perform efficient pre-complementation, perhaps using inducible promoters or artificial chromosomes, to make this work. For many pathways there are numerous genes-of-interest, and perhaps a practical starting point would be to survey which of these is amenable to complementary gene expression to apply the power of reverse genetics across the malaria parasite life cycle.

4.5 References

1. Wiley JD, Merino EF, Krai PM, McLean KJ, Tripathi AK, Vega-Rodríguez J, et al. Isoprenoid precursor biosynthesis is the essential metabolic role of the apicoplast during gametocytogenesis in *Plasmodium falciparum*. Eukaryotic cell. 2015;14:128-39.
2. Hunter WN. The non-mevalonate pathway of isoprenoid precursor biosynthesis. Journal of Biological Chemistry. 2007;282:21573-77.
3. Bitok JK, Meyers CF. 2 C-methyl-D-erythritol 4-phosphate enhances and sustains cyclodiphosphate synthase IspF activity. American Chemical Society Chemical Biology. 2012;7:1702-10.
4. Jomaa H, Wiesner J, Sanderbrand S, Altincicek B, Weidemeyer C, Hintz M, et al. Inhibitors of the nonmevalonate pathway of isoprenoid biosynthesis as antimalarial drugs. Science. 1999;285:1573-76.
5. Qidwai T, Jamal F, Khan MY, Sharma B. Exploring drug targets in isoprenoid biosynthetic pathway for *Plasmodium falciparum*. Biochemistry Research International. 2014;2014.
6. Wu W, Herrera Z, Ebert D, Baska K, Cho SH, DeRisi JL, et al. A chemical rescue screen identifies a *Plasmodium falciparum* apicoplast inhibitor targeting MEP isoprenoid precursor biosynthesis. Antimicrobial Agents and Chemotherapy. 2015;59:356-64.
7. Yao Z-K, Krai PM, Merino EF, Simpson ME, Slebodnick C, Cassera MB, et al. Determination of the active stereoisomer of the MEP pathway-targeting antimalarial agent MMV008138, and initial structure–activity studies. Bioorganic and Medicinal Chemistry Letters. 2015;25:1515-19.
8. Cassera MB, Gozzo FC, Fabio L, Merino EF, Del Portillo HA, Peres VJ, et al. The methylerythritol phosphate pathway is functionally active in all intraerythrocytic stages of *Plasmodium falciparum*. Journal of Biological Chemistry. 2004;279:51749-59.
9. Howe R, Kelly M, Jimah J, Hodge D, Odom AR. Isoprenoid biosynthesis inhibition disrupts Rab5 localization and food vacuolar integrity in *Plasmodium falciparum*. Eukaryotic cell. 2013;12:215-23.
10. Painter HJ, Morrisey JM, Vaidya AB. Mitochondrial electron transport inhibition and viability of intraerythrocytic *Plasmodium falciparum*. Antimicrobial Agents and Chemotherapy. 2010;54:5281-87.

11. Mullin KA, Lim L, Ralph SA, Spurck TP, Handman E, McFadden GI. Membrane transporters in the relict plastid of malaria parasites. Proceedings of the National Academy of Sciences. 2006;103:9572-77.

12. Lim L, Sayers CP, Goodman CD, McFadden GI. Targeting of a transporter to the outer apicoplast membrane in the human malaria parasite *Plasmodium falciparum*. PLoS One. 2016;11:e0159603.

13. Lim L, McFadden GI. The evolution, metabolism and functions of the apicoplast. Philosophical Transactions of the Royal Society of London B: Biological Sciences. 2010;365:749-63.

14. Banerjee T, Jaijyan DK, Surolia N, Singh AP, Surolia A. Apicoplast triose phosphate transporter (TPT) gene knockout is lethal for *Plasmodium*. Molecular and Biochemical Parasitology. 2012;186:44-50.

15. Yeh E, DeRisi JL. Chemical rescue of malaria parasites lacking an apicoplast defines organelle function in blood-stage *Plasmodium falciparum*. PLoS biology. 2011;9:e1001138.

16. Silvestrini F, Lasonder E, Olivieri A, Camarda G, van Schaijk B, Sanchez M, et al. Protein export marks the early phase of gametocytogenesis of the human malaria parasite *Plasmodium falciparum*. Molecular and Cellular Proteomics. 2010;9:1437-48.

17. Nair SC, Brooks CF, Goodman CD, Strurm A, McFadden GI, Sundriyal S, et al. Apicoplast isoprenoid precursor synthesis and the molecular basis of fosmidomycin resistance in *Toxoplasma gondii*. Journal of Experimental Medicine. 2011;208:1547-59.

18. Baumeister S, Wiesner J, Reichenberg A, Hintz M, Bietz S, Harb OS, et al. Fosmidomycin uptake into *Plasmodium* and *Babesia*-infected erythrocytes is facilitated by parasite-induced new permeability pathways. PLoS One. 2011;6:e19334.

19. Haussig JM, Matuschewski K, Kooij TW. Experimental genetics of *Plasmodium berghei* NFU in the apicoplast iron-sulfur cluster biogenesis pathway. PLoS One. 2013;8:e67269.

20. Sparr C, Purkayastha N, Kolesinska B, Gengenbacher M, Amulic B, Matuschewski K, et al. Improved efficacy of fosmidomycin against *Plasmodium* and *Mycobacterium* species by combination with the cell-penetrating peptide octaarginine. Antimicrobial Agents and Chemotherapy. 2013;57:4689-98.

21. Bushell E, Gomes AR, Sanderson T, Anar B, Girling G, Herd C, et al. Functional profiling of a *Plasmodium* genome reveals an abundance of essential genes. Cell. 2017;170:260-72. e8.

22. Partow S, Siewers V, Daviet L, Schalk M, Nielsen J. Reconstruction and evaluation of the synthetic bacterial MEP pathway in *Saccharomyces cerevisiae*. PLoS One. 2012;7:e52498.

23. Guggisberg AM, Amthor RE, Odom AR. Isoprenoid biosynthesis in *Plasmodium falciparum*. Eukaryotic cell. 2014;13:1348-59.

24. Sauret-Güeto S, Botella-Pavía P, Flores-Pérez Ú, Martínez-García JF, San Román C, León P, et al. Plastid cues posttranscriptionally regulate the accumulation of key enzymes of the methylerythritol phosphate pathway in *Arabidopsis*. Plant Physiology. 2006;141:75-84.

25. Cassera MB, Merino EF, Peres VJ, Kimura EA, Wunderlich G, Katzin AM. Effect of fosmidomycin on metabolic and transcript profiles of the methylerythritol phosphate pathway in *Plasmodium falciparum*. Memorias do Instituto Oswaldo Cruz. 2007;102:377-84.

26. Guggisberg AM, Park J, Edwards RL, Kelly ML, Hodge DM, Tolia NH, et al. A sugar phosphatase regulates the methylerythritol phosphate (MEP) pathway in malaria parasites. Nature Communications. 2014;5:4467.

27. Rathnapala UL, Goodman CD, McFadden GI. A novel genetic technique in *Plasmodium berghei* allows liver stage analysis of genes required for mosquito stage development and demonstrates that *de novo* heme synthesis is essential for liver stage development in the malaria parasite. PLoS Pathogens. 2017;13:e1006396.

28. Janse CJ, Ramesar J, Waters AP. High-efficiency transfection and drug selection of genetically transformed blood stages of the rodent malaria parasite *Plasmodium berghei*. Nature Protocols. 2006;1:346.

29. Lin J-w, Annoura T, Sajid M, Chevalley-Maurel S, Ramesar J, Klop O, et al. A novel 'Gene Insertion/Marker Out'(GIMO) method for transgene expression and gene complementation in rodent malaria parasites. PLoS One. 2011;6:e29289.

30. Sturm A, Graewe S, Franke-Fayard B, Retzlaff S, Bolte S, Roppenser B, et al. Alteration of the parasite plasma membrane and the parasitophorous vacuole membrane during exo-erythrocytic development of malaria parasites. Protist. 2009;160:51-63.

31. Odom AR, Van Voorhis WC. Functional genetic analysis of the *Plasmodium falciparum* deoxyxylulose 5-phosphate reductoisomerase gene. Molecular and Biochemical Parasitology. 2010;170:108-11.

32. Nagaraj VA, Sundaram B, Varadarajan NM, Subramani PA, Kalappa DM, Ghosh SK, et al. Malaria parasite-synthesized heme is essential in the mosquito and

liver stages and complements host heme in the blood stages of infection. PLoS Pathogens. 2013;9:e1003522.

33. Chudakov DM, Matz MV, Lukyanov S, Lukyanov KA. Fluorescent proteins and their applications in imaging living cells and tissues. Physiological Reviews. 2010;90:1103-63.

34. Andersen JB, Sternberg C, Poulsen LK, Bjorn SP, Givskov M, Molin S. New unstable variants of green fluorescent protein for studies of transient gene expression in bacteria. Applied and Environmental Microbiology. 1998;64:2240-6.

35. Sturm A, Amino R, van de Sand C, Regen T, Retzlaff S, Rennenberg A, et al. Manipulation of host hepatocytes by the malaria parasite for delivery into liver sinusoids. Science. 2006;313:1287-90.

36. Ralph SA, van Dooren GG, Waller RF, Crawford MJ, Fraunholz MJ, Foth BJ, et al. Tropical infectious diseases: Metabolic maps and functions of the *Plasmodium falciparum* apicoplast. Nature Reviews Microbiology. 2004;2:203-16.

37. Chang WC, Song H, Liu HW, Liu P. Current development in isoprenoid precursor biosynthesis and regulation. Current Opinion in Chemical Biology. 2013;17:571-79.

38. Imlay LS, Armstrong CM, Masters MC, Li T, Price KE, Edwards RL, et al. *Plasmodium* IspD (2-c-methyl-d-erythritol 4-phosphate cytidyltransferase), an essential and druggable antimalarial target. American Chemical Society Infectious diseases. 2015;1:157-67.

39. Morris WL, Ducreux LJ, Hedden P, Millam S, Taylor MA. Overexpression of a bacterial 1-deoxy-d-xylulose 5-phosphate synthase gene in potato tubers perturbs the isoprenoid metabolic network: Implications for the control of the tuber life cycle. Journal of Experimental Botany. 2006;57:3007-18.

40. Brown AC, Eberl M, Crick DC, Jomaa H, Parish T. The nonmevalonate pathway of isoprenoid biosynthesis in *Mycobacterium tuberculosis* is essential and transcriptionally regulated by DXS. Journal of Bacteriology. 2010;192:2424-33.

41. Kajiwara S, Fraser PD, Kondo K, Misawa N. Expression of an exogenous isopentenyl diphosphate isomerase gene enhances isoprenoid biosynthesis in *Escherichia coli*. Biochemical Journal. 1997;324:421-26.

42. Carretero-Paulet L, Cairó A, Botella-Pavía P, Besumbes O, Campos N, Boronat A, et al. Enhanced flux through the methylerythritol 4-phosphate pathway in

Arabidopsis plants overexpressing deoxyxylulose 5-phosphate reductoisomerase. Plant Molecular Biology. 2006;62:683-95.

43. Liu HS, Jan MS, Chou CK, Chen PH, Ke NJ. Is green fluorescent protein toxic to the living cells? Biochemical and Biophysical Research Communications. 1999;260:712-17.

4.6 Tables and figures

Table 4.6.1: List of Primers used in this study

Gene		5'-3' (restriction sites in italics)	Expected size (bp)
oTPT			
Comp	SP	*GGCGCC*TTCCTAGGCGTTACATAATGAAGGAAAATGACA	1042
	ASP	*AGATCT*AATAATAGAATAAAGAAATGCCCCGATAA	
KO 5'	SP	*GCTAGC*TGCATAACACCCGGATTTG	1065
	ASP	*GGTACC*TCCGTGATATGTTGGTATCTGTG	
KO 3'	SP	*CCGCGG*CAATTATCGGGGCATTTCTT	1247
	ASP	*AAGCTT*CGCGCTTAACAAGAGTGACA	
IspF			
Comp	SP	*GGCGCC*TTAAAGAATGAAATATGGAACAATTAAGTC	864
	ASP	*GGATCC*AGTTTTAGGAATTAACAAAACATTGGC	
KO 5'	SP	*GCTAGC*TCCAATTACGACATTTGCCACA	590
	ASP	*GGTACC*CCTTGCCCTATTCGCATTCC	
KO 3'	SP	*CCGCGG*ACATATTTTTCTGATTTGTTCA	815
	ASP	*AAGCTT*TGGAACTTACCCCTTCCATA	
DXR			
Comp	SP	*GGCGCC*TAAATAAATGAGAACGCTTATTAATTTGC	1519
	ASP	*GGATCC*AGAACTTATTTTCCTATTATATATATCCATG	
KO 5'	SP	*GCTAGC*TTGCTATTTTTGGCTTGTCG	821
	ASP	*GGTACC*TTTTTACTCGACGCCTGTTA	
KO 3'	SP	*CCGCGG*TGTATAATACATTCATGCGTGG	812
	ASP	*AAGCTT*AGCATATATAAATGTATCAAATCATGC	
EF-1α	SP	TGCAGCCCAGCTTAATTCTTAATTCTTTTCGAGCTC	597
	ASP	CCTATGTTTTATAAAATTTTTTATTTATTTATAAGC	
PDF	SP	TGGCGCCCAATTTCTTTGGTGTTAATATG	693
	ASP	GAATTCACCTAGGGTGTATGATATGCAAACTTAG	
DG3'	SP	GGGCCCGGGTTCAGGAAACTTTTGTGTG	1083
	ASP	CTTAAGGCGCGCCATTCAGTTTGCCTATTTGC	
Screening primers			
GIMO	SP	TCAATGATTCATAAATAGTTGGACTTG	1356
	ASP	CCCAGAATTCCCATGAACTG	
GFP in GIMO	SP	AACTGAAAAAGAGCGCAAATG	1570
	ASP	CCCAGAATTCCCATGAACTG	
DXR KO 5'	SP	AGCCGAGCAAGATGACATACT	1054
	ASP	TCAATGATTCATAAATAGTTGGACTTG	

DXR KO 3’	SP	GACGATGCAGTTTAGCGAAC	1834
	ASP	TGGATTTATTTGTTGATGATGGCCT	
DXR WT 5’	SP	AGCCGAGCAAGATGACATACT	1024
	ASP	TCCTATACTCCCTGTACTCCCA	
DXR WT 3’	SP	TCTGGTGGACCATTTCAAAACT	1381
	ASP	TGGATTTATTTGTTGATGATGGCCT	
tdTom--ato of DXR KO	SP	GGGCGAGGAGGTCATCAAAG	2145
	ASP	ACATGTGCAACTTCCTGGGA	

Table 4.6.2: Generation of parasites with gene complementary copy

Gene	Attempt	Vector A	Restriction enzymes used	Vector B	Restriction enzymes used	Reason for ligation	Result
oTPT Comp	1	Int6HSP70GFPHAcam3'	*Kas*I, *BamH*I-HF	oTPT Comp in pGEM	*Kas*I, *Bgl*II	To insert the oTPT complementary gene in to the vector	Did not get bacterial colonies post transformation
	2	Int6HSP70GFPHAcam3'	*EcoR*I-HF, *Xma*I	pBART sil6 (1)	*EcoR*I-HF, *Xma*I	To make the previous kanamycin resistant vector Ampicillin resistant	Vector I
		Vector I	*EcoR*I-HF, *BamHI*-HF	oTPT Comp in pGEM	*EcoR*I-HF, *Bgl*II	To insert the complementary gene	Vector II
		Vector II	*Kas*I, *Avr*II	PDF promoter (primers: Table 4.6.1)	*Kas*I, *Avr*II	To insert the promoter	Transfection done (cut with *Bgl*I and *Nae*I)
	3	pBART sil6 (1)	*Zra*I, *Xma*I	DG3' sequence PCR amplified using primers: Table 4.6.1)	*Xma*I, blunt end	To facilitate efficient double cross-over recombination by inserting a multiple cloning site (MCS) in to the vector	pBART sil6+DG3
		pBART sil6+DG3	*Nae*I, *Asc*I	Vector I	*Nae*I, *Asc*I		Vector III
		Vector III	*EcoR*I-HF, *BamH*I-HF	oTPT Comp in pGEM	*EcoR*I-HF, *Bgl*II	To insert the complementary oTPT	Vector IV
		Vector IV	*Kas*I, *Avr*II	PDF promoter	*Kas*I, *Avr*II	To insert the promoter	Transfection done (vector V)
	4	Vector V	*Kas*I	EF-1α PCR amplified using primers (Table 4.6.1) in pGEM	*Kas*I	To replace the PDF promoter with EF-1α promoter	Transfection done (cut with *Asc*I and *Nae*I)
	5	Int6 HSP70 GFPHA in	*EcoR*I-HF, *BamH*I-HF	oTPT Comp in pGEM	*EcoR*I-HF, *Bgl*II	To use a more suitable vector for efficient	Vector VI

		pBKS				transfection	
		Vector VI	*Kas*I	EF-1α PCR amplified using primers (Table 4.6.1) in pGEM	*Kas*I		Transfection done (cut with *Not*I and *Asc*I)
DXR and IspF	1	Int6 HSP70 GFPHA in pBKS	*EcoR*I-HF, *BamH*I-HF	Comp gene in pGEM	*EcoR*I-HF, *BamH*I-HF	To insert the complementary gene	Vector VII
		Vector VII	*Kas*I, *EcoR*I-HF for DXR and *Kas*I, *Not*I for IspF	EF-1α PCR amplified using primers (Table 4.6.1) in pGEM	*Kas*I, *EcoR*I-HF for DXR and *Kas*I, *Not*I for IspF	To insert the promoter region	Transfection done (cut with *Not*I and *Asc*I)

Formation of pINT6 5'3' HG (2); the kanamycin resistant vector contains intergenic sequence 5' and 3' flanks and HSP70 5'-FP-HSP703'. Then, HA cam 3' PCR was ligated in to the vector using *EcoR*I and *Sac*II to make Int6HSP70 GFPHA cam3'rc.

Formation of Int6 HSP70 GFPHA in pBKS; Int6HSP70GFPHAcam3' vector cut with XmaI and KasI to ligate to Int63'5' in PBlusk. To make Int63'5' in PBlusk, pBluescript SK was cut and ligated in to introduce Int6 3'5.

Below diagram summerises the series of transfection events (from attempt 2 to 5 of oTPT gene and attempt 1 for DXR and IspF genes in Table 4.6.2) performed to generate the complementary gene constructs using different promoters and vectors.

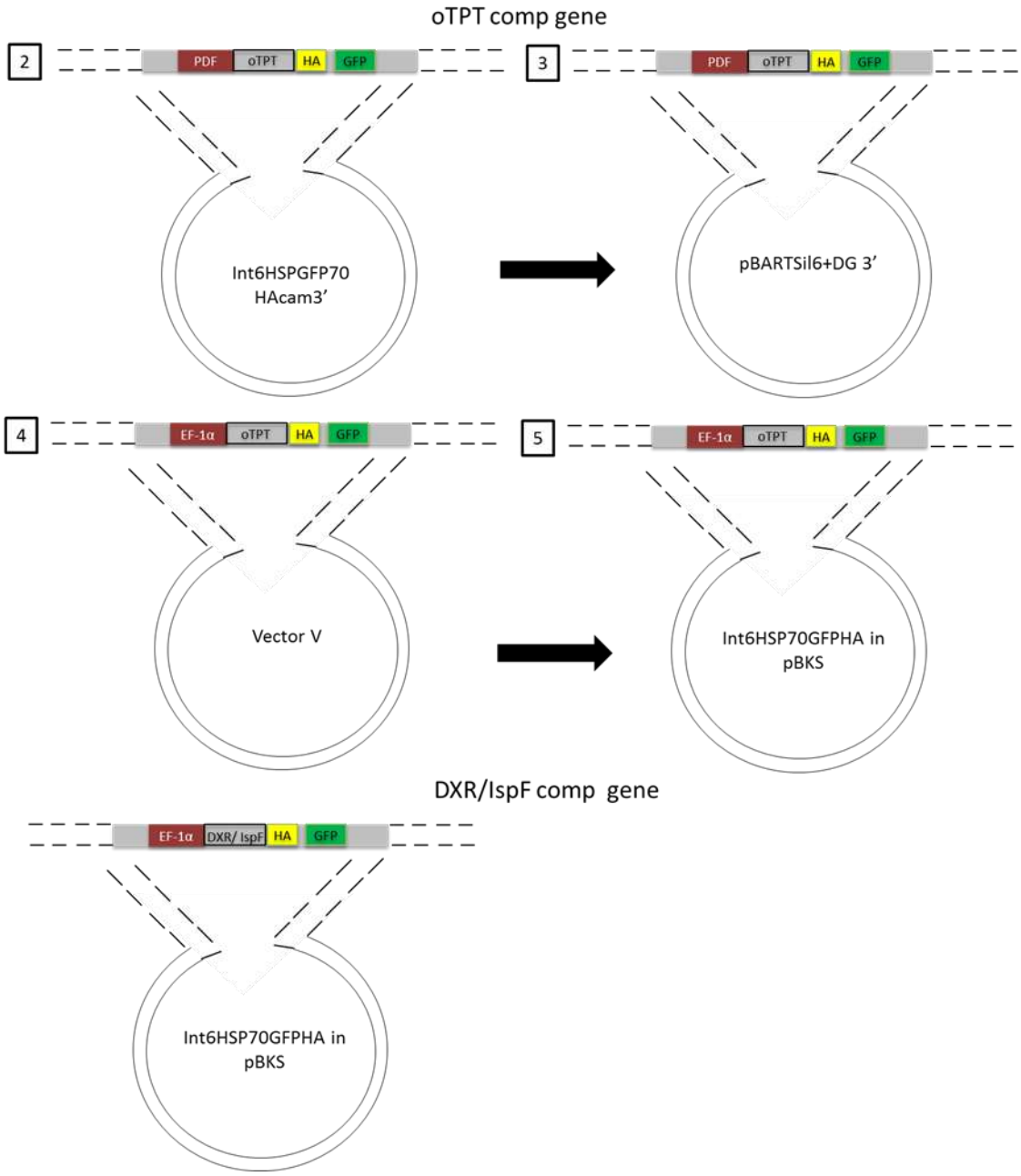

Table 4.6.3: Generation of parasites with gene knockout constructs inserted

Gene	Vector A	Vector B	Restriction enzymes used	Result
oTPT	pLDSKTm	oTPT 3'KO in pGEM	*Sac*II, *Hind*III-HF	Vector I
	Vector I	oTPT 5'KO in pGEM	*Kpn*I-HF, *Nhe*I-HF	oTPT KO in pLDSKTm
DXR	pLDSKTm	DXR 3'KO in pGEM	*Sac*II, *Hind*III-HF	Vector II
	Vector II	DXR 5'KO in pGEM	*Kpn*I-HF, *Nhe*I-HF	DXR KO in pLDSKTm
IspF	pLDSKTm	IspF 3'KO in pGEM	*Sac*II, *Hind*III-HF	Vector III
	Vector III	IspF 5'KO in pGEM	*Kpn*I-HF, *Nhe*I-HF	IspF KO in pLDSKTm

For the entire three gene-knockout constructs, first the 3' flank amplified by PCR and ligated in to pGEM intermediate vector was ligated in to pLDSKTm vector using *Sac*II and *Hind*III-HF. The resulting vector was then ligated in to the PCR amplified 5' flank of the gene in pGEM intermediate vector using *Kpn*I-HF and *Nhe*I-HF

The below diagram depict the three gene knockout constructs and the vector pLDSKTm which was used to generate the gene knockout parasites.

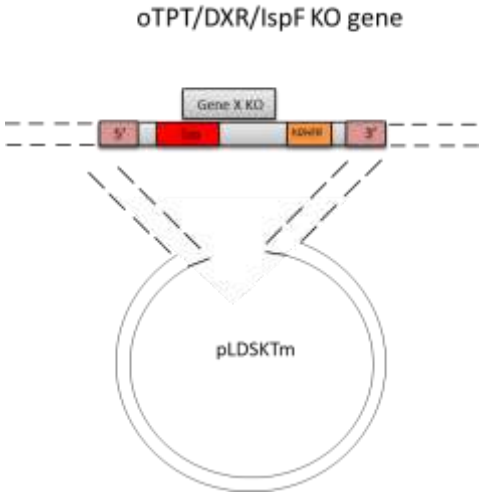

Table 4.6.4: Number of detached cells and merosomes of parasites depending on their colour at 70 hpi (number of biological trials=1)

Strain	Number of detached cells and merosomes			
	red	green	red and green	colourless
DXR $Comp^{GFP}$ KO^{Tm} x DXR^{WT}	3	2	28	14
DXR WT^{GFP} x DXR WT^{RFP}	35	30	17	4

References of Tables

1. Kooij TW, Rauch MM, Matuschewski K. Expansion of experimental genetics approaches for *Plasmodium berghei* with versatile transfection vectors. Molecular and Biochemical Parasitology. 2012;185(1):19-26.

2. Rathnapala UL, Goodman CD, McFadden GI. A novel genetic technique in *Plasmodium berghei* allows liver stage analysis of genes required for mosquito stage development and demonstrates that *de novo* heme synthesis is essential for liver stage development in the malaria parasite. PLoS pathogens. 2017;13(6):e1006396.

Figures

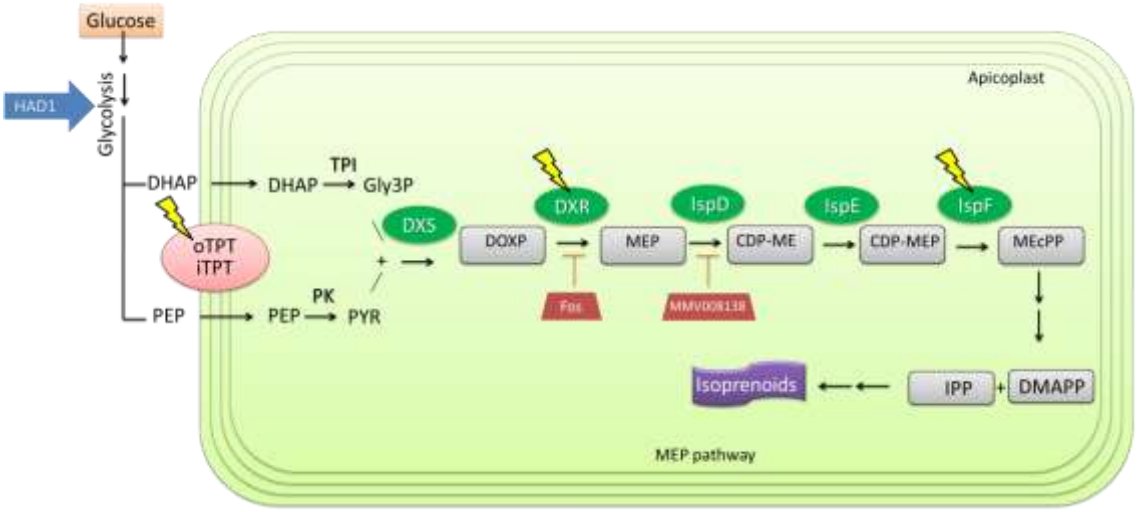

Figure 4.6.5: The MEP pathway for isoprenoid biosynthesis. The MEP pathway initiates with two triose phosphate transporters oTPT and iTPT that reside in the apicoplast membrane and import DHAP and PEP in to the apicoplast. The imported DHAP is converted to Gly3P by TPI, and PEP is converted into PYR by PK. Precursors of the MEP pathway Gly3P and PYR combined to generate DOXP courtesy of DXS, and a series of biochemical reactions leads to production of IPP and DMAPP. The DXR of the MEP pathway is specifically inhibited by Fos and the target of MMV008138 is IspD. The precursors for the pathway, DHAP and PEP are generated through glycolysis. By catalyzing the dephosphorylation of cytosolic phosphometabolites of glycolysis, HAD1 acts as a negative regulator of the MEP pathway (1). The enzymes involved in the pathway are denoted with green colour circles and the drugs that target DXR and IspF genes are shown inside red colour boxes. Three yellow colour arrows represent the three gene targets of this study.

TPT, triose phosphate transporters; DHAP, dihydroxyacetone phosphate; Gly3P, glyceraldehyde-3-phosphate; TPI, triose phosphate isomerase; PEP, phosphoenol pyruvate; PYR, pyruvate; PK, pyruvate kinase; CDP-ME, 4-diphosphocytidyl-2-C-methylerythritol; CDP-MEP, 4-diphosphocytidyl-2-C- methyl-D-erythritol 2-phosphate; DMAPP, dimethylallyl pyrophosphate; DXR, DOXP reductase; IPP, isopentenyl pyrophosphate; IspD, CDP-ME synthase; IspE, CDP-ME kinase; IspF, MEcPP synthase, HAD; haloacid dehalogenase-like hydrolase

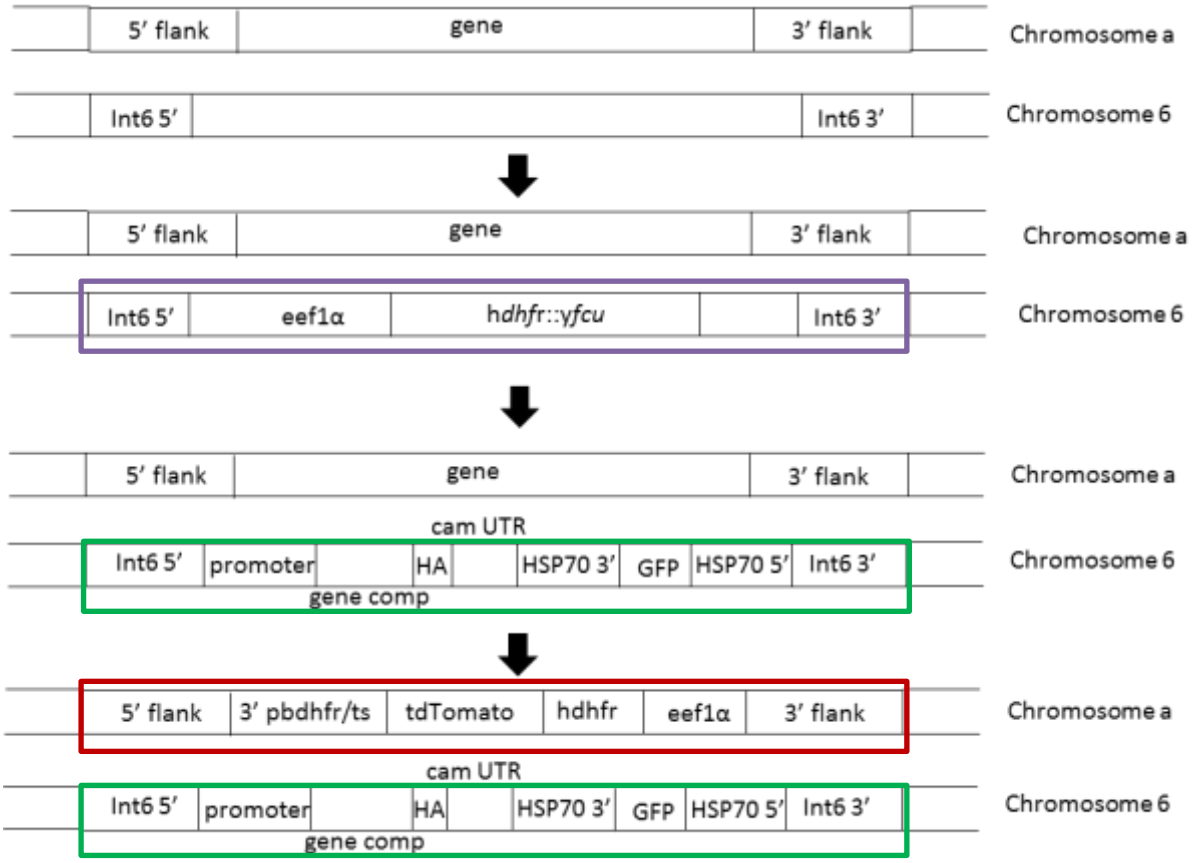

Figure 4.6.6.I: A simplified illustration of step-wise modifications introduced into the parasite chromosomes to generate parasites with an extra gene and with the endogenous gene being knocked out. An intragenic region of chromosome 6 of *P. berghei* has been replaced with the GIMO construct (2) as shown within the purple box. The GIMO contains the positive-negative selectable marker (*h*dhfr::*y*fcu), which enables negative selection of parasites with 5-FC. Next, the GIMO is replaced by a new construct to generate parasites with the extra gene/complementary gene of interest (green box). In this construct, a gene specific promoter is integrated to drive the extra gene coupled with a HA tag and a *Pb* calmodulin 3'UTR the GFP is driven by HSP70 promoter. The endogenous gene locus (gene of interest) on chromosome "a" from the same parasite strain is next replaced with a cassette containing a tdTomato fluorescent marker, drug selectable marker, *h*DHFR, all driven by the promoter EF-1α (red box). Parasites with this construct integrated are selected (positive selection) by pyrimethamine. The final, pyrimethamine resistant parasite strain after this complete procedure must contain only one copy of the gene of interest (extra copy on chromosome 6) with both tdTomato and GFP being expressed.

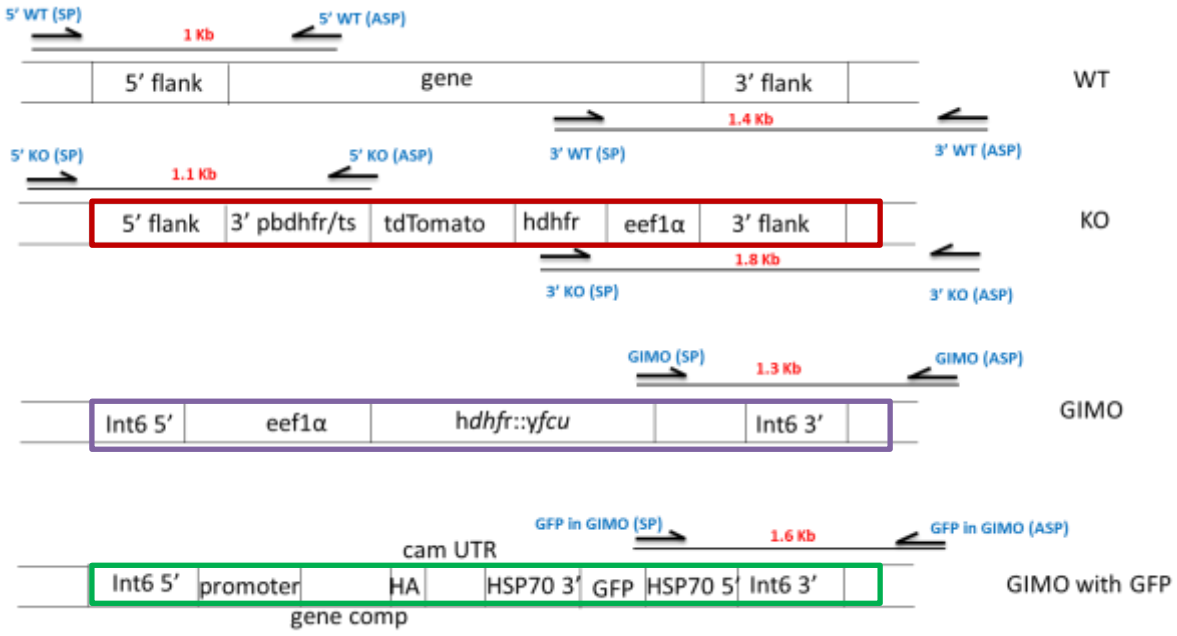

Figure 4.6.6.II: PCR genotyping strategy of parasites at different stages of genetic modifications.

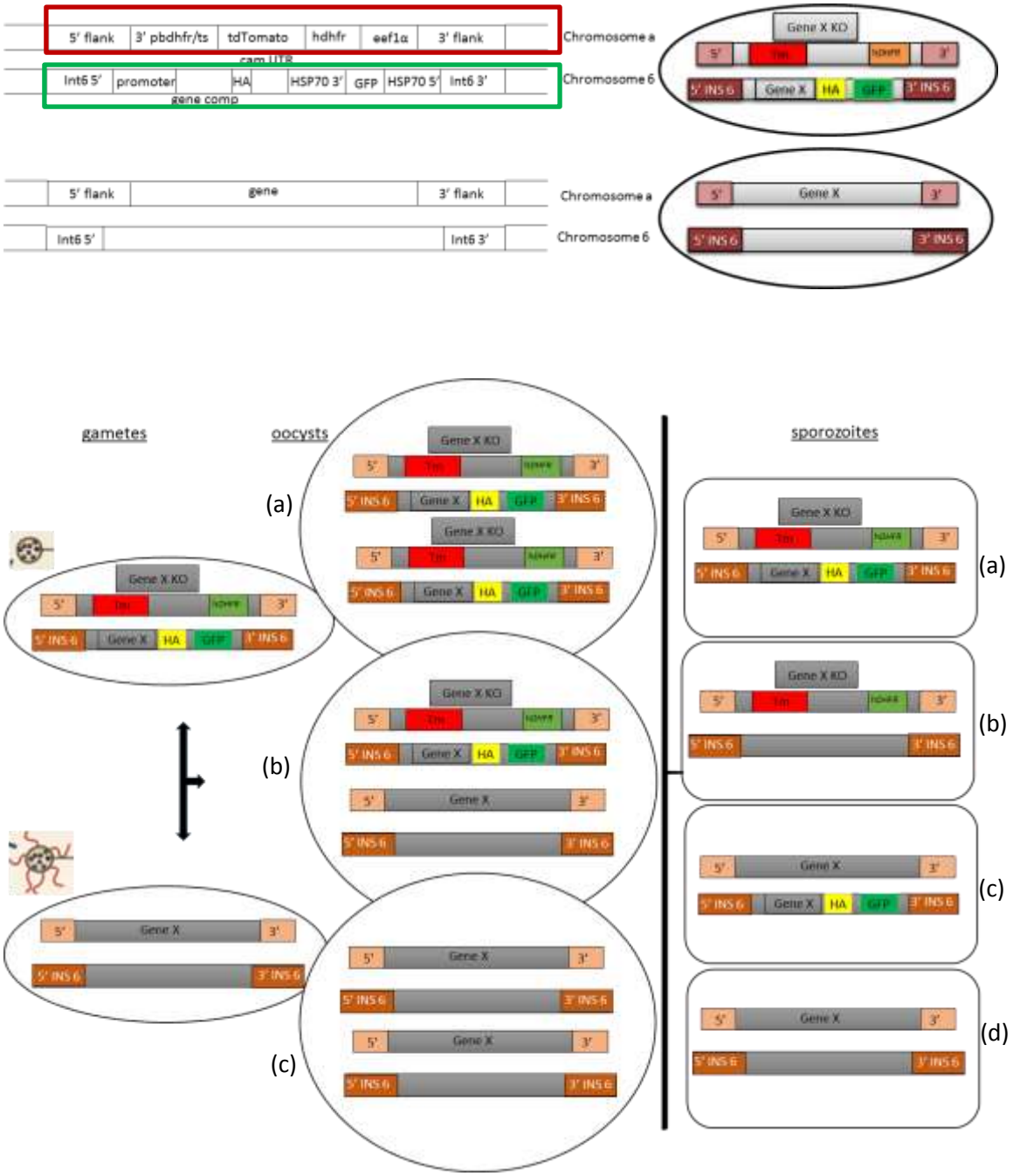

Figure 4.6.7: Expected outcome of the parasites (red and green gene X KO^{Tm}Comp^{GFP} parasites crossed to a colourless wildtype) post sexual reproduction and recombination inside the mosquito. The first parent parasite contains the extra gene X with GFP (green) and the knocked-out gene with tdTomato (red). The other parent is a wildtype *P. berghei* strain with no fluorescent or drug resistance markers inserted. Following the fusion of two gametes (n) of two strains, parasites undergo these subsequent stages; zygote (2n), ookinete (4n), oocysts (~1000n) while sexual

recombination takes place. The self-fertilization of two orange (red+green) gametes produces orange oocysts (a) while the colourless wildtype gametes make colourless oocysts (c). Cross fertilization of the two parent gametes will give rise to orange coloured oocysts with a different genotype (b). Once all these parasites enter their usual haploid salivary gland sporozoite stage (n), four phenotypes are expected. The two parent phenotypes will be recovered [orange (a) and colourless (d)] along with two recombinants expressing only red (b) or only green (c). The parasite with red has the knocked-out gene X while the green-only parasite receives the complementary gene. From this point onwards, the red only parasite with the knockout in the gene of interest can be easily followed up for the rest of the life cycle.

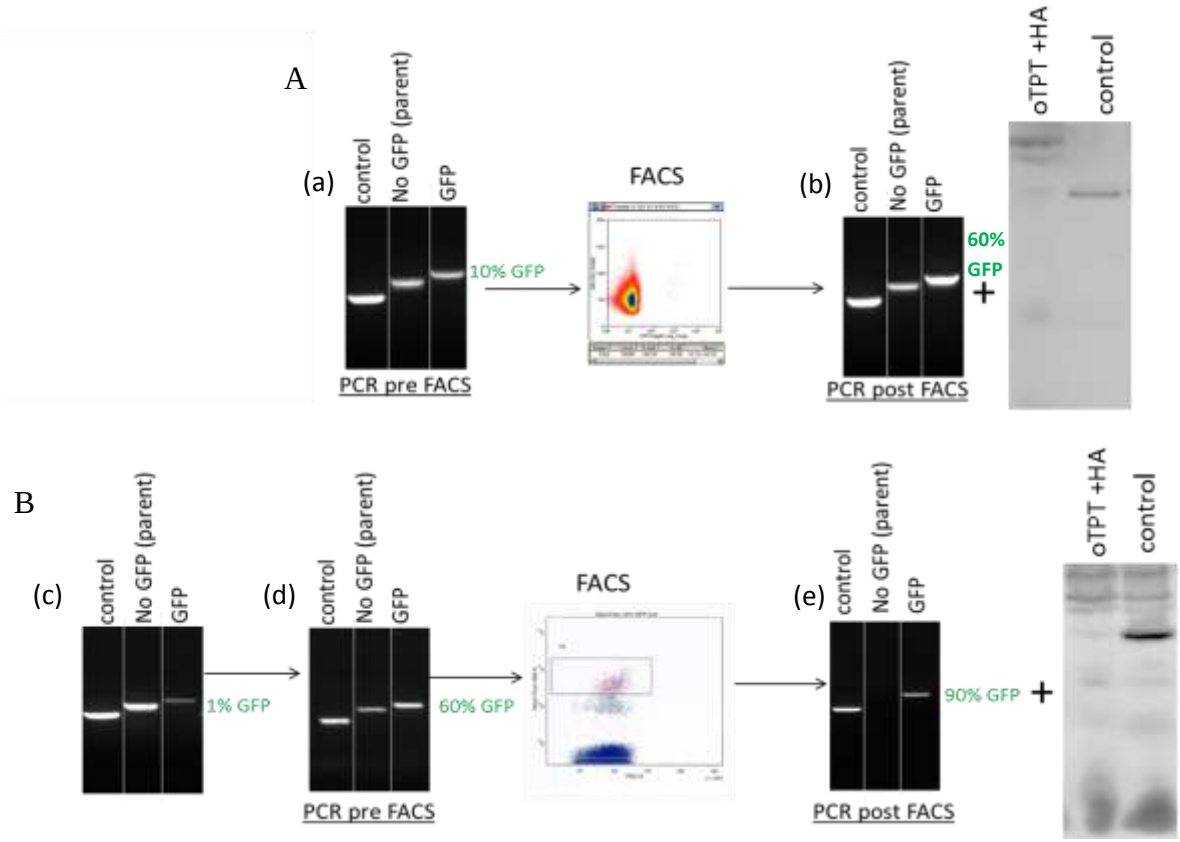

Figure 4.6.8: oTPT complementary (oTPT comp) gene construct generation. The primers used (Table 4.6.1) are (i) control; to amplify a known region of parasite genome to confirm the quality of gDNA and PCR conditions in general (ii) No GFP; to amplify the GIMO region with no GFP inserted (iii) GFP; to amplify the GFP insertion of chromosome 6 (refer to Fig 4.6.6.II). (A) A gel image (a) of a PCR reaction showing the presence of approximately 10% of GFP expressing parasites with the oTPT complementary and PDF promoter integrated. Note the presence of GIMO parent parasites in a larger proportion. After optimising the transfection conditions pre- FACS, the percentage has been increased to approximately 60% (b) post sort but a protein band was absent in the western blot to indicate the expression of HA with the complementary gene. (B) Transfection of parasites to integrate oTPT comp copy and the EF-1α promoter resulted in ~1% of GFP parasites by observing parasites under fluorescence microscopy and per the gel image (c). Second transfection to insert the same genetic construct yielded ~60% of the desired strain (d) and was subjected to sorting. Post sorting, the population with GFP insertion has been increased up to 90% out of total population as shown in the figure (e). But none of the parasites expressed HA tag to confirm the extra oTPT protein production.

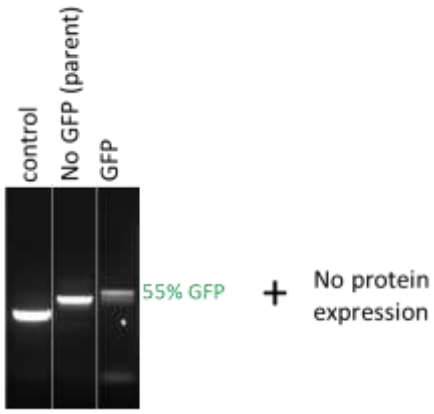

Figure 4.6.9: Generation of parasites with IspF complementary (IspF comp) gene inserted. The primers used are similar to Fig 4.6.8. The transfection of IspF comp copy driven by EF-1α promoter in to *Pb*ANKA GIMO parasites resulted in approximately 55% of parasites with GFP expression but with no HA tag detectable, suggesting the lack of extra IspF protein expression by the parasites.

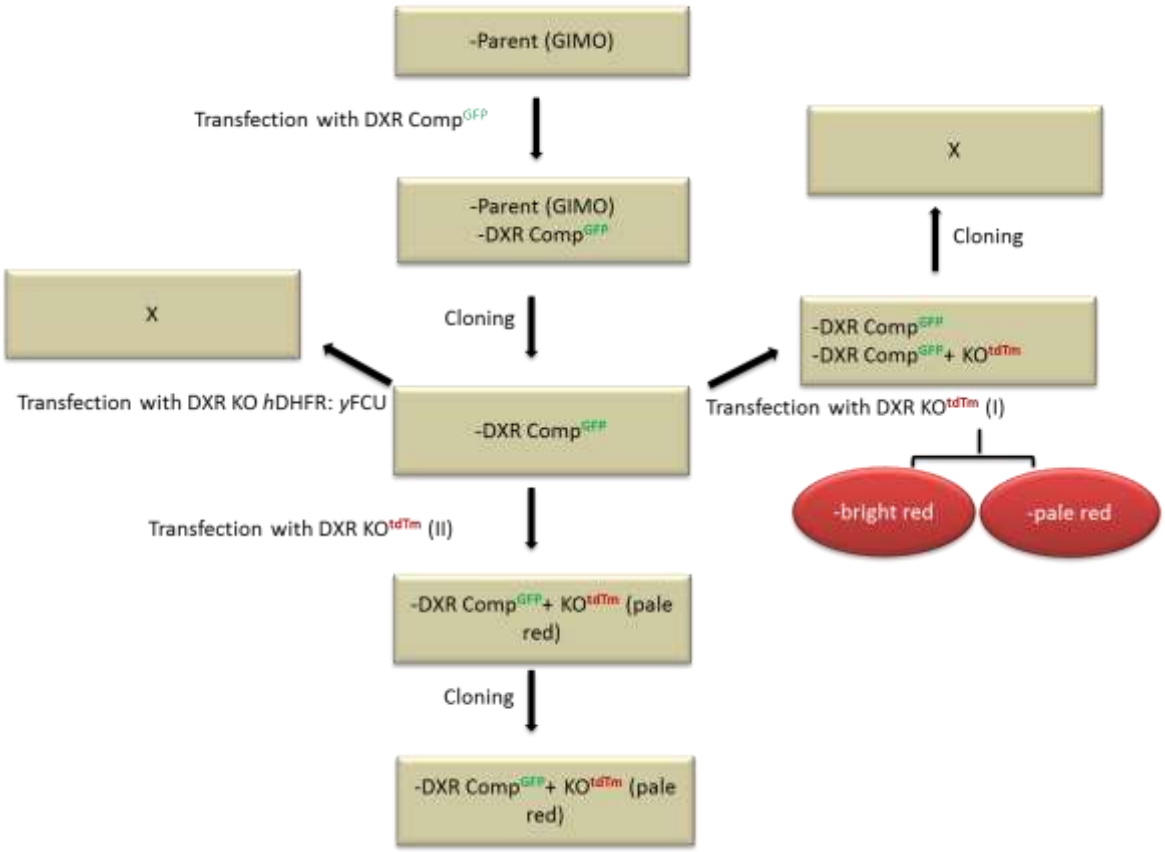

Figure 4.6.10.I: A summary flow chart showing steps of transfections and sub-cloning attempts performed to generate parasites having both the complementary DXR with GFP and the DXR knockout with tdTomato expression (DXR Comp^{GFP}KO^{Tm}). The first transfection was performed to insert the DXR complementary construct with GFP (DXR Comp^{GFP}) in to *P. berghei* GIMO strain where a mixed population of the parent and DXR Comp^{GFP} obtained. By sub-cloning, a single strain of DXR Comp^{GFP} was separated. Next transfection (i) was performed to insert DXR KO^{Tm} in to the previous DXR Comp^{GFP}. In the resultant population, three phenotypes of parasites were observed within two genotypes; parent DXR Comp^{GFP} (green) and DXR Comp^{GFP}KO^{Tm} (bright red with green and pale red with green). Five attempts to sub-clone the DXR Comp^{GFP}KO^{Tm} were not successful. In order to avoid the colour diminishing phenotype of knockouts (pale red with green colour), another transfection was performed with a new knockout construct where the tdTomato marker has been replaced with *h*DHFR:*y*FCU, a positive-negative selectable marker. Since this particular transfection was not positive, a second transfection (ii) with the initial knockout construct (with tdTomato marker; DXR KO^{Tm}) was attempted where almost all the parasites obtained post transfection contained both red and green thus DXR

Comp^{GFP}KO^{Tm}. Finally, by sub-cloning, a single parasitic strain of DXR Comp^{GFP}KO^{Tm} was generated.

Figure 4.6.10.II

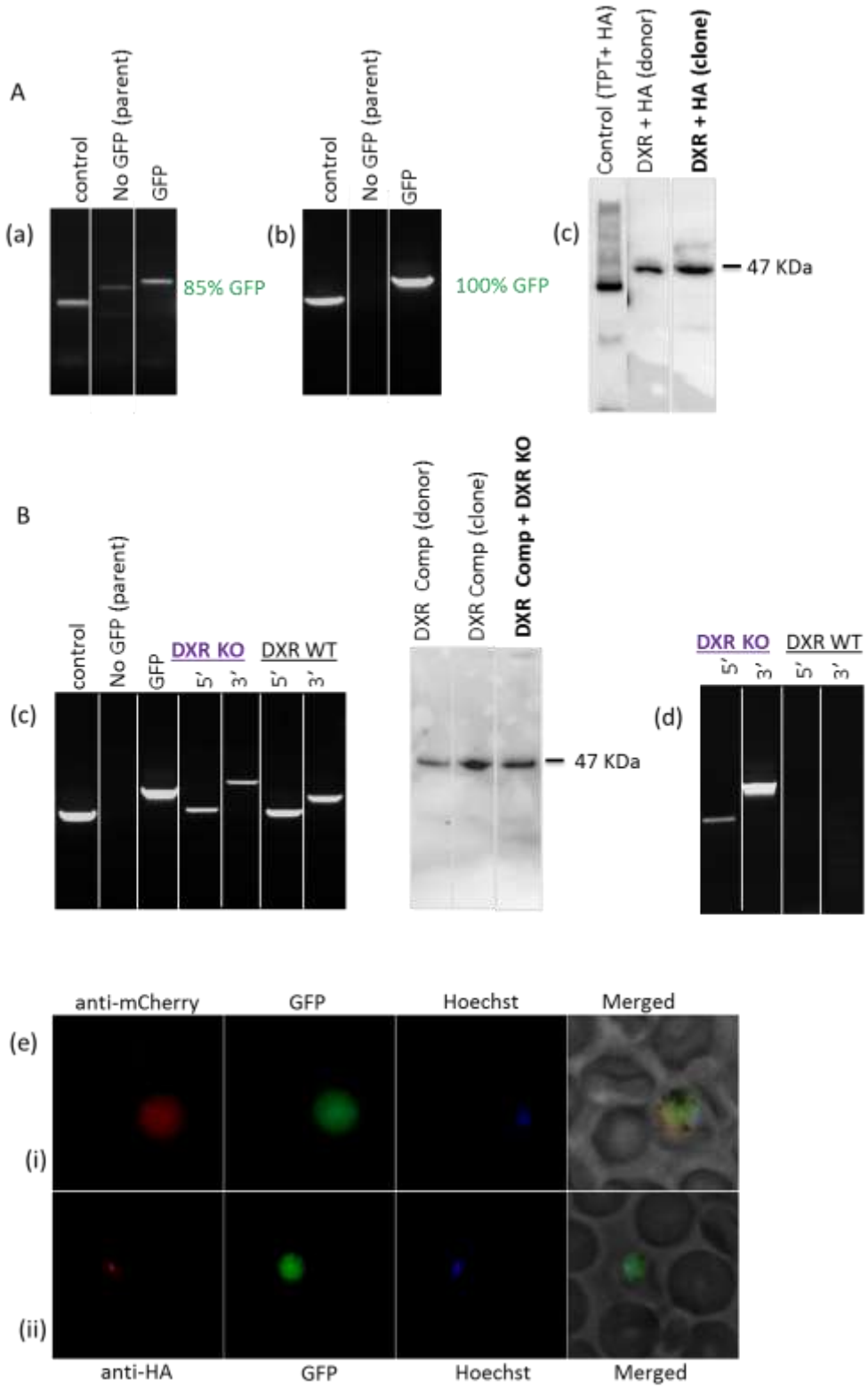

Figure 4.6.10.II: Generation of parasites with DXR complementary gene (DXR comp) driven by EF-1α inserted. The primers used are (i)-(iii)-refer to Figs 4.6.6.II, 4.6.8 (iv) DXR KO; to screen amplify the 5' and 3' ends of knockout construct integrated in to the genome (v) DXR WT; to screen amplify the 5' and 3' ends of the DXR endogenous gene (Fig 4.6.6.II). (A) Initial transfection which yielded ~85% of GFP parasites (a) also expressed the HA tag of a 47 kDa mass as per the western blot (b) cloning of the parasites (100% GFP) resulted in only the desired strain with HA tag inserted and expressed (c). (B) Insertion of the DXR knockout construct resulted in DXR knockout parasites but an appreciable number of DXR wildtype parasites still remained (c). Finally, a single parasitic strain (clone), having the knockout DXR with no DXR wildtype parasites was confirmed by PCR as per the next gel image shown (d). Due to the dimmer red/ tdTomato expression of the knockout parasites, an IFA was performed on (e) (i) parasites stained with anti-mCherry antibody to enhance the red colour of DXR knockouts (ii) parasites with only the DXR complementary gene copy, incubated with anti-HA/546 antibody to detect the HA expression.

(d) (e) (ii))

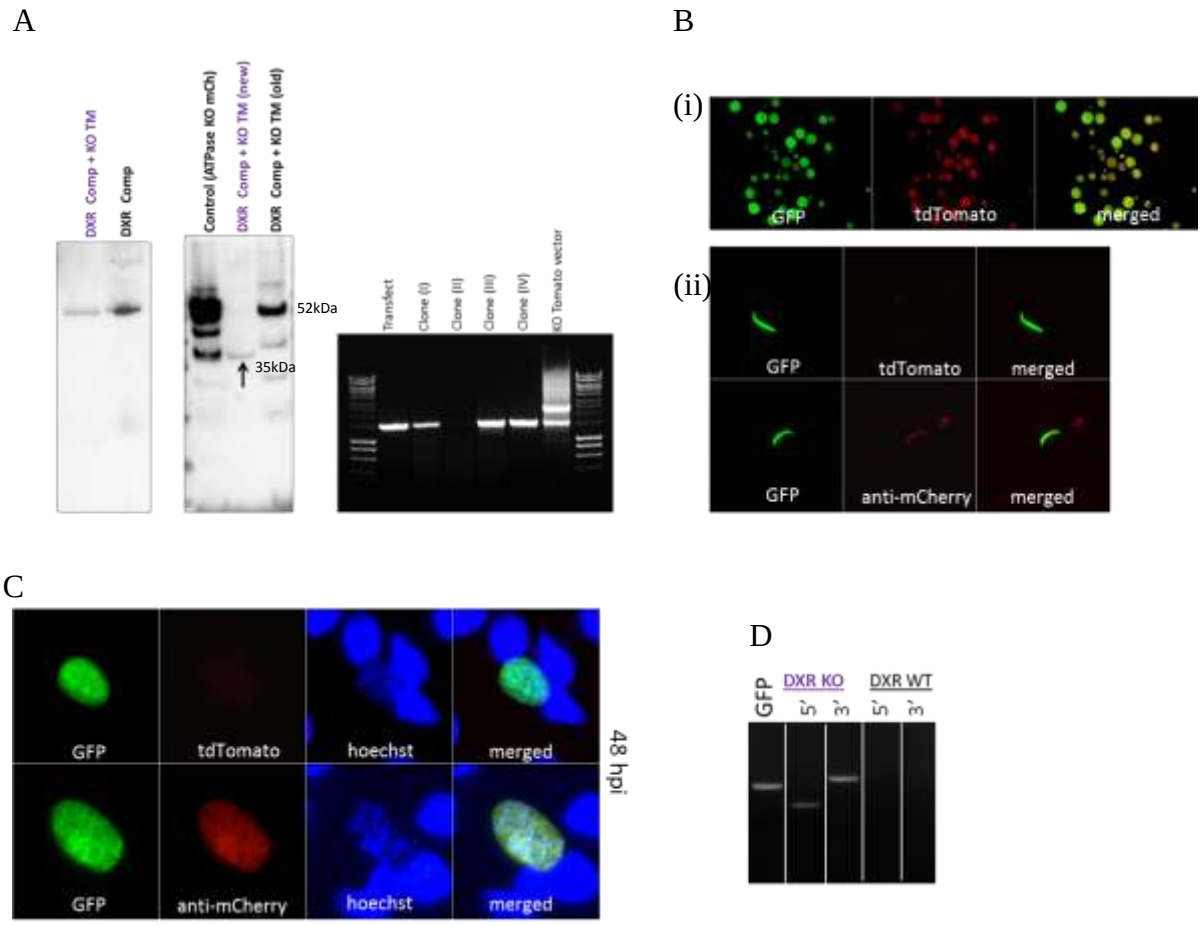

Figure 4.6.11: Confirmation of tdTomato expression of DXR Comp^{GFP} KO^{Tm} throughout the parasite life cycle (A) Blood stage parasites with the DXR complementary copy and the knockout (DXRComp^{GFP} KO^{Tm}) was first confirmed by a western blot with antibodies against anti-HA and anti-mCherry. The expected mass of DXR with HA (47 kDa) is apparent, but the protein band decorated by the anti-mCherry antibody (arrow head) was beolow the expected mass (~35 kDa vs 52 kDa). A set of PCR reactions [primers; tdTomato of DXR KO (Table 4.6.1), DNA; the intial transfectant DXRComp^{GFP} KO^{Tm} (transfect), four parastic strains from the sub-cloning of DXRComp^{GFP} KO^{Tm} (clone I-IV) and the final bacterial vector used for the transfection] was performed to amplify a region in the genome that includes the tdTomato insertion. The PCR bands obtained were below the expected size (~1.5 vs 2.1 kb; Table 4.6.1). (B) Mosquito stage growth of DXRComp^{GFP} KO^{Tm} parasites (i) oocysts day 12 post infection where a relatively bright red colour from tdTomato expression can be seen (ii) salivary gland sporozoites (day 21 post infection) with native tdTomato (the red colour is barely visible without staining with an antibody) and anti-mCherry antibody staining (the red colour expression is enhanced) respectively. (C) Parasite growth in *in-vitro* liver cells (HepG2 cells) 48 hours post infection; with

tdTomato and anti-mCherry incubation respectively, to detect tdTomao signal of the knockout parasites. Eventhough the native tdTomato expression is hardly visible, the staining with anti-mCherry antibody enhanced the colour expression (D) Phenotyping of P0 parasites (performed by biting strategy). A description of the primers used is in Figs 4.6.6.II, 4.6.10.II. The PCR shows recovery of parasites with GFP, knockout DXR (primers designed to target the gene disruption in both 5' and 3' flanks) and the absence of wildtype DXR gene in the parasite respectively. Since only the DXRComp^{GFP} KO^{Tm} was used as the donor strain (without crossing to a wildtype) it was expected to recover only parasites having GFP expression (coming from the DXR Comp^{GFP}) and the knockout (from DXR KO^{Tm}). Absence of any parasites with wildtype DXR gene further confirmed the previous finding and further validated the function of the designed construct.

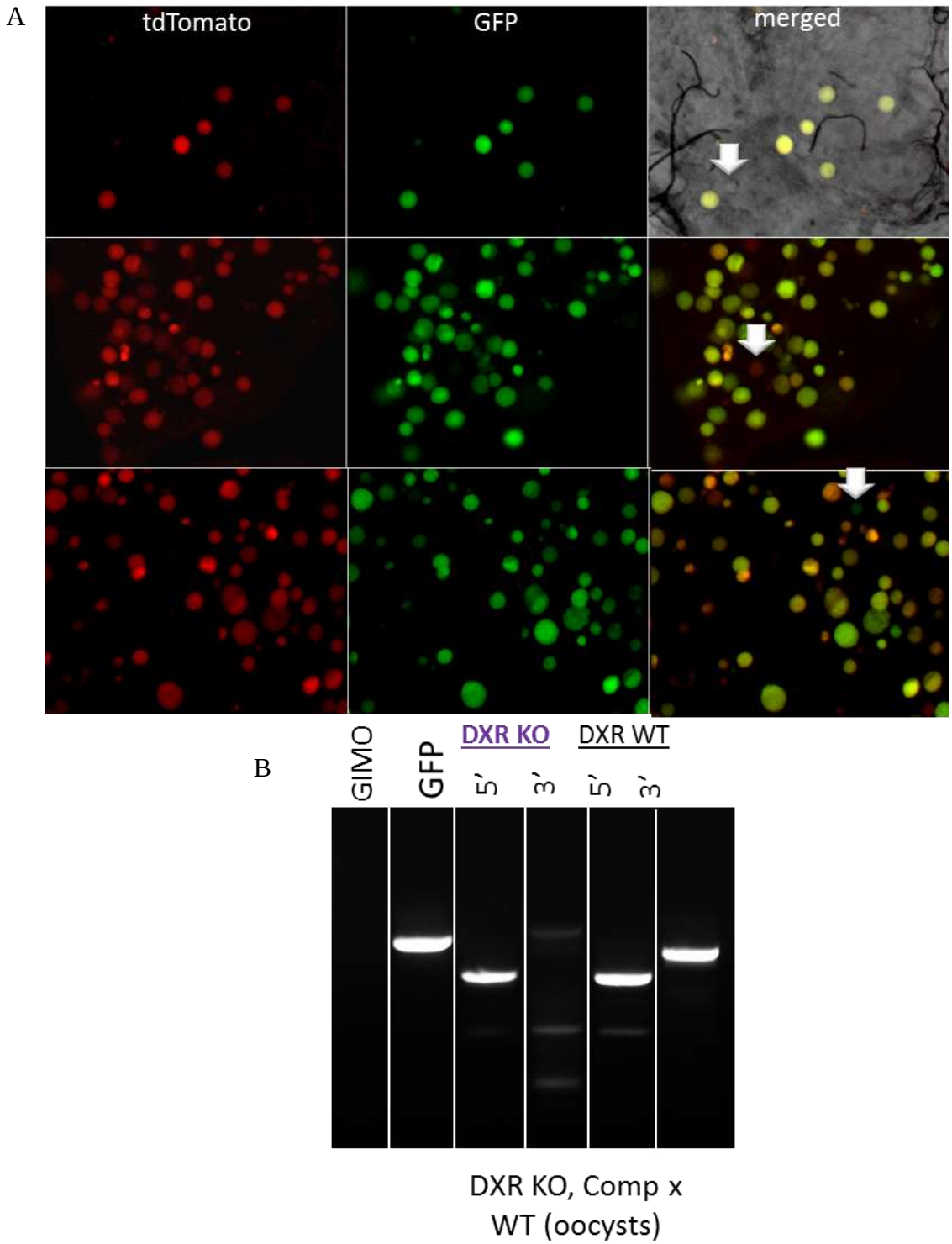

Figure 4.6.12: Oocysts development of DXR Comp^{GFP} KO^{Tm} crossed to wildtype (DXR Comp^{GFP} KO^{Tm} x DXR^{WT}) parasites day 12 post infection (A) the three arrow heads show a colourless, red and green colour oocysts respectively. The colourless oocysts must have originated from self-fertilization of wildtype gametes, and the orange coloured oocysts (which are in the majority) should come from either self-fertilization of the orange parent gamete or from the cross-fertilization of orange parent and the

wildtype gametes. The single colored oocysts (red-only and green-only) are not genetically possible suggesting that fluorescence expression silencing occurred. (B) Gel image of a PCR, run using DXR $Comp^{GFP}$ KO^{Tm} x DXR^{WT} oocysts DNA. The primers used are in Figs 4.6.6.II, 4.6.10.II. The PCR confirms, colourless oocysts observed are not GIMO integrated parasites (if survived even after a series of sub-cloning events post first transfection). Further, since the PCR is performed on all the oocysts in the population regardless of the each oocysts colour, it is anticipated to see all the expected genetic combinations of parasites (Fig 4.6.7), parasites with GFP expression (DXR $Comp^{GFP}$), parasites having knockout DXR (primers were designed to detect the disruption of the gene in both ends 5' and 3') and wildtype DXR gene (using primers to amplify the intact DXR gene from both ends 5' and 3').

A

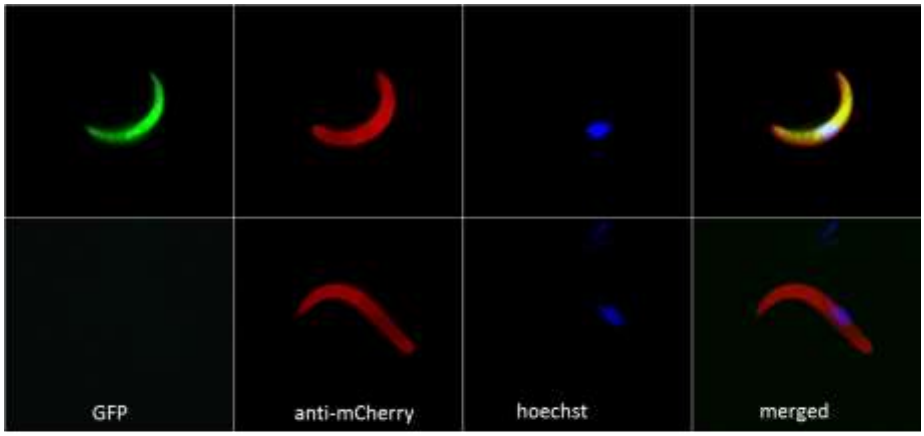

B

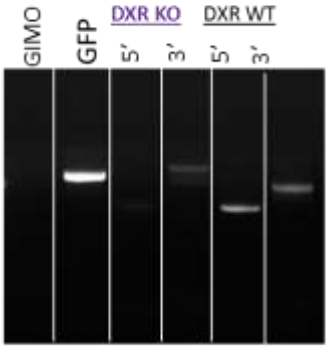

DXR KO, Comp x
WT (sporozoites)

Figure 4.6.13: Sporozoite development of DXR Comp^{GFP} KO^{Tm} x DXR^{WT} parasites in salivary glands day 21 post infection (A) IFA of sporozoites incubated with anti-mCherry antibody and Hoechst DNA strain; two phenotypes of sporozoites could be seen; first an orange coloured sporozoite which was expected and an unexpected red only sporozoite, possibly resulting from the silencing of GFP expression in some parasites. Since the red only sporozoites with the DXR knockout, may have a "silenced" GFP expression therefore contain the complementary DXR gene as well, it is difficult to intepret the data at this point whether the DXR knockout can form sporozoites or not. (B) A PCR reaction run with salivary gland sporozoite DNA of DXR Comp^{GFP} KO^{Tm} x DXR^{WT} shows the presence of GFP expression (complementary DXR gene), knockout and wildtype DXR gene (the primers amplify both 5' and 3' flanks of the gene to further confirm the disrupted/ intact DXR gene) respectively. A description of primers used are in Figs 4.6.6.II, 4.6.10.II. As expected, there are no parasites still containing GIMO region in their genome as well as there are parasites with GFP expression (coming from the DXR Comp^{GFP}). Both DXR knocked-out parasites (DXR KO^{Tm}) and parasites with a wildtype DXR (DXR ^{WT})are also present in the salivary gland sporozoite population.

A

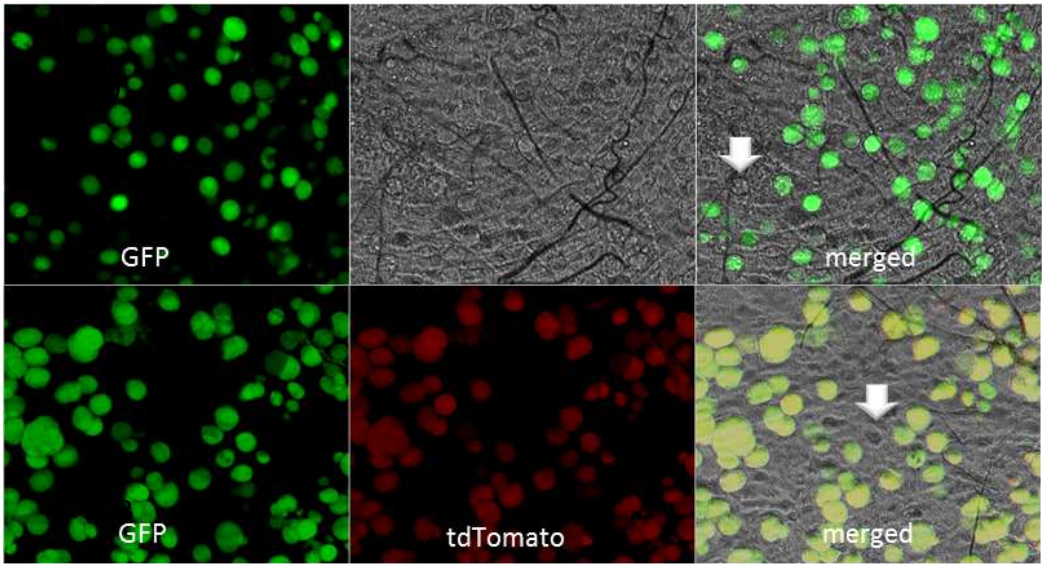

B

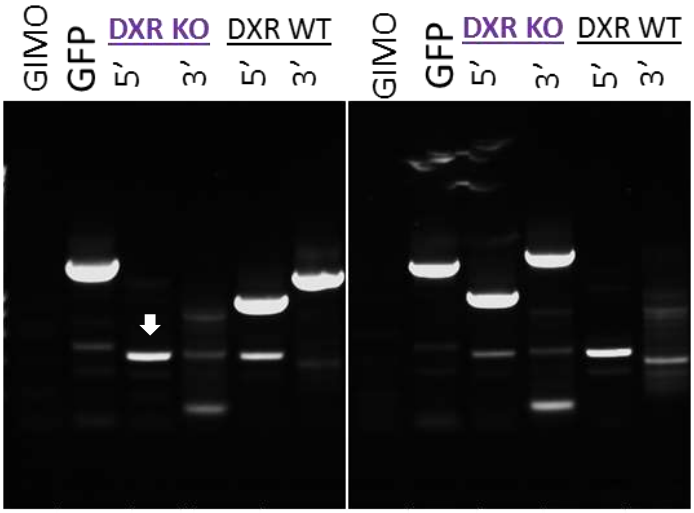

Figure 4.6.14: Oocyst development of the two donor parasitic strains: DXR Comp^{GFP} and DXR Comp^{GFP} KO^{Tm} (A) oocysts day 12 post infection (i) oocysts of DXR Comp^{GFP}; arrow head showing unexpected colourless oocysts (ii) DXR Comp^{GFP} KO^{Tm}; arrow head showing (unexpected) colourless oocysts. (B) A PCR reaction to confirm the absence of GIMO parents/ presence of parasites with GFP/ absence of DXR knockouts/ presence of parasites with DXR wildtype in DXR Comp^{GFP} strain oocysts respectively. Although a band is apparent for the 5' knockout of DXR (arrow head), it is

not the expected size (Table 4.6.1), and it seems the same band apperas in all the PCR reactions in this gel image. The next section of the same gel image shows absence of GIMO parents/ presence of GFP parasites and DXR knockouts/ absence of DXR wildtype parasites respectively in oocysts coming from the DXR Comp^{GFP} KO^{Tm} strain. A description of the primers used is in Figs 4.6.6.II, 4.6.10.II

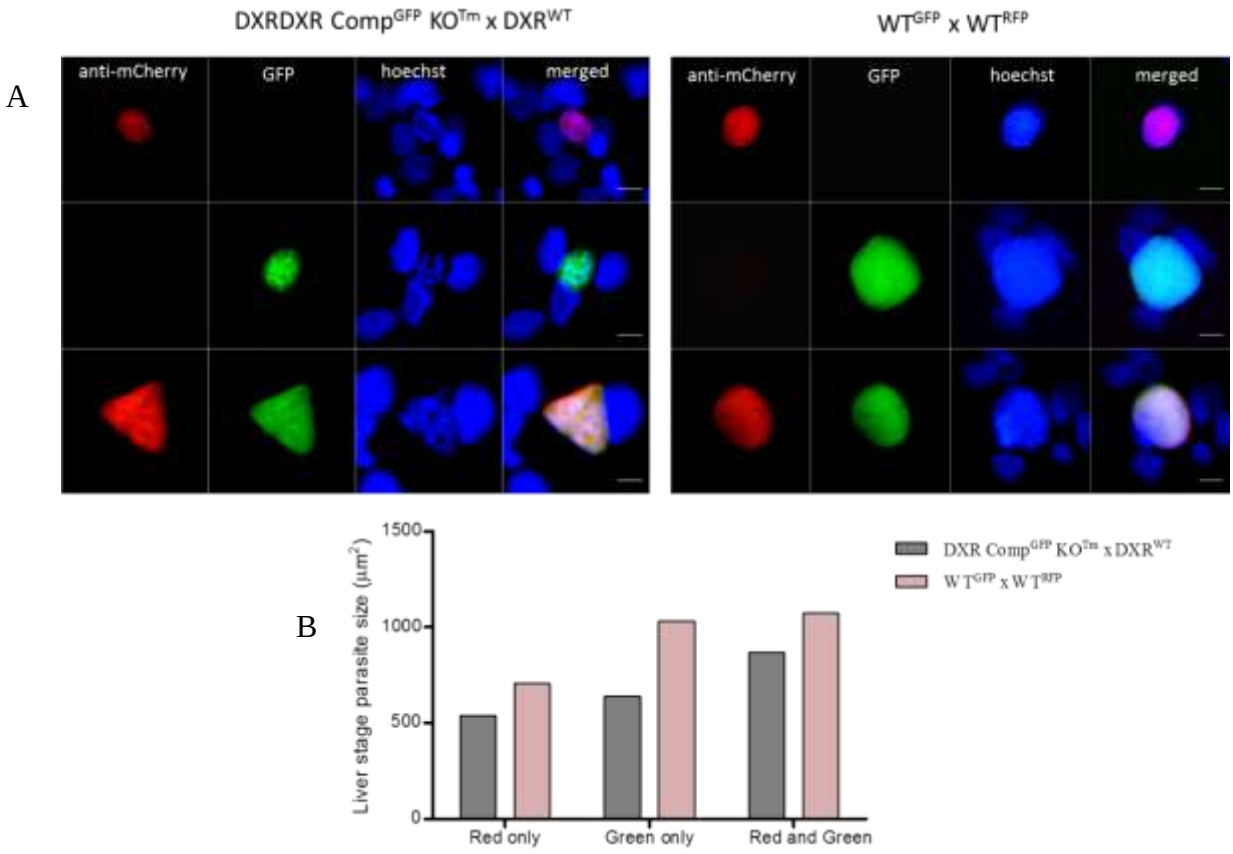

Figure 4.6.15: In-*vitro* liver stage growth of DXR Comp^{GFP} KO^{Tm} x DXR^{WT} parasites and their control (WT^{GFP} x WT^{RFP}) (A) IFA of parasites incubated with anti-mCherry antibody and Hoechst in HepG2 cells 68 hpi showing red (recombinants), green (recombinants), and orange colour parent parasite respectively. Scale bar: 20µm (B) Graph showing comparison of average size of liver stage parasites post 68 hpi as per their colour expression (a statistical analysis was not performed due to the insufficient number of red colour parasites in the sample, parasite size is depicted in µm^2). Colourless liver stage parasites originating from the wildtpe DXR parent (DXR^{WT}) are possibly be present in this population, but their size cannot be analysed without the expression of a fluorophore.

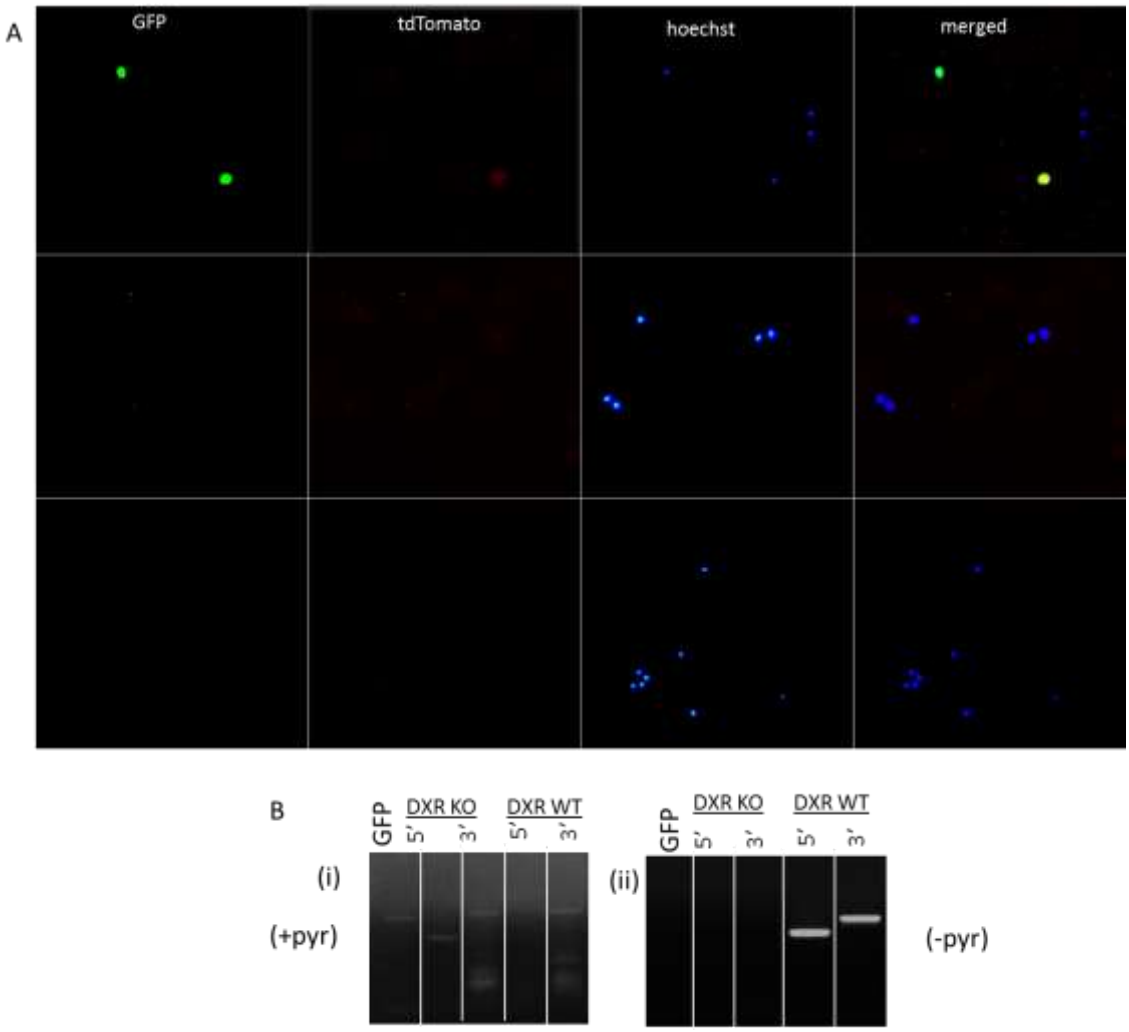

Figure 4.6.16: P0 stage growth of DXR Comp^{GFP} KO^{Tm} x DXR^{WT} (A) Fluorescence microscopy images (X10) of P0 parasites obtained from IV injecting 10000, 1000 sporozoites and by bite-back respectively. Note the presence ofparasites with GFP only and parasites with both GFP and tdTomato expression, but only in the 10000 sporozoites IV injected mouse. It is unclear the reason behind not recovering any parasite having fluorophores (only colourless parasites are seen with the use of DNA stain) from the mice infected with either 1000 sporozoite IV injection or by bite-back. However, the presence of only GFP expressing parasites (in the mouse infected with 10000 sporozoites) confirms the recovery of DXR Comp^{GFP} and the orange coloured parasites are recombinants (with both DXR Comp^{GFP} and DXR KO^{Tm}). (B) PCR reactions showing (i) recovery of GFP expressing parasites with knockouts in DXR gene coming from the DXR Comp^{GFP} KO^{Tm} (all the PCR bands in this gel image are

less bright.Neverthelss there are PCR amplicons that are expected). Since these P0 parasites were pyrimethamine treated, there are no pyrimethamine sensitive DXR wildtype parasites recovered (a faint band is present under the DXR WT 3' screen primer pair, but is not in the expected size; Table 4.6.1) as well as DXR Comp^{GFP} parasites should not be recovered since they are also sensitive to pyrimethamine. (ii) Pyrimethamine un-treated parasites have only the wildtype DXR gene as per the PCR genotyping, while the absence of DXR knockout parasites was noted. Few GFP expressing parasites were recovered as P0 by IV injecting 10000 sporozoites but the PCR of same parasite gDNA was negative for GFP expression possibly due to the low number of GFP parasites present. A description of the primers used is in Figs 4.6.6.II, 4.6.10.II

References for figures

1. Guggisberg AM, Park J, Edwards RL, Kelly ML, Hodge DM, Tolia NH, et al. A sugar phosphatase regulates the methylerythritol phosphate (MEP) pathway in malaria parasites. Nature Communications. 2014;5:4467.

2. Lin JW, Annoura T, Sajid M, Chevalley-Maurel S, Ramesar J, Klop O, et al. A novel 'Gene Insertion/Marker Out'(GIMO) method for transgene expression and gene complementation in rodent malaria parasites. PLoS One. 2011;6:e29289.

Chapter 5

The genetic complementation approach at the mosquito stage; future prospects

5.1. Introduction

Substantial efforts are underway to develop new prophylactic drugs and vaccines against malaria. The liver stage is a logical place to focus some of this effort. As the first point of infection in the human host, the liver is an obvious place to target prophylaxis, which would eliminate an infection before it has the chance to amplify further in the blood stage. Interruption of the liver stage, particularly the late liver stage, also seems to be the most efficacious way of generating sterile immunity, so the liver stage is also important for vaccine development (1). During the obligatory liver stage, parasites show a dramatic increase in numbers within a relatively short period of time, and this stage is asymptomatic (1). However, despite its great potential as a prophylactic target, and its potential value for vaccination, there are serious limitations to studying the liver stage. Accessing parasites in human livers is impractical so the key approach is to study this stage *in-vitro* or *in-vivo* using mice. Another limitation is constraints of our current reverse genetic approach. At present, we can only transfect parasites at blood stage. This means that transfectants must be generated at blood stage and then passaged through mosquitoes before they can be phenotyped in the liver, either *in-vitro* or *in-vivo*. Clearly, any genetic intervention that hinders this life cycle passage (i.e. gene essential at blood and/or mosquito stage) is problematic for studies focusing on the hepatic stage. My overarching goal in this thesis has been to explore simple genetic methods to investigate apicoplast, mitochondrial metabolic activity in the liver stage of rodent malaria parasites.

All apicoplast metabolic pathways, with the notable exception of isoprenoid precursor synthesis, are dispensable during blood stage malaria parasite growth. From this we can deduce that the parasite is able at this stage to scavenge most of the required metabolites from the host; red blood cells. In contrast to the blood stage, the definitive host (the anopheline mosquito) represents a less nutrient rich niche, apparently requiring the parasites to activate more metabolic pathways to survive (2). Increased requirement for functional metabolic pathways in the mosquito host creates a blockade for gene

knockout strains, which typically can not be taken beyond the mosquito stage and back into a naïve vertebrate host for liver studies.

I have modified a previously established method where a mosquito stage indispensable knockout strain is crossed to a wildtype strain to complement and bridge null alleles through the mosquito stage. My innovation was to tag the two strains with two fluorescent markers, which opened up the possibility to live image different parasite genotypes in mosquitoes and also to extend the study into the liver stage and further. Using this novel approach, I have provided compelling evidence that heme pathway deficient parasites fail to grow in liver. Additionally, I have made one of the first assessments of how malaria parasites make use of their energy metabolism in the liver stage. I further modified this technique with the goal of studying how parasites with blood stage essential gene knockouts in isoprenoid precursor synthesis grow in their hepatic stage.

5.2 Heme biosynthesis is essential for liver stage malaria parasites

Malaria parasites presumably need heme for their cytochromes in their mitochondrial electron transport chain. The unusual hybrid mitochondrial/apicoplast heme synthesis pathway of malaria parasites is dispensable at blood stage, but required in mosquitoes. It is believed that parasites can scavenge sufficient heme from the host red blood cells but must resort to synthesis in mosquitoes. However, prior to my study there was no direct genetic study to show whether or not heme synthesis is required in the liver stage of malaria parasites. I applied the genetic complementation approach to fill in the remaining gaps of the heme story in the liver stage using a ferrochelatase (FC) knockout in *P. berghei*. I showed that FC knockout parasites are able to commence the liver stage infection but are unable to complete the hepatic stage due to a growth defect from mid to late liver growth. This is the first time that a detailed study of liver stage development of a heme synthesis deficient parasite has been performed (3) and not only has this facilitated establishment of the genetic complementation tactic but also highlighted the significance of heme biosynthetic pathway in future prophylactic drug development.

I have also postulated (3) that not all the genes in the heme pathway will act the same in the liver stage as the parasite has differential abilities to compensate for loss of heme pathway components. Thus, it will be worthwhile to apply this same technique to other genes in the pathway to get a more complete idea of the pathway functions, which will

inform the prophylactic drug development process focusing on this initial stage of human infection.

5.3 Mitochondrial energy metabolism of liver stage malaria parasites

Malaria parasites utilise anaerobic glycolysis during blood stage, probably because this is the fastest way to grow. However, in the mosquito stage the parasites need their mitochondrial ATP synthase β subunit to generate ATP (2). Using my genetic complementation technique, I have been able to show that the ATPase β knockout parasites grow similar to wildtype parasites during the liver stage. The fact that malaria parasites do not require ATP synthase β subunit for liver stage energy metabolism suggests that this stage might also rely on glycolysis to generate most of its ATP. It is also possible that the parasite might manipulate host cells to obtain ATP.

To extend my investigations of liver stage malaria parasite energy metabolism I investigated the essentiality of three ETC and Krebs/ tricarboxylic acid (TCA) cycle related gene knockouts by crossing them with wildtype parasites at mosquito stage to obtain knockout sporozoites via complementation. This preliminary investigation forewent the fluorophore tagging of genotypes to take advantage of time saving, off-the-shelf knockout constructs. Nevertheless, by studying the knockout growth in liver and P0 blood stages, I found that α-ketoglutarate dehydrogenase (KDH), a TCA cycle associated gene, is probably not essential for liver stage parasites. Conversely, two subunits of the succinate dehydrogenase (SDH) in mitochondrial ETC appear, in this preliminary assessment, to be essential for liver stage.

Further confirmation of these preliminary data (study on KDH and two subunits of SDH) is essential. This will require a detailed study of the liver stage using a clonal strain of colour tagged knockout lines. In addition, it will be beneficial to study the relationship between host energy precursors, glucose availability and the ability of parasites (including β knockout parasites) to alter their energy demand in the liver (4). So far, complex I and III have been subjected to studies in liver and I have studied complex II and V of the ETC. Thus, a detailed liver stage study of complex IV would complete the big picture of ETC essentiality in the liver stage of malaria parasites. Furthermore, experiments on TCA cycle associated genes will be essential to paint a full picture of the over-all energy demands and metabolism of liver stage malaria parasites.

5.4 A new strategy to generate blood stage essential gene knockout parasites

Blood stage malaria parasites require isoprenoid precursors as the only essential *de-novo* synthesised metabolite in the apicoplast (5), but the function of this isoprenoid synthesis pathway in mosquito and liver stages remains elusive. The main obstacle to reaching the mosquito stage is the inability to knockout these blood stage essential genes. Thus, reverse genetic study of the apicoplast isoprenoid biosynthesis pathway of mosquito and liver stage resident parasites required a new strategy. I generated blood stage parasites that have a defect in an endogenous isoprenoid synthesis pathway gene (DXR) but survive courtesy of a complementary gene copy inserted at a remote locus. I subsequently allowed the genes to be independently assorted during sexual recombination and segregation at the mosquito stage to study DXR knockout parasites in the liver. After various obstacles, I was able to generate what I believe to be DXR deficient sporozoites with which to infect liver cells *in-vitro* and *in-vivo*, validating this approach. However, due to apparent random shutting-off of fluorescent markers in DXR constructs, and the difficulties encountered in expressing exogenous copies of oTPT and IspF gene products in parasites, it was difficult to reach any firm conclusion as to the consequence of isoprenoid pathway deficiency on liver stage parasites.

Since my implementation of this new concept suggests it could be tractable, the next steps would be modification of existing genetic constructs for the DXR gene designed to make this study more fruitful. Because the correct colour tagging of parasites is mandatory for this study, major emphasis must be put on applying new, less toxic fluorescent markers, which will hopefully prevent random silencing of colours I experienced in my experiments. In addition to using different fluorescent markers, the use of different epitope tags to separate knockouts from other genotypes could extend the utility of this concept. Further, selecting an appropriate promoter to drive the exogenous gene expression appears to be crucial. To this end it might be strategic to examine gene expression data for the gene-of-interest before selecting a promoter to drive the complementary copy. The choice of transgene promoters in malaria parasites is not currently extensive, but judicious choices, or even use of regulatable promoters, might expedite the insertion of the pre-complementation copy of the gene of interest.

5.5 Conclusion and future directions

5.5.1 Genetic complementation through the mosquito stage

With this project, I have introduced a novel yet simple technique that can be used to analyse the malaria parasite liver stage with the tremendous power of reverse genetics. When a gene of interest is essential for the mosquito stage of parasites, it is difficult to go further into their hepatic stage. Considering the long list of mosquito stage essential genes discovered to date (Table 1.3.1) my technique, which is relatively straightforward and requires no special strains or facilities beyond an insectary, should have widespread application in liver stage biology.

My incorporation of fluorescent markers to track knockout and wild type loci in progeny of crosses is a simple yet powerful innovation for malaria parasite molecular genetics. By using the long established genetic crossing technique to mix two parasitic strains and hence to by-pass the defects in the non-haploid mosquito stage offers a simple way to track knockouts by live imaging cell microscopy that are otherwise lethal in mosquitoes (Table 1.3.2). Moreover, my introduction of pyrimethamine treatment as a secondary screening tool to facilitate detection of low frequency blood stage knockout parasites in P0 mice that are potentially below the threshold detection level of PCR and fluorescent microscopy is a further important feature of this technique.

The malaria parasite oocyst is a biologically unusual cell. It contains multiple haploid nuclei, each the product of meiotic recombinations of the parental gene set, yet they reside within a common cytoplasm to which they all contribute proteins. This phenomenon, referred to as heterokaryptic polyploidy, is key to my complementation-by-crossing strategy; a functional gene can be introduced from one parent to bridge parasites through the oocyst stage until they revert to haploidy again at sporogony. The oocyst stage is also a ‘bottleneck’ stage of malaria parasite life cycle (6) at which parasite numbers are lowest at the beginning of oocyst development but increase exponentially by releasing thousands of sporozoites after what is a relatively protracted phase (~10-15 days) of expansion (7). Therefore, the oocyst stage is vitally important as an intervention point for transmission blocking strategies. The more we can learn about it, the better.

In addition, I have reported the carry-over of shared proteins from the oocyst stage into further stages (i.e. sporozoites). This phenomenon is little studied, and I attempted to further clarify this phenomenon by tracking to what extent the shared proteins (fluorophores in my case) are carried over. I envisage great opportunity for new experiments to resolve this rather unique process. The carryover of, not only fluorescent proteins but also stage specific proteins or signalling molecules, as well as up-regulation of immune components specific for the stage of parasite development could be investigated by fluorescent tagging and cross complementation in oocysts (8-12).

It is known that the longer the parasites remain in the liver, the better the immune response if they fail to successfully progress to blood stage. Indeed, various attenuated strains designed to fail at late liver stage are effective vaccines (13). Therefore, it is important to perform comprehensive studies on parasite growth in their hepatic stage. Using my strategy, it is possible to see exactly, (i) if parasites grow normally or have any defects and if so (ii) when defects appear and (iii) whether viable parasites exit the liver and infect erythrocytes. Complementation by crossing to perform such comprehensive liver stage studies should open up a new avenue for vaccine development.

Despite the simplicity and wide applicability of my novel strategy, there are certain limitations which must be considered. First, if the knockout strain shows a growth delay in blood stage compared to the partner wildtype strain, obtaining approximately similar number of parasites in to the mixed population can be problematic. Similarly, study of gametocyte, zygote and ookinete stage essential genes, which precede oocysts, will not be facilitated by my approach (though some complementation likely occurs in the tetraploid ookinetes). Similarly, sporozoite stages and early liver stage essential genes will also not be complemented since they have returned to haploidy, though depending on the longevity of the shared products carry-over from the sporoblast mother cell these cells may experience some temporary complementation.

The aforementioned technical limitations notwithstanding, the sheer simplicity, the applicability to any laboratory established malaria strain, and the flexibility of use should see this novel technique open up a vast array of previously impossible gene studies of malaria liver stage. For example, it appears appropriate to use this system to screen genes specific for sporozoite development as this could lead to discovery of

potential second generation pre-eythrocytic vaccine candidates (14). In the meantime, the heme metabolic pathway is now known to be essential for both mosquito and liver stages (3, 15-19). However, as previously mentioned, not all the genes in the heme pathway be good candidates for vaccine or prophylactic drug targets, but there is a possibility that at least one gene of the pathway to have necessary characteristics. Based on rodent malaria trials (in which apicoplast FASII is dispensable in oocysts) it had been hoped that FASII knockouts, which die late in liver stage and induce immunity would make excellent attenuated strains (20). However, apicoplast fatty acid biosynthesis (FAS II) is required for sporozoite development in *Plasmodium falciparum* (21). Thus, FASII attenuation vaccination strategy was abandoned but might now be re-explored using my new complementation technique to generate FAS II deficient liver stage parasites and study in detail whether *P. falciparum* FAS II, similar to *P. berghei* and *P. yoelii* (22) is essential for liver stage completion. Indeed, one can even imagine a scenario where the FASII deficient line was complemented (crossed) with a FASII wild type line that also had a different liver stage deficiency to create a 'super' attenuated strain with zero risk of blood stage breakthrough.

5.5.2 Genetic complementation at blood stage coupled with the independent assortment of genes during sexual recombination

Since I have established a new technique to study mosquito stage essential genes in liver stage, my next attempt was to expand this technique to study blood stage indispensable genes in liver stages. Overall my aim was to develop a unique technique that enables complete study of a gene across the malaria life cycle regardless of stage essentiality.

Parasites with knockouts in blood stage essential genes are difficult to recover unless the missing product has been somehow supplemented. However, introduction of an extra copy of the targeted gene into a null locus of a chromosome prior to deletion of the target later enabled DXR, a blood stage essential isoprenoid pathway gene to be knocked out.

Of the three isoprenoid synthesis pathway related genes I chose to work with, I found that not all were readily amenable to this strategy. First, emphasis should be put on to the possible inhibitory effect of exogenous gene products being available for parasites prior to the gene knockout, coupled with the cellular regulatory mechanisms. It is

similarly important to wisely select a promoter to drive the extra gene product. Most constitutive promoters such as CMV, EF-1α can drive a hundred-fold increase in the amount of a protein they express (23). Even though EF-1α successfully expressed the exogenous DXR in my study, the potential increase in the protein/exogenous product expression could have a major influence on the sub-cellular location of the fused protein (23). In the meantime, the PDF promoter that I used as an apicoplast specific promoter did not drive any expression of the complementary copy, preventing the subsequent knockout of the targeted endogenous locus. However, it is hard to predict which promoter works for which gene but it may be beneficial to use a strong and a constitutive promoter to drive a complementary gene such as I have used for DXR gene study. Thirdly, live genotyping of parasites by fluorescent markers can be confounded by random silencing of the markers, which made liver stage study of my DXR gene problematic. Often, the attachment of a fluorescent protein to a gene of interest has no major impact but problems may arise when the protein is over-expressed (23). Moreover, the larger fluorescent tags such as tdTomato can affect folding and maturation of the attached proteins (24). Additionally, GFP has also been reported to cause cellular toxicity in certain organisms (25), which would be a good explanation of what I observed in some parasites with exogenous DXR expressing GFP. Finally, there are incidents of variants of red fluorescent protein causing mis-regulation and mis-targeting of protein of interest (23). Instead of using different fluorescent markers, epitope tagging with either HA, c-Myc or His could also be a better option. Perhaps a combination of both fluorescent proteins and epitope tagging will lead to more reliable results. Whatever the case, it seems essential to carefully choose markers for this study, be it fluorescent markers or epitope tags.

Nonetheless, my pre-complementation study is one of the first studies where a reverse genetic assessment of a blood stage essential gene has been undertaken in liver stage, which represents a significant forward leap in malaria parasite molecular genetics. This less-complicated and clever blood stage strategy, tied with the simple mosquito stage genetic complementation, could well prove to be the next step towards a new era of malaria genetics.

5.6 References

1. Prudêncio M, Mota MM, Mendes AM. A toolbox to study liver stage malaria. Trends in Parasitology. 2011;27:565-74.

2. Sturm A, Mollard V, Cozijnsen A, Goodman CD, McFadden GI. Mitochondrial ATP synthase is dispensable in blood-stage *Plasmodium berghei* rodent malaria but essential in the mosquito phase. Proceedings of the National Academy of Sciences. 2015;112:10216-23.

3. Rathnapala UL, Goodman CD, McFadden GI. A novel genetic technique in *Plasmodium berghei* allows liver stage analysis of genes required for mosquito stage development and demonstrates that *de novo* heme synthesis is essential for liver stage development in the malaria parasite. PLoS Pathogens. 2017;13:e1006396.

4. Meireles P, Sales-Dias J, Andrade CM, Mello-Vieira J, Mancio-Silva L, Simas JP, et al. GLUT1-mediated glucose uptake plays a crucial role during *Plasmodium* hepatic infection. Cellular Microbiology. 2017;19.

5. Yeh E, DeRisi JL. Chemical rescue of malaria parasites lacking an apicoplast defines organelle function in blood-stage *Plasmodium falciparum*. PLoS Biology. 2011;9:e1001138.

6. Smith RC, Barillas-Mury C. *Plasmodium* oocysts: Overlooked targets of mosquito immunity. Trends in Parasitology. 2016;32:979-90.

7. Smith RC, Vega-Rodríguez J, Jacobs-Lorena M. The *Plasmodium* bottleneck: Malaria parasite losses in the mosquito vector. Memorias Do Instituto Oswaldo Cruz. 2014;109:644-61.

8. Bushell ESC, Ecker A, Schlegelmilch T, Goulding D, Dougan G, Sinden RE, et al. Paternal effect of the nuclear formin-like protein MISFIT on *Plasmodium* development in the mosquito vector. PLoS Pathogens. 2009;5.

9. Kappe SHI, Gardner MJ, Brown SM, Ross J, Matuschewski K, Ribeiro JM, et al. Exploring the transcriptome of the malaria sporozoite stage. Proceedings of the National Academy of Sciences of the United States of America. 2001;98:9895-900.

10. Laurentino EC, Taylor S, Mair GR, Lasonder E, Bartfai R, Stunnenberg HG, et al. Experimentally controlled downregulation of the histone chaperone FACT in *Plasmodium berghei* reveals that it is critical to male gamete fertility. Cellular Microbiology. 2011;13:1956-74.

11. Raine JD, Ecker A, Mendoza J, Tewari R, Stanway RR, Sinden RE. Female inheritance of malarial lap genes is essential for mosquito transmission. PLoS Pathogens. 2007;3.

12. Voorberg-van der Wel A, Zeeman AM, van Amsterdam SM, van den Berg A, Klooster EJ, Iwanaga S, et al. Transgenic fluorescent *Plasmodium cynomolgi* liver stages enable live imaging and purification of malaria hypnozoite-forms. PLoS One. 2013;8:e54888.

13. Butler NS, Schmidt NW, Vaughan AM, Aly AS, Kappe SH, Harty JT. Superior antimalarial immunity after vaccination with late liver stage-arresting genetically attenuated parasites. Cell Host and Microbe. 2011;9:451-62.

14. Arama C, Troye-Blomberg M. The path of malaria vaccine development: Challenges and perspectives. Journal of Internal Medicine. 2014;275:456-66.

15. Nagaraj VA, Padmanaban G. Insights on heme synthesis in the malaria parasite. Trends in Parasitology. 2017.

16. Nagaraj VA, Sundaram B, Varadarajan NM, Subramani PA, Kalappa DM, Ghosh SK, et al. Malaria parasite-synthesized heme is essential in the mosquito and liver stages and complements host heme in the blood stages of infection. PLoS Pathogens. 2013;9:e1003522.

17. Rizopoulos Z, Matuschewski K, Haussig J. Distinct prominent roles for enzymes of *Plasmodium berghei* heme biosynthesis in sporozoite and liver stage maturation. Infection and Immunity. 2016.

18. Ke H, Sigala PA, Miura K, Morrisey JM, Mather MW, Crowley JR, et al. The heme biosynthesis pathway is essential for *Plasmodium falciparum* development in mosquito stage but not in blood stages. Journal of Biological Chemistry. 2014;289:34827-37.

19. Sigala PA, Crowley JR, Henderson JP, Goldberg DE. Deconvoluting heme biosynthesis to target blood-stage malaria parasites. Elife. 2015;4.

20. Shears MJ, Botté CY, McFadden GI. Fatty acid metabolism in the *Plasmodium* apicoplast: Drugs, doubts and knockouts. Molecular and Biochemical Parasitology. 2015;199:34-50.

21. van Schaijk BC, Kumar TS, Vos MW, Richman A, van Gemert G-J, Li T, et al. Type II fatty acid biosynthesis is essential for *Plasmodium falciparum* sporozoite development in the midgut of *Anopheles* mosquitoes. Eukaryotic cell. 2014;13:550-59.

22. Vaughan AM, O'Neill MT, Tarun AS, Camargo N, Phuong TM, Aly AS, et al. Type II fatty acid synthesis is essential only for malaria parasite late liver stage development. Cellular Microbiology. 2009;11:506-20.

23. Crivat G, Taraska JW. Imaging proteins inside cells with fluorescent tags. Trends in Biotechnology. 2012;30:8-16.

24. Chudakov DM, Matz MV, Lukyanov S, Lukyanov KA. Fluorescent proteins and their applications in imaging living cells and tissues. Physiological Reviews. 2010;90:1103-63.

25. Liu HS, Jan MS, Chou CK, Chen PH, Ke NJ. Is green fluorescent protein toxic to the living cells? Biochemical and Piophysical Research Communications. 1999;260:712-17.

Appendix: Publication

PLOS | PATHOGENS

RESEARCH ARTICLE

A novel genetic technique in *Plasmodium berghei* allows liver stage analysis of genes required for mosquito stage development and demonstrates that *de novo* heme synthesis is essential for liver stage development in the malaria parasite

Upeksha L. Rathnapala, Christopher D. Goodman‡*, Geoffrey I. McFadden‡

School of BioSciences, University of Melbourne, Parkville, Victoria, Australia

‡ These authors are joint senior authors on this work.
* deang@unimelb.edu.au

OPEN ACCESS

Citation: Rathnapala UL, Goodman CD, McFadden GI (2017) A novel genetic technique in *Plasmodium berghei* allows liver stage analysis of genes required for mosquito stage development and demonstrates that *de novo* heme synthesis is essential for liver stage development in the malaria parasite. PLoS Pathog 13(6): e1006396. https://doi.org/10.1371/journal.ppat.1006396

Editor: Ashley M Vaughan, Seattle Biomedical Research Institute, UNITED STATES

Received: February 15, 2017

Accepted: May 3, 2017

Published: June 15, 2017

Data Availability Statement: All raw data files are available from the figshare database (https://figshare.com) doi number 10.4225/49/583b9330c7361.

Funding: This study was funded by the Australian Research Council grant DP160104980, www.arc.gov.au, and the National Health and Medical Research Council grant APP1106213, www.nhmrc.gov.au, awarded to GIM. The funders had no role in

Abstract

The combination of drug resistance, lack of an effective vaccine, and ongoing conflict and poverty means that malaria remains a major global health crisis. Understanding metabolic pathways at all parasite life stages is important in prioritising and targeting novel anti-parasitic compounds. The unusual heme synthesis pathway of the rodent malaria parasite, *Plasmodium berghei*, requires eight enzymes distributed across the mitochondrion, apicoplast and cytoplasm. Deletion of the ferrochelatase (FC) gene, the final enzyme in the pathway, confirms that heme synthesis is not essential in the red blood cell stages of the life cycle but is required to complete oocyst development in mosquitoes. The lethality of FC deletions in the mosquito stage makes it difficult to study the impact of these mutations in the subsequent liver stage. To overcome this, we combined locus-specific fluorophore expression with a genetic complementation approach to generate viable, heterozygous oocysts able to produce a mix of FC expressing and FC deficient sporozoites. These sporozoites show normal motility and can invade liver cells, where FC deficient parasites can be distinguished by fluorescence and phenotyped. Parasites lacking FC exhibit a severe growth defect within liver cells, with development failure detectable in the early to mid stages of liver development *in vitro*. FC deficient parasites could not complete liver stage development *in vitro* nor infect naïve mice, confirming liver stage arrest. These results validate the heme pathway as a potential target for prophylactic drugs targeting liver stage parasites. In addition, we demonstrate that our simple genetic approach can extend the phenotyping window beyond the insect stages, opening considerable scope for straightforward reverse genetic analysis of genes that are dispensable in blood stages but essential for completing mosquito development.

study design, data collection and analysis, decision to publish, or preparation of the manuscript.

Competing interests: The authors have declared that no competing interests exist.

Author summary

Combating, and ultimately eliminating, malaria requires drugs that hit the parasite at all stages of its life cycle. Deletions of parasite metabolism genes can expose where and when a certain metabolic pathway is essential, and hence vulnerable to drugs. However, once a parasite gene has been deleted, it is difficult to examine that parasite beyond the point in the life cycle where that gene is essential because the parasites die. We developed a simple genetic complementation strategy to bridge malaria parasites through the mosquito life stage when they carry a genetic defect that otherwise specifically stops them completing this stage. Our strategy allows the phenotypic analysis of any such defect in the subsequent life stages, in any genetically tractable parasite species. It does not require specific background lines, or the chemical or physical treatment necessary for conditional knockout approaches and can be applied to any of the ~50 genes already known to be specifically required for development in the mosquito. This includes genes of the heme synthesis pathway. Malaria parasites are obliged to synthesize the iron-managing molecule heme to complete their development in mosquitoes. We used our genetic complementation strategy to bridge malaria parasites lacking the final enzyme in the heme synthesis pathway through the mosquito phase and back into a vertebrate. We discovered that parasite-generated heme is crucial for the parasite to complete the liver phase of vertebrate development; absence of this enzyme prevents parasites from progressing to the symptomatic blood phase. Our results indicate that blocking parasite heme production should work as a prophylactic intervention to prevent the progression of incipient malaria infections into the deadly blood phase.

Introduction

Malaria is a life-threatening disease caused by five species of *Plasmodium* parasites, with *P. falciparum* being the most deadly. The on-going emergence of drug resistance threatens malaria control efforts [1] and highlights the need for new drugs and novel approaches for controlling the spread of this disease. *Plasmodium berghei* is a widely-used mouse malaria model and a dominant tool for reverse genetic studies in malaria [2]. The *P. berghei* genome is largely homologous to the genome of the human parasites, which permits experiments that are difficult to perform with human subjects [3]. Experimental access to the entire life cycle is arguably the most important advantage of rodent malaria parasites as it facilitates study of transmission dynamics, exoerythrocytic stage vaccines, and prophylactic drugs.

Genome manipulation is an essential tool for understanding key events in the *Plasmodium* life cycle. Stable transfection of the parasite and modification of its genome by homologous recombination are now common procedures [4]. A significant limitation of the method is that the parasite genes essential at one life stage cannot be characterized in subsequent stages. In the growing list of loss of function mutations that can survive the blood stages, many are found to fail during development in the mosquito; possibly due to the increased metabolic requirements in this stage of the life cycle [5]. Failure to produce infective sporozoites limits the possibilities for studying the role of these genes in the liver stage. Given the unique features of the hepatic stage of the life cycle, particularly the low parasite burden and the role in generation of sterile immunity [6], understanding parasite biology at this stage is of great importance. Thus, temporal gene inactivation is needed in functional studies to test protein function during liver stage development. A small number of genes essential in other life stages have been successfully ablated using conditional knockout strategies in *P. berghei* to analyse liver stage

function [7, 8], and other conditional strategies are available. But these strategies can present significant limitations in terms of which species can be tested, the complexity of plasmid construction, the need for specific parasite lines, requirements for specific chemical or physical treatments during the life cycle, and unpredictable variations in the effectiveness of the gene ablation. Such drawbacks have limited the use of these techniques and severely hampered analysis of parasite liver stage responses to gene deletion [9, 10] largely precluding reverse genetic approaches to this important life cycle phase.

Heme is essential in malaria parasites, playing an important role as a precursor for cytochrome production in the mitochondrial electron transport chain. *Plasmodium* parasites encode and express all the enzymes for a complete heme biosynthesis pathway, and heme biosynthesis was initially considered a potential drug target against malaria parasites [11]. However, the *de novo* heme synthesis pathway enzymes are dispensable during the blood stage of the parasite life cycle [12–15]. It appears that parasites still require heme, but in the blood stage they can scavenge pathway intermediates, heme and/or heme synthesizing enzymes, from the host red blood cell [12, 14, 16]. However, these alternate sources are apparently not sufficient or accessible enough during the mosquito stages of the parasite life cycle, where parasites lacking heme-synthesizing enzymes fail to complete sporozoite development in the oocyst [12, 13, 15].

Given the essentiality of the endogenous heme biosynthesis pathway in the mosquito stages of the parasite life cycle, it is hardly surprising that there is minimal data available about the liver stage growth of heme deficient parasites. Parasites lacking the first enzyme in the heme biosynthesis pathway, aminolevulinic acid synthase (ALAS) can only complete the life cycle if mosquitoes are fed aminolevulinic acid (d-ALA), the product of ALAS [12, 15]. This chemical complementation approach has been effectively employed to generate infective ALAS-minus sporozoites and demonstrate that parasites can scavenge d-ALA from the host liver and, thereby, partially restore parasite viability [15]. While it is clear that parasites can survive the loss of ALAS, this finding does not directly address whether parasite synthesized heme is essential for liver stage development. Aminolevulinic acid is a stable compound that appears to be available for uptake from the host cell cytoplasm, possibly by the same mechanism that imports parasite synthesized d-ALA into the apicoplast where the next steps in the pathway are localized. It remains unclear if the other compensatory mechanisms available to parasites in the red blood cell, particularly the ability to scavenge FC and/or heme, are available to the parasite during liver stage infection.

A chemical complementation approach is not available for the final stage of the heme biosynthesis pathway, namely conversion of protoporphyrin IX and iron to heme by ferrochelatase (FC) in the mitochondrion, so we set out here to address this limitation by applying a genetic complementation method to rescue parasites with a deletion of the FC gene. By combining locus-specific fluorescence tagging with the ability of sexual outcrossing to bridge parasites through the mosquito life stages [17], we generated viable sporozoites that lacked the FC gene but were capable of infecting liver cells *in vitro* and *in vivo*. The specific fluorescent labelling of parasites lacking FC allowed detailed exploration of the reliance on heme for parasite development in the liver stage. Our fluorescence-tagging complementation strategy gives a straightforward method for reverse genetic analysis of various blood-stage dispensable/mosquito-stage essential genes that is useable in all genetically tractable, fertile *Plasmodium* species and requires no special conditions.

Materials and methods

Experimental animals

Male asmu:Swiss mice aged between 4–6 weeks obtained from Monash Animal Research platform were used in all the experiments.

Ethics statement

All animal experiments were carried out as per the National Health and Medical Research Council—Australian Code for the Care and Use of Animals for Scientific Purposes 2013 (8th edition) guidelines and were permitted by the University of Melbourne Animal Ethics committee under Ethics ID 1413078.1. Anesthesia using ketamine/xylazine, euthanasia via slow fill carbon dioxide followed by cervical dislocation.

Parasites

The *Pb*nek-4ko strain [18] was provided by Oliver Billker (Wellcome Trust Sanger Institute, Hinxton, Cambridge, UK). *Pb ANKA* parasites lines expressing GFP, tdTomato and mCherry fluorescence markers were developed in our laboratory based on [19]. See Supplementary Methods for a full description of the generation of these lines.

Generation of *Plasmodium berghei* ^{FC} knockout parasites

To generate the *P. berghei* FC (Pb ANKA_114070) knockout parasites (FC^{KOmCh}), the selection cassette from pLChSKD, a modified version of pL0006 (MRA-775) with the hDHFR replaced by mCherry fused to hDHFR via a viral 2A skip peptide [20], was ligated into the *Xho*I/*Bgl*II sites of pL0006 containing regions flanking the FC gene [16] to create pFCChSKD. See Supplementary Methods for a full description of pLChSKD plasmid construction. *Pb*ANKA parasites were transfected with *Hind*III/*Eco*RI linearized pFCChSKD, genotyped by PCR (see S1 Table for primer sequences) and cloned as previously described [5, 21].

Infection of *Anopheles stephensi*

All parasite strains used for coinfection crossing experiments were inoculated by intraperitoneal injection into naïve mice and assessed for fluorescence and genotype at day 3. 2.5 x 10^5 parasites from each strain were mixed and used to infect a naïve mouse by intravenous (IV) injection. The mice were infected with the following combinations of *P. berghei* parasitic strains.

1. FC^{KOmCh} x FC^{WT}-GFP–Parasites having FC replaced with ChSKDHFR mixed with parasites having a wild type FC locus and expressing GFP from a different genetic locus
2. FC^{KOmCh} nek-4wt x FC^{WT}-nek-4ko—Parasites with a wild type nek4 locus and having FC replaced with ChSKDHFR mixed with parasites carrying a wild type FC gene but lacking nek-4.
3. FC^{WT}-mCh x FC^{WT}-GFP–parasites with a wild type FC locus and expressing mCherry from another genetic locus mixed with FC wild type parasites expressing GFP from another genetic locus.
4. FC^{WT-}mCh x FC^{WT}-nek-4ko—parasites with wild type FC and nek4 loci and expressing mCherry from another genetic locus mixed with non-fluorescent parasites with a wild type FC locus but lacking nek-4.

Adult females of *A. stephensi* (MR4) reared under standard insectary conditions (adult mosquitoes were grown at 27˚C with humidity of 80% and light: dark photoperiod of 14:10 hours with a 1 hour ramp in) were allowed to feed on 4–6 weeks old Swiss mice anesthetized with ketamine/xylazine 3 days following coinfection. A minimum of three independent infections were done for all crosses.

Assessment of mosquito stage development

Twelve days after infection, mosquito midguts were removed, imaged using a Leica DM 2500 epifluorescence microscope (20x) and counted. Oocyst size was measured using Fiji (ImageJ 1.46a, Wayne Rasband, National Institutes of Health).

Salivary gland sporozoite numbers were counted using a standard haemocytometer and averaged per mosquito. Salivary gland sporozoite motility 21 days post-infection was analysed by immunofluorescence assay (IFA) [22]. Slides were probed with primary antibodies against anti-circumsporozoite protein (1: 500; a gift from Louis Schofield, Walter and Eliza Hall Institute) and mCherry (1: 250; Abcam ab167453). FC^{KOmCh} nek-4wt x FC^{WT}-nek-4ko parasites were probed with Alexa Fluor 488 goat anti-mouse IgG and Alexa Fluor 546 goat anti-rabbit IgG (1:1000; Molecular Probes) secondary antibodies. FC^{KOmCh} x FC^{WT}-GFP parasites were probed with Alexa Fluor 633 goat anti-mouse IgG and Alexa Fluor 546 goat anti-rabbit IgG (1:1000; Molecular Probes/ThermoFisher) secondary antibodies. Salivary gland sporozoite gDNA was extracted and used as template for nested PCR to confirm the presence of FC^{KOmCh} parasites.

In vitro liver stage development analysis

Growth and IFAs of pre-erythrocytic forms were performed as described [23]. To determine size and nuclear content, parasites were stained with rabbit anti-mCherry (1: 250; Abcam ab167453)/Alexa Fluor 546 goat anti-rabbit IgG (1:1000; Molecular Probes/ThermoFisher) and Hoechst 33342 (5μg/ ml). Images collected at 40x magnification with the Leica DM 2500 microscope were analysed in Fiji to measure parasite size in μm^2. Student t-test (unpaired) was used to compare the average growth size differences 24, 48 and 68 hours post infection for parasites pooled from 6 independent experiments. For nuclear content, Chi-squared analysis was used to assess pooled data from two independent experiments.

To further assess parasites development in liver cells, parasites grown for 68 hours in three independent experiments were stained with both rabbit anti-mCherry, (1: 250; Abcam ab167453) and mouse anti-Pf merozoite surface protein-1 (MSP-1) (1: 100; a gift from Paul Gilson, Burnet Inst) followed by Alexa Fluor 546 goat anti-rabbit IgG Probes and Alexa Fluor 488 goat anti-mouse IgG (1:1000; Molecular Probes/ThermoFisher) for the FC^{KOmCh}-nek4-wt x FC^{WT}-nek4-ko. For the FC^{KOmCh} x FC^{WT}-GFP cross, Alexa Fluor 633 goat anti-mouse IgG and Alexa Fluor 546 goat anti-rabbit IgG (1:1000; Molecular Probes/ThermoFisher) were used as secondary antibodies. MSP-1 expression was compared using Fisher's exact test of data pooled from three independent experiments (801 parasites assessed).

To determine the ability of parasites to complete liver stage development *in vitro*, merosomes were counted at 70 hpi using an Olympus CKX41 compound fluorescence microscope at 40x magnification.

To confirm the presence of FC knockout parasites in liver by PCR, naïve mice were (IV) infected with 20,000 sporozoites. Forty to 42 hours post infection, mice were sacrificed, their livers harvested and genomic DNA was extracted for use as template in a nested PCR reaction. See S1 Table/S1 Fig for primer sequences and PCR strategy.

Analysis of sporozoite infectivity and ability to infect naïve mice

For bite-back infection, mosquitoes were given access to anesthetized Swiss mice (4–6 weeks old) until at least 20 mosquitoes had fed. For IV infection, salivary gland sporozoites were isolated from salivary glands 21–24 days after infection, counted and IV injected at 1000 or 10,000 sporozoites/mouse. Time to patency and the subsequent development of asexual stage

parasites, were monitored by fluorescence microscopy and Giemsa stained blood smears from 3 days post infection onwards. Genotyping by PCR was done as described above.

For each pyrimethamine selection of FC^{KOmCh} parasites, two mice were simultaneously infected from a single cage of mosquitoes. One mouse was given pyrimethamine in its drinking water (70μg/ ml) while the other was not treated. Once parasites were detected in the untreated mice, they were analysed for fluorescence and genotype and then given pyrimethamine in drinking water (70μg/ ml) to clear all the parasites. After parasites were cleared (day 4) pyrimethamine was removed and mice were observed for 7 days to test for recrudescence.

Statistical analysis

All statistical analysis was done using GraphPad Prism (GraphPad Software, La Jolla California USA)

Results

Deletion of the ferrochelatase gene arrests parasite development in the oocysts stage

Pb ANKA_114070 encodes FC, the last enzyme of the heme biosynthesis pathway [24]. We interrupted the *Pb* ANKA_114070 locus by double cross over homologous recombination introducing the selectable marker, human dihydrofolate reductase (*h*DHFR) fused to a fluorescent mCherry tag and driven by the constitutive *Pb* EF-1α promoter, into the FC coding sequence (S1 Fig). Parasites carrying this FC deletion are denoted as FC^{KOmCh}. When *Anopheles stephensi* mosquitoes fed on mice infected with FC^{KOmCh}, oocysts developed in these mosquitoes but no salivary gland sporozoites were observed (Table 1). This is consistent with previous reports that FC is dispensable at the blood stage and early sexual stages but crucial for completion of sporozoite development [12, 13, 16].

Crossing ferrochelatase deficient parasites with those carrying a wild type ferrochelatase gene complements the defect in oocyst development and sporozoite production

To determine if the effects of the FC deletion during the mosquito stage could be complemented by a wild type copy of the allele (denoted FC^{WT}), we crossed our FC^{KOmCh} with two different strains carrying intact FC genes: either FC^{WT} parasites expressing GFP inserted into the intergenic locus of chromosome 6 [19], or a female sterile line FC^{WT}-nek-4ko [18]. To control for any effects of fluorophore expression on oocyst generation and development, we also generated control crosses of the fluorescent lines with parasites with a wild type FC locus. Mice were dual infected and *A. stephensi* mosquitoes fed on these dual infected mice to generate the various crosses. Expected genotypes of the oocysts and sporozoites from the two crosses are depicted in Fig 1A and 1B.

The replacement of the FC coding region with *h*DHFR fused to mCherry in FC^{KOmCh} parasites allows tracking of FC^{KO} genotype throughout sexual reproduction. In mosquitoes fed on mice infected with both FC^{KOmCh} and FC^{WT}-GFP, after sexual recombination and oocyst formation in mosquitoes, three oocyst genotypes could be identified 12 days post infection: FC^{KOmCh} (red), FC^{WT}-GFP (green), and FC^{KOmCh} x FC^{WT}-GFP recombinants (orange) (Fig 1C).

Mosquito infectivity, as measured by infection rate and oocyst load, was not significantly different ($P>.05$, one-way ANOVA) between FC^{KOmCh} and FC^{WT}-mCh parasites when crossed to either FC^{WT}-GFP or FC^{WT}-nek-4ko parasites (Table 1). This confirms previous

Table 1. Life cycle progression and infectivity of FC^{KOmCh} parasites following outcrossing.

Parasite lines	Number of infections	Infection rate (%)/ Oocysts per mosquito* (n = number of infected mosquitoes)	Sporozoites per mosquito (n = number of mosquitoes dissected)	Transmission to naïve mice**		Time to patency (days) **
				IV injection (n = number of sporozoites injected)	bite-back	
FC^{KOmCh} parent	2	47 ± 29/ 203 ± 34 (n = 13)	0 n = 22	(NA)***	0/1	N/A
FC^{KOmCh} x FC^{WT}-GFP	4	79 ± 5/ 172 ± 30 (n = 33)	6367± 1206 n = 72	n = 1000–1/1 n = 10 000–1/1	4/4	4.5
FC^{WT}-mCh x FC^{WT}-GFP	3	80 ± 2/ 161 ± 33 (n = 24)	6101± 233 n = 78	(ND)	3/3	5
FC^{KOmCh}nek-4wt x FC^{WT}-nek-4ko	8	86 ± 4/ 181 ± 21 (n = 75)	5330± 906 n = 142	n = 1000–1/1 n = 10 000–1/1	4/4	4.75
FC^{WT}-mCh-nek-4wt x FC^{WT}-nek-4ko	5	79 ± 6/ 241± 28 (n = 43)	10913± 3482 n = 94	n = 10 000–1/1	3/3	4.5

*The number of oocysts per midgut reflect only mCherry expressing oocysts from infected mosquitoes

**Transmission and days to patency data do not include results of experiments involving pyrimethamine treatment.

****Pb*** FC^{KOmCh} parasites do not produce salivary gland sporozoites when self-fertilized, so IV injection was not possible.

NA = not applicable. ND = Not done.

https://doi.org/10.1371/journal.ppat.1006396.t001

findings [12, 15] that the parasite heme synthesis enzymes do not play an essential role in the early mosquito life stages in *P. berghei*.

FC deletion restricts the growth of oocysts (Fig 1C and 1D). Fluorescence tags allowed us to determine the genotype (presence/absence of active FC gene) of each oocyst. In the FC^{KOmCh} x FC^{WT}-GFP cross, oocysts with only mCherry fluorescence (red) are the product of FC^{KOmCh} self-fertilization, and they exhibit the reduced oocyst growth phenotype (Fig 1C and 1D) characteristic of parasites lacking ferrochelatase, or other heme synthesizing enzymes [15]. FC^{KOmCh} self-fertilized parasites (red in the cross) are not significantly different in size to oocysts produced when mosquitoes are infected with FC^{KOmCh} alone (Fig 1D). In contrast, orange oocysts, which carry both FC^{KOmCh} and FC^{WT}-GFP genes, are significantly larger than exclusively FC^{KO} oocysts (red) and equivalent in size to FC^{WT}-GFP oocysts (green), which are self-fertilized progeny of the GFP containingparent from FC^{KOmCh} x FC^{WT}-GFP cross. A comparable increase in size was also seen in the oocysts from the FC^{KOmCh}-nek-4wt x FC^{WT}-mCh-nek-4ko cross. Because the FC^{WT}-mCh-nek-4ko line is female sterile [18], no colourless oocysts were produced, and in the absence of a second fluorophore it is not possible to distinguish FC^{KOmCh} nek-4wt self-fertilization oocysts (red) from FC^{KOmCh} nek-4wt x FC^{WT}-mCh-nek-4ko recombinants (red). Nevertheless, the mCherry expressing oocysts from the FC^{KOmCh} nek-4wt x FC^{WT}-mCh-nek-4ko cross are, on average, significantly larger than oocysts arising from infections with FC^{KOmCh} alone (Fig 1D).

Complementation of the FC knockout by crossing to FC^{WT} strains not only restored normal oocyst growth but also enabled development of sporozoites, with robust numbers of salivary gland sporozoites produced in all our crosses (Table 1). Red sporozoites could be observed in the mosquito midgut at day 17 and in the salivary glands at day 21 post-infection (Fig 1E). Sporozoites contain only a single haploid nucleus, so red sporozoites predict the presence of FC^{KOmCh} genotype in the sporozoites generated by the cross and this was confirmed by PCR (Fig 1F). Therefore, we conclude that introduction of a wild type FC gene by sexual

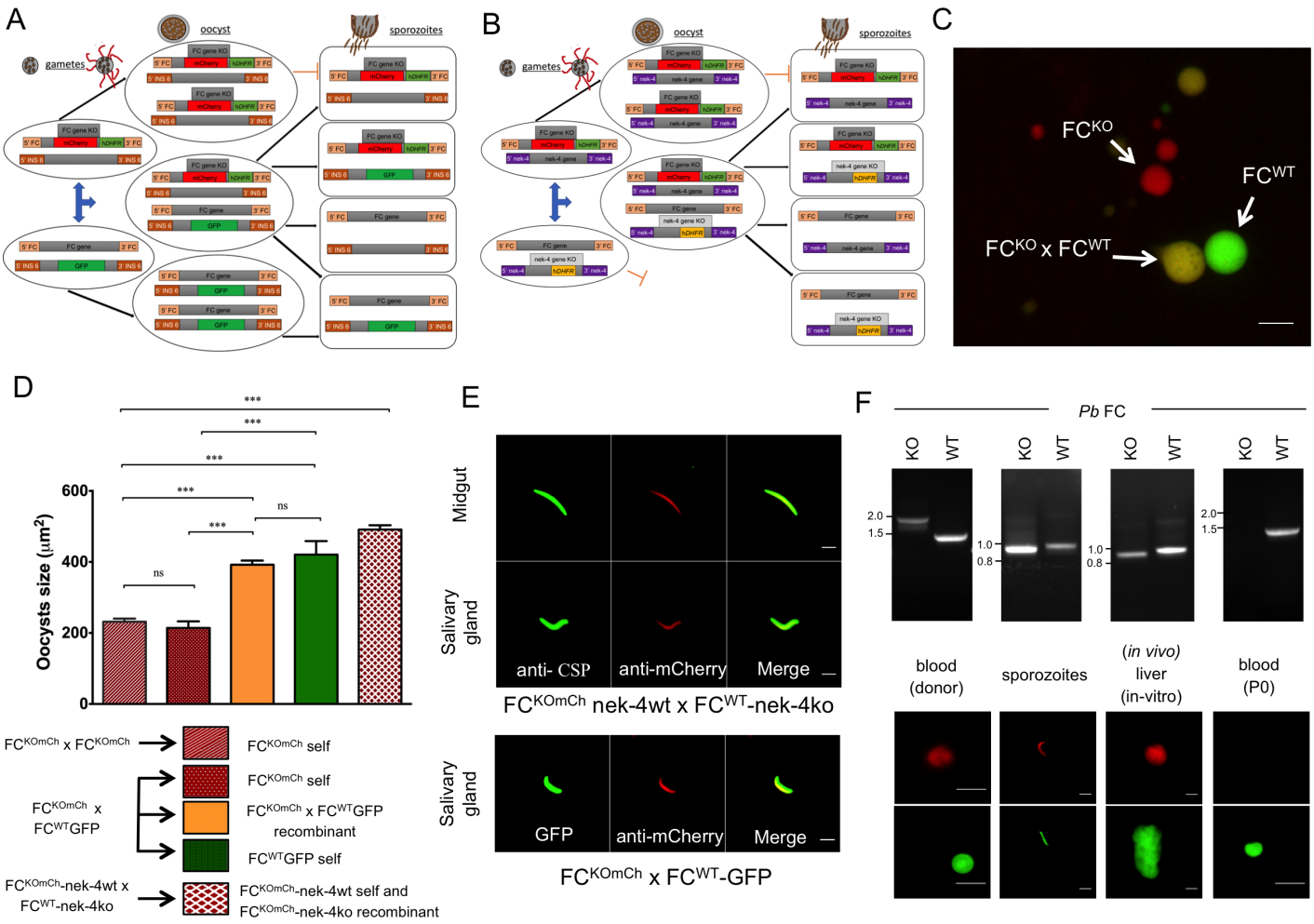

Fig 1. Crossing FC^{KOmCh} to FC^{WT} parasites allows normal development of FC^{KOmCh} sporozoites. A) Schematic representation of the predicted parasite genotypes at the polyploid oocyst stage and haploid sporozoite stage after allowing mosquitoes to feed on mice dually infected with FC^{KOmCh} and FC^{WT}-GFP parasites. Three genetic combinations are possible in the polyploid oocyst: self- fertilization yielding oocysts with only the FC^{KOmCh} or the FC^{WT}-GFP allele or outcrossing creating an oocyst with both FC^{KOmCh} and the FC^{WT}-GFP alleles. Following sporogony, the parasite returns to the haploid state yielding four possible genetic combinations of the FC^{KOmCh} and the FC^{WT}-GFP genes: The original FC^{KOmCh} or FC^{WT}-GFP alleles alone, a combination of both the FC^{KOmCh} and FC^{WT}-GFP alleles or parasites carrying neither allele. B) Schematic representation of the predicted parasite genotypes at the polyploid oocyst stage and haploid sporozoite stage after allowing mosquitoes to feed on mice dually infected with FC^{KOmCh}–nek4-wt and FC^{WT}-nek4-ko parasites. The nek4ko mutation prevents self-fertilization of this parasite line, so two genetic combinations are possible in the polyploid oocyst: self- fertilization yielding oocysts with only the FC^{KOmCh} allele or outcrossing creating an oocyst with both FC^{KOmCh} and the FC^{WT}-nek4ko alleles. Following sporogony, the parasite returns to the haploid state yielding four possible genetic combinations of the FC^{KOmCh} and the FC^{WT}-nek4ko genes: The original FC^{KOmCh} or FC^{WT}-nek4ko alleles alone, a combination of both the FC^{KOmCh} and FC^{WT}-nek4ko alleles or parasites carrying neither allele. C) A midgut infected by feeding on an FC^{KOmCh} x FC^{WT}-GFP infected mouse showing the presence of the three oocyst phenotypes. Red oocysts are self-fertilized FC^{KOmCh} parasites, green are self-fertilized FC^{WT}-GFP, and orange oocysts are FC^{KOmCh} x FC^{WT}-GFP recombinants. scale bar: 20μm. (D) Complementation of the FC^{KO} phenotype demonstrated by comparing the mean surface area of oocysts from FC^{KOmCh} self-fertilization with oocysts produced by the FC^{KOmCh} x FC^{WT}-GFP and FC^{KOmCh} nek-4wt x FC^{WT}-nek-4ko crosses. The female specific defect resulting from the nek4-ko genotype prevents development of colourless FC^{WT}-nek-4ko oocysts, so all oocysts produced from FC^{KOmCh} nek-4wt x FC^{WT}-nek-4ko crosses carry the FC^{KOmCh} and are red in colour. ns; not significant, ***—*P* value <0.0001 (Student t test) (E) Immunofluorescence assay showing the presence of mCherry fluorescence, and hence the presence of the FC^{KOmCh} allele in midgut (day 17 post infection) and salivary gland (day 21 post infection) sporozoites from the FC^{KOmCh} nek-4wt x FC^{WT}-nek-4ko cross and the salivary gland sporozoites from the FC^{KOmCh} x FC^{WT}-GFP cross. scale bar: 10μm F) FC genotype (by PCR) and matching fluorescent phenotype of parasites through the complete life cycle showing the presence of parasites carrying both the FC^{KOmCh} and FC^{WT} genes until the liver stage of the life cycle. Parasites carrying the FC^{KOmCh} fail to complete liver stage development so neither red fluorescence nor the FC^{KOmCh} gene is detectable in the subsequent blood stage infection. Sporozoite and liver stage genotypes were assessed with a nested PCR reaction, yielding a band of different size to that seen in blood stages. scale bar: 10μm.

https://doi.org/10.1371/journal.ppat.1006396.g001

crossing can restore oocyst growth and sporozoite production to FC^{KO} parasites. We noted that all the sporozoites from the FC^{KOmCh} nek-4wt x FC^{WT}-nek-4ko cross were red, despite the expectation that half of the sporozoite population should carry the colourless FC^{WT} genotype and, therefore, not fluoresce. The presence of both FC^{KOmCh} and FC^{WT} parasites was confirmed by PCR (Fig 1F). This suggests that fluorescent protein was being carried over from the oocyst and interfering with visual genotyping of sporozoites in the midgut and salivary glands.

To further examine the apparent carryover of fluorescent protein from the oocyst to the sporozoites, we crossed parasites with either GFP or tdTomato inserted in the same genetic locus (Fig 2A), namely the intergenic region of chromosome 6 [19]. Oocysts from this cross exhibited three different colours (green, red and orange) indicating that the lines had successfully crossed and also self-fertilised (Fig 2B). Unlike the polyploid oocysts, haploid sporozoite progeny from this cross can inherit only one fluorophore gene, either GFP or tdTomato (Fig 2A). Nevertheless, in addition to exclusively green or red sporozoites, we observed many sporozoites that contained both fluorophores (orange parasites highlighted with arrows in Fig 2C). We conclude that sporozoite formation involves carryover of significant oocyst cytoplasm, resulting in dual-coloured sporozoites emerging from the heterozygous oocysts. All parasites had reverted to exclusively GFP or tdTomato once the sporozoites invaded liver cells and developed into early exoerythrocytic forms (Fig 2B). Similarly, only red or green parasites were observed when these parasites progressed in to blood stage following bite-back (Fig 2B)

FC^{KO} sporozoites are liver infective both *in vitro* and *in vivo* but have severe growth defects and fail to complete liver stage development

To examine the viability of FC^{KOmCh} sporozoites, we tested their motility *in vitro*, and their infectivity both *in vitro* and *in vivo*. No significant difference between the number of motile sporozoites, or in their levels of motility, was observed between FC^{KOmCh} and FC^{WT} sporozoites (S2 Table, S2 Fig). FC^{WT} parasites had slightly more sporozoites with maximal motility (> 10 trails), but this difference was not statistically significant ($P>0.05$).

Sporozoites recovered from complemented FC^{KOmCh} lines were used to infect *in vitro* cultures of HepG2 liver cells, and parasite development was assessed by IFA at 24, 48 and 68 hours. By 24 hours, any residual fluorescent protein seen in the sporozoites is lost and the liver parasites can be unequivocally genotyped by fluorescence expression, with mCherry expression denoting the FC^{KOmCh} genotype. FC^{KOmCh} liver parasites (red) could be detected at 24, 48 and even 68 hours post infection from either of the complementation crosses (Fig 3A). The FC^{KOmCh} (red) parasites were smaller than FC^{WT} parasites at all three time points, although the difference only becomes statistically significant at 48 and 68 hours (Fig 3A and 3B). This size defect correlated with a significant reduction ($P<0.0001$) in the number of nuclei produced in FC^{KOmCh} parasites at 68 hpi (Fig 3C). To further assess progress through liver stage development, the production of merozoite surface protein-1 (MSP-1) was measured in FC^{KOmCh} parasites. Significantly fewer FC^{KOmCh} parasites (45%) were MSP-1 positive than FC^{WT} type parasites (79%) (Fig 3D, $P<0.001$) suggesting a mid-stage liver stage defect [25–28].

To determine if the smaller size, reduced nuclear content, and impaired MSP-1 expression in FC^{KOmCh} liver stage parasites foreshadowed an inability to complete the liver stage of the life cycle we counted merosomes, which are groups of membrane-bound merozoites that bud off the infected liver cell and represent the end-product of the parasite's liver stage development [29]. Merosomes were readily recovered, but none contained red fluorescent parasites, indicating that FC^{KOmCh} parasites could not complete the liver stage *in vitro* (Table 2). We conclude that FC^{KOmCh} parasites can infect liver cells *in vitro* but cannot complete liver stage development.

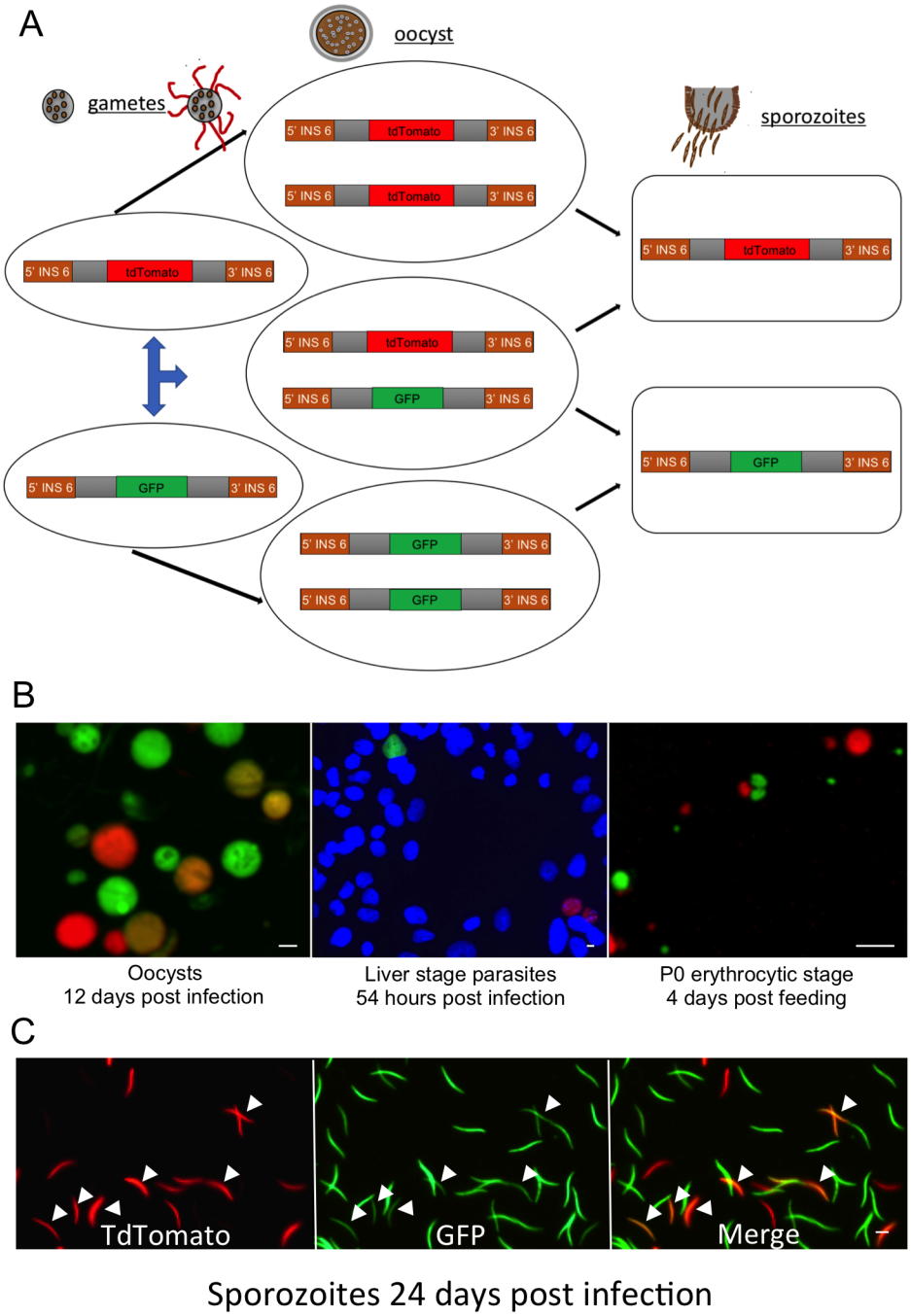

Fig 2. Sporozoite development involves significant carryover of oocyst cytoplasm. A) Schematic representation of the predicted parasite genotypes at the polyploid oocyst stage and haploid sporozoite stage after allowing mosquitoes to feed on mice dually infected with parasites expressing either GFP or tdTomato. The fluorophore is inserted into the same genetic locus in each parasite line, so three genetic combinations are possible in the polyploid oocyst: self- fertilization yielding oocysts with either the GFP or tdTomato allele, whereas outcrossing generates a heterzygous oocyst with both the GFP and tdTomato alleles. Following sporogony, the parasite returns to the haploid state and can carry either the GFP or tdTomato allele, but not both. B) Progeny of the GFP x tdTomato cross through the life cycle. Three oocyst phenotypes are present, GFP only (green) and tdTomato only (red) from self-fertilizations and heterozygous, polyploid parasites expressing both fluorophores (orange). Only two phenotypes, GFP (green) or tdTomato (red) are present in haploid liver and red blood cell stages. C) Sporozoites generated from crossing GFP and tdTomato parasites showed many haploid sporozoites still carrying both fluorphores (arrow heads). Single colour (green or red) sporozoites are presumably offspring from self-fetilizations, while two-colour (orange) sporozoites are from recombinant oocysts.

https://doi.org/10.1371/journal.ppat.1006396.g002

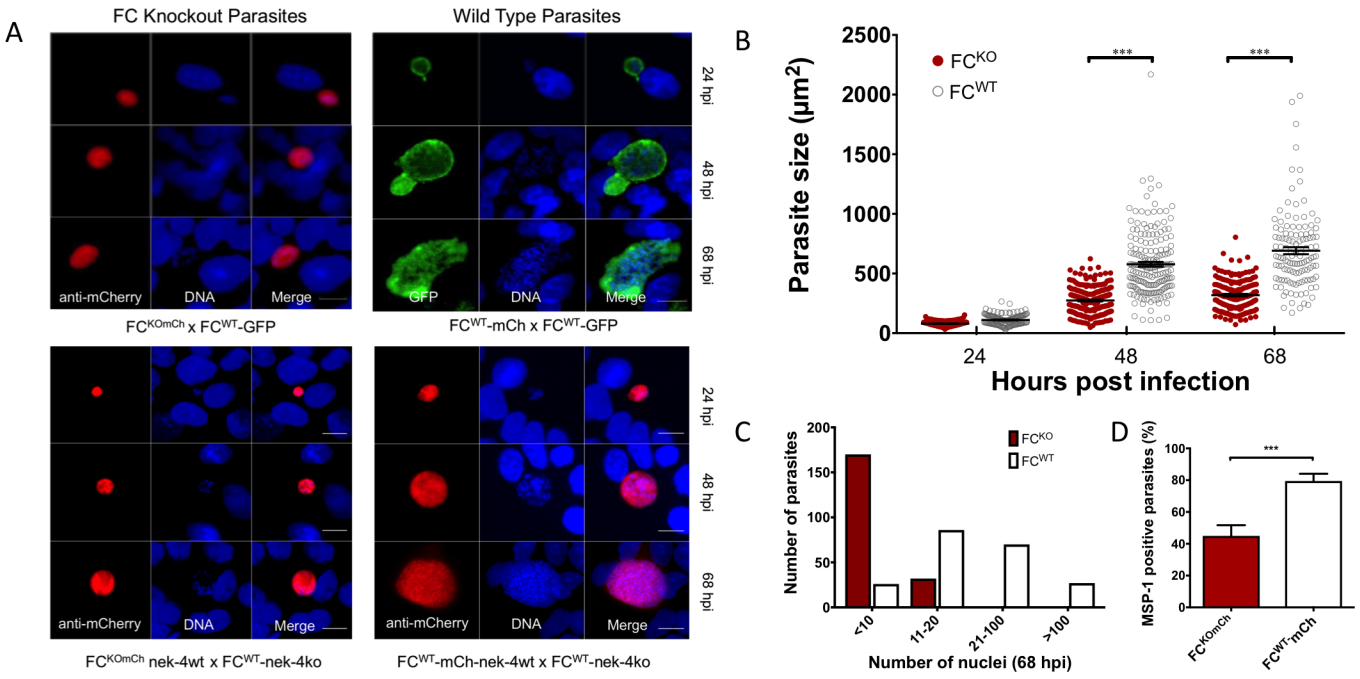

Fig 3. Parasites lacking FC have a severe liver stage growth phenotype. A) Immunofluorescence assay of FC^{KOmCh} and FC^{WT} parasites grown in HepG2 liver cells for 24, 48 and 68 hours post infection (hpi) showing the reduced growth of FC^{KOmCh} parasites. scale bar 20 μm. B) Quantification of liver stage parasite size showing that FC^{KOmCh} parasites are significantly smaller than FC^{WT} parasites after 48 and 68 hours of incubation in HepG2 cells. ***—P value < 0.0001 (Student t-test), data pooled from six independent experiments. C) Quantification of parasite nuclei 68 hours after infection showing that FC^{KOmCh} parasites produced significantly fewer nuclei than FC^{WT} parasites by 68 hpi. P value <0.0001 (χ^2). D) Immunofluorescence assay of MSP-1 expression, a marker for mid to late stage parasite development in the liver stage. FC^{KOmCh} parasites have a defect in MSP-1 expression, with only 45% of FC^{KOmCh} parasites producing MSP-1 compared to 79% of FC^{WT}. ***—P value <0.001 (Fisher's exact test) 801 parasites assessed, pooled from three independent experiments with no fewer than 58 parasites measured in any one sample. Error bars show 99% confidence interval.

https://doi.org/10.1371/journal.ppat.1006396.g003

To assay FC^{KOmCh} liver development *in vivo*, we used both bite-back and IV injection of purified salivary gland sporozoites to infect naïve mice. Positive PCR of FC^{KOmCh} parasites in mice livers 40–42 hours after IV injection of complemented sporozoites demonstrates that these parasites can successfully infect mouse hepatocytes *in vivo* (Fig 1F). To test if FC^{KOmCh} parasites could complete the liver stage in naïve mice, we then tested for blood stage parasites by microscopy and PCR. Blood stage patency was achieved in standard times frames from either mosquito bites or intravenous injection of sporozoites from each of our crosses, including those with FC^{KOmCh} parasites as one parent (Table 1). However, fluorescence microscopy revealed no mCherry expressing parasites in any of the infected mice (Fig 4A) indicating that parasites carrying FC^{KOmCh} could not complete the liver stage *in vivo*. All other expected gene combinations following recombination were detected by PCR, including the nek-4ko allele transmitted via the male FC^{WT}-nek-4ko gamete, confirming that recombination had occurred (Figs 4B and S3).

To exclude the possibility that FC^{KOmCh} parasites were present at levels below the threshold of detection by microscopy or PCR, we applied pyrimethamine selection to the P0 mice infected with sporozoites generated by the FC^{KOmCh} x FC^{WT}-GFP cross. The FC^{WT}-GFP

Table 2. Production of FC^{KOmCh} merosomes following outcrossing (no. of trials = 3).

	FC^{KOmCh}	FC^{WT}-mCh
70 hours post infection	0	21.6 ± 6

https://doi.org/10.1371/journal.ppat.1006396.t002

parasites lack pyrimethamine resistance, so drug pressure should selectively recover any FC^{KOmCh} parasites (in which *h*DHFR disrupts their FC gene) that had completed the liver stage. Following infection with sporozoites from the FC^{KOmCh} x FC^{WT}-GFP cross, one group of mice was immediately treated with pyrimethamine. These mice remained free of parasites for 14 days after infection. A second group of mice were left untreated following sporozoite infection and then treated with pyrimethamine after the infection was established (7 days after infection). All parasites were cleared after four days of pyrimethamine treatment, and no recrudescence was detected. These experiments eliminate the possibility that a small number of FC^{KOmCh} parasites complete the liver stage but are being masked by a larger population of FC^{WT} parasites. This confirms that the deletion of FC is lethal during the exoerythrocytic stage of *P. berghei*. FC^{KOmCh} parasites can establish, but not complete, a liver stage infection and this prevents them from generating a blood stage infection.

Discussion

We confirmed that *P. berghei* rodent malaria parasites with a disrupted FC gene are viable during blood stage, can infect mosquitos and produce oocysts, but that these oocysts fail to

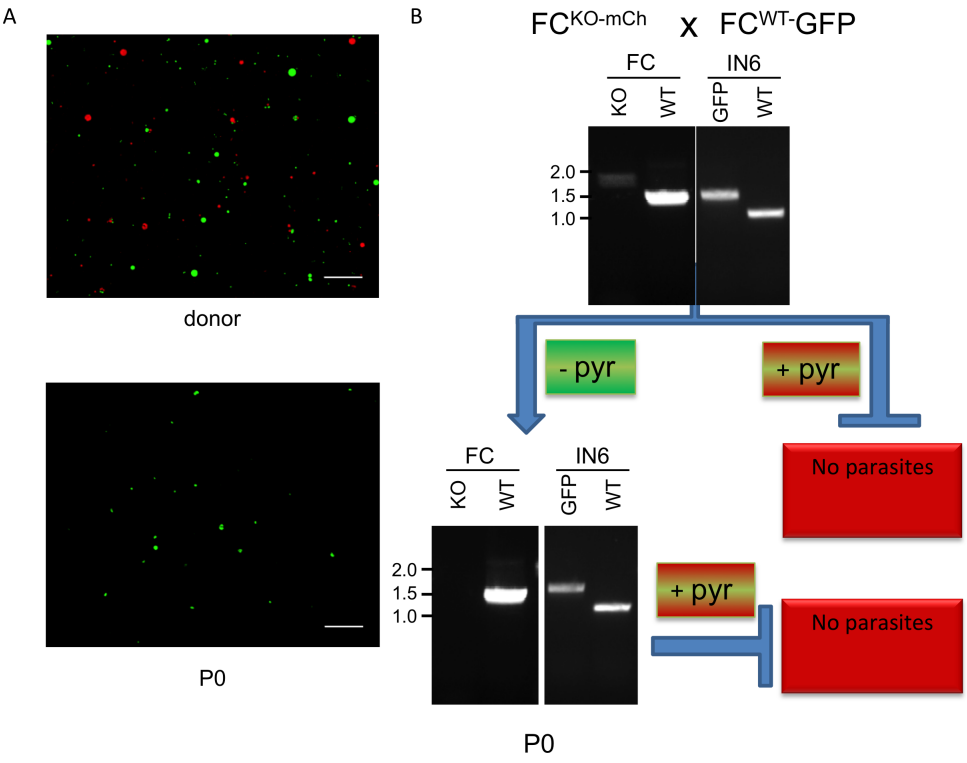

Fig 4. FC deficient parasites cannot complete the liver stage *in vivo*. (A) Epi-fluorescent images comparing the expression of mCherry and GFP before and after transmission. Both GFP and mCherry are visible in parasites recovered from the blood of a donor mouse dual infected with FC^{KOmCh} and FC^{WT}-GFP parasites (upper panel). In contrast only GFP expression is observed in a naïve mouse infected with the progeny (P0) of this cross (lower panel), confirming the essential nature of FC during liver stage development. scale bar: 100μm. B) Summary of the genotypes and pyrimethamine resistance phenotype following infection of naïve mice with sporozoites from the FC^{KOmCh} x FC^{WT}-GFP cross. PCR screening detects parasites with both of the FC and GFP alleles in the donor mouse used to infect mosquitoes. The FC^{KOmCh} genotype cannot be detected in the blood of mice infected by parasites found in those mosquitoes, demonstrating its lethality in the liver stage. Pyrimethamine selection for parasites carrying the hDHFR inserted in the FC locus kills all parasites, confirming that FC^{KOmCh} sporozoites cannot infect naïve mice. FC^{WT}-GFP parasites are susceptible to pyrimethamine treatment and are, therefore, not present after drug treatment.

https://doi.org/10.1371/journal.ppat.1006396.g004

produce sporozoites. As with many other mutants with their first observable effect in the mosquito stage, the absolute block in sporozoite production by heme pathway deletion mutants essentially prevents any subsequent assessment of the viability of these mutants in the sporozoite and liver stages. Our aim was to create a simple genetic system to complement the deletion of any mosquito stage essential gene using a heme enzyme as a test case. It has been a common strategy in *Plasmodium* parasites that can be transmitted in the lab, to complement mosquito stage defects by crossing mutant parasites to wild type parasites (S3 Table). This simple technique takes advantage of the heterokaryotic, polyploid nature of the mosquito stages to determine if the deleted gene is essential for transmission. However, this approach does not allow phenotypic analysis in the early stages of the mammalian infection because it yields a mixed population of wild type and mutants parasites that are indistinguishable from each other. By inserting a fluorescent marker into the deleted locus, we can definitively identify mutant parasites following recombination, thus enabling phenotypic characterization of these parasites during liver stages. Using this technique, we analysed the late mosquito, and early mammalian stage phenotype of the final enzyme in heme synthesis, FC.

We were able to generate haploid FC^{KO} sporozoites (Fig 1F), and (in agreement with findings for parasites lacking ALAS but chemically complemented with d-ALA) these FC^{KOmCh} sporozoites showed no significant defects in motility (S2 Fig, S2 Table) and could infect liver cells both *in vivo* and *in vitro* (Figs 1F and 3). ALAS is the first enzyme in the heme synthesis pathway and FC is the last, so it is reasonable to assume that the entire synthesis pathway is not essential for sporozoites. We note, however, that all sporozoites from the forced outcross to a colourless, female sterile parasite line (FC^{WT}-nek-4ko) contained mCherry, even though the genotyping confirmed the presence of sporozoites carrying the non-fluorescent FC^{WT} locus (Fig 1F). This suggested significant carryover of mRNA, protein and/or heme from the cytoplasm of the multinucleate oocyst that could transiently complement FC^{KOmCh} sporozoites. By crossing parasites expressing different fluorophores from the same genetic locus we confirmed that sporozoites can contain proteins expressed in the oocyst even when they lack the gene encoding these proteins (Fig 2). Therefore, the FC^{KOmCh} sporozoite phenotypic data must be interpreted with caution until further studies clarify the nature and persistence of the products carried over from the shared oocyst cytoplasm to the haploid sporozoite.

Parasites in mosquito and hepatic cells are postulated to have fewer host cell resources available to them in comparison to parasites in the erythrocytic environment [14]. Indeed, mitochondrial chemiosmotic respiration is significantly increased as parasites transition to the non-red blood cell stages, reflecting the activation of oxidative phosporyhylation to generate ATP [30]. Thus, it is not surprising that this stage has high demands for heme cores for cytochromes and that *de novo* heme biosynthesis is essential during the protracted oocyst stage of the *Plasmodium* life cycle, [5, 12, 13, 15]. Supplementing ALAS deficient parasites by exogenously applying the product of this enzyme during the mosquito stages has proven an elegant method to look at the role of the initial heme synthesis enzyme in the liver stage of parasite development [12, 15]. However, the complexity of the *Plasmodium* heme biosynthetic pathway, particularly being spread over three cellular compartments, suggests that the parasite may have differential abilities to compensate for loss of heme pathway components.

In our system, the specific phenotype of FC deficient parasites could be assessed throughout the entirety of liver stage development. Reassuringly, at the first phenotypic assessment at 24 hours, parasites could be definitively classified based on the expression of mCherry, suggesting there is no detectable carry over of fluorphores, and presumably other proteins, from the sporozoite at this early liver stage. It remains possible that very early liver stage development could be affected by residual protein from the oocyst, although the absence of any oocyst derived fluorphores at 24 hours post infection suggest a very limited contribution of oocyst derived

products to overall development in the liver stage. mCherry expressing FC knockout parasites were present throughout the life cycle up to 68 hpi, but these had significant growth defects that arrest their progress in the middle of liver stage development. The reduced expression of MSP-1 (Fig 3D) further suggests that FC^{KOmCh} parasites are significantly impaired in the ability to develop normally beyond ~50 hours after liver cell invasion, the point at which MSP-1 is detectable [25]. This developmental block was confirmed by the slower growth rate (Fig 3A and 3B), reduced number of nuclear division (Fig 3C) and inability to complete development, as demonstrated by the inability to produce merosomes (Table 2).

In vivo transmission confirmed the *in vitro* liver stage phenotype of FC^{KOmCh} parasites. Mutant parasites could be detected in the mouse liver 40–42 hours after infection with sporozoites (Fig 1F) but could not be detected in the subsequent blood stage infection by fluorescence or PCR, even when mice were infected by 10-fold more sporozoites than are required to generate 100% infection rates in the naïve mouse strain tested (Figs 4B and S3, Table 1). Recovery of all other combinations possible from sexual recombination confirmed successful crossing and infection of the naïve mice (Figs 4B and S3). The ability to specifically select for FC^{KOmCh} parasites using pyrimethamine treatment provided a further tool to assay for parasites carrying the FC^{KOmCh} locus, ensuring that no population of mutant parasites was present at levels below the sensitivity of our PCR screen and masked or overgrown by FC^{WT} parasites during subsequent blood stage infection. These screens also support the specific link between the observed phenotype and the FC locus. Rigorous, discipline-standard experimental technique in the development of the FC^{KOmCh} parasite line strongly supports a single, specific integration in this parasite line. However, the strict correlation observed between fluorescence, drug resistance and the FC gene deletion following sexual recombination and drug selection confirms that the observed phenotype is specifically caused by deletion of the FC locus.

Deletion of FC causes a different defect in parasite liver stage growth both *in vitro* and *in vivo* than that observed for parasites lacking the upstream heme pathway enzyme ALAS [15]. Although it was initially reported that ALAS activity is essential to generate infectious sporozoites [12], a subsequent study found that *P. berghei* parasites can partially compensate for the loss of ALAS activity [15] allowing them to maintain limited infectivity *in vivo* [15]. An *in vitro* analysis showed that these parasites can complete the liver stage and produce a limited number of merosomes in the absence of ALAS activity [15] presumably by scavenging sufficient d-ALA from the host cell to compensate for the loss of this enzyme. In contrast, our data suggest such scavenging cannot compensate for the lack of FC activity. The *in vitro* liver stage phenotype observed for FC^{KOmCh} parasites is far more severe than that for parasites lacking ALAS and no merosome production was observed. This agrees with the *in vivo* findings that FC^{KOmCh} parasites can infect the liver but not complete this life stage.

The marked difference between knockouts of the first enzyme in the synthesis pathway and the last, likely relates to differences in the stability of the two products and their localization within the host cell. Heme is a highly reactive molecule that can be a significant generator of oxygen radicals [31], whereas d-ALA is stable enough to survive prolonged periods in culture or in sucrose solution fed to mosquitoes. After d-ALA formation by ALAS in the host mitochondrion, this substrate is transported to the host cell cytoplasm where ALAD, the next enzyme in the pathway is located. This makes it much more likely that salvageable levels of d-ALA are available in the host liver cell cytoplasm. In contrast, in a hepatic cell FC, and the heme it produces, are located in the mitochondrion. This organellar localization is likely to restrict the free diffusion of reactive heme into the liver cell cytoplasm, where the parasite is located, thus preventing the parasite from salvaging enough heme to compensate for a loss of the FC enzyme. By contrast, red blood cells lack any internal cellular structure, so parasites are surrounded by all the enzymes of the heme pathway and by copious amounts of cytosolic

haemoglobin. Parasites are also actively degrading haemoglobin in their food vacuole, making more heme available and apparently rendering FC dispensable at this stage [12, 13, 16].

The essential nature of FC during the *P. berghei* liver stages described here completes the picture of heme requirements, either endogenous or scavenged, for survival across all stages of the parasite life cycle. It also contrasts the differing ability of the parasite to scavenge host resources to compensate for a loss of enzymes in the *de novo* synthesis pathway. In the red blood cell, the abundance of freely accessible heme, heme pathway intermediates and host cell enzymes allows the parasite to rely on scavenging to meet its heme needs. Host resources appear less available or less accessible during the mosquito stages, making a loss of any heme-synthesizing enzyme during the insect stage lethal. Sporozoites apparently do not require heme synthesis, perhaps having sufficient heme on board after sporogony to underpin their needs. Alternatively, sporozoites would have to scavenge for their heme requirements in the mosquito hemocoel, vertebrate skin, blood capillaries and liver. The liver stage appears more complicated, with the parasites able to partially compensate for the loss of ALAS by scavenging d-ALA from the host cytoplasm. However, in the absence of FC parasites are unable to access sufficient quantities of host heme (or FC) to survive this stage. This suggests that targeting heme synthesis with prophylactic drugs in the parasite and host cells is still possible, but must be carefully considered, given the ability of the parasite to compensate for the loss of certain steps in the pathway. In contrast, the phenotype of parasites lacking FC suggests that heme synthesis may not be an ideal pathway to target for genetic attenuation vaccine strategies, which are more effective the longer the parasite grows in the liver [32].

Despite its importance in vaccine development and prophylaxis, hepatic growth of malaria parasites remains one of the least explored areas of parasite biology. Reverse genetic approaches to liver stage analysis have been hampered by two aspects of *Plasmodium* molecular genetics: only blood stages can be genetically modified, and getting from the blood stage to the liver stages means that these genetically modified parasites must traverse the entire life cycle. Thus, analysis of liver stage phenotypes was compromised by the difficulty in generating infectious sporozoites in mutant parasites with lethal phenotypes at earlier life stages. The complementation strategy outlined here presents a straightforward, simple to implement, and widely applicable approach to extending the analysis window for the burgeoning list of gene mutations (S3 Table) that show their first effects during the mosquito stages. Thus, complementation provides a powerful tool to dissect the biology of the parasite during its earliest, most vulnerable stage in the mammalian host.

Supporting information

S1 Text. Supplementary methods.
(DOCX)

S1 Fig. Generation of FC^{KOmCh} and FC^{WT}-GFP and PCR genotyping strategy. A) FC^{KOmCh} B) GFP in intergenic region of chromosome 6 C) nek4-ko [18].
(TIF)

S2 Fig. Motility of FC^{KOmCh} salivary gland sporozoites. (ns; not significant; $P>.05$, χ^2 test); A) percentage of motile sporozoites observed B) representative image of a motile sporozoites and trails labelled with anti-CSP/AlexaFluor 488 antibodies (green). scale bar: 10μm.
(TIF)

S3 Fig. PCR Genotyping of donor parasites and P0 parasites generated by crossing FC^{KOmCh} nek-4wt x FC^{WT}-mCh-nek-4ko.
(TIF)

S1 Table. List of PCR primers and predicted product sizes.
(DOCX)

S2 Table. Motility of FC^{KOmCh} salivary gland sporozoites.
(DOCX)

S3 Table. Partial list of *Plasmodium* spp. pathways/genes shown to be essential for mosquito stage development that could be candidates for analysis with the described genetic complementation strategy.
(DOCX)

Acknowledgments

Vanessa Mollard for assistance with training and mice handling, Anton Cozijnsen for assistance with mosquito rearing, infections and salivary gland dissection, and Joachim Kloehn for assistance with mouse dissection.

Author Contributions

Conceptualization: CDG GIM.

Data curation: ULR CDG.

Formal analysis: CDG ULR.

Funding acquisition: GIM.

Investigation: ULR CDG.

Methodology: ULR CDG.

Project administration: CDG GIM.

Resources: ULR CDG GIM.

Supervision: CDG GIM.

Validation: ULR CDG GIM.

Visualization: ULR CDG GIM.

Writing – original draft: ULR.

Writing – review & editing: ULR CDG GIM.

References

1. WHO. World malaria report 2013: World Health Organization; 2014.
2. Jambou R, El-Assaad F, Combes V, Grau GE. *In vitro* culture of *Plasmodium berghei*-ANKA maintains infectivity of mouse erythrocytes inducing cerebral malaria. Malar J. 2011; 10:346. https://doi.org/10.1186/1475-2875-10-346 PMID: 22118493
3. Kooij TW, Carlton JM, Bidwell SL, Hall N, Ramesar J, Janse CJ, et al. A *Plasmodium* whole-genome synteny map: indels and synteny breakpoints as foci for species-specific genes. PLoS Pathog. 2005; 1 (4):e44. https://doi.org/10.1371/journal.ppat.0010044 PMID: 16389297
4. Carvalho TG, Thiberge S, Sakamoto H, Menard R. Conditional mutagenesis using site-specific recombination in *Plasmodium berghei*. Proc Natl Acad Sci USA. 2004; 101(41):14931–6. https://doi.org/10.1073/pnas.0404416101 PMID: 15465918

5. Sturm A, Mollard V, Cozijnsen A, Goodman CD, McFadden GI. Mitochondrial ATP synthase is dispensable in blood-stage *Plasmodium berghei* rodent malaria but essential in the mosquito phase. Proc Natl Acad Sci USA. 2015; 112(33):10216–23. https://doi.org/10.1073/pnas.1423959112 PMID: 25831536
6. Prudencio M, Mota MM, Mendes AM. A toolbox to study liver stage malaria. Trends Parasitol. 2011; 27 (12):565–74. https://doi.org/10.1016/j.pt.2011.09.004 PMID: 22015112
7. Lacroix C, Giovannini D, Combe A, Bargieri DY, Spath S, Panchal D, et al. FLP/FRT-mediated conditional mutagenesis in pre-erythrocytic stages of *Plasmodium berghei*. Nat Protoc. 2011; 6(9):1412–28. https://doi.org/10.1038/nprot.2011.363 PMID: 21886105
8. Kalanon M, Bargieri D, Sturm A, Matthews K, Ghosh S, Goodman CD, et al. The *Plasmodium* translocon of exported proteins component EXP2 is critical for establishing a patent malaria infection in mice. Cell Microbiol. 2016; 18(3):399–412. https://doi.org/10.1111/cmi.12520 PMID: 26347246
9. Suarez C, Volkmann K, Gomes AR, Billker O, Blackman MJ. The malarial serine protease Sub1 plays an essential role in parasite liver stage development. PLoS Pathog. 2013; 9(12):e1003811. https://doi.org/10.1371/journal.ppat.1003811 PMID: 24348254
10. de Koning-Ward TF, Gilson PR, Crabb BS. Advances in molecular genetic systems in malaria. Nat Rev Microbiol. 2015; 13(6):373–87. https://doi.org/10.1038/nrmicro3450 PMID: 25978707
11. Surolia N, Padmanaban G. *de novo* biosynthesis of heme offers a new chemotherapeutic target in the human malarial parasite. Biochem Biophys Res Commun. 1992; 187(2):744–50. PMID: 1356337
12. Nagaraj VA, Sundaram B, Varadarajan NM, Subramani PA, Kalappa DM, Ghosh SK, et al. Malaria parasite-synthesized heme is essential in the mosquito and liver stages and complements host heme in the blood stages of infection. PLoS Pathog. 2013; 9(8):e1003522. https://doi.org/10.1371/journal.ppat.1003522 PMID: 23935500
13. Ke H, Sigala PA, Miura K, Morrisey JM, Mather MW, Crowley JR, et al. The heme biosynthesis pathway is essential for *Plasmodium falciparum* development in mosquito stage but not in blood stages. Journal Biol Chem. 2014; 289(50):34827–37.
14. Sigala PA, Crowley JR, Henderson JP, Goldberg DE. Deconvoluting heme biosynthesis to target blood-stage malaria parasites. Elife. 2015; 4.
15. Rizopoulos Z, Matuschewski K, Haussig J. Distinct prominent roles for enzymes of *Plasmodium berghei* heme biosynthesis in sporozoite and liver stage maturation. Infect Immun. 2016. 84(11):3252–3262. https://doi.org/10.1128/IAI.00148-16 PMID: 27600503
16. Smith CM, Jerkovic A, Puy H, Winship I, Deybach JC, Gouya L, et al. Red cells from ferrochelatase-deficient erythropoietic protoporphyria patients are resistant to growth of malarial parasites. Blood. 2015; 125(3):534–41. https://doi.org/10.1182/blood-2014-04-567149 PMID: 25414439
17. Trueman HE, Raine JD, Florens L, Dessens JT, Mendoza J, Johnson J, et al. Functional characterization of an LCCL-lectin domain containing protein family in *Plasmodium berghei*. J Parasitol. 2004; 90 (5):1062–71. https://doi.org/10.1645/GE-3368 PMID: 15562607
18. Reininger L, Billker O, Tewari R, Mukhopadhyay A, Fennell C, Dorin-Semblat D, et al. A NIMA-related protein kinase is essential for completion of the sexual cycle of malaria parasites. J Biol Chem. 2005; 280(36):31957–64. https://doi.org/10.1074/jbc.M504523200 PMID: 15970588
19. Kooij TW, Rauch MM, Matuschewski K. Expansion of experimental genetics approaches for *Plasmodium berghei* with versatile transfection vectors. Mol Biochem Parasitol. 2012; 185(1):19–26. https://doi.org/10.1016/j.molbiopara.2012.06.001 PMID: 22705315
20. Straimer J, Lee MCS, Lee AH, Zeitler B, Williams AE, Pearl JR, et al. Site-specific genome editing in *Plasmodium falciparum* using engineered zinc-finger nucleases. Nat Methods. 2012; 9(10):993-+. https://doi.org/10.1038/nmeth.2143 PMID: 22922501
21. Janse CJ, Ramesar J, Waters AP. High-efficiency transfection and drug selection of genetically transformed blood stages of the rodent malaria parasite *Plasmodium berghei*. Nat Protoc. 2006; 1(1):346–56. https://doi.org/10.1038/nprot.2006.53 PMID: 17406255
22. Combe A, Moreira C, Ackerman S, Thiberge S, Templeton TJ, Menard R. TREP, a novel protein necessary for gliding motility of the malaria sporozoite. Int J Parasitol. 2009; 39(4):489–96. https://doi.org/10.1016/j.ijpara.2008.10.004 PMID: 19000911
23. Sturm A, Graewe S, Franke-Fayard B, Retzlaff S, Bolte S, Roppenser B, et al. Alteration of the parasite plasma membrane and the parasitophorous vacuole membrane during exo-erythrocytic development of malaria parasites. Protist. 2009; 160(1):51–63. https://doi.org/10.1016/j.protis.2008.08.002 PMID: 19026596
24. Ralph SA, van Dooren GG, Waller RF, Crawford MJ, Fraunholz MJ, Foth BJ, et al. Tropical infectious diseases: metabolic maps and functions of the *Plasmodium falciparum* apicoplast. Nat Rev Microbiol. 2004; 2(3):203–16. https://doi.org/10.1038/nrmicro843 PMID: 15083156

25. Combe A, Giovannini D, Carvalho TG, Spath S, Boisson B, Loussert C, et al. Clonal conditional mutagenesis in malaria parasites. Cell Host Microbe. 2009; 5(4):386–96. https://doi.org/10.1016/j.chom.2009.03.008 PMID: 19380117

26. Yu M, Kumar TR, Nkrumah LJ, Coppi A, Retzlaff S, Li CD, et al. The fatty acid biosynthesis enzyme FabI plays a key role in the development of liver-stage malarial parasites. Cell Host Microbe. 2008; 4 (6):567–78. https://doi.org/10.1016/j.chom.2008.11.001 PMID: 19064257

27. Annoura T, Ploemen IH, van Schaijk BC, Sajid M, Vos MW, van Gemert GJ, et al. Assessing the adequacy of attenuation of genetically modified malaria parasite vaccine candidates. Vaccine. 2012; 30 (16):2662–70. https://doi.org/10.1016/j.vaccine.2012.02.010 PMID: 22342550

28. Falkard B, Kumar TR, Hecht LS, Matthews KA, Henrich PP, Gulati S, et al. A key role for lipoic acid synthesis during *Plasmodium* liver stage development. Cell Microbiol. 2013; 15(9):1585–604. https://doi.org/10.1111/cmi.12137 PMID: 23490300

29. Sturm A, Amino R, van de Sand C, Regen T, Retzlaff S, Rennenberg A, et al. Manipulation of host hepatocytes by the malaria parasite for delivery into liver sinusoids. Science. 2006; 313(5791):1287–90. https://doi.org/10.1126/science.1129720 PMID: 16888102

30. Jacot D, Waller RF, Soldati-Favre D, MacPherson DA, MacRae JI. Apicomplexan energy metabolism: carbon source promiscuity and the quiescence hyperbole. Trends Parasitol. 2016; 32(1):56–70. https://doi.org/10.1016/j.pt.2015.09.001 PMID: 26472327

31. Sigala PA, Goldberg DE. The peculiarities and paradoxes of *Plasmodium* heme metabolism. Annu Rev Microbiol. 2014; 68:259–78. https://doi.org/10.1146/annurev-micro-091313-103537 PMID: 25002093

32. Butler NS, Schmidt NW, Vaughan AM, Aly AS, Kappe SH, Harty JT. Superior antimalarial immunity after vaccination with late liver stage-arresting genetically attenuated parasites. Cell Host Microbe. 2011; 9(6):451–62. https://doi.org/10.1016/j.chom.2011.05.008 PMID: 21669394